ABSTARCT

Researchers focused on developing herbal therapies as pharmacological medicines to treat liver cirrhosis that is accompanied by distortion in liver functions. This study evaluated the mechanisms of the hepatoprotective activity of *Vitex negundo* (VN) and *Caesalpinia sappan* (CS) ethanolic extracts on thioacetamide (TAA)-induced liver cirrhosis in male rats. A computer-aided prediction of hepatoprotective activity was primarily performed with prediction activity spectra of substances (PASS) program. The antioxidant properties of the crude extracts of VN and CS were evaluated by 2,2-diphenyl-1-picrylhydrazyl (DPPH), ferric reducing antioxidant power (FRAP), total phenolic content (TPC) and total flavonoid content (TFC) assays. The hepatoprotective effects of the plant extracts were measured against TAA-induced liver damage in a rat model over a period of 12 weeks. Male *Sprague Dawley* (SD) rats were given (0.03% w/v) TAA in their drinking water with daily oral administration of 100 mg/kg and 300 mg/kg from each plant. Silymarin (SY) was used as a reference drug that was orally administered to the animals at a daily dose of 50 mg/kg. At the end of the experiment, the liver was evaluated by the body and liver weight changes, liver gross morphology as well as histopathology, and biochemical measurements of liver parameters, AP, ALT, AST, GGT, LDH, total protein, albumin, bilirubin, serum glucose and lipid profile. The degree and stages of liver fibrosis were determined by Masson's trichrome staining. Hepatic cytochrome P450 2E1 (CYP2E1), matrix metalloproteinase (MMP-2 and MMP-9) and tissue inhibitor of metalloproteinase (TIMP-1) were measured. Oxidative stress was measured by malondialdehyde (MDA) level. The protective activity of VN and CS extracts were evaluated through the liver level of antioxidant enzymes (SOD, CAT and GPx). Protein expression of pro-fibrogenic TGF-β1, α-SMA and proliferating

cell nuclear antigen (PCNA) proteins in the liver were determined and confirmed by immunohistochemical study and Western blot analysis. VN and CS extracts were tested for their cytotoxicity by 3-(4,5-dimethylthiazol-2-yl)-2,5-diphenyltetrazolium (MTT) assay, measuring LDH and caspase-3 enzymes against hepatocarcinoma cell lines (HepG2) and antioxidant activity against hydrogen peroxide (H_2O_2)-induced oxidative damage in embryonic normal liver cell line (WRL-68). PASS-predicted plant activity efficiently helped in selecting the promising antioxidant, hepatoprotectants and antiproliferative pharmaceuticals with high accuracy. Our findings showed that VN and CS ethanol extracts significantly reduced the impact of TAA toxicity, and they were effectively hepatoprotective as evidenced by improved liver histopathology, immunohistochemistry and biochemistry, comparable to that of SY. The mechanism of the hepatoprotective effects of VN and CS were proposed to be through neutralizing the ROS as well as attenuation of the endogenous antioxidant activities: CAT, SOD, GPx and MDA. Additionally, VN and CS treatment had normalised the expression of TGF-β1, α-SMA, PCNA, MMPs and TIMP-1 proteins. In conclusion, the results of the present study indicate that VN and CS ethanol extracts were non-toxic and safe when administered orally, these plants possessed hepatoprotective, antioxidant and antiproliferative activities probably due to the presence of negundoside, vitegnoside and sappanchalcone as explored by PASS in VN and CS plant, respectively.

ABSTARK

Penyelidik memberi tumpuan kepada membangunkan terapi herba sebagai ubat-ubatan untuk merawat farmakologi sirosis hati yang disertai dengan penyelewengan dalam fungsi hati. Kajian kali ini ingin menilai mekanisme aktiviti hepatoprotektif daripada ekstrak etanol Vitex negundo (VN) dan Caesalpinia sappan (CS) pada tikus jantan yang menghidap sirosis hepar akibat dirawat dengan thioacetamide (TAA). Satu ramalan bantuan komputer ke atas aktiviti antioksidan hepatoprotektif utama dilakukan menggunakan program spectra aktiviti ramalan bahan (PASS). Sifat antioksidan ekstrak mentah daripada VN dan CS telah diuji dan dinilai dengan menggunakan diphenyl pcryl hydrazyl (DPPH), kuasa penurunan ferik (FRAP), jumlah kandungan flavonoid (TFC) dan kandungan jumlah fenol (TPC). Kesan hepatoprotektif ekstrak tumbuhan tersebut diukur menggunakan model tikus Sprague Dawley (SD) jantan dengan kerosakan hepar yang disebabkan oleh rawatan TAA melebihi 12 minggu. Tikus telah diberi (0.03% w/v) TAA di dalam air minuman harian haiwan berkenaan berserta dengan ekstrak setiap tumbuhan pada dos 100 mg/kg dan 300 mg/kg. Silymarin (SY) telah digunakan sebagai ubat rujukan, sebagai perbandingan, yang diberi secara oral mengikut dos harian sebanyak 50 mg/kg. Pada akhir tempoh 12 minggu, kerosakan hepar telah dinilai dengan perubahan berat badan dan berat hepar, morfologi kasar hepar serta histopatologi dan nilai ukuran parameter biokimia hepar (AP, ALT, AST, GGT dan LDH), di samping paras protein, albumin, bilirubin, serum glukosa dan profil lipid. Tahap dan peringkat fibrosis hepar ditentukan dengan pewarnaan Masson Trichrome. Cytochrome hepar P450 2E1 (CYP2E1), matriks metalloproteinase (MMP-2 dan MMP-9) serta tisu perencat metalloproteinase (TIMP-1) juga diukur. Tekanan oksidatif diukur dengan paras malondialdehid (MDA). Aktiviti pelindungan ekstrak VN dan CS diukur

melalui paras enzim antioksidan (SOD, CAT dan GPx) dalam hepar. Pengekspresian protein pro-fibrogen TGF-β1, α-SMA dan antigen nuklear sel pembiak (PCNA) dalam hepar haiwan telah ditentukan dan disahkan menggunakan kajian immunohistokimia dan analisis *Western blotting*. Ekstrak VN dan CS telah diuji tahap ketoksikan masing-masing dengan menggunakan penilaian (3-(4,5-dimethylthiazol-2-YL)-2,5-diphenyltetrazolium (MTT), pengukuran enzim dehidrogenase laktat dan caspase-3 dilakukan ke atas sel-sel terbitan hepatocarcinoma (HepG2), manakala aktiviti pelindungan dilakukan ke atas sel hepar embrio normal (WRL-68) yang mengalami kerosakan oksidatif akibat rawatan hidrogen peroksida (H_2O_2). Ramalan PASS dengan darjah ketepatan yang tinggi telah dapat menentukan aktiviti tumbuhan serta sifat-sifat kandungan farmaseutikal telah membantu dalam menentukan kandungan fito bagi setiap tumbuhan. Rawatan dengan ekstrak VN dan CS telah dapat mengurangkan dengan ketara kesan ketoksikan TAA pada hepar. Ini menunjukkan bahawa kedua-dua tumbuhan tersebut mengandungi bahan hepatoprotektif yang berkesan sehingga dapat membaikpulih kerosakan hepar seperti yang dilihat dalam dapatan histopatologi, immunohisto-kimia dan biokimia tisu hepar setanding dengan SY. Mekanisme bagi kesan hepatoprotektif ekstrak VN dan CS dicadangkan sebagai melalui kaedah peneutralan ROS dan pengurangan aktiviti antioksidan endogen: CAT, SOD, GPx dan MDA. Selain itu, rawatan VN dan CS telah menormalkan ekspresi TGF-β1, αSMA, PCNA, MMPs dan protien TIMP1. Sebagai kesimpulan, dapatan daripada kajian ini menunjukkan bahawa ekstrak etanol VN dan CS adalah tidak toksik dan selamat jika diambil secara oral; tumbuhan ini mengandungi bahan hepatoprotektif, antioksidan dan mempunyai kesan immunomodulatori mungkin kerana kandungan fito dan sebatian aktifnya (negundoside, vitegnoside dan sappanchalcone) seperti yang diramalkan oleh PASS.

ACKNOWLEDGMENT

Foremost, a very deep thankful to Allah Subhanahu Wa Taala, that helped me to manage myself to handle this project satisfactorily. I would like to express my sincere gratitude to my advisor Prof. Dr. Normadiah Binti M. Kassim and my co-supervisor Prof. Dr. Mahmood Ameen Abdullah for the continuous support of my Ph.D study and research, for their patience, motivation, enthusiasm and immense knowledge. Their guidance helped me in all the time of research and writing of this thesis. Many thanks to University of Malaya for PPP PS grant, all the staff in animal house, Anatomy and Biomedical Science Departments, Faculty of Medicine, University of Malaya.

I would like to thank my parents for giving birth to me at the first place and supporting me spiritually throughout my life and for always being there when I needed to talk through how I was feeling about my work and for all of their moral support

My final, and most heartfelt, acknowledgment must go to my daughter Dalia, my son Yousif and my sister Abbeer and her husband Wageeh. They have worked diligently, and successfully. Their support, encouragement, and companionship have turned my journey through graduate school into a pleasure. For all that, and for being everything I am not, they have my everlasting love.

LIST OF CONTENTS

LIST OF FIGURES

LIST OF TABLES

LIST OF SCHEMES

LIST OF SYMBOLS AND ABBREVIATIONS

%	Percentage
α-SMA	α-smooth muscle actin
α-TOH	α-Tocophenol
µmol/ L	micromol per liter
Alb	Albumin
ALT	Alanine aminotransferase
ANOVA	Analysis of variance
AP	Alkaline phosphatase
AST	Aspartate aminotransferase
BHT	Butylated hydroxyl toluene
BOH	Binucleation of hepatocytes
BDE	Bond dissociation energy
^{o}C	Degree celcius
Cm	Centimetre
CS	*Caesalpinia sappan*
CAT	Catalase
CT	Computerized axial tomography
CCl4	Carbon tetra chloride
CV	Central vein
CYP2E1	Cytochrome P450 2E1
DMEM	Dulbecco's modified eagle's medium
dL	Decilitre
DMSO	Dimethyl sulfoxide

DPPH	Diphenyl picryl hydrazyl
DPX	Dibutyl phathalate Xylene
DW	Distilled water
ECM	Extracellular matrix
Fe^{2+}	Ferrous ion
FBS	Fetal bovine serum
Fe^{3+}	Ferric ion
FD	Fatty degeneration
FDA	Food and Drug Administration
FDN	Fatty degenerative nodule
Fe -TPTZ	Ferric - Tris 2 Pyridyl – s Trizine
FRAP	Ferric reducing antioxidant power
Gm	Gram
GGT	Gamma glutamyl transferase
GPx	Glutathione peroxidase
HBV	Hepatitis B Virus
HCV	Hepatitis C Virus
H and E	Hematoxyline and Eosin
HSC	Hepatic stellate cell
hrs	hours
INR	international normalized ratio
IU/L	International unit per litre
L	Litre
LD_{50}	Lethal dose 50
LDH	Lactate dehydrogenase

LM	Light microscope
M	Metre
Mg	Milligram
Min	Minute
Mm	Millimetre
μmole	Micromole
μm	Micrometre
Ml	Millilitre
Mmole	Milimole
mmol/ L	Milimole per litre
Nm	Nanometre
nmol/mg	Nano mole per milligram
MMP_S	Matrix metalloproteinases
MDA	Malondialdehyde
TBA_2	Thiobarbituric acid
MMPs	Matrix metaloproteinases
MRI	Magnetic resonance imaging
MTT	3-(4,5-dimethylthiazol2-yl)-2,5-diphenyltetrazolium bromide assay
NaCl	Sodium chloride
NR	Nodular regeneration
NRH	Nodular regenerative hyperplasia
NS	Normal saline
PBD	Proliferation of bile duct
PBS	Phosphate buffer saline

PDGF	Platelet-derived growth factor
PVDF	Poly vinylidene doflouride membrane
PT	Portal traid
P value	Level of significance
Rpm	Revolution per minute
ROS	Reactive oxidative species
RSC	Radical scavenging capacity
RH	Regenerative hepatocytes
SDS	Sodium dodecyl sulphate
Sec	Second
SD	*Sprague Dawley*
SEM	Standard error of the mean
SGOT	Serum glutamic oxaloacetic transaminase
SGPT	Serum glutamic pyruvate transaminase
SOD	Superoxide dismutase
TAA	Thioacetamide
TASO	Thioacetamide –S oxide
Tcp	Twinning of cell plates
TFC	Total Flavonoid content
TGF-β1	Transforming growth factor β
TIMP1	Tissue inhibitor of matrix metalloproteinase 1
TIMP2	Tissue inhibitor of matrix metalloproteinase 2
TPC	Total phenolic content
UV	Ultraviolet
VN	*Vitex negundo*

LIST OF APPENDICES

Chapter 1

Introduction

1.1 The Beginning

Diseases of the liver are common in medical practice. Fibrosis, defined as the excessive deposition of an extracellular matrix in an organ, it is the main complication of chronic liver damage (Guyot et al., 2006). In many cases, the fibrosis can not be treated, and chronicity develops. In about one-third of patients with chronic liver disease, liver cirrhosis develops (Koek et al., 2007). Liver fibrosis is reversible, whereas cirrhosis is irreversible, this probably due to the fibrous scarring and hepatocellular degeneration. It is associated with prominent morbidity and mortality (Ueki et al., 1999). Several biological and biochemical alterations are occurred, resulting in hepatic cirrhosis (Kadir et al., 2011), which inevitably lead to liver dysfunction and anatomic aberrations (Sheldon, 1994). Cirrhosis is the eighth leading cause of death in diseased population over the world and the cost of cirrhosis, which is expressed in terms of human suffering, hospital costs and loss of productivity is high because loss of liver function affects the body in many ways (Derek, 1994).

Liver cirrhosis is a critical stage of liver disease where chronic inflammation of liver cells has caused an extensive build-up of scar tissue within the liver (Muñoz, 1991). Most of the liver diseases have the potential to progress to this stage and with various presentations (Rigby & Schwarz, 2001). Liver cirrhosis is a consequence of fibrotic changes that occur in a chronically damaged liver as in alcoholic abuse, viral hepatitis and inherited metabolic diseases (Hsiao et al., 2007).

The exact prevalence of cirrhosis worldwide is unknown. It was estimated at 0.15% or 400 000 in the United States of America, which accounted for more than 25000 deaths and 373 000 hospital discharges in 1998. Similar numbers have been reported from Europe, and numbers are even higher in most Asian and African countries where chronic viral hepatitis B or C is common (Schuppan & Afdhal, 2008). Epidemiological studies have identified a number of factors that contribute to the risk of developing cirrhosis such as regular (moderate) alcohol consumption, an age older than 50 years and male gender (Derek, 1994).

Alcoholic liver disease and hepatitis C are the most common causes in developed countries, whereas hepatitis B is the prevailing cause in most parts of Asia and Africa (Schuppan & Afdhal, 2008). And almost innumerable varieties of chemical substances may produce liver cirrhosis such as, carbon tetrachloride (CCl_4), chloroform and thioacetamide (TAA) in certain doses (Muñoz, 1991). TAA-induced rat liver cirrhosis has been shown to resemble the human disease and serves as a suitable animal model for studying the human liver cirrhosis caused by free radical-mediated lipid peroxidation (Müller et al., 1988).

The current treatments of liver cirrhosis are limited in removal of the underlying injurious stimulus (Cruz et al., 2005). Liver cirrhosis is considered as an irreversible process (Reif et al., 2004). However, treatment can stop or delay further progression and reduce the possible complications. In spite of extensive research in the medical field, there is no drug in the modern system of medicine that can be claimed to cure liver cirrhosis (Agarwal et al., 2006). As the pathological assessment is regarded as the gold standard for evaluating the extent of fibrosis, in this study, we will adopt an acceptable staging criterion for rodent model fibrosis. This staging fibrotic system is not just a

classification criterion, but it is also a useful tool to judge the effect of new anti-fibrotic agents (Zhao et al., 2008).

There has been a substantial increase in the use of complementary or alternative therapies (herbal therapy), based on free radical scavenging or antioxidant properties to treat patient with liver diseases. Among these herbals are Chinese herbal medicines, olive leaf extract, turmeric, and milk thistle are used to treat liver diseases such as acute viral hepatitis, alcoholic liver diseases and cirrhosis (Bass, 1999).

The extract of *Vitex negundo* (VN) leaves was found to possess hepato-protective activity against liver damage (Mahalakshmi et al., 2010; Tandon et al., 2008; Tasduq et al., 2008; Yang et al., 1987). Similarly, many studies have been conducted to determine the hepatoprotective effect of *Caesalpinia sappan* (CS) crud extract against different agents-induced hepatotoxicity in rats (Sarumathy et al., 2011; Srilakshmi et al., 2010). Antioxidants are our 1st line defence in protecting the liver against TAA-induced injury and reducing reactive oxidative species in several human diseases and experimental models of liver dysfunction (Balkan et al., 2001; Bruck et al., 1999) such as *Curcuma longa* (Turmeric) (Salama et al., 2013), and *Androgaraphis paniculata* (Trivedi & Rawal, 2000) to prevent drug-induced hepatotoxicity has been correlated with their free radical scavenging property. The antioxidant system involves both endogenous and exogenous sources, both functions actively and synergistically to effectively neutralize free radicals like 2,2-diphenyl-1-picrylhydrazyl (DPPH) (Buijnsters et al., 2001).

Inspired by these results, we were keen to discover whether oral administration of ethanolic extract of both VN and CS can prevent the extent of toxic effect of TAA-induced liver cirrhosis in rat. Could the antioxidant activity of VN and CS extract be

evaluated by DPPH, antioxidant enzymes and lipid peroxidation assays? Can VN and CS extracts restore the liver function, glucose level and lipid profile parameters in TAA-induced liver cirrhosis in rats? Furthermore, can VN and CS extracts maintain or at least protect the normal macroscopic and microscopic features in liver of the experimental rats?

We were also keen to understand how these plants' extracts behave as antiproliferative agents against heaptocarcinoma cell lines (HepG2) under certain conditions. Do VN and CS extracts have apoptotic and cytotoxic effect on HepG2 cells? The attempt to answer these questions forms the basis for the present investigations.

The discovery of new effective drugs for treatment of liver cirrhosis still remains a top priority. In practice, patients with liver cirrhosis are often prescribed a cocktail of medicines, each of these medicines acts on a single target. It may be expected that medicines acting simultaneously on different targets will allow physicians to treat patients more flexibly and to reduce the intake of medicines, hence, reducing the side effects (Lagunin et al., 2003). This method does not solve the problem. In contrast to this approach, the computer program prediction of activity spectra for substances (PASS) (Hade, 2012) simultaneously predicts more than 700 types of biological activity on the basis of the structural formulas of a substance. The availability of several hundred types of biological activity already predicted and the data on the relationships between mechanisms of action and pharmacological effects allowed us to select compounds that act on different molecular targets and cause the same pharmacological effect.

We decided in the light of circumstances under which we would be working, to give more serious attention to the role of VN and CS extracts. We recognize that these require understanding the role of antioxidant properties with the effective assistance of

prediction of activity spectra for substances software (PASS). The 2nd stage would be to subject this understanding on its role as hepatoprotective agents in rats. The 3rd stage would be to evaluate the cytotoxic effect of VN and CS extracts on HepG2 cells. Subsequent discussion throughout this study would reveal many surprises in the store for us.

1.2 Objectives of the Study

1.2.1 General objectives

1. To investigate the hepatoprotective activity of VN and CS ethanol extracts against TAA-induced liver cirrhosis in male *Sprague Dawley* rats.
2. To study the mechanism underlying the hepatoprotective activity of VN and CS in TAA–induced liver cirrhosis in rats.
3. To study the *in vitro* bioactivities of VN and CS crude ethanolic extract on normal embryonic liver cells (WRL68) and hepatocarcinoma cell lines (Hep G 2).

1.2.2 Specific objectives

1. To predict and explore the active principle compounds of VN and CS by using PASS program.
2. To determine the *in vitro* antioxidant properties of VN and CS extracts.
3. To determine the macroscopic and microscopic changes in TAA-induced liver cirrhosis in rats treated with VN and CS extracts.
4. To determine the role of VN and CS extracts on the liver function test, serum glucose and lipid profile parameters in TAA–induced liver cirrhosis in rats.

5. To determine the antifibrotic effect of VN and CS extracts on down regulation of tansforming growth factor-β1 (TGF-β1), α-smooth muscle actin (α-SMA) and proliferating cell nuclear antigen (PCNA) proteins expressions by immunohistochemical staining and Western blot analysis in TAA-induced liver cirrhosis in rats.
6. To investigate the hepatic oxidative stress marker, endogenous antioxidant enzymes activities, hepatic cytochrome P450 2E1 (CYP2E1) level and matrix metalloproteinases (MMPs) activities of VN and CS extracts in TAA-induced liver cirrhosis in rats.
7. To examine the *in vitro* cytotoxicity effect of VN and CS extracts on normal embryonic liver cells (WRL68) and hepatocarcinoma cell lines (HepG 2).

Chapter 2

Literature Review

2.1 Gross Anatomy and Histology of Liver

Except for the skin, the liver is the biggest organ in the body. It is reddish–brown in colour, weighs about 1.5 kg or about 2% in an adult body weight (Keith et al., 2009). It is situated under the diaphragm, below the ribs on the right hypochondrium of the abdomen. Normally, it extends from the right fifth intercostal space in the mid-clavicular line down to the right costal margin (Swanson & Kim, 2004) The liver is anatomically divided into two unequal lobes by the falciform ligament (Figure 2.1), whereby the right lobe is bigger than that of the left lobe (Portmann, 2006). The caudate lobe lying posteriorly along the inferior vena cava in front of the hepatic porta while the quadrate lobe lying anteriorly between the gallbladder and round ligament. They are attached to its posterior-inferior surface (Leonard, 1995). Surgically, the point of division between the right and left hepatic lobes is at the porta hepatis where the hepatic artery and portal vein divide into right and left branches (Portmann, 2006). It has the capacity to regenerate its own tissue (Sheldon, 1994). Clinical terms referring to the liver mostly start with "hepato" or "hepatic" from the Greek word for liver (hepar) (Tortora & Derrickson, 2008).

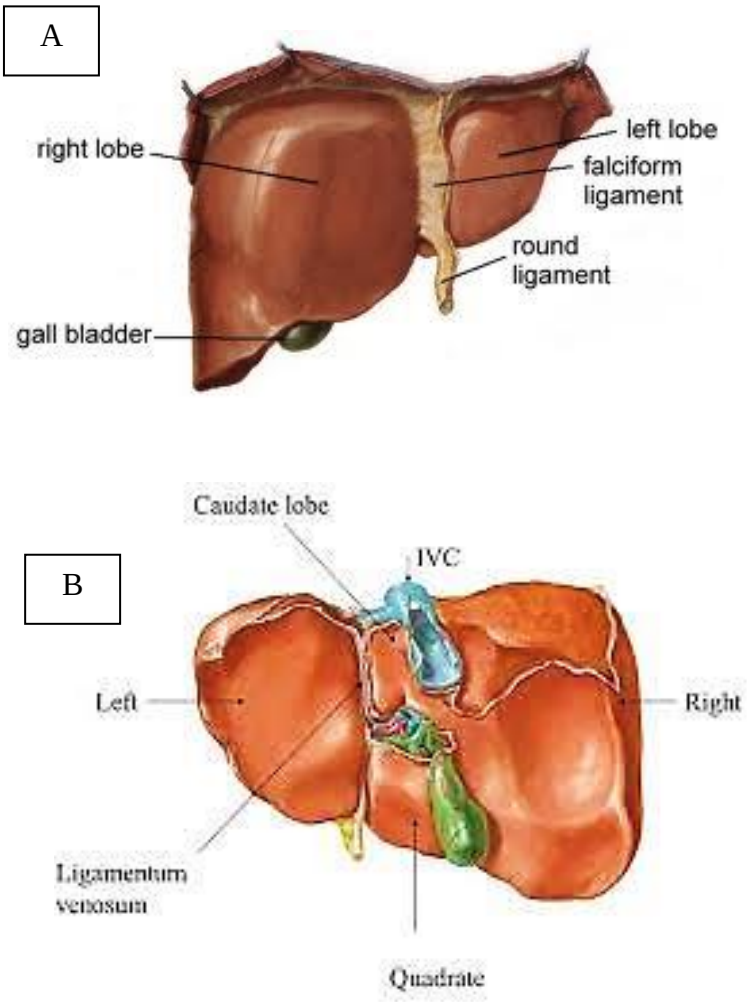

Figure 2.1: Liver A. Anterior surface. B. Posterior surface

[Adapted from (Abrahams et al., 2008)]

Both lobes are made up of thousands of lobules, which are the functional units of the liver, defined as the classic lobule of Kiernan. Each lobule is polygonal, generally hexagonal, and each is 1–2 mm in diameter. It is composed of a labyrinth of interconnected hepatocyte plates, which are separated by endothelium-lined sinusoids. Each lobule is crossed by a central structure, the centrilobular vein. The hepatocyte plates radiate out from the centrilobular vein to the perimeter of the lobule. The portal triads comprise the portal vein, hepatic artery, and bile ductule, and the surrounding

connective tissue are typically found at the angles of the polygon (Eroschenko & di Fiore, 2012).

Based on the blood supply, the functional unit of the liver is the acinus, which is composed of three different zones as shown in Figure 2.2. The peripheral zone or zone 1 is located near the portal tract, the centrolobular zone or the zone 3 surrounds the vena centrolobularis, while the liver parenchyma situated in between zone 1 and zone 3 is zone 2 (Junqueira & Carneiro, 2005). It is apparent that zone 1 is better oxygenated, and this is where many synthetic processes occur, such as albumin production. In contrast, zone 3 has many enzymes involving detoxification reaction (Levison & Reid, 2008).

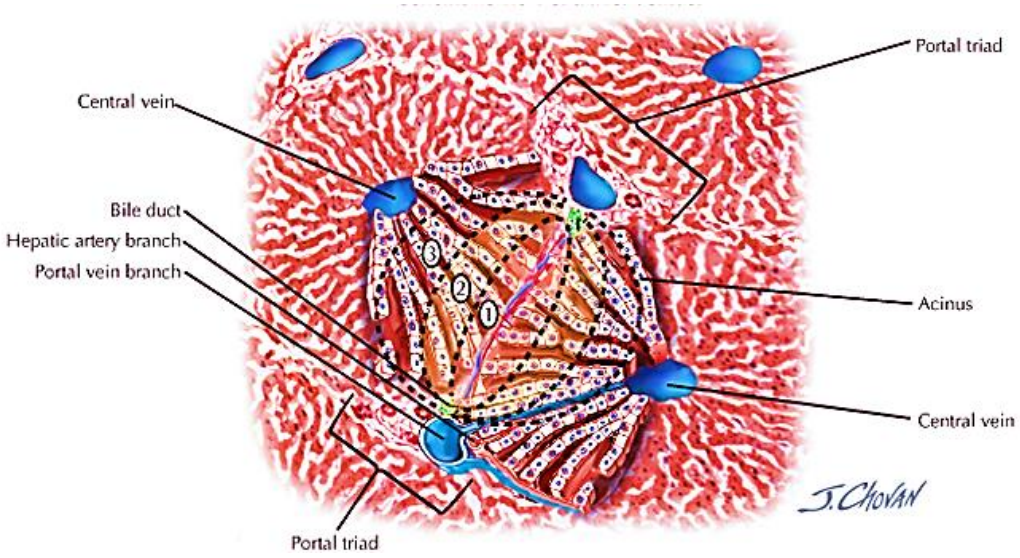

Figure 2.2: The hepatic zones of the liver

[Adapted from (Ovalle et al., 2013)]

Most of the blood in the liver (70-80 %) comes from the portal vein arising from the stomach, intestine and spleen, the rest (20-30 %) is supplied by the hepatic artery (Morton et al., 2011). Blood enters the lobules through branches of the portal vein and hepatic artery, and then flows through small channels called sinusoids, which lie in between the hepatocytes (Cunningham & Van Horn, 2003).

These blood vessels enter the liver at the porta hepatis. The hepatic veins drain posteriorly into the inferior vena cava. The liver is supplied by sympathetic nerve fibres from T7 to T10, that synapse in the celiac plexus along with the right and left vagus nerves and the right phrenic nerve (Swanson & Kim, 2004). Nerve fibres accompany the hepatic artery and bile ducts into the liver parenchyma and innervate Glisson's capsule, the investing membrane of the organ. Lymphatic vessels draining the liver merge at the porta hepatis, and most lympatics accompany the inferior vena cava into the mediastinum (Cunningham & Van Horn, 2003).

In the liver of an adult, hepatocytes occupy 78% of the tissue volume; non-hepatocytes account for 6.3% of the tissue volume and the remaining 15.7% is the extracellular space (Fan & Steer, 2006). Hepatocytes are arranged in plates of one-cell thick. The non-hepatocytes include the endothelial cells, phagocytic Kupffer cells and hepatic stellate cells (HSCs) and portal fibroblast while the extracellular space consists of connective tissues (Portmann, 2006).

The cells of the liver are apparently identical and differ only in their position in the columns along which blood flows from the intestinal tract to the heart (Sheldon, 1994).

2.2 Functions of the Liver

Liver is an important regulating organ in the human body, it is a distinctive organ which functions as a metabolic and biochemical transformation factory (Luxon, 2006). It is essential in the maintenance of metabolic homeostasis by processing dietary amino acids, carbohydrates, lipids, and vitamins; metabolizing cholesterol and toxins; producing clotting factors and storing glycogen.

The liver receives blood that contains substances which are absorbed or secreted by the gastrointestinal organs including the pancreas, intestine, stomach and spleen via the hepatic portal vein at a rate of 1.5 L per min (Jeffrey, 2000). In the meantime, the oxygenated blood is supplied to the liver by the hepatic artery. The substances that enter the liver are then modified or re-synthesised completely to new chemicals which are subsequently returned to the bloodstream or to the bile for excretion. For example, drugs that undergo first-past metabolism might be modified and activated or inactivated in the liver before they enter the systemic blood circulation or remain unchanged (Luxon, 2006). Bile passes in the opposite direction to blood flow, from the canaliculi which are formed between the plates of hepatocytes to the bile ducts (Levison & Reid, 2008).

The liver synthesizes, regulates, stores and secretes many types of substances that enter the liver via the blood flow. It also plays a role to purify, detoxify and neutralize toxins, poisons and unwanted substances that enter the body either by inhalation or ingestion. Without the normal function of the liver, one might not survive (McEwen, 1996).

2.3 Liver Diseases

Because of the multidimensional functions and strategic location of the liver, it is disposed to many diseases. The most common diseases of the liver are acute hepatitis (inflammation), chronic (long duration) hepatitis, alcohol damage, fatty liver, cirrhosis (scarring), α1 antitrypsin deficiency, progressive familial intrahepatic cholestasis, biliary atresia and cancer. These diseases accelerate liver's derangement; however, with its ability to regenerate, it only produces symptoms after long-term damage (Friedman & Keeffe, 2011). Liver regeneration is the response to different injuries induced by external stimuli; it involves consequent changes in the growth factor production, gene expression, and morphologic structure (Kumar et al., 2012).

2.3.1 Liver cirrhosis

The word cirrhosis is originally obtained from the Greek word “kirrhos” that means orange-yellow discoloration (Kuntz & Kuntz, 2008). Cirrhosis is a worldwide health problem; it is a complication of several liver diseases that is described by abnormal structure and function of the liver. It is the scarring of the liver in response to development of regenerative nodules surrounded by fibrous septa as a consequence of long-term liver injury. The scar tissue blocks the flow of blood through the liver and slows down the production of various substances and proteins, including hormones, nutrients, as well as slowing down detoxifying toxins and drugs. As portal congestion progresses, the spleen also becomes congested and leading to splenomegaly and other complications (Tsukada et al., 2006).

Liver cirrhosis is a serious medical problem with significant morbidity and mortality rates and according to the National Institutes of Health in the USA, cirrhosis is

the 12th leading cause of death and within the top 15 most important causes of death of 1990 to 2020 as assumed by global burden disease study (Murray & Lopez, 1997). Previously, liver cirrhosis is thought to be an irreversible process due to the parenchyma collapse and its replacement with collagen, but currently it considered as wound-healing process in response to chronic liver damage. In general, treatment could delay or stop further progression of liver damage and reduce complications (Mann et al., 2003).

2.3.1.1 Causes of liver cirrhosis

Liver cirrhosis is among the most serious diseases. It may develop as a consequence of chronic inflammation caused by free radicals generated by viruses, toxins, unhealthy fats, alcohol, and some drugs or antibodies that attack liver cells (Friedman & Schiano, 2004). Numerous clinical studies have demonstrated that patients with chronic hepatitis B virus (Liaw et al., 1988) and hepatitis C virus infection may progress to liver cirrhosis (Poynard et al., 1997). More than 60-70% of individuals infected with HCV develop chronic liver disease with intermittent necrosis and fibrosis, while a significant number progress to cirrhosis and even to hepatocellular carcinoma (Schuppan & Afdhal, 2008). However, some liver cirrhosis occurs in patients without evidence of hepatotropic viral infection. Tobacco smoking and alcohol consumption have been shown to play a role in causing liver cirrhosis too (Corrao et al., 1994). Nevertheless, biliary obstruction, primary or secondary biliary cirrhosis and non-alcoholic fatty liver, autoimmune liver diseases, hemochromatosis, alpha-1 antitrypsin deficiency, Wilson's disease, and liver cell injury due to toxic chemicals such as certain antibiotics, chemotherapeutic agents, aflatoxin, thioacetamide, carbon-tetrachloride, chlorinated hydrocarbons, etc. can also give rise to liver cirrhosis with less likely to

other causes of cirrhosis, which include parasitic infections and prolonged exposure to environmental toxins (Heidelbaugh & Bruderly, 2006).

2.3.1.2 Molecular pathogenesis of liver cirrhosis

Normal liver contains hepatocytes, Kupffer cells, and hepatic stellate cell (HSC) with low levels of collagen I, III and IV. Type I and III collagen are present in approximately equal amounts and constitute from 0.5% to 2% of total protein in the normal liver (Pierce et al., 1987). Complex cellular and molecular mechanisms resulting from chronic activation of tissue repair mechanism following liver tissue injury have been characterised (Arthur, 1998). In a fibrotic liver, there is a substantial increase deposition of most matrix proteins but in particular, the interstitial collagens type I and III. These collagens are not only present in greater amounts but also deposited in abnormal sites within the liver microanatomy (Reid et al., 2008). A special form of mesenchymal cell which acts as a facultative (myo) fibroblast (HSC), also known as the Ito cell, is found within the perisinusoidal space of Disse (the area between the hepatocytes and the endothelium of the liver sinusoids) whereas the portal fibroblasts are embedded in the portal tract connective tissue around portal structures (Crawford, 2002). These types of cells are the major cell type associated with the formation of scar tissue in response to liver damage. The scar replaces the damaged liver cells thus, preventing the liver from functioning properly and it not only reduces the blood supply, but also limiting the metabolic and detoxification processes (Antoine et al., 2007).

The fibrotic process involves various cells and different factors in bringing about an excessive fibrogenesis with disruption of intercellular contacts and interactions of extracellular matrix composition. However, Kupffer cells, together with mononuclear cells and HSCs are by far the key-players in liver fibrosis. They are triggered and

favoured by a series of chemical mediators, with a prominent role played by the TGF-β1(Poli, 2000).

In liver, the inflammation process gives rise to different pathways of lymphocyte recruitment and migration, probably directly related to type of insult. These pathways involve portal tract, sinusoid and hepatic vein. Composition and distribution of the inflammatory infiltration may include T lymphocytes (more peripheral) B lymphocytes (mainly central), plasma cells, histiocytes (granuloma), eosinophils, neutrophils, natural killer (NK) cells, and mast cells, which in turn give rise to secondary changes such as phenotypic differences among different vascular compartments (Gutiérrez-Ruíz et al., 2002).

Leukocytes that are recruited to the liver during injury act with Kupffer cells in producing substances that modulate stellate cell behavior. Monocytes and macrophages are involved in inflammatory actions by producing large amounts of nitric oxide (NO) and inflammatory cytokines such as tumour necrosis factor-α (TNF-α) which have a direct stimulatory effect on stellate cell collagen synthesis.

In recent years, a significant role of proinflammatory cytokines such as TNF-α, has been indicated to be responsible for the onset of liver disease in clinical observations and other cytokines in patients and in studies with animal models. Kupffer cells, the resident macrophages in the sinusoids of the liver, have been widely implicated in hepatic injury such as endotoxin–mediated live injury (Portmann, 2006). Kupffer cells respond to the endotoxin challenge by producing a battery of cytokines and chemokines, including TNF-α, interleukin (IL)-1β , IL-6, and prostaglandin E2 (Thurman et al., 1999). The influx of Kupffer cells coincides with the appearance of stellate cell activation markers. Kupffer cells can stimulate matrix synthesis, cell

proliferation, and release of retinoids by stellate cells through the actions of cytokines especially TGF-β1 and reactive oxygen intermediates.

In the injured liver, HSCs are regarded as the primary target cells for inflammatory and oxidative stimuli, they are transformed into myofibroblast-like cells when activated. This activation is results in a loss of cellular retinoid, but induces the synthesis of α-smooth muscle actin (α-SMA) and large quantities of the major components of the extracellular matrix (ECM), including collagen types I, III, and IV, fibronectin, and laminin (Cassiman et al., 2001). During the active hepatofibrogenesis, HSCs become the major ECM producing cell type, with a predominant production of collagen type I. Activation of HSC is regulated by several soluble factors, including cytokines TGF-β1, chemokines, growth factors, and products of oxidative stress as well as by extensive changes in the composition and organization of the extracellular matrix components.

There is evidence to show that the products of lipid peroxidation modulate collagen gene expression in HSC (Bedossa et al., 1994). Among all the cytokines and growth factors produced, TGF–β and IL- 6 are the two main fibrogenic cytokines. While HSC activation is taking place in liver and cytokines and signal transduction pathways are being stimulated, TGF–β1 plays a central role in fibrosis, contributing to influx and activation of inflammatory cells as well as activation of HSC. TGF-β is produced by Kupffer cells and HSCs, it up-regulates the transcription of collagen I genes and induces the expression of TIMP-1, a tissue inhibitor of matrix metalloproteinases, involved in collagen degradation. There are four members of the family of the TIMPs have been so far (Arthur, 1998). Interestingly, these TIMPs are able to inhibit all matrix metalloproteinases (MMPs), IL- 6 which is produced by HSC from normal or cirrhotic livers, it up-regulates the expression of TGF-β in HSC from

cirrhotic livers. Recent work indicates that reactive oxygen intermediates in general, and H_2O_2 in particular, are important mediators of TGF-β actions in HSC (Friedman, 1997). Following cell activation *in vivo*, HSCs express the genes encoding the key components required for matrix degradation such as MMP-l and -2 (Atzori et al., 2009). In a normal liver, matrix protein degradation is accomplished by a family of enzymes called MMPs. To date, four subclasses of MMPs have been defined on the basis of relative substrate specificity. Stellate and Kupffer cells are certainly recognized as the source of MMPs (Cawston, 1998). However, through the activation of tissue inhibitor of TIMP-l and -2, activated HSCs also inhibit the activity of interstitial collagenases, which degrade fibrillar collagen. Most of the hepatocellular injury inducer and subsequently hepatic inflammation, finally result in HSC activation and collagen deposition (McPhee & Hammer, 2009). Although hepatocytes are the major cells for oxygen utilization, non-parenchymal cells also found to be the sources of reactive oxygen species (ROS) and may thereby contribute to hepatocyte necrosis and/or HSC activation (Schuppan & Afdhal, 2008).

Furthermore, Kupffer cells can be activated by a variety of stimuli to produce ROS. ROS include hydrogen peroxide (H_2O_2), hydroxyl (OH), superoxide (O_2) and nitric oxide (NO) free radicals, that are highly heterogeneous in terms of reactivity against cellular targets. Inflammatory cells, such as Kupffer cells and the invading mononuclear cells, release cytokines, TGF-β l and platelet derived growth factor (PDGF) that contribute to the fibrogenic response to liver injury (Figure 2.3). Furthermore, TGF-β l is a key fibrogenic mediator that can enhance ECM deposition and inhibit MMP activity (Casini et al., 1993). It is also noteworthy that TGF- β1 is an inhibitor of the proliferation of hepatocytes, and at higher concentrations, TGF- β1 induces oxidative stress leading to hepatocyte apoptosis. Consequently, the fibrous

tissue septa separates the hepatocyte nodules, which eventually replace the entire liver architecture, leading to decreased blood flow throughout the liver.

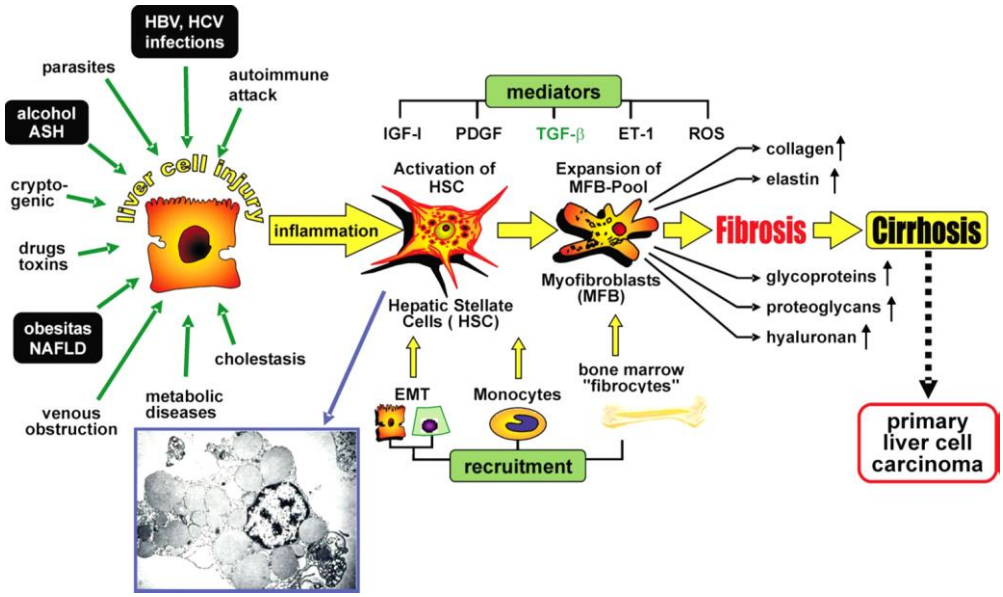

Figure 2.3: Molecular pathogenesis of Liver cirrhosis

[Adapted from (Gressner et al., 2007)]

Oxidative stress plays a role in many chronic liver diseases. The imbalance between the free radicals and antioxidants, such as vitamin E, is the cause of lipid peroxidation. Peroxidation of lipids containing poly unsaturated fatty acids, in particular, impairs the structure of biological membranes and this has a significant role in pathogenesis of many diseases (Kuzu et al., 2007). Antioxidants neutralize and pair with the free radicals, transform them from being harmful to harmless and reducing the cell damage. If the imbalance cannot be restored and the inflammation cannot be stopped, eventually, liver cirrhosis develops (Friedman, 2000). Phenolic antioxidants and their derivatives have been known for a long period of time to have widespread

applications in pharmaceutical, textiles, plastics, polymers, oil, pesticides, dye stuffs, explosives, fluorescent brightener and many other industries (Cotelle, 2001). Since our experiment is designed to induce liver cirrhosis by using hepatotoxin TAA, therefore, more elaboration on drug-induced cirrhosis will be explained here.

2.4 Drug-Induced Cirrhosis

Humans are exposed to a wide range of lipophilic chemicals, including drugs, xenobiotics, certain vitamins, carcinogens, pesticides, and other environmental pollutants. This characteristic enables them to cross the membranes of intestinal cells. Moreover, these drugs are rendered more hydrophilic by biochemical processes in the hepatocyte, yielding water-soluble products that are excreted in urine or bile (Weinshilboum, 2003). This hepatic biotransformation involves oxidative pathways, primarily by way of the cytochrome P-450 enzyme system (Guengerich, 2007).

Following the metabolic steps, which usually include conjugation to a glucuronide or a sulfate or glutathione, the hydrophilic product, is exported into the plasma or bile by transport proteins located on the hepatocyte membrane. Subsequenty, it is excreted by the kidney or the gastrointestinal tract.

Compounds that cause liver injury can be classified into those that are chemically stable (direct hepatotoxins) and those whose metabolism forms chemically-reactive species (indirect hepatotoxins). Most currently-used agents that can cause drug-induced liver injury are indirect hepatotoxins. Their hepatic metabolism gives rise to electrophilic drug metabolites and free radicals. Among the various hepatotoxins used to induce liver cirrhosis in laboratory animals are TAA, the most potent chemical because of its rapid elimination and cumulative injury when it is given intermittently. Furthermore, TAA is very effective in producing liver cirrhosis in laboratory rodents.

Besides, different methods of TAA administration have been used in experimental animals for the production of fibrosis and cirrhosis in the liver, such as via intraperitoneal or subcutaneous administration, or by mixing the chemical with the diet, or in the drinking water (Dashti et al., 1997).

2.4.1 Thioacetamide (TAA)

2.4.1.1 Properties of TAA

TAA is an organic compound with a formula CH_3CSNH_2, Figure 2.4 which appears as a white crystal under standard conditions. It has a few synonyms such as acetothioamide, ethanethioamide, thiacetamide and thioacetamidic acid. It is soluble in water and ethanol, with a melting point between 110-115 °C. TAA is stable at room temperature (Cinghită et al., 2008).

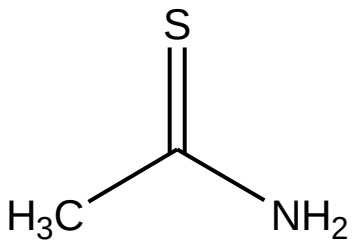

Figure 2.4: Structure of TAA

[Adapted from (Hanaa, 2007)]

2.4.1.2 Uses of TAA

In laboratories, TAA can serve as a source of sulphur in the synthesis of organic compounds such as rubber chemicals, curing agents, cross linking agents, metallurgy, pesticides, and pharmaceuticals. Besides, it is used as a stabilizer of motor fuels and in

purification of hydrochloric and sulphuric acids. It is also used in leather processing (Hanaa, 2007). TAA is a hepatotoxic and hepatocarcinogenic agent that is still widely used in qualitative inorganic analysis as a substitute for hydrogen sulphide gas. Besides, TAA was first used to control the decay of oranges and then as a fungicide (Spira & Raw, 2000).

Shortly, after administration it converts to TAA–S oxide (TASO) by the mixed function oxidase system and TASO is transformed into TAA S, S–dioxide as shown in Scheme 2.1 which is with or without further oxidized species exerts the toxic effect which is then distributed among several organs including plasma, liver, kidney, bone marrow, adrenals and other tissues. Then, TAA undergoes an extensive metabolism to acetate and finally excreted through the urine within 24 hrs (Spira & Raw, 2000). TAA is known to induce centrilobular hepatic necrosis, liver cirrhosis, hepatocellularcarcinoma and bile duct proliferation (Schuppan & Afdhal, 2008). TAA-induced liver fibrosis is caused by free radical-mediated lipid peroxidation (Spira & Raw, 2000). In chronic TAA intoxication, substantial liver fibrosis and prominent regenerative nodules development are associated with portal hypertension and the hyperdynamic circulation characteristic of liver cirrhosis (Heidelbaugh & Bruderly, 2006).

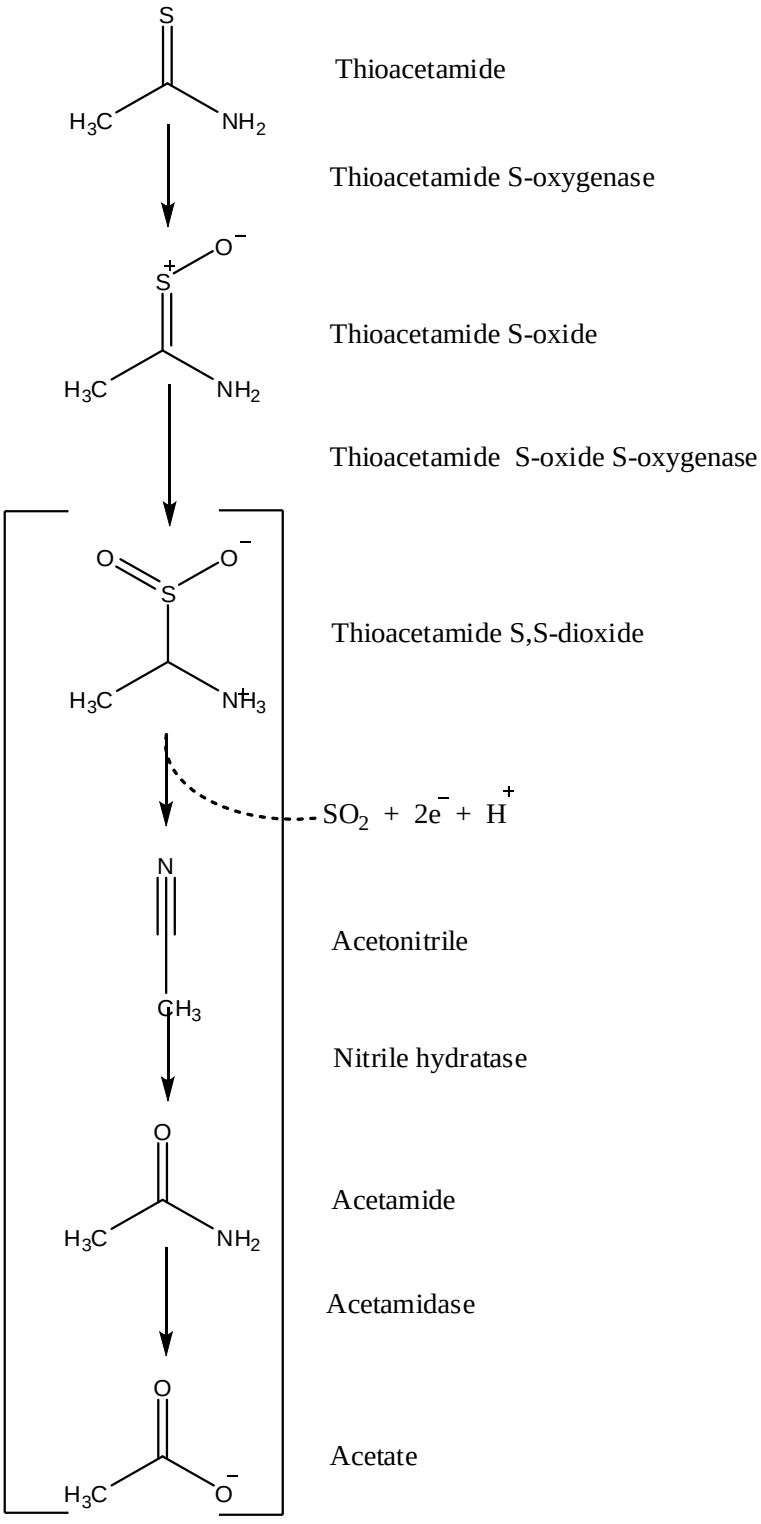

Scheme 2.1: Metabolism of thioacetamide

[Adapted from (Spira & Raw, 2000)]

2.5 Symptoms, Signs and Complications of Liver Cirrhosis

Cirrhosis is often indolent, silent, asymptomatic, and unsuspected until complications of liver disease are present. Approximately, 80 to 90 % of liver parenchyma must be destroyed before liver failure is manifested clinically (Heidelbaugh & Bruderly, 2006). Many people with liver cirrhosis are asymptomatic in the early stages. However, when the liver is distorted and loses its functions, symptoms become apparent. The symptoms are anorexia, weight loss, weakness, fatigue and osteoporosis due to vitamin D malabsorption and subsequent calcium deficiency (Heidelbaugh & Bruderly, 2006).

In later stage, jaundice may occur as the bile pigment that is secreted by the liver is retained due to biliary obstruction. Moreover, the blocked bile ducts will worsen with retention of bile in the liver, causing less amount of bile reaching the gallbladder (Derek, 1994). The other complications of liver cirrhosis include nail changes (Muehrche's line and Terry's nails when the proximal two-thirds of the nail plate appears white with distal one-third red) associated with edema and ascites due to reduction in albumin synthesis; bruising and bleeding as a result of reduction of clotting factor synthesis; itching, accumulation of toxins (urea) in the blood or brain, sensitivity to medication, portal hypertension, varices, insulin resistance and type 2 diabetes, liver cancer and problems in other organs like the gonads (Sheldon, 1994).

The fate of most patients with liver cirrhosis is the death secondary to infection. Common complications include pneumonia, gastrointestinal haemorrhage and hepatic coma (Sheldon, 1994). Today, hepatic coma is the most frequent and most common cause of death, as infection and haemorrhages are overcome more successfully by modern management methods (Sheldon, 1994).

Liver cirrhosis is usually associated with infertility, so much so that pregnancy is rarely considered in liver cirrhosis. However, if portal hypertension do exists secondary to cirrhosis in a pregnant patient hemorrhage from the oesophageal varices is a major risk. Haematemesis is most likely to occur during the second stage of labour, secondary to a combination of the increased plasma volume, raised intra- abdominal pressure from the pregnant uterus causing increase in systemic venous pressure which is transmitted directly to the varices. Defect in coagulation may also increase the risk of a post-partum haemorrhage (Derek, 1994). In male patients, gynecomastia, loss of male hair pattern due to conversion of androstenedione to oestrone and oestradiol and reduced oestradiol degradation in the liver (Schuppan & Afdhal, 2008). The term "cirrhosis" was first introduced in 1826 by Laennec. It refers to the orange or tawny surface of the liver as seen at autopsy. Macroscopically, the liver enlarges with irregular external surface and has nodular appearance. It usually became shrunken and yellowish but in some cases became enlarged and yellow such as in alcoholic fatty cirrhosis, or large and green in biliary obstruction and rusty in hemochromatosis. A variation in colors, sizes, shapes and consistency of the nodules helps in the identification of the etiology. Based on the size of the nodules, cirrhosis was classified to micro nodular (nodules $\leq$ 3 mm), macro nodular (nodules >3 mm) and the mixed cirrhosis which consists of a variety of nodules with different sizes (Wanless, 2004). Histological criteria for cirrhosis (Figure 2.5) is characterised by vascularized fibrotic bands, which link the portal tracts with each other and with the central veins. The microscopic feature includes regeneration of hepatic nodules, deposition of connective tissue between these nodules and destruction of other normal tissues of the liver: including the sinusoids, the space of Disse, and other vascular structures (Schuppan & Afdhal, 2008).

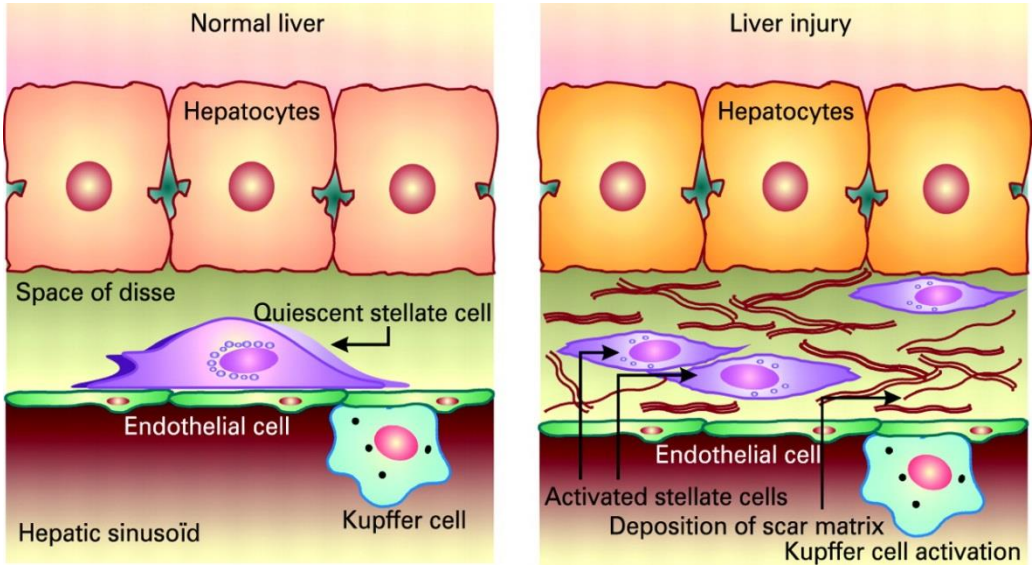

Figure 2.5: Histological criteria of chronic hepatic injury

[Adapted from (Asselah et al., 2009)]

2.6 Diagnosis of Liver Cirrhosis

Currently, there is no serologic test to diagnose cirrhosis accurately (Friedman & Schiano, 2004). To date, diagnosis of liver cirrhosis can be done by analyzing blood samples, performing ultrasound examination, computerized axial tomography (CT) scan, magnetic resonance imaging (MRI), radioisotope or laparoscope imaging. Most clinical tests of liver function can be detected from the biochemical functions of the liver such as the enzymes released when there is plasma membrane damaged of the hepatocytes (Kaplowitz & DeLeve, 2007). A liver biopsy is necessary to confirm the diagnosis with the sample of liver tissue examined under the microscope (Friedman & Schiano, 2004). A physical examination may reveal an enlarged liver or spleen, distended abdomen, yellow eyes or skin (jaundice), red spider- like blood vessels on the

skin (spider nevi), excess breast tissue, small testicles in men, contracted fingers, or dilated veins in the abdominal wall (Sheldon, 1994).

2.6.1 Liver function test

Liver function test is a common blood test. It stands for a wide range of normal functions performed by the liver. The term liver function test is a misnomer because the assay in most standard liver panels does not reflect the function of the liver correctly (Heidelbaugh & Bruderly, 2006). Common tests that are used to evaluate liver function include: albumin, alkaline phosphatase (AP), alanine aminotransferase (ALT), aspartate aminotransferase (AST), gamma glutamyl transpeptidase (GGT), prothrombin time (PT), serum bilirubin, and urine bilirubin (Levison & Reid, 2008).

2.6.1.1 Serum liver enzymes

Inflammation of the hepatocytes results in elevation of the ALT and AST. ALT, also called serum glutamic pyruvate transaminase (SGPT) is an enzyme present in the hepatocytes. ALT is the most sensitive marker for liver cell damage. When a liver cell is damaged, ALT leaks into the bloodstream and causes its level in the blood to increase. However, the ALT level may or may not correlate with the degree of cell death or inflammation. On the other hand, AST is another enzyme that reflects hepatocytes injury. It is also called serum glutamic oxaloacetic transaminase (SGOT). It is less specific for liver disease because it is also present in red blood cells, kidney, cardiac and skeletal muscle cells. Therefore, AST has been used as a cardiac marker (Levison & Reid, 2008). However, the ratios between ALT and AST are useful in assessing the etiology of liver enzyme abnormalities in the patients (Šídlová et al., 2002). Alkaline phosphatase (AP) is another enzyme found in the cells lining the biliary ducts of the

liver. Inflammation of the biliary tract cells will mostly cause the increase in the level of AP. It is synthesised mostly in the liver and bone, sometimes in the intestines and kidneys. High levels of AP may indicate bone or liver damage (Derek, 1994).

2.6.1.2 Serum bilirubin

Bilirubin is derived mainly from haem, when erythrocytes get old or damaged. This releases hemoglobin, which is broken down to heme as the globin parts are turned into amino acids. The heme is then turned into unconjugated bilirubin in the reticuloendothelial cells of the spleen. This unconjugated bilirubin is not soluble in water. It is then bound to albumin and transported to the liver (Friedman & Keeffe, 2011). Bilirubin metabolism occurs primarily in the liver. It is taken up by the liver paranchymal cells, conjugated in the smooth endoplasmic reticulum, and secreted into the bile. A low level of bilirubin (about 1 mg/dL) normally circulates throughout our body, but it is too faint to be visible (Sheldon, 1994). Conjugation is the process by which bilirubin is readily excreted in the bile and in order to be conjugated, bilirubin must have been acted on by hepatocytes. Basically, bilirubin in the liver is conjugated with glucuronic acid by the enzyme glucuronyl transferase, making it soluble in water. Much of it goes into the bile and thus out into the small intestine. However, 95% of the secreted bile is reabsorbed by the intestines and reach the liver by portal circulation and then resecreted by the liver into the small intestine. This process is known as enterohepatic circulation (Lascelles & Donaldson, 1990). In any hepatic injury, the liver does not process enough conjugated bilirubin (water soluble-direct) which is called total bilirubin (MacSween, 1994). On the other hand, unconjugated (indirect) bilirubin, when it is elevated, the cause is usually outside the liver, typically gallstones. Total

bilirubin testing measures the amount of bilirubin in the bloodstream (Lascelles & Donaldson, 1990).

2.6.1.3 Gamma glutamyl transpeptidase (GGT)

Specific to the liver and a more sensitive marker for cholestatic damage than AP, Gamma glutamyl transpeptidase (GGT) may be elevated even in minor, sub-clinical levels of liver dysfunction and act as surrogate marker of alcohol abuse (Levison & Reid, 2008).

2.6.2 Full blood count

Occult bleeding may cause anemia (macrocytic, normocytic or microcytic), complete blood count with platelets should be performed if liver abnormality is suspected (Heidelbaugh & Bruderly, 2006). Thrombocytopenia plays an important role in intensification of damage and fibrosis of liver tissues. The level of platelets damage depends on severity of the course of liver disease (Panasiuk et al., 2005).

2.6.3 Coagulation screen

Abnormalities of coagulation are sensitive tests of liver function. A prolonged prothrombin time indicates a deficiency in any of the factors VII, X, V, prothrombin, or fibrinogen, which is usually observed in cases of vitamin K deficiency, a liver disease or disseminated intravascular coagulation (Friedman & Schiano, 2004). The prothrombin time and its derived measure of international normalized ratio (INR) is the measurement of the extrinsic pathway of coagulation. The normal prothrombin time is around 12 - 15 seconds, the normal range for the INR is 0.8 - 1.2 (Friedman & Schiano, 2004).

2.6.4 Total serum protein

A total serum protein test measures the total amount of protein in the blood. It also measures the amount of two major groups of proteins in the blood; albumin and globulin (Fan & Steer, 2006). Albumin is synthesised mainly in the liver. It maintains blood from leaking out of the blood vessels. Albumin also helps to carry some drugs and other substances through the blood and is important for tissue growth and healing (Fan & Steer, 2006). A low serum albumin indicates poor liver function which is usually characterised by the presence of ascites. This is more marked in chronic liver failure caused by cirrhosis (Friedman & Schiano, 2004). As for globulin, it is made up of different proteins called alpha, beta, and gamma types. Some globulins are synthesised by the liver, while others are made by the immune system. Serum globulin can be separated into several subgroups by serum protein electrophoresis (Fan & Steer, 2006).

A test for total serum protein reports separate values for total serum protein, albumin and globulin. The amounts of albumin and globulin also are compared (albumin/globulin ratio). Normally, there is a little more albumin than globulin and the ratio is greater than 1. A ratio less than 1 or much greater than 1 gives clues about problems in the body (Fan & Steer, 2006).

2.6.5 Lactate dehydrogenase enzyme (LDH)

The LDH represents a group of enzymes that are involved in carbohydrate metabolism, catalyses the conversion of lactate to pyruvate, which is an important step in energy production in cells (Lascelles & Donaldson, 1990). LDH is found in many tissues such as the heart, liver, kidney, skeletal muscle, brain, red blood cells and lung.

As the cells die, LDH is released and finds its way into the blood. Low LDH occurs in hypoglycemia, while elevated LDH indicates the presence of damage to cell causing a rupture in the cellular cytoplasm (Lascelles & Donaldson, 1990).

2.6.6 Lipid profile

Liver plays an essential role in lipid metabolism, therefore, it is reasonable to expect an abnormal lipid profile in cases of liver dysfunction (Ghadir et al., 2010). There is prominent decline in plasma cholesterol and triglyceride (TG) levels in patients with severe hepatitis and hepatic failure because of reduction of lipoprotein biosynthesis. The normal total serum cholesterol depends upon normal hepatocellular enzymatic activities. In extra-hepatic biliary obstruction, there is a significant rise in the total serum cholesterol, while in hepatocellular diseases the total cholesterol concentration of the serum may be normal or slightly reduced, and a marked drop indicates poor prognosis in liver cirrhosis(Lascelles & Donaldson, 1990).

2.6.7 Liver biopsy

Liver biopsy is a procedure whereby tiny pieces of liver tissue are removed and sent to a laboratory for examination. Liver biopsy may be performed via percutaneous, trans-jugular, laparoscopic, open operative or ultrasonography or CT-guided fine-needle approaches. The tissue is then prepared and stained and viewed under the microscope for signs of damage or disease. The histology of the tissue helps the physician to make a specific diagnosis and determine the extent and severity of the condition and therefore provides vital information for determining treatment (Crawford, 2002).

2.7 Prevention

There are several ways to reduce the risk of developing liver cirrhosis:

i. Stop abusing alcohol or limiting the amount and frequency of intake for those who drink alcohol.

ii. Avoiding high-risk sexual behaviour such as unprotected sexual contact with multiple partners.

iii. Wearing protective clothing and a facemask for people who are in contact with synthetic chemicals, such as cleaning products and pesticides.

iv. Vaccination of susceptible patients against hepatitis B.

v. Eating a well-balanced, low-fat diet and taking vitamins.

2.8 Current Therapeutic Approaches for Liver Cirrhosis

2.8.1 Early stage

Treatment options for common liver diseases such as cirrhosis, fatty liver, and chronic hepatitis are problematic. The best way to prevent further progression in liver cirrhosis at early stages is to remove the causative agent (Friedman & Schiano, 2004). For instance, cirrhosis caused by alcohol abuse is treated by refraining from alcohol. Meanwhile, the treatment involves medications for hepatitis-related cirrhosis. This approach is effective in inhibiting the progression of liver fibrosis in most cases. The other approaches used for liver cirrhosis include suppressing hepatic inflammation, inhibition of activation and proliferation of HSC_S, modulation of collagen synthesis and degradation, and hepatic stellate cell-specific targeting of antifibrotic therapy (Ramón & David, 2001).

In diseases where oxidative stress plays an important role clinically, antioxidant therapy is given, for example vitamin E, flavonoids, silymarin, ursodeoxycholic acids, N- acetyl cysteine, betaine and selenium (Rice-Evans, 2001). Mostly, the treatment aims at the following:

i. Preventing further damage to the liver
ii. Treating the complications of cirrhosis.
iii. Preventing the development of liver cancer or detecting it early.

2.8.2 Treatment for complications

Treatment will also include remedies for complications. These approaches are: (i) diuretics for the treatment of oedema in the legs or abdomen, (ii) vitamins and mineral supplements, (iii) calorie supplements to maintain nutrition, (iv) laxatives to prevent constipation and to reduce the chances of the toxic substances from the bowel bypassing the liver and reaching the brain, causing drowsiness, confusion and coma (Sheldon, 1994), (v) a liver transplant is necessary when complications cannot be controlled or when the liver becomes so damaged from scarring and completely stops functioning. Physicians and patients are in need of effective therapeutic agents with a low incidence of side-effects, the plants products potentially constitute such a group (Newman et al., 2003).

2.8.3 End stage

Persistent liver cell damage will result in the progression of the liver fibrosis to end-stage liver cirrhosis, characterised by a septal and perisinusoidal fibrosis (Schuppan

& Afdhal, 2008). Finally, liver transplantation may be considered in patients with end-stage cirrhosis when the liver damage is extensive (Bayless & Diehl, 2005).

2.9 Experimental Models for Fibrosis

2.9.1 *In vivo* animal models

Several *in vivo* animal models have been designed to mimic different causes of the development of liver fibrosis in humans as close as possible. The four most commonly used are discussed here briefly. Firstly, as a model for toxicity-induced chronic liver damage progressing to fibrosis and cirrhosis is by administration of several toxic compounds, including CCl_4 (Nussler et al., 2014), galactosamine (Vasanth Raj et al., 2010) and TAA (Shirin et al., 2013). Furthermore, liver damage can be caused by administration of cupric (Toyokuni et al., 1989). Secondly, cholestasis induced-liver fibrosis by occlusion of the bile duct is often used in experimental animals (Muriel et al., 1994) and it is characterised by increased proliferation of bile-duct epithelial cells (Schuppan & Afdhal, 2008). Thirdly, infection with Schistosoma can be used to induce liver fibrosis (Wu et al., 1982). Finally, a methionine can be administered to experimental animals to induce fibrosis, inflammation, and increased lipid content of the liver (George et al., 2003).

In vivo models for studying liver fibrosis got many advantages over *in vitro* models and this is because this model allows for the inclusion of various effects on organs and systems in the development of liver fibrosis. In addition to that, different types of fibrosis with different underlying causes and antifibrotic drugs can be clearly studied which closely similar to development of fibrosis in humans. However, still there is a disadvantage of experimental animals models like largely restricted to rodent

and may be of limited predictive value for human disease, in addition to high discomfort for the experimental animals.

2.9.2 *In vitro* cell lines models

In vitro culture models have the advantage of relatively well-controlled variables and are generally accepted as a very effective method for safety testing. Hence, *in vitro* culture models that employ human liver cells or (WRL 68) cells could be a reliable method for predictive studies on drug toxicity and metabolism in the pharmaceutical industry by expressing hepatocyte specific function, such as Cytochrome P450 and albumin production, which can provide an adequate in vitro liver model for many mechanistic studies of signal transduction, gene expression, metabolism and toxicology (Saad et al., 2006).

Thus, WRL 68 cells were used in this study. The usage of these cells as an *in vitro* hepatic model has been validated in some studies, and the morphologic as well as the functional characteristics of the cell lines have been determined. (Bucio et al., 1995) suggested that WRL 68 cells secrete alpha-feto protein and albumin and they exhibit a cytokeratin pattern similar to other hepatic cultures. In another study, they found that human liver cells are the most suitable *in vitro* model for biotransformation in human liver and are of great importance for toxicological and pharmaceutical studies (Wilkening et al., 2003).

Another type of cell which is used in this study is the hepatocarcinoma cell lines (HepG2) cell lines, which are the liver cancer cells. In human biotransformation studies, cultures of primary normal liver cells and HepG2 cell line are frequently used in *vitro* models (Brandon et al., 2003). Based on the results of their study, they concluded that

normal human liver cells are a valuable *in vitro* model to identify compounds that are potentially toxic to humans, as compared to the liver cancer cells.

2.10 Antioxidant and Liver Cirrhosis

Antioxidants are compounds that dispose, scavenge and suppress the formation of free radicals, or oppose their actions. Generally, antioxidants scavenge free radicals through four mechanisms. The first mechanism involves termination of free radicals production by electron donation. In the second mechanism, ROS initiator is removed by antioxidant. The third mechanism is by reducing the potency of ROS. Antioxidant serves as transition metal catalysts chelating agent in the fourth mechanism. It protects the human body against free radical attacks that may cause pathological conditions such as liver cirrhosis (Hasani-Ranjbar et al., 2009). Moreover, lipid peroxidation was significantly increased along with significant decreased in antioxidant levels in patients with alcoholic liver disease (Shinde & Ganu, 2009). In recent years there has been increasing interest in the presence and availability of compounds in plant materials that may possess bioactive properties, in particular, antioxidant activity. Plant antioxidants are composed of a broad variety of different substances like polyphenolic compounds, tocopherols or terpenoids. Most antioxidants isolated from higher plants are phenolic compounds (e.g. phenolic acids, tannins, coumarins, anthraquinones, flavonoids) (Rice-Evans, 2004). Basically, the antioxidant activity of phenolic compounds was found to be due to their scavenging and redox properties, through neutralizing and quenching free radicals (Galato et al., 2001). Several anti-inflammatory, anti-necrotic, potent antifibrotic and hepatoprotective agents have recently been shown to have an antioxidant and/or anti-radical scavenging mechanism as part of their activity. Cells are equipped with different kinds of cellular enzymes and compounds that may fight against

ROS and to maintain the redox homeostasis of cell. For example, antioxidant enzymes such as superoxide dismutase (SOD), catalase (CAT) and glutathione peroxidase (GPx) play important roles in scavenging the free radicals and preventing cell injury. Molecules such as vitamin C and E inhibit lipid peroxidation in cell. When the mechanism of antioxidant protection becomes unbalanced in human body, antioxidant supplement may be used to help reduce oxidative damage (Bergendi et al., 1999).

2.11 Liver Cirrhosis and Medicinal Plants

For thousands of years, the medicinal plants have formed the basis for treatment of diseases in traditional medicine and continue to play a major role in the primary health. Herbal extracts have been used in the treatment of liver injuries for over 2,000 years. Up to now, more than 160 plant-derived substances from 101 plant families have been recognized regarding their hepatoprotective activity (Negi et al., 2008). World Health Organization (WHO) reported that 80% of the world population rely on the use of traditional medicine which is predominantly based on plant materials (Bauer, 1998). Moreover, all drugs approved by the US Food and Drug Administration (FDA), finding that 42% of the 1031 drugs approved between 1981 and 2002 are associated with natural products (Jones et al., 2006). The available synthetic drugs to treat liver disorders in this condition also cause further damage to the liver. Hence, herbal drugs have become increasingly popular and their use is wide-spread. The use of natural remedies for the treatment of liver diseases has a long history, starting with the Ayurvedic treatment, and extending to the Chinese, European and other systems of traditional medicines. The 21st century has seen a paradigm shift towards therapeutic evaluation of herbal products in liver disease models by carefully synergizing the strengths of the traditional systems of medicine with that of the modern concept of

evidence-based medicinal evaluation, standardization and randomized placebo controlled clinical trials to support clinical efficacy (Thyagarajan et al., 2002). Different herbal plants as natural sources have been evaluated for the treatment of hepatocellular damage in experimental animal models (Luper, 1998).

In recent years many researchers have examined the effects of plants used traditionally by indigenous healers and herbalists to support liver function and treat diseases of the liver. In most cases, research has confirmed traditional experience and wisdom by discovering the mechanisms and modes of action of these plants as well as reaffirming the therapeutic effectiveness of certain plants or plant extracts in clinical studies. Several hundred plants have been examined for use in a wide variety of liver disorders. Just a handful has been fairly well researched. The latter category of plants include: Silybum marianum (milk thistle), Picrorhiza kurroa (kutkin), Curcuma longa (turmeric), Camellia sinensis (green tea), Chelidonium majus (greater celandine), Glycyrrhiza glabra (licorice), and Allium sativa (garlic) (Luper, 1998). The constituents of plant extracts have immune stimulating, liver protective and anti-inflammatory actions.

The herbs stimulate hepatocytes production and for repairing and regeneration of hepatocytes. Accumulative evidence for the effectiveness against fibrosis is now available for several plant-derived antioxidants. The most successful liver protective natural product is silymarin, a flavonolignan from the seeds of milk thistle *Silibum marianum L*. This extract is used exclusively for liver protection. Silymarin proved to be antifibrogenic in a rat fibrosis model (Jia et al., 2001), where it led to a reduction of hepatic collagen accumulation by more than 35 %. It is well known that silymarin and its component silibinin have potent antioxidant activity (Shaker et al., 2010). Medicinal plants are an important source of antioxidants (Rice-Evans, 2004). The secondary

metabolites such as phenolics and flavonoids from plants have been reported to be potent free radical scavengers. They are found in all parts of plants such as leaves, fruits, seeds, roots and bark (Mathew & Abraham, 2006).

2.11.1 Silymarin (SY)

SY (Figure 2.6) is the flavono lignan extracted from the dried seeds of milk thistle *Silybum marianum*. It is a combined mixture of four flavono lignan isomers, namely isosilybin, silybin, silychristin and silydianin and with a molecular formula $C_{25}H_{22}O_{10}$ (Pradhan & Girish, 2013).

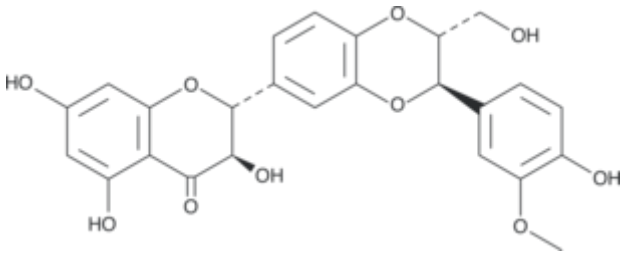

Figure 2.6 **:** Chemical structure of silymarin

[Adapted from (Katiyar et al., 1997)]

The pharmacological properties of SY have been well defined and the hepatoprotective profile was reported both *in vitro* and *in vivo*. It has been documented to prevent the liver from injuries induced by various toxins or chemicals by performing anti-lipid peroxidative, antioxidative, antifibrotic, membrane stabilizing, anti-inflammatory, liver regenerating and immunomodulatory activities. Its main action have been investigated to be through promoting protein synthesis, controlling inflammation, regenerating liver tissue, protecting against glutathione depletion and enhancing glucuronidation (Cragg & Newman, 2005). SY is also reported to enhance the activity of RNA-polymerase I, combined to toxic-free iron and blocks the uptake of toxins such

as Amanitaphalloides toxin (Yadav et al., 2008). Furthermore, other promising activities of SY has been reported to include anticancer activity, regulation of apoptosis and inflammation process, as neuroprotective agent with its neurotropic activities, to prevent and treat cardio-pulmonary problems, to treat skin problems and acts as steroid hormones receptors (Křen & Walterova, 2009).

Studies demonstrated that SY protects liver tissue from a wide variety of toxins such as acetaminophen (Muriel et al., 1992), TAA (Wong et al., 2012), CCl_4 and D-galactosamine (Chrungoo et al., 1997). SY has also been found to protect liver cells from ischemic injury and stimulate liver regeneration, (Wu et al., 1993), radiation (Kropacova et al., 1998), iron toxicity and viral hepatitis (Rashed, 2011). Both in vivo and in vitro studies showed significant increase in the formation of ribosomes and DNA synthesis as well as increased in protein synthesis which interestingly was only measured in the damaged livers. This due to the ability of SY to imitate a physiologic regulator, so the silybin fits into a specific binding site on the polymerase, thus stimulating ribosome formation (Ewelina et al., 2013).

Besides, SY could reduce or reverse liver fibrosis in animals by 30-35% in comparison with controls (50 mg/kg/day, human dose = 3500 mg/day) for six weeks by (Boigk et al., 1997) reducing the conversion of HSCs into myofibroblasts and down-regulation of the gene expression for extracellular matrix components (Fuchs et al., 1997). In addition, SY has been shown to have significant renal protectant (Wenzel et al., 1996), antiarthretic activity and anti-inflammatory effects, including mast cell stabilization (Fantozzi et al., 1986) inhibitions of neutrophil migration (Puerta et al., 1996), Kupffer cell inhibition, leukotriene synthesis inhibition and prostaglandin formation (Dehmlow et al., 1996).

Overall, the mechanism of hepatoprotective action of SY have been investigated to be through four actions (Pradhan & Girish, 2006): (i) Free radical scavenging activity, increasing of glutathione cellular content and lipid peroxidation lowering property, (ii) membrane permeability regulation and increasing the membrane stability against damages caused by xenobiotic, (iii) regulation of nuclear expression through steroid like effects, and (iv) inhibit the formation of myofibroblasts from HSCs which release collagen and subsequently causes hepatic cirrhosis.

2.12 Medicinal Plants Investigated in the Current Experiment

2.12.1 *Vitex negundo* (VN)

2.12.1.1 Morphology and distribution

VN plant is credited with innumeral medicinal qualities validated by modern science and used since ancient times. It belongs to family of Verbenceae (Table 2.1) and the genus consists of 250 species and most of them have commercial and medicinal importance (Tandon, 2005). VN is commonly called five- leaved chaste tree or Monk's Pepper; it is a large aromatic shrub or sometimes a small slender with quadrangular branchlets, about 2-5 m in height and mainly distributed in tropical to temperate regions, especially in Malaysia, India at the warmest zones and Western Himalayas (Tandon, 2005).

Table 2.1: Botanical Classification of *Vitex negundo*

Kingdom	**Plantae**
Subkingdom	Tracheobionta
Super Division	Spermatophyta
Division	Magnoliophyta
Class	Magnoliopsida
Sub Class	Asteridae
Order	Lamiales
Family	Verbenaceae
Genus	*Vitex*
Species	*negundo*

[Adapted from(Singh, P. et al., 2011)]

The leaves have a typical five foliolate pattern in palmate arrangement with 4-10 cm long (Singh, P. et al., 2011), hairy beneath and pointed at both ends while the flowers are numerous, bluish purple and become dark when ripened. The fruit is succulent, black and rounded when matured, whereas roots cylindrical, long woody, tortuous with gray brown colour (Tandon, 2005).

Figure 2.7: *Vitex negundo*

[Adapted from (Tandon, 2005)]

2.12.1.2 Chemical constituents of VN

Phytochemical studies on VN have been applied and afforded several types of compounds such as volatile oils, liganans, flavonoids, iridoids, terpenes (triterpenes, diterpenes, sesquiterpenes) and steroids. At the same time, eight compounds from VN crud extract were isolated by activity guided fractionation methods (Gautam et al., 2010). These compounds are illustrated in Table 2.2.

The leaves contain an alkaloid, flavonoids like flavones, luteolin-7-glucoside, casticin, iridoid, glycosides, an essential oil and other constituents like vitamin C, carotene, glucononital, benzoic acid, β-sitosterol and glycoside (Tandon, 2005).

Table 2.2: Active components identified in VN extract (GC MS study)

No.	Name of the compound	Molecular Formula
1	5-hydroxy-7, 4'-dimethoxy flavone	$C_{17}H_{14}O_5$
2	5-hydroxy-3,6,7,3',4'-pentamethoxy flavone	$C_{20}H_{20}O_8$
3	5,7-dihydroxy- 6,4'-dimethoxy flavanone	$C_{17}H_{16}O_6$
4	5,3'-dihydroxy-7,8,4'-trimethoxy flavanone	$C_{18}H_{18}O_7$
5	7,8-dimethyl herbacetin-3-rhamnoside	$C_{23}H_{24}O_{11}$
6	agnuside	$C_{22}H_{26}O_{11}$
7	negundoside	$C_{23}H_{28}O_{12}$
8	vitegnoside	$C_{22}H_{20}O_{12}$

[Adopted from (Gautam et al., 2010)]

2.12.1.3 Traditional, medicinal uses and biological activities

The plant has a pungent, bitter, acrid taste so used in various traditional remedies in the treatment of stomach-ache, antihelmintic, promotes the growth of hair, useful in disease of the eye, inflammation, enlargement of spleen, bronchitis, asthma and painful teething in children (Singh, et al., 2011). The root is used as an antidote to snake venom, tonic, expectorant, antipyretic, diuretic and it was used in the treatment of otalgia, arthritis, dyspepsia, rheumatism, leprosy, wounds, ulcers, malarial fever, urinary tract infection (Sharma et al., 2005) . The leaves are aromatic, tonic and vermifuge, the juice of the leaves was used in the treatment of ulcers and swelling of joints (Kirtikar & Basu, 2008).

A preliminary acute toxicity study of ethanolic leaf extract in albino rats by oral rout found it to be practically nontoxic, as its LD50 dose was recorded as 7.58 g/Kg body weight with no histomorphological changes in liver, stomach, heart and lung at any dose of the extract studied (Tandon, 2005).

The whole parts of the plant showed a potent source of natural antioxidants (Sharma et al., 2010). 1, 2 di-substituted idopyranose, the isolated compound from VN

extract showed protection of hepatocytes, nephrocytes and pancreatic β-cells probably by its action against NF-kB and induced-nitric oxide synthase iNOS mediated inflammation in streptozotocin-induced diabetes (Manikandan et al., 2011).

Besides, petroleum ether fraction from the ethanol extract of VN seeds showed analgesic and antinociceptive activity (Zheng et al., 2010), stimulates hair root and promotes blood circulation and hair growth (Matsumoto et al., 1993). The hepatoprotective activity of VN leaf ethanolic extract at doses of 100, 250 and 500 mg/kg body weight in rats was investigated against hepatotoxicity produced by administering a combination of three anti-tubercular drugs isoniazid 7.5 mg/kg, rifampicin 10 mg/kg and pyrazinamide 35 mg/kg 45 min prior to anti-tubercular challenge for 35 days duration (Tandon et al., 2008).

Furthermore, oral administration of 250 mg/kg body weight of alcoholic extract of VN in rats was found to be effective in preventing liver damage obtained by CCl_4 (Avadhoot & Rana, 1991) and ibuprofen (Mahalakshmi et al., 2010) and d-galactosamine (Yang et al., 1987), was evident by morphological, biochemical and functional parameters.

In addition, negundoside revealed hepatoprotective effect against CCl_4 induced toxicity in HuH-7 cells via inhibition of lipid peroxidation, followed by an improved intracellular calcium homeostasis and inhibition of Ca^{+2} dependent proteases (Tasduq et al., 2008).

2.12.2 *Caesalpinia sappan* (CS)

2.12.2.1 Morphology and distribution

CS is commonly named as Brazil or Sappan, it belongs to family of Caesalpiniaceae (Table 2.3). The species are being used traditionally and have a variety of medicinal properties (Badami et al., 2004). CS tree or shrub is mostly cultivated in gardens because of large and ornamental yellow flowers; it is propagated from seed and is quickly growing. The height of this shrub is about 10 m and widely distributed in South India, West Bengal, Malaysia and Sri Lanka and throughout the Asian tropics (Badami et al., 2004). The wood is orange red, hard and very heavy; the leaves are large and bearing small prickles at the base; and the seeds are ellipsoid and black (Badami et al., 2004) (Figure 2.8).

Table 2.3: Botanical classification of *Caesalpinia sappan*

Kingdom	**Plantae**
(unranked)	Angiosperms
(unranked)	Eudicots
(unranked)	Rosids
Order	Fabales
Family	*Caesalpiniaceae*
Genus	*Caesalpinia*
Species	*sappan*

[Adapted from (Badami et al., 2004)]

Figure 2.8: *Caesalpinia sappan*

[Adapted from (Badami et al., 2004)]

2.12.2.2 Chemical constituents of CS

A great deal of chemical investigations have been carried out on heartwood and other part of the CS plant in the presence of active constituents such as triterpenoids, flavonoids, oxygen heterocycles, lipids, steroids and amino acids in the heartwood and seeds have been reported, and the main phenolic compound in sappan extract was divided into 4 structural sub-types: brazilin, chalcone, protosappanin and homisoflavonoid (Fu et al., 2008). The ethanol extract of CS is a complex mixture of many constituents and 12 compounds were isolated from 70% ethanol extraction of CS (Sarumathya et al., 2011). Their structures were elucidated based on GC-MS data (Table 2.4).

Table 2.4: Active Components identified in CS extract (GC MS study)

No.	Name of the compound	Molecular Formula
1	Propane, 1,1,3-triethoxy	$C_9H_{20}O_3$
2	2-Furancarboxaldehyde, 5-(hydroxymethyl)-	$C_6H_6O_3$
3	Bicyclo[7.2.0]undec-4-ene,4,11,11-trimethyl-8-methylene-,[1R-(1R*,4Z,9S*)]-	$C_{15}H_{24}$
4	Naphthalene, 1,2,3,5,6,8a-hexahydro-4,7-dimethyl-1-(1-methylethyl)-, (1S-cis)- [Synonyms: Cadina-1(10),4-diene]	$C_{15}H_{24}$
5	Caryophyllene oxide	$C_{15}H_{24}O$
6	1,2,3,5-Cyclohexanetetrol, (1à,2á,3à,5á)-	$C_6H_{12}O_4$
7	3-O-Methyl-d-glucose	$C_7H_{14}O_6$
8	n-Hexadecanoic acid	$C_{16}H_{32}O_2$
9	1,2-Benzenedicarboxylic acid, diisooctyl ester	$C_{24}H_{38}O_4$
10	4,7,10,13,16,19-Docosahexaenoic acid, methyl ester, (all-Z)	$C_{23}H_{34}O_2$
11	Cyclodecacyclotetradecene,14,15-didehydro-1,4,5,8,9,10,11,12,13,16,17,18,19,20-tetradecahydro-	$C_{22}H_{32}$
12	9,12,15-Octadecatrienoic acid, 2-[(trimethylsilyl)oxy]-1-[[(trimethylsilyl)oxy]methyl]ethyl ester, (Z,Z,Z)	$C_{27}H_{52}O_4Si_2$

[Adopted from (Sarumathya et al., 2011)]

One of the chemical components for this plant is sappanchalcone. It has been shown that using different concentrations of sappanchalone proportionately increase heme oxygenase (HO)-1 protein expression and enzyme activity in both human dental pulp (HDP) and human periodontal ligament cells (HPDL). It also protected HDP cells from H_2O_2-induced cytotoxicity and ROS prodoction. In addition, sappanchalcone is seen to inhibit interleukin-1b (IL-1b), tumour necrosis factor-a (TNF-a), interleukin-6 (IL-6) and interleukin-12 (IL-12) release in addition to inducible nitric oxide synthase (iNOS) and cyclooxygenase-2 (COX-2) expression in HPDL cells (Jeong et al., 2010).

3-(4,5-Dimethylthiazol2-yl)-2,5-diphenyltetrazolium bromide assay (MTT) assay using different densities of CS phenols have effects of inhibiting the growth of Hela cells (Zou et al., 2010) and human ovarian cancer (Zhang et al., 2010) and

inducing cancerous cells to die by increasing the expression of caspase-3, 9 which tend to be time and dosage dependent.

Isoliquiritigenin 2'-methyl ether (ILME) which is isolated from CS extract has anti-oral cancer effects by a mechanism in which heme oxygenase-1 protien is up regulated via a pathway involving MAP kinases, NF-kB, and Nrf2. using MTT assay, fluorescence microscopy, flow cytometry, and Western blotting. Thus, ILME could be considered to be a potential chemotherapeutic target for anti-oral cancer treatment strategies (Lee et al., 2010).

Brazilein, a compound obtained in a large amount from CS extract which has long been used in traditional medicine in China, has some pharmacological activities. HepG2 cells were treated with brazilein and analyzed for survivin protein and mRNA levels by Western blotting and real-time RT-PCR. Besides, brazilein also have been studied for its antitumour effect for treating human leukemia, kidney cancer, liver cancer, lung cancer, rectal cancer, gastric cancer, esophagus cancer or mammary cancer (Qiang, 2007).

2.12.2.3 Medicinal uses of CS

Acute toxicity study for CS ethanolic extract was done and there were no mortality or gross behavioural changes between rats with the highest dose of 2000 mg/kg orally (Sarumathy et al., 2011). Methanolic extract of CS revealed the antimicrobial activity and bactericidal activity against five food-borne pathogens, *E. coli, S. aureus, S. typhimurium, B. cereus* and *L. monocytogenes* (Lee & Min, 2011).

CS is among the most widely employed medicinal plants throughout a large part of Asia and Africa. CS extract exhibits different therapeutic effects include potent

antiallergic activity on antigen-induced b-hexosaminidase release (Yodsaoue et al., 2009), neuroprotective effect against glutamate-induced neurotoxicity in primary cultured rat cortical cells (Moon et al., 2010). CS extract has an effective component for improving and treating acne because it shows a good antimicrobial effect against propionibacterium acnes and can be used in skin-external-use drug compounds and cosmetic compounds for treating acne (Kim et al., 2009).

Additionally, (Wang et al., 2010) explored that brazilein extract from CS entered in the medicinal preparations for treating cerebral ischemia, myocardial ischemia, dysmenorrhea, irritable bowel syndrome, anxiety disorder, pain, immune hyperfunction, vasospasm, headache, coronary heart disease, and angina pectoris. In other cases, extract from CS was used for treating ascites, tumour and leukemia (Xu et al., 2009), arteriosclerosis (Park et al., 2008). This could be due to the antioxidant activity which is capabile in scavenging superoxide anions, hydrogen peroxide, and hydroxyl radicals (Hu et al., 2008).

Moreover, CS extract has been shown to have antidiabetic or hypoglycemic effects against alloxan diabetic mice. Furthermore, a study revealed that daily administration of 100 mg brazilin/kg body weight, for 10-30 days, normalized the suppressed activities of lysosomal enzymes in the kidney of alloxan diabetic mice (Moon, 1986).

Seven compounds from methanolic extract of CS used in an *in vitro* studies using the J774.1 cell line showed anti-inflammatory effects through their inhibitory effects on nitric oxide (NO) and prostaglandin E2 (PGE2) production and their suppressive effects on tumour necrosis factor-a (TNF-a), interleukin-6 (IL-6), cyclooxygenase- 2 (COX-2), and inducible nitric oxide synthase (iNOS) mRNA

expression (Washiyama et al., 2009). The ethanolic extract of CS also showed significant attenuation of collagen-induced arthritis in rats by decreasing the levels of IL-1b, IL-6, TNF-a and PGE2 in serum and the expression of COX-2 in paw cartilage (You-Zhi et al., 2011).

Both *in vitro* and *in vivo* studies have shown the powerful antioxidant activity of ethyl acetate, methanol and water extracts of CS as evidenced by the low IC50 values in both 1,1-diphenyl-2-picryl hydrazyl (DPPH) and nitric oxide methods when compared with rutin and ascorbic acid (Yang et al., 2010) have approved that CS can be used as a traditional medicinal plants for treating adiposis hepatica, alcoholic hepatitis, liver cirrhosis, hepatic fibrosis and ascites caused by alcoholism. It was observed that the incubation of rat hepatocytes with $BrCCl_3$ resulted in a significant increase in lipid peroxidation leakage of cytoplasmic enzymes, and glutathione depletion. The $BrCCl_3$ toxicity on hepatocytes was reduced by treatment with braziline (Moon et al., 1992). Additionally, wistar and albino rat models were used for the investigation of *in vivo* hepatoprotective properties of aqueous and methanolic extract of CS (100 and 200 mg/kg body weight) against CCl_4-induced liver damage revealed potent hepatoprotective activity of CS at 200 mg/kg body weight, which was comparable with that of the standard SY used in the similar test dose (Srilakshmi et al., 2010)

In another *in vivo* study, ethanolic extract of CS is reported to protect the rat liver from acetaminophen induced liver damage at doses of 100 and 200 mg/kg body weight as well as 250 and 500mg/kg (Sarumathya et al., 2011). However, no in vivo experimental data is available on the hepatoprotective effect of ethanolic extract of CS against TAA-induced liver fibrosis in rats.

2.13 Prediction of Activity Spectra for Substances (PASS)

The complex and diverse chemical structures of natural products provide the basis for advancement of various biological targets (Mallikadevi et al., 2012). In fact, natural products have historically been invaluable as a source of therapeutic agents, however, in the past decade, research into natural products in the pharmaceutical industry has declined, owing to issues such as the lack of compatibility of traditional natural-product extract libraries with high-throughput screening. Therefore, recent technological advances that help to address these issues, coupled with unrealized expectations from current lead-generation strategies, have led to a renewed interest in natural products in drug discovery (Koehn & Carter, 2005). Virtual screening is of specific significance to understand the pharmacological action of the plant compounds (Pramely & Leon, 2012). Many biological activates like anxiolytic and anticonvulsants (Athina et al., 2007), antihypertensive (Lagunin et al., 2003), antitumour and antibacterial (Pogrebnyak, 1998) have been discovered after the screening with PASS and confirmed by the experimental testing. PASS software (Lagunin et al., 2000) , which predicted more than 300 pharmacological effects, biological and biochemical mechanisms based on the structural formula of the substance, was efficiently used for this study to reveal new multitalented actions for the isolated components of VN and CS extracts.

2.14 Immunomodulatory Activity

An immunomodulator is a substance used for its effect on the immune system, which can inhibit, stimulate or modulate the immune system. The immunostimulants are investigated to enhance body's immunity against infection, allergy, and cancer. In healthy individuals the immunostimulants are expected to serve as prophylactic by

enhancing the basal levels of immune response, while in individuals with impairment of immune response as immunotherapeutic agent (Agarwal & Singh, 1999). Some medicinal plants and their active components such as Ginseng, Echinacea and Astragalus possess immunomodulatory properties and show potential against malignant diseases and infections (Block & Mead, 2003). The *in vitro* methods used to study immunomodulation are principally based on the assessment of the proliferation, the metabolic activity and the activation of immune cells (measurement of cytokine production). A few methods are being widely used to evaluate the immunomodulating activity based on the assessment of the proliferation, metabolic activity such as Methyl tetrazolium (MTT) assay and cell number quantitation (direct cell counting using a hemocytometer) (Durrieu et al., 2005).

2.15 Aim of the Study

To date, no studies on the development of effective anti-fibrotic drugs relay mostly on in vivo animal experiments and as no efficient treatment for liver fibrosis is yet available, extensive research is on-going to develop new anti-fibrotic drugs. Activation of HSCs and the development of liver fibrosis is multicellular processes also involve hepatocytes, Kupffer cells, and sinusoidal endothelial cells. Therefore, when studying these processes and the effects of potential anti-fibrotic compounds there on, intercellular interactions should be taken into account.

Interestingly, a very recent patent was effectively produced using a new composition of treatment and prevention of liver disease based-on plants' extracts (Shukla, 2013). Accordingly, our aim of the research described in this thesis to evaluate whether VN and CS are suitable as hepatoprotective agents against liver fibrosis and as

a test-system for anti-fibrotic compounds based primarily on the rich literature review with the support of PASS prediction program.

Concurrently, a part of this study will also provide the cytotoxic and antiproliferative effects of the crude extract from the leaves and aerial parts of VN and CS on the normal liver cells and hepatocarcinoma cell lines.

Chapter 3

Materials and Methods

3.1 Materials

3.1.1 Collection and identification of plant materials

The fresh leaves of VN and CS were used in this study. They were obtained from Kampung Baru, Sungai Ara, Penang, Malaysia. Their botanical identity is determined and authenticated in the Department of Pharmacy, Faculty of Medicine, University of Malaya, Kuala Lumpur, Malaysia with voucher specimen number (KLU 34968) and (KLU 47313), respectively.

3.1.2 Animals

A sixty six healthy adult male Sprague Dawley rats weighing in the range of 150-250 gm at the beginning of the study were purchased from the Animal House, University of Malaya. They were kept in specially prepared cages at room temperature (23 -32 °C) with 12 hrs light/12 hrs dark photoperiod and at 50% to 60% humidity in order to maintain the normal circadian rhythm in the animal room. The rats were fed ad labitum with rodent food pellet and water. Water was given through a special dropper – tipped bottles placed in the cages. The handling of animals is accordance to the experimental protocols which were approved by the Institutional Animal Care and Use Committee, University of Malaya (UM IACUC) with an ethics number

ANA/18/05/2012/FAAK in University of Malaya Grant No. (PG087-2012B) and (UM/MoHE/HIR Grant E000045-20001).

3.1.3 WRL 68 and HepG2-cells

For the cell culture experiments, two types of cells were used, the normal embryonic liver cells (WRL 68) and hepatocarcinoma cells (HepG2). HepG2 cells are perpetual adherent, epithelial in morphology and routinely used for toxicology studies (Wilkening et al., 2003). Both types of cells were obtained from Department of Biomedical Science, Faculty of Medicine, University of Malaya.

3.1.4 Chemicals and consumables

95% ethanol solution, industrial graded (R & M chemical, Essex, UK) and filter paper (Whatman No.1, England) for the preparation of the plant extract. Tween-20 Polyoxyethylene Sorbitan 10% (Merck, Germany) was used as a solvent for the extract. Diphenyl-2- Picrylhydrazyl (DPPH) reagent (Sigma-Aldrich, Germany), Ascorbic acid (Sigma-Aldrich, Germany) and Butylated hydroxyl toluene (BHT) (Sigma - Aldrich, Germany) were used for DPPH assay. Folin-Ciocalteu reagent, ascorbic acid, potassium persulfate, methanol, Folin-Ciocalteu reagent, gallic acid, natrium carbonate (Na2CO3) (Thermo Fisher scientific ,USA), Acetic acid glacial (Sigma, Germany), 2, 4, 6- Tris (2-pyridyl)-s- trizine (TPTZ) (Merck, Germany), HCl 37 %,(Merck, India), FeCl3 of purity less than 98 % (Merck, India) and FeSO4.7H2O (Merck, Germany) were used for Ferric reducing antioxidant power (FRAP) assay.

The chemicals that are used in cell culture tests included 3-(4, 5-dimethylthiazol-2-yl)-2,5-diphenyltetrazolium bromide (MTT reagent), Foetal Bovine Serum (FBS),

dimethyl sulphoxide (DMSO), Dulbecco´s phosphate buffered saline purchased from (Merck, Darmstadt, Germany). Ethidium bromide aqueous solution, Hydrogen peroxide 30%, Centrifuge tubes, 15 ml and 25 ml, Centrifuge tube, 50 ml, Tissue culture flasks, 25cm2 , 96 well plates (Fisure Scientific Malaysia), Power wave X 340 ELISA plate reader (from BIO-TEK instruments, Winooski, VT, USA).

Thioacetamide (Sigma-Aldrich, Germany) for induction of liver cirrhosis in the rats. SY was purchased from International Laboratory (USA). Syringes and oral feeding needles size 18 (Terumo, Japan), blood tubes with activated gel, blood tubes with sodium citrate (Terumo, Japan), NaCl (Merck, Germany) and phosphate buffer saline (Ajax Chemicals, Australia) for the experiment. Deionized water (Sigma, Germany) and malondialdehyde (MDA) Assay Kit (Cayman Chemical Company, USA). Catalase (CAT) (Item No. 707002), superoxide dismutase (SOD) (Item No. 706002) and glutathione peroxidase (GPx) (Item No. 703102) to measure antioxidant enzymes in vitro and in vivo (Cayman Chemical Company, USA).

Enzyme-linked immunosorbent assay (ELISA) kit for Cytochrome P450 2E1 (Item No. SEA988Ra) (Uscn, Life Science Inc.) was used for determination of hepatic CYP2E1. Matrix metalloproteinase enzymes (MMP-2 and MMP-9) and their partial regulator tissue inhibitor of metalloproteinase (TIMP-1) were assayed by enzyme-linked immunosorbent assay kit following the kits' manuals (Uscn Life Science E 90100 Ra, SEA553Ra and SEA552Ra, China), respectively. Caspase-3/CPP32 Colorimetric Assay Kit (Catalog # K106-25) (Bio vision) for detecting apoptosis in cancer cells, LDH Cytotoxicity assay Kit (Item No. 10008882) (Cyman chemical company) for measuring the level of lactate dehydrogenase enzyme in cultured cells.

Concentrated formalin 38–40%, xylazine, ketamine (Sigma-Aldrich, Gillingham, UK), Di-natrium hydrogen phosphat (Merck, Germany), sodium dehydrogen phosphate monohydrate (Sigma - Aldrich, Germany), toluene (Merck, Germany), xylene (BDH Laboratory supplies, England), paraplast paraffin (Microm International, USA) and dibutyl phathalate xylene (DPX) (Merck, Germany), Coverslips (24x50 mm), Fisure Scientific Malaysia for histological study.

For immunohistochemical and Western blot study, TGF-β1, α-smooth muscle actin (α-SMA) and proliferative cellular nuclear antigen (PCNA) determination, Mouse Monoclonal [2Ar2] to TGF-β1 immunohistochemistery kit (ab64715) (Abcam) and Rabbit polyclonal to α-SMA immunohistochemistery kit (ab5694) (Abcam) were used. and PCN (Anti-PCNA antibody [PC10] - Proliferation Marker ab29) (Abcam). Primary standard antibody β-actin (Santa Cruz Biotechnology, Inc), Ice-cold lysis buffer [(50mM Tris-HCL pH 8.0, 120mM NaCl, 0.5% NP-40, 1mM PMSF)] (abcam), sodium dodecyl sulphate (SDS) sample buffer (abcam), poly vinylidene difluoride membrane (PVDF) (Bio-Rad, USA) were used.

3.1.5 Apparatus/ Equipments

The apparatus used in this study were: weighing machine (Ederan Medical, Germany), blender (Panasonic, China), rotary evaporator (Heidolph Laborata-control Rotary Evaporator 4000, Canada), oven (Thelco 6M, USA) and freeze-drying machine (LabConco, Kansas City, MO, USA), Genie-2 vortex (Scientific Industries Inc., USA) for plant extraction.

Incubator (Ederan Medical, Germany), water bath (Leica HI 1210, Germany), Magnetic stirrer (Age Glass 13659, USA), vortex mixer (Age Glass PC-610, USA),

glass-teflon homogenizer (Polytron, Heidolph RZR 1, Germany), centrifuge machine (Biofuge Primo R, Heraeus, Germany) and spectrophotometer (Shimadzu UV - 1601 UV, Netherlands) for measuring lipid peroxidation product (MDA) and Ferric reducing antioxidant power (FRAP) assay. Automated tissue processing machine (Leica TP1020, Germany), Microtome (Leica RM 2135, Germany) and Image analyzer (Leica CTR.MIC., German), light microscope (Leica, German) for histopathological study, trinocular inverted phase contrast microscope (Olympus, Japan), fluorescence microscope (Leica). Serum and blood specimens were determined by blood analysis machine (Maxcom ISO 9001, China). For protein electrophoresis in Western blot analysis, semi dry transfer unit (Hoefer TE 70X, USA) was used.

3.2 Methods

3.2.1 Computational evaluation of biological activity

The biological activity spectra of the phytoconstituents for VN and CS plants were obtained using PASS software. PASS prediction tool is constructed using 20,000 principal compounds from the MDDR database (Figure 3.1) (produced by Accelrys and Prous Science) (Koehn & Carter, 2005). Generally, natural products research requires the utilization of virtual screening methods to find new lead substances. Currently, with development of sophisticated bioinformatics software's such as PASS, it has become feasible to explore the hidden pharmacological potential of selected traditional medicinal plants based on their phytoconstituents.

We assume that PASS is an intrinsic way to represent the activity of each active component qualitatively and provides the basis to include the data collected from many different sources into training test.

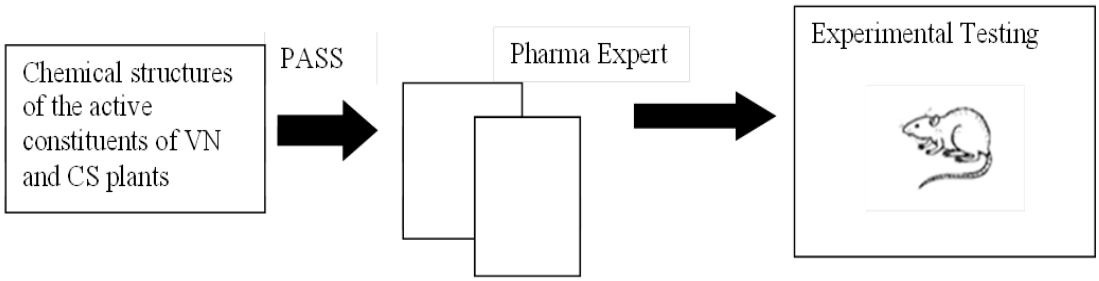

Figure 3.1: PASS processing

3.2.2 Extraction of VN and CS plants

The dried and ground leaves of VN and CS plants were weighed, then homogenized in 95% ethanol at a ratio of 1:10 of plant to ethanol. The mixture was left to soak for 4 days at 25 ºC with occasional shaking and stirring. Later the mixture was filtered through a filter paper and the resulting liquid was concentrated under reduced pressure at 45 ºC to obtain a dark gummy–green extract for each plant (Lisina et al., 2011). The concentrated extracts were then frozen and finally lyophilized with freeze dryer, yielding the crude extract of the leaves of VN and CS. Percentage yield of VN crude extract was 18% and for CS was 4.3 %. This was calculated by using the following formula:

$$\%\ \text{of yield} = \frac{\text{Weight of crude extracts in gm}}{\text{Weight of powdery sample in gm}} \times 100\%$$

Each extract was then dissolved in 10% Tween-20 before being given orally to the animals.

3.2.3 Experimental design

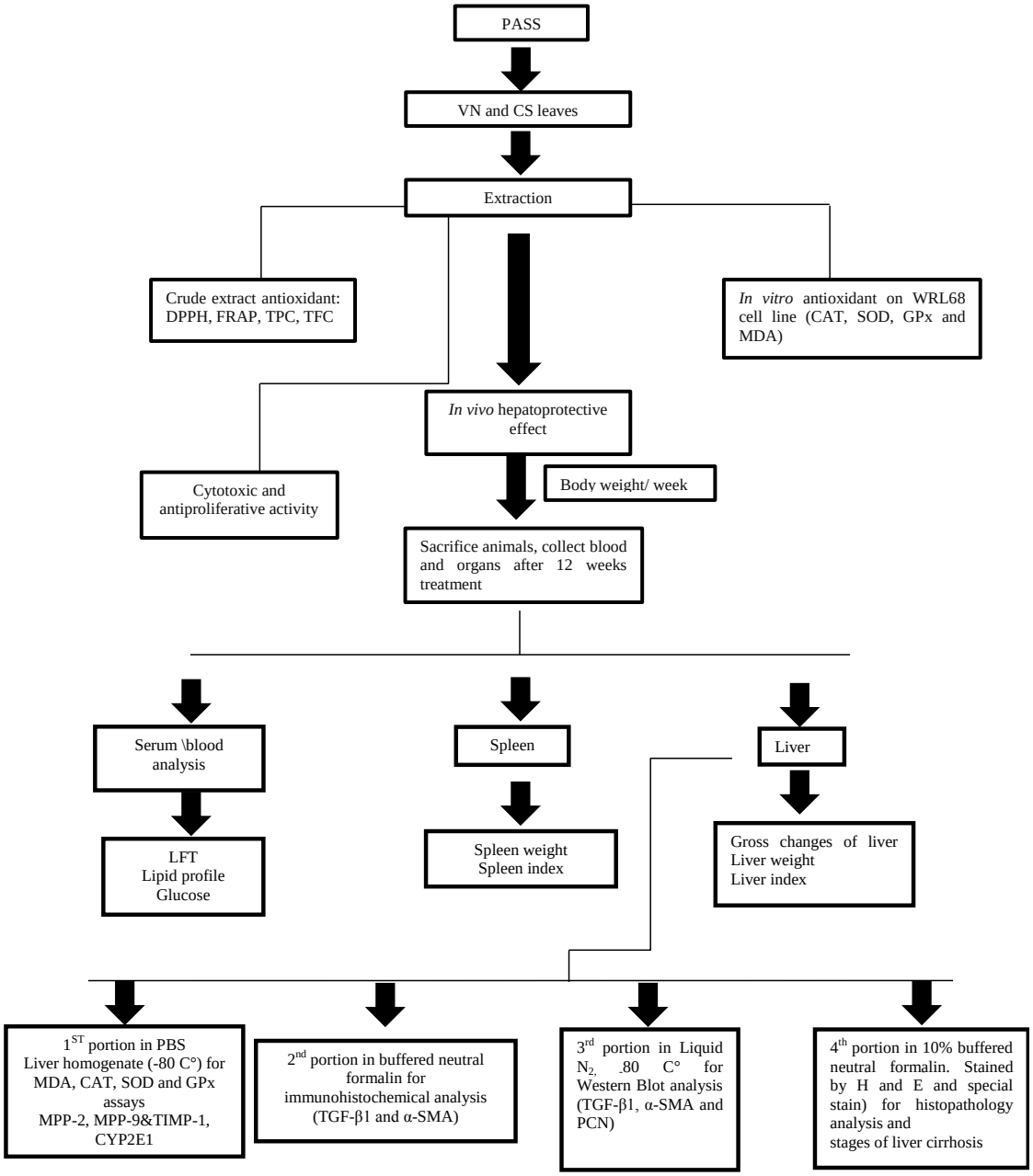

3.2.4 Crude extracts antioxidant

The investigated plants were examined to determine their antioxidant activity using the following assays: Diphenyl-2- picrylhydrazyl (DPPH), Ferric reducing antioxidant power (FRAP), total phenolic content (TPC) and total flavonoid content (TFC).

3.2.4.1 Radical scavenging activity of VN and CS

The scavenging activity for DPPH free radicals of VN and CS extracts was determined (Gorinstein et al., 2003). The hydrogen atom or electron donation ability of VN and CS extracts was measured from the bleaching of purple coloured ethanol solution of DPPH. The capacity of this extract to scavenge the lipid-soluble DPPH radical, which results in the bleaching of the purple colour exhibited by the stable DPPH radical, was monitored at an absorbance of 515 nm (Gülçin et al., 2007). Basically, 195 µl of various concentration of DPPH were added with 5µl of diluents and absorbance at 515 nm was read. 5µl of samples/standard were loaded, and followed by 195 µl of DPPH reagent (x40 dilution). Plate was read for 2 hrs with 20 min intervals at the lowest temperature on the micro titer plate. Lower absorbance of the reaction mixture indicated higher free radical scavenging activity. The DPPH concentration (µmole) in the reaction medium was calculated from the calibration curve and determined by linear regression. The capability to scavenge the DPPH• radical was calculated using the following equation:

DPPH• scavenging effect (%) = (Control A –Sample A / Control A) ×100

Where in Control A was the initial concentration of the stable DPPH radical without the test compound and sample A was the absorbance of the remaining concentration of DPPH• (Gorinstein et al., 2003). This assay provides information on

the reactivity of test compounds with a stable free radical. Because of its odd electron, DPPH• gives a strong absorption band at 515 nm in visible spectroscopy. This test was conducted in triplicate. The extract concentration providing 50% inhibition (IC50) was calculated from the graph of inhibition percentage plotted against extract concentration (3.125, 6.25, 12.5, 25 and 50 µg/ml), (Appendix B1 and B2).

3.2.4.2 Ferric reducing antioxidant power (FRAP) assay

The FRAP assay measures the change in absorbance at 593 nm due to the formation of blue coloured Fe^{2+}-tripyridyltriazine (Fe-TPTZ) compound from the colourless oxidized Fe^{3+} form by the action of electron donating antioxidants (Benzie, 1999). The experiment was conducted at 37 °C under pH 3.6 condition with a blank sample in parallel. In the sample reduce Fe^{3+}/tripyridyltriazine complex, present in stoichiometric excess, to the blue Fe^{2+} form, with an increase in absorbance at 593 nm.

Briefly, 50 µl from the dissolved extract was added to 1.5 ml freshly prepared and pre warmed (37 °C) FRAP reagent (300 mM acetate buffer, pH3.6, 10 mM TPTZ in 40 mM HCl and 20 mM $FeCl_3.6H_2O$ in the ratio of 10 : 1 : 1) and incubated at 37 °C for 10 min. The absorbance of the sample was read against reagent blank (1.5 ml FRAP reagent+50 µl distilled water) at 593 nm. Increased absorbance of the reaction mixture indicated increased reducing power. Ascorbic acid, gallic acid BHT and quercetine were used as standards. All analyses were run in triplicate and results averaged, (Appendix B3 and B4).

3.2.4.3 Quantitative estimation of total phenolic contents (TPC) of extracts

TPC of the two plants extracts were determined using Foli–Ciocalteu reagent (Horwitz, 1980) and by using quercetine as a standard. The samples were inserted into different test tubes and mixed thoroughly with 5 ml Folin-Ciocalteu reagent. After 5 min, 4 ml of 7.5% sodium carbonate (Na_2 CO_3) was added and allowed to react for 2 hrs at room temperature. The absorbance was measured at 765 nm using microplate reader spectrophotometers. Samples were measured in three triplicates. Standard curve of quercetine solution (62.5, 125, 250, 500, 1000) was prepared using the similar procedure. The results were expressed as mg quercetine /g extract sample using the following equation based on the calibration curve: y=0.0023 x, R2=0.9965, where x is the absorbance and y was the quercetine equivalent (mg/g). This assay was carried out in triplicate, (Appendix B5 and B6).

3.2.2.4 Quantitative estimation of total flavonoid contents (TFC) of extracts

TFC of each sample of plant extract was determined by aluminium chloride colorimetric method (Harborne & Williams, 2000). Briefly, 0.5ml of extract solutions (1mg /1ml) were added to a separate test tube and mixed with1.5 ml of 95 % ethanol, 0.1ml of 1M of potassium acetate, 0.1 ml of aluminium chloride and 2.8 ml of distilled water. After that, the mixtures were incubated for 30 min at room temperature. The absorbance readings were taken spectrophotometrically at 415 nm. A yellow colour indicated the presence of flavonoids. Total flavonoid content was expressed as milligrams of quercetin equivalent to gram of dried plant material, (Appendix B7 and B8).

3.2.5 *In vitro* antioxidant effect of VN and CS extracts on H_2O_2- induced oxidative damage in WRL68 cell lines

The VN and CS extracts were used for *in vitro* antioxidant experiment. Approximately, 1000 µl of the WRL 68 cell line suspension were seeded in 12-well flat bottom micro titer plates at 2 × 106 cells/ml in Dulbecco's modified eagle's medium (DMEM) containing 10 % (v/v) foetal bovine serum (FBS) and allowed to attach overnight. On the second day, the cells were treated with 100 µg of each VN and CS extract in triplicate according to Table 3.1 and incubated at 37 °C with 5 % CO_2 for 2 hrs. The treated cells were induced by 100 µl of freshly prepared 1000 µM H_2O_2 and re-incubated for 2 hrs. The H_2O_2-treated and untreated cells after removing the medium, were harvested, washed twice with phosphate buffer saline (PBS) and lysed in lysis buffer (25 mmol/l Tris-HCl). WRL 68 cell lysates were prepared in a 0.5 ml cold PBS (pH 7.4). The cell debris was removed by centrifugation at 100 rpm for 10 min at 4 °C using refrigerated centrifuge Rotofix 32 (Hettich Zentrifugen, Germany). All samples were sonicated for 5 min with 10 sec rest after each min. The samples were kept at -20 °C until utilised (Chen et al., 2006). The supernatant was used for the estimation of the following antioxidant using commercially available kits (Cayman Chemical Company, USA): malondialdehyde (MDA) (Item No. 10009055), superoxide dismutase (Item No. 706002) and glutathione peroxidase (Item No. 703102) activities, (Appendices B 9, B10 and B11).

Table 3.1: *In vitro* antioxidant for cell line experimental design

Group	**Oxidant agent (1000 µM H_2O_2)**	**Treatment (100 µg/ml)**
Normal	No oxidant agent (100 µl medium)	No treatment (10 µl solvent)
H_2O_2	10 µl	No treatment (10 µl solvent)
VN	10 µl	VN ethanol extract (10 µl)
CS	10 µl	CS ethanol extract (10 µl)

3.2.6 *In vivo* assays

3.2.6.1 Preparation of thioacetamide (TAA)

TAA from (Sigma-Aldrich, Switzerland) and all other chemicals used were of analytical grade and purchased mostly from Sigma-Aldrich and Fisher. TAA stock solution of 5 gm/l was prepared by diluting the pure TAA which is in the crystal form. The amount of TAA needed was diluted in distilled water in 0.03% w/v and stirred well until all the crystals were dissolved and given to the rats with their drinking water.

3.2.6.2 Preparation of silymarin (SY)

SY with 80% purity, (International Laboratory, USA) used as a standard drug, was dissolved in Tween 20 (10% w/v) and orally administered to rats at a dose of 50 mg/kg body weight (Salama et al., 2013).

3.2.6.3 Preparation of 10% Tween-20

To prepare 100 ml of this dissolvent, 10 ml of 10% Tween-20 was added to 90 ml of distilled water.

3.2.6.4 Preparation of 0.9% normal saline

Nine gm of NaCl was added to 1 L of distilled water.

3.2.6.5 Preparation of phosphate buffer saline pH 7.3± 0.2

One tablet of sodium chloride 8.0 mg, potassium chloride 0.2 mg, di-sodium hydrogen phosphate 1.15 mg and potassium dehydrogen phosphate 0.2 mg was dissolved in 100 ml of distilled water at 25 °C.

3.2.6.6 Preparation of 10% fresh formalin (buffered formalin)

To prepare 1 L of fresh formalin, 6.5 gm di-natrium hydrogen phosphate with 4 gm sodium dihydrogen phosphate monohydrate were dissolved with 900 ml of PBS and 100 ml concentrated formalin (38-40%).

3.2.6.7 Animal experimental design

Experimental design is shown in Table 3.2. The rats were randomly divided into 11 groups, each of which consisted of 6 rats. The animals were acclimatized under standard laboratory conditions for a period of two weeks before the commencement of the experiment. Group 1 (normal control) rats were administered orally with 10% Tween 20 (5 ml/kg) daily. Group 2 (hepatotoxic or TAA group), rats were given 0.03% TAA with their drinking water and this protocol is according to the recommendation of a previous study (Müller et al., 1988). Group 3, the rats were gavaged daily with low dose of 100 mg/kg VN orally. Group 4, the rats were gavaged daily with low dose of 100 mg/kg VN+0.03%TAA in drinking water. Group 5 rats were gavaged daily with 300 mg/kg VN and Group 6 rats were gavaged with 300 mg/kg VN+0.03%TAA in drinking water. Group 7 the rats were gavaged with low dose of 100 mg/kg CS orally. Group 8 the rats were gavaged with low dose of 100 mg/kg+0.03%TAA in drinking water. Group 9 rats were gavaged daily with CS 300 mg/kg. Group 10, the rats were gavaged daily with 300 mg/kg CS+0.03% TAA in drinking water. Group 11 the rats were gavaged daily with 50 mg/kg SY+0.03% TAA. The experiment was carried out for a total of 12 weeks. The animals were given water ad libitum. The body weights of the animals were recorded weekly starting from day 0 and throughout the experiment. Throughout the experiment, all criteria of taking care of animals prepared by the National Academy of Sciences and outlined in the "Guide for the Care and Use of laboratory Animals" were complied (Clark et al., 1997).

Table 3.2: Experimental groups of the rats treated with each plant

Group	Name of the group	0.03% TAA in drinking water	Oral feeding
1	Normal control	-	Water, ad libitum and 10% Tween 20
2	(Hepatotoxic)TAA	TAA	Water , ad libitum
3	VN100	-	100mg/kg VN in 10% Tween 20
4	VN100+TAA	TAA	100mg/kg VN in 10% Tween 20
5	VN300	-	300mg/kg VN in 10% Tween 20
6	VN300+TAA	TAA	300mg/kg VN in 10% Tween 20
7	CS100	-	100mg/kg CS in 10% Tween 20
8	CS100+TAA	TAA	100 mg/kg CS in 10% Tween 20
9	CS300	-	300mg/kg CS in 10% Tween 20
10	CS300+TAA	TAA	300mg/kg CS in 10% Tween 20
11	SY+TAA	TAA	50mg/kg SY in 10% Tween 20

At the end of the 12^{th} week, the rats were anaesthetized by intramuscular injection of 50 mg/kg ketamin mixed with xylazine 5 mg/kg. The abdomen and thoracic cavities were opened by a mid-ventral abdominal incision on each animal. The liver and spleen were carefully observed for any gross pathology. Through the jugular vein, blood was withdrawn and collected into the plain tube with activated gel for determination of the liver function test and lipid profile, while the tube with sodium floride/ Na_2 EDTA, was used for serum glucose determination.

For serum analysis, the blood sample was allowed to clot, centrifuged and the serum was sent to the Clinical Diagnosis Laboratory of Medical Centre (CDL) in University Malaya Hospital to use the blood analysis machine. The livers and spleens were isolated, washed with normal saline, blotted with filter papers and weighed. The liver and spleen indices were calculated as the percentage of the body weight. Liver for each rat was dissected out immediately into four small parts. Two parts were taken from

the right lobe and kept in 10% formalin for determination of histological assessment of hepatic pathology and immunohistochemical analysis. While 3rd and 4th parts were washed in 0.9 % NaCl and was kept in phosphate buffer saline and stored at –80 °C until required for determination of the extent of lipid peroxidation, endogenous antioxidant enzymes, hepatic CYP2E1 level and matrix metalloproteinase enzymes (MMP-2, MMP-9 and TIMP-1) and Western Blot analysis.

3.2.6.8 *In vivo* antioxidant in liver tissue

Liver samples were washed immediately with ice cold saline to remove as much blood as possible. Liver homogenates (10 % w/v) were prepared in a cold 50 mM PBS (pH 7.4) using homogenizer in ice. The cell debris was removed by centrifugation at 4500 rpm for 15 min at 4°C using refrigerated centrifuge Rotofix 32 (Hettich Zentrifugen, Germany). The supernatant was used for the estimation of the following in vivo antioxidant using commercially available kits from (Cayman Chemical Company, USA): malondialdehyde (MDA) or thiobarbituric acid reactive substance (TBARS) (Item No. 10009055, superoxide dismutase (SOD) (Item No. 706002) and glutathione peroxidase (GPx) (Item No. 703102) and Catalase (CAT) (Item No. 707002) activities. All assays performed according to the instruction manual of the manufacturer, (Appendices B9, B10, B11 and B12).

3.2.6.9 Assessment of hepatic CYP2E1 level

To demonstrate the effect of the crude extracts of VN and CS on the level of CYP2E1 as an important enzyme in the biotransformation of TAA in the liver microsome (Amali et al., 2006), the tissue homogenate from all rats was tested for the level of CYP2E1 enzyme by following the instructions of Uscn Life Science (SEA988Ra, China). Briefly, 100 µL of the sample was incubated with pre-coated capture antibody specific to CYP2E1 in duplicate in 96-well plate for 2 hrs at 37 °C. After brief rinsing, the sample was incubated for 1 hour at 37 °C with 100 µL of biotin-conjugated secondary antibody followed by three times washing using 350 µL washing buffer (1x). 100 µL Streptavidin-Horse radish peroxidase (HRP) was added to the sample and incubated for 30 min at 37 °C followed by 5 repeated washes. 90 µL Tetramethylbenzidine (TMB) was added to the sample as a colorimetric reagent and incubated for 20 min. Finally, the reaction was stopped using 50 µL of H_2SO_4 and the absorbance was read at 450 nm, (Appendix B13).

3.2.6.10 Evaluation of matrix metalloproteinase enzymes (MMP-2 and MMP-9) and TIMP-1

MMP-2 and MMP-9 and their partial regulator TIMP-1 play a role in liver damage (Okazaki et al., 2003). For this purpose, the following assay was conducted to demonstrate the effect of VN and CS extracts on these enzymes in the liver tissue homogenate collected from the rats of all groups as mentioned previously and assayed in duplicate by enzyme-linked immunosorbent assay kit following the kits' manuals (Uscn Life Science E90100Ra, SEA553Ra and SEA552Ra, China), (Appendices B15, B17 and B19).

3.2.6.11 Histological evaluation of the liver

In order to obtain good sections for microscopy, the fixed tissues were first dehydrated to remove aqueous fixative and tissue water. Next, the tissues were cleared to remove the dehydrating agent. Finally, sections of the randomly selected fixed liver specimens from each group were embedded in paraffin and processed for light microscopy by staining the individual sections with Hematoxyline and Eosin (H and E) stain and Masson's Trichrome stain, mounted with neutral DPX medium and examined under light microscope. The photomicrographs were captured with a Nikon microscope Digital camera (Nikon, Tokyo, Japan).

1. Techniques for processing the tissues

a. Fixation

Tissue processing was started with fixation using 10% buffered formalin. The purpose of fixation is to preserve the tissues permanently in life-like state as much as possible after removal of the tissues. The tissues were trimmed into small pieces of about 1 cm in size and then placed in cassettes containing fresh formalin of 10:1 ratio of fixative to tissue for 48 hour.

b. Tissue processing technique

The technique of getting fixed tissue into paraffin is called tissue processing. The main steps in this process involved:

i. Dehydration, water from the tissues was removed by a procedure called dehydration through a series of alcohol

ii. Clearing, the removal of dehydrant was done with toluene that is miscible with the embedding medium, paraffin. Toluene is more tolerant of small amounts of water left in the tissues and less toxic than xylene.

iii. Infiltration and impregnation, the tissues were infiltrated with embedding agent, usually, the paraffin in oven less than 60 °C. The protocol is provided in appendix B21.

All the above processes were done by using automatic tissue processor, which performed fixation, dehydration, clearing and paraffin impregnation of tissues in a programmed sequence.

iv. Tissue embedding, the tissues were manually transferred from the cassettes and placed into the prepared moulds with molten paraffin over them, with proper orientation of tissue in the block of paraffin.

c. Sectioning

Once the paraffin blocks cooled down and hardened, the blocks were trimmed into an appropriately-sized block and put into a freezer with temperature under -4 °C for 1 hour before sectioning. Each block was then mounted in a specially designed slicing machine, a microtome. They were cut with steel knife into sections of 5 µm thickness. These sections were floated in a 40 °C water bath and then they were picked up on labelled glass microscopic slides. All these slides were air-dried followed by drying in 50 °C oven.

d. Staining

All slides were deparaffinised by running them through xylenes I, II for 5 min each before staining, in order to dissolve and remove the paraffin wax out of the tissues. Slides were then hydrated through a series of alcohol to allow water soluble dyes to penetrate the sections. The stains used in our experiment were H and E and a special stain Masson's Trichrome, used for detecting of collagen and elastic fibrous tissues

i. Staining technique for Hematoxylin and Eosin

The preparation method of hematoxylin and eosin is provided in appendix B22. Paraffin sections (5 µm thick) of liver tissue were dewaxed in xylene, hydrated through a series of decreasing concentration of alcohol to water then immersed in hematoxylin for 15 min. Sections were then differentiated with 1% Acid alcohol and washed in a running tap water. This is, followed by staining the sections with eosin for 5 min. Finally, the sections were dehydrated in series of increasing concentration of alcohol, cleared in xylene, mounted with DPX and covered with a glass cover slip (Bancroft & Cook, 1994).

ii. Staining technique for Masson's Trichrome

The preparation method for Masson's trichrome staining is provided in appendix B23. Sections were brought to water, stained with lugol's iodine for 5 min, then decolourized with 5% sodium thiosulphate and washed with a running tap water until clear and before staining with Weigert's iron hematoxylin for 20 min. Sections were decolourized with 1% acid alcohol and tap water, then stained with 1% ponceau-fuchsin for 5 min, mordant in 1% phosphomolybdic acid for 5 min and stained with 2% light green, then differentiated with 1% acetic acid. Finally, the sections were dehydrated in series of increasing concentration of alcohol, cleared in xylene, mounted with DPX and covered with a glass cover slip (Bancroft & Cook, 1994).

3.2.6.12 Staging criterion for hepatic fibrosis for experimental groups

Each section was subjectively scored by two blinded experienced observers including an anatomist and histopathologist for evidence of fibrosis, fatty change, architectural distortion and regenerative nodules. The extent of bile duct proliferation and fibrosis with accompanying inflammation by using H and E stain were duly graded

by semi-quantitative method on a scale between zero and six (Zhao et al., 2008). Stage 0 values were indicative of normal hepatic architecture in which there was no evidence of bile duct proliferation, inflammation or fibrosis whereas stage 6 reflected a gross disturbance of hepatic architecture typified by marked proliferation of the bile ducts with severe inflammation and a very conspicuous fibrotic response (Table 3.3) and (Figure 3.2). Each sample was observed at x10 magnification. The degree of fibrosis was expressed as the mean of 10 different fields in each slide (Kuzu et al., 2007).

Table 3.3: Staging criterion for experimental hepatic fibrosis in rats

Stages/ Scores	**Categorical description**
0	No fibrosis
1	Mild fibrosis started and extended from hepatic central venules
2	CV-CV fibrotic septa were formed
3	Multiple CV-CV fibrotic septa incompletely compassed and divided hepatic lobule
4	CV-CV septa connected with each other completely dividing hepatic lobule, into rectangle –like pseudo-lobule, portal tract(P)usually located in the center (early stage of cirrhosis)
5	Moderate CV-P bridging septa divided pseudo-lobule further, the number of smaller sized nodules less than 50% (incomplete cirrhosis)
6	Multiple CV-P bridging septa divided pseudo-lobule further, the number of smaller sized nodules more than 50% (complete cirrhosis)

CV, central vein; P, portal tract

[(Adopted from (Zhao et al., 2008)]

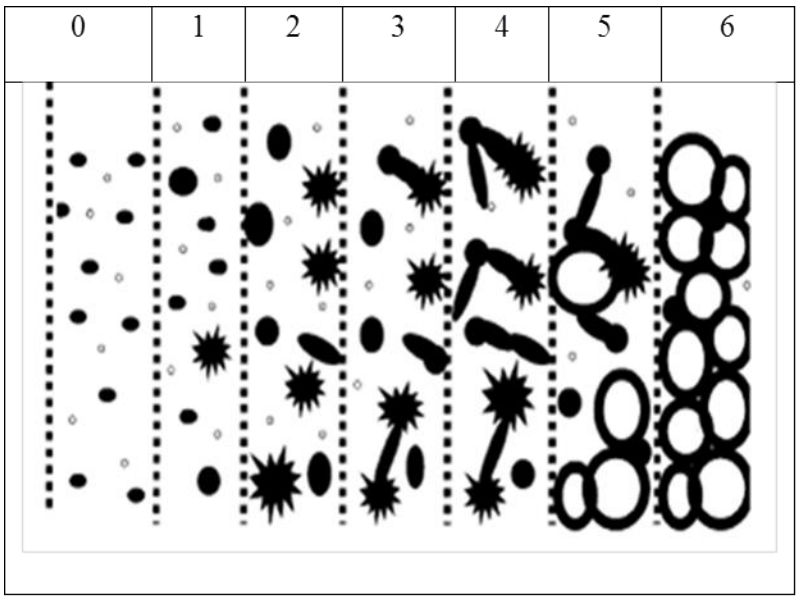

Figure 3.2 : Diagrammatic representations of the seven stages of the fibrosis

[Adopted from (Goodman, 2007)]

A two blinded experienced observers including an Anatomist and Histopathologist confirmed the histopathologic analysis. The histology of the livers from each group of herb treated rats was compared to that of the positive control group which was treated with (TAA) G2 group, G 1 and G 11. These comparisons were to confirm the effect of the herbs in TAA-treated groups.

3.2.6.13 Immunohistochemical localization of transforming growth factor-β1 (TGF-β1) and α smooth muscle actin (α-SMA) in rat liver

For the qualitative determination of TGF-β1 and αSMA, Mouse Monoclonal [2Ar2] to TGF-β1 (100ug) immunohistochemistery kit (ab64715) (Abcam) and Rabbit polyclonal to α-SMA immunohistochemistery kit (ab5694) (Abcam) was used respectively. Briefly, by using poly-L-lysine-coated slides liver sections were prepared and heated in an oven (Venticell, MMM, Einrichtungen, Germany) for 25 min at 60 ^{o}C. After heating, liver sections were deparaffinised in xylene and hydrated in a series of

graded alcohol. Antigen recovery procedure was conducted in 10 mM sodium citrate buffer boiled in a microwave. Staining method was conducted following the company's guidelines (Dako Cytomation, USA). Briefly, 0.03% hydrogen peroxide sodium azide was used to block endogenous peroxidase for 5 min and then sections were carefully washed with clean wash buffer. After washing, the sections were incubated with the monoclonal antibody of TGF-β1 (diluted to 1:50) at 37 °C for 60 min. and with rabbit anti-rat α-smooth muscle actin antibody (1:200) for 30 min. Following gentle washing with wash buffer, the sections were re-incubated for 15 min with streptavidin-HRP. After washing, the sections were incubated with Diaminobenzidine-substrate chromagen for over 7 min followed by washing and counterstaining with hematoxylin for 5 seconds. Tissue sections were finally washed with running water, dehydrated by series of alcohols and cover slipped to microscopically examine the cytoplasmic brown granule was marked as a positive expression of TGF-β1 and the brown-stained positive antigens for α-SMA. The protocols are provided in appendices B24 and B25 respectively.

A two blinded experienced observers, including an Anatomist and Histopathologist confirmed the immunohistochemical analysis. The histology of the livers from each group of herb treated rats was compared to that of the positive control group which was treated with the normal and TAA groups. These comparisons were to confirm the effect of the herbs in TAA-treated groups (Kadir et al, 2011).

3.2.6.14 Western blot analysis of TGF-β1, α-SMA and proliferative cellular nuclear antigen (PCNA) expression

An analytic technique used to detect specific proteins in a given sample of tissue, homogenate or extract. Identification is based on the transfer of proteins from gel

(polyacrylamide gel) to poly vinylidene difluoride membrane (PVDF) or nitrocellulose membrane and eventually detects a target protein based on its property to specifically bind to an antibody.

The protein is usually separated by sodium dodecyl sulfate (SDS)-page, based on the size of protein particles by electrophoresis then followed by blotting the protein onto membrane by probing with antibodies. It is important to transfer the proteins to membranes from gels for the efficient binding with the probe antibody as polyacrylamide gel is not particularly amenable to the diffusion of large molecules. The attachment of specific antibodies to specific immobilised antigens onto the membrane can be readily visualized by indirect enzyme immunoassay techniques, usually using a chromogenic substrate which produces an insoluble product.

This analysis was used to investigate the expression of fibrosis-related proteins which included TGF-β1 (ab64715), abcam, αSMA (ab5694) (abcam) and mouse monoclonal Anti-PCNA antibody [PC10] - Proliferation Marker ab29 (Abcam). Briefly, livers were homogenized in an ice-cold lysis buffer [(50mM Tris-HCL pH 8.0, 120mM NaCl, 0.5% NP-40, 1mM PMSF)]. Lysates were centrifuged at 14,800g for 30 min, and aliquots of supernatant containing 30 µg proteins were boiled in SDS sample buffer for 5 min before electrophoresis on 10% SDS–polyacrylamide gel. After electrophoresis, proteins were transferred to PVDF (Bio-Rad, USA) using semi dry transfer unit (Hoefer TE 70X, USA), and the blots were blocked with 5% non-fat milk in TBS-Tween buffer (0.12M Tris-base,1.5M NaCl, 0.1% Tween 20) for 1 hr at room temperature and then washed in PBS buffer. The membranes were then incubated at 4 °C overnight with primary antibodies, β-actin (1:2000) Santa Cruz Biotechnology, Inc, CA, USA, TGF-β1 (1:2000), α-SMA (1:5000), and PCNA (1:500) were purchased from (abcam), (Appendices B24, B25 and B26).

The membranes were then incubated for 1 hr at room temperature with goat anti-mouse and goat anti-rabbit secondary antibodies conjugated with alkaline phosphatase (i-DNA, USA) at a ratio of 1:1000 and then washed twice with TBST for 10 min three times on an orbital shaker. Then, blots were developed using the BCIP/NBT (Santa Cruz, USA) solution for a period of 5-30 min to detect the target protein band as a precipitated dark blue colour.

3.2.7 Cytotoxic and antiproliferative activity

3.2.7.1 Cell viability assay

3.2.7.1.1 Handling and maintaining cells

In this test, 2 types of cells were used namely normal embryonic liver cells (WRL 68) and hepatocarcinoma cells (HepG2). Handling and maintaining of cells were performed in a biologic safety cabinet or tissue culture hood. The biological safety cabinet was first cleaned with 70% alcohol prior to use. Then, the cabinet was disinfected with UV light for 5 min. Two beakers, each for solid waste and liquid waste respectively, centrifuge tube and its holder, two small flasks, 100 µl, 1000 µl and 5000 µl micropipette and their tips were disinfected with UV light for 5 min inside the biological safety cabinet prior to starting the procedures. Caution needs to be taken not to put any liquid materials under the UV light. Liquid materials were placed under the cabinet later on when the solid materials have been disinfected. Liquid materials that were used are DMEM, and PBS.

In order to handle the cells, it is mostly important to make sure that the cells are confluent. Confluent means that the cells grow until they are attached or merged very closely to each other and to the wall of the flask. Cells usually take 24 hrs to be confluent after being sub-cultured; however, it depends on the type of cells. During the

research project, most WRL 68 cells were confluent after 24 hrs, but HepG2 cells took more than 24 hrs to be confluent.

After making sure that a flask with confluent cells was chosen, the media was discarded into the liquid waste beaker. The cells were then washed with PBS. In order to detach the cells from the wall of the flask, trypsin was pipetted into the flask. The process of detachment requires incubation for about 5 to 10 min inside the cell culture incubator. This is so because the incubator's temperature is similar to normal human body temperature.

3.2.7.1.2 Methyl tetrazolium (MTT) assay

Both HepG2 and WRL68 cells were cultured in the DMEM (Sigma-Aldrich, UK), supplemented with 10 % (v/v) FBS (J R Medical, Inc, USA) and 1 % (v/v) penicillin-streptomycin solution (Sigma-Aldrich, UK), using 75 cm2 flasks in a 37 °C in humidified 5% CO2 incubator. Briefly, the cells were plated into 96-well plates at density 1.5×104/well in final volume of 100µl culture medium per well. The following day, cells were treated with various concentration of each plant extract at doses of 6.25, 12.5, 25, 50,100 and 200 µg/ml and maintained at 37 °C with 5% CO_2 for 24, 48 and 72 hrs. Sample without treatment was used as negative control. At the end of incubation period, 20µL of MTT reagent was added to each well and incubated again for 4 hrs at 37 °C with 5% CO2, then 100 µL of DMSO was added into each well and the absorbance was determined at 540 nm using ELISA reader. The cell viability percentage was calculated using:

A550nm (sample)/A550nm (control) ×100

Where A (sample) is the absorbance of wells containing different concentrations of plant extract and A (control) is the absorbance of control wells containing cell culture

medium without samples. The experiment was carried out in triplicates (Nugraheni et al., 2011), (Appendix B27).

a. Cell observation using an inverted microscope

HepG2 cell lines were grown in 96-well plates and treated with VN and CS ethanolic extracts separately. The cells were then washed with 1× PBS (Sigma). Morphological and confluence changes in the cells in both the treated and untreated group were observed under ×10 magnification by a trinocular inverted phase contrast microscope (Olympus, Japan).

b. Acridine orange/ethidium bromide (AO/EB) staining

AO/EB is a double staining to distinguish necrotic and apoptotic cells. If alive and dead cells can be distinguished in the same microscopic field by different colours. It is also possible to distinguish apoptotic from necrotic cells on the basis of their nuclear morphology. The dual staining with acridine orange and ethidium bromide was performed based on the protocol previously described (Allen et al., 1997). Cells were seeded in six well plates for 72 hrs and subjected to treatment with VN and CS separately. After incubation, cells were harvested by trypsinization and washed with PBS, then stained with 0.1mg/ml acridine orange and 0.1mg/ml ethidium bromide. Stained cell suspension 10 µl was placed on a clean glass slide and covered with a cover slip. The cells were then observed under UV fluorescence microscope (Leica) in both red channel (590 nm) and green channel (520-550 nm) and within 30 min before the fluorescence colour starts to fade, (Appendix B28).

The status of cells can be identified by counting the number of each cell exhibiting staining pattern (Abelson et al., 2000).

(i). Bright green chromatin with organized cell structure (viable cells with normal nuclei, live cells).

(ii). Bright green chromatin that is highly condensed or fragmented (viable cells with apoptotic nuclei, early phase of apoptosis)

(iii). Bright orange chromatin with organized cell structure (nonviable cells with normal nuclei, necrotic cells).

(iv). Bright orange chromatin that is highly condensed or fragmented (non-viable cells with apoptotic nuclei, late phase of apoptosis).

3.2.7.2 Detection of apoptosis in HepG2 cells by measuring caspase-3 enzyme activity

Caspase-3 activity was assessed using the caspase-3 Colorimetric Assay Kit (BioVison, Catalog #K106-25), following the manufacturer's instructions is based on spectrophotometric detection of the chromophore *p*-nitroaniline (*p*NA) after cleavage of a specific substrate DEVD-pNA. The protocol is provided in appendix B29. The HepG2 cells were seeded in sterile 60 mm dishes, and at the end of VN and CS treatment, the cells were washed with PBS and lysed in lysis buffer provided by the kit. After freezing and thawing three times, the cell lysate was centrifuged at 20,000× g at 4 ˚C for 15min. The supernatants were collected and DEVD-pNA was then added and incubated for 1-2 hrs at 37 ℃. The concentration of the pNA released was measured at 405 nm, and the quantity of pNA was calculated from a calibration curve of pNA standard. Caspase-3 activity was expressed spectrophotemetrically compared to the control untreated cells. The experiment was carried out in triplicates (George et al., 2010).

3.2.7.3 Lactate dehydrogenase enzyme release (LDH) in HepG2 and WRL68 cells

To determine the effect of VN and CS extracts on membrane permeability in HepG2 and WRL 68 cells, LDH release assay was used. Basically, LDH cytotoxicity assay kit (item No. 10008882) measures cell death in response to chemical compounds using a coupled two-step reaction. In the first step, LDH catalyses the reduction of NAD^+ to NADH and H^+ by oxidation of lactate to pyruvate. In the second step of the reaction, diphorase uses the newly-formed NADH and H^+ to catalyze the reduction of a tetrazolium salt (INT) to highly-colored formazan, which absorbs strongly at 490-520 nm. The amount of formazan produced is propotional to the amount of LDH released into the culture medium as a result of cytotoxicity. The cells were seeded in 96-well culture plates at a density of 2 × 104 cells/well in 100 µL volume and allowed to grow for 18 hrs before treatment. After treatment, the plates were incubated for 24, 48 and 72 hrs, respectively. Then, the supernatant 40 µL was transferred to a new 96 well to determine LDH release, 40 µL was added to the original plate for determination of total LDH. An aliquot of 0.1 M potassium phosphate buffer 100 µL, pH 7.5 containing 4.6 mM pyruvic acid was mixed to the supernatant using repeated pipetting. Then, 0.1 M potassium phosphate buffer 100 µL, pH 7.5 containing 0.4 mg/mL reduced *β*-NADH was added to the wells. The kinetic changes were read for 1 min using ELISA micro plate reader in absorbance at wavelength 340 nm. This procedure was repeated with 40 µL of the total cell lysate to determine total LDH U/well (Al-Qubaisi et al., 2011). The protocol is provided in appendix B30.

3.3 Statistical Analysis

All data were expressed as mean ± standard error of the mean (SEM) and statistical analysis was performed using SPSS for Windows version 17.0 (SPSS Inc. Chicago, IL, USA). One-way analysis of variance (ANOVA) followed by Bonferroni post hoc test was applied to test for statistically significant differences between groups at $P < 0.05$.

For pathological scoring for the staging of liver cirrhosis, the following formula was used:

$$A = \frac{X1(Y1) + X2(Y2) + X3(Y_3)}{N}$$

A= Average
X= Score
Y= Stage or grade
N= Number of specimens

The minimum inhibitory concentration (IC50) was determined by using Masterplex2010 software (5Parameters logistics).

Chapter 4

Results

4.1 PASS Prediction and Assistant Experimental Design

In order to accelerate the search for potent natural product, computer-aided drug discovery program PASS was used to predict the hepatoprotective, antioxidant and antiproliferative properties. PASS prediction tools are constructed using 20000 principal compounds (Lagunin et al., 2003) and about 4000 kinds of biological activity on the basis of structural formula with mean accuracy about 90% (Pogrebnyak, 1998). The result of prediction is presented as the list of activities with appropriate Pa and Pi ratio. Pa and Pi are the estimates of probability for the compound to be active and inactive, respectively. It is reasonable that only those types of activities may be revealed by the compound, which Pa > Pi. If Pa > 0.3 the compound is likely to reveal this activity in experiments, but in this case the chance of being the analogue of the known pharmaceutical agents for this compound is also high. Thus, potential biological effects of the plant constituents were predicted by PASS program based on structure activity relationship (SAR) analysis of the training set containing thousands of compounds which have many kinds of biological activity. Therefore, before we started our experiments, we used PASS program to validate whether VN and CS constituents based on SAR strategy is in agreement with the SAR of the training set of the PASS database. For the training set, two subsets of databases of drugs and non-drugs are used.

Accordingly, a portion of the predicted biological activity spectra (lipid peroxidase inhibitor, antioxidant, free radical scavenger, hepatoprotectant, caspase-3 stimulant and antiproliferative) for the VN and CS extracts isolated compounds are given in Table 4.1 and Table 4.2 respectively.

In Table 4.1, we found that 7, 8 dimethyl herbacetin 3-rhamnoside, agnuside, negundoside and vitegnoside showed highest percentage of hepatoprotective activity (91.2%, 98.3%, 98.6% and 92.4%) in comparison to other compounds. Moreover, vitegnoside and 7,8-dimethyl herbacetin 3-rhamnoside shared similar features including antioxidant, free radical scavenging activity and lipid peroxidation inhibition. On the other hand, 5,3'-dihydroxy-7,8,4'-trimethoxy flavanone showed highest antiproliferative activity (88.6%) while 7,8- dimethyl herbacetin 3-rhamnoside have the strongest caspase-3 stimulant activity (81.2%).

Table 4.1: Part of the predicted biological activity spectra for the phytoconstituents of VN extract

Chemical compounds	Biological activity											
	Lipid peroxidation inhibitor		Antioxidant		Free radical scavengers		Hepatoprotectant		Caspase-3 stimulant		Antiproliferative	
	Pa	Pi	Pa	Pi	Pa	P	Pa	Pi	Pa	Pi	Pa	Pi
5-hydroxy-7,4'dimethoxy flavone	0.813	0.003	0.699	0.004	0.786	0.003	0.717	0.007	0.741	0.009	0.737	0.012
5-hydroxy-3,6,7,3',4'-Pentamethoxy flavone	0.765	0.004	0.671	0.004	0.765	0.003	0.744	0.006	0.706	0.011	0.754	0.011
5, 3' dihydroxy-7, 8, 4'-trimethoxy flavanone	0.798	0.004	0.749	0,004	0.849	0.002	0.741	0.006	0.778	0.007	0.886	0.005
(5,7-dihydroxy-6,4'dimethoxy flavanone	0.711	0.005	0.644	0.004	0.751	0.003	0.658	0.009	0.734	0.009	0.855	0.005
7, 8 dimethyl herbacetin 3-rhamnoside	0.952	0.002	0.874	0.003	0.973	0.001	0.912	0.002	0.812	0.005	0.817	0.007
Agnuside	0.304	0.062	0.788	0.003	0.518	0.009	0.983	0.001	0.679	0.012	0.445	0.005
Negundoside	0.415	0.031	0.598	0.005	0.698	0.004	0.986	0.001	0.611	0.006	0.554	0.014
Vitegnoside	0.920	0.002	0.798	0.003	0.956	0.001	0.924	0.002	0.749	0.008	0.715	0.013

Pa—probability “to be active”; Pi—probability “to be inactive”

Table 4.2 showed that the highest hepatoprotective activity was belonged to Sappanchalcone (92%) in comparison to the rest. Although 3-deoxy sappanchalcone and 3-omethybrazilin showed > 50% of antioxidant, radical scavenging and lipid peroxidation inhibition activities, however, sappanchalcone showed the strongest activity (83%, 95% and 81%) respectively. On the other hand, sappanchalcone showed high antiproliferative (87.1%) property, while the strongest caspase-3 stimulant belonged to 3-deoxy sappanchalcone (89.9%).

Table 4.2 Part of the predicted biological activity spectra for the phytoconstituents of CS extract.

Chemical compounds	Biological activity											
	Lipid peroxidation inhibitor		Antioxidant		Free radical scavengers		Hepatoprotectant		Caspase-3 stimulant		Antiproliferative	
	Pa	Pi	Pa	Pi	Pa	Pi	Pa	Pi	Pa	Pi	Pa	Pi
Protosappanin A	0.495	0.017	0.324	0.019	0.360	0.021	0.264	0.076	0.415	0.045	0.617	0.024
Protosappanin B	0.419	0.030	0.416	0.011	0.366	0.021	0.454	0.024	0.758	0.008	0.602	0.026
Lyoniresinol	0.355	0.048	0.246	0.,037	0.233	0.054	0.383	0.035	0.319	0.104	0.390	0.078
(8S,8'S)-bisdihydrosiringenin	0.415	0.031	0.610	0.004	0.424	0.015	0.434	0.027	0.442	0.038	0.251	0.066
Sappanchalcone	0.810	0.003	0.83	0.003	0.95	0.001	0.92	0.002	0.517	0.025	0.871	0.003
3-deoxy sappanchalcone	0.655	0.006	0.49	0.007	0.626	0.005	0.590	0.013	0.899	0.003	0.788	0.009
brazilein	0.372	0.043	0.304	0.022	0.440	0.014	-	-	0.326	0.097	0.729	0.021
3-omethybrazilin	0.423	0.029	0.292	0.024	0.733	0.004	0.314	0.055	0.542	0.022	0.343	0.044
Brazilin	0.393	0.037	0.293	0.024	0.667	0.004	0.280	0.067	0.416	0.045	0.326	0.049
sappanone B	0.410	0.032	0.377	0.014	0.392	0.018	0.302	0.059	0.483	0.030	0.173	0.135
3-deoxysappanone B	0.445	0.024	0.384	0.014	0.351	0.022	0.288	0.064	0.417	0.045	0.422	0.028
3-deoxy-4-O-methylepisappanol	0.350	0.050	0.276	0.028	0.262	0.041	0.260	0.079	0.466	0.033	0.364	0.038

Pa—probability “to be active”; Pi-probability“to be inactive”

4.2 Antioxidant Properties of VN and CS Extracts

4.2.1 Mean inhibition of 1,1–diphenyl–2–picrylhydrazyl free radicals

DPPH assay was utilized to evaluate the ability of the investigated VN and CS ethanolic extracts to act as donors of hydrogen atoms or electrons in transformation of DPPH radical into its reduced form DPPH-H. The scavenging activities of VN, CS extracts, ascorbic acid, gallic acid and BHT against stable free radicals (DPPH) were compared as shown in Figure **4.1**.These tested extracts possessed radical scavenging activity, and this activity was increased by increasing the concentration of the sample extract. Percentage of radical scavenging activity for VN extract at the highest concentration was 79.43±1.3, BHT 82.53±1.7, gallic acid 89.51±1.14 and ascorbic acid 90.65±1.34. The percentage of inhibition of VN extract was significantly ($P< 0.05$) lower than the BHT, gallic acid and ascorbic acid. The maximum inhibitory concentration (IC50) to inhibit 50% of the DPPH free radicals for VN extract was at 13.31 µg/ml as shown in Table 4.3. CS extract could reduce the stable purple-coloured radical DPPH into the yellow-coloured DPPH-H. Figure **4.1** shows that CS extract possessed radical scavenging activity and this activity was increased by increasing the concentration of the sample extract. Percentage of radical scavenging activity at the highest concentration of CS was 68.25±1.06.

The maximum inhibitory concentration (IC50) to inhibit 50% of the DPPH-free radicals for CS extract was 23.07µg/ml as shown in Table 4.3. Results indicate that the ability of CS to scavenge DPPH is lower than that of VN which has better scavenging activity that approaches the capacity of the standard BHT.

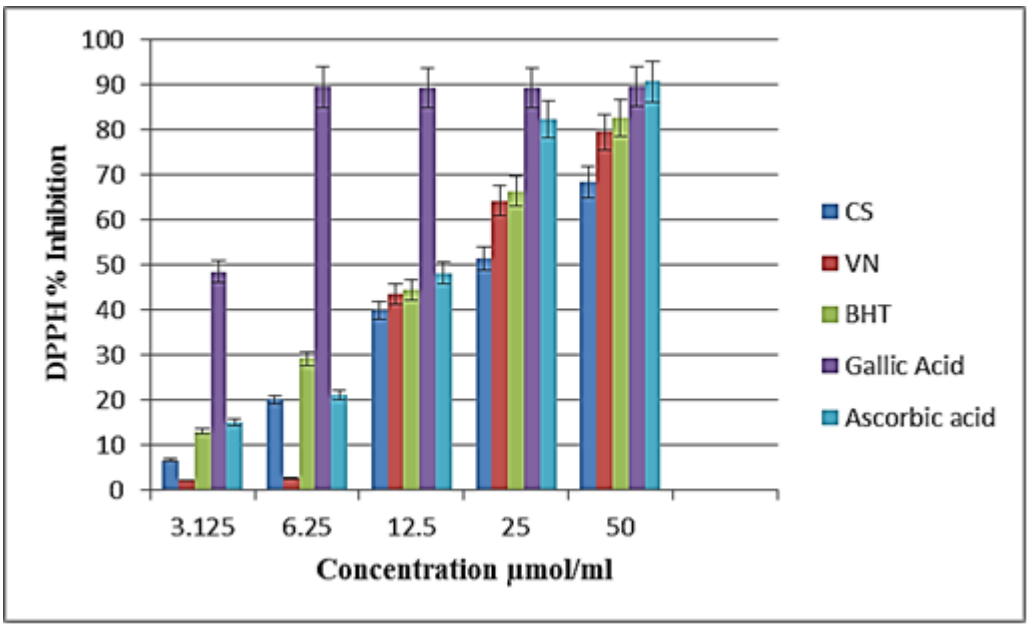

Figure 4.1: The percentage of scavenging activity of ethanolic extract of VN and CS gainst DPPH.

Table 4.3: IC50 value and % inhibition of the DPPH radical scavenging assay

µmol/ml		**Max. inhibition % ± S.E.M** [a]			
	VN	CS	BHT	Gallic acid	Ascorbic acid
3.125	2.35 ±0.07	6.75±0.35	13.05 ±0.07	48.4 ± 0.01	15.1 ±0.14
6.25	2.58 ± 0.4	20.1± 0.14	29.15 ±0.21	89.3 ±0.51	21.24 ±0.86
12.3	43.5 0.47	39.9±0.5	44.5 ±0.07	89.1 ±1.27	48.06 ±1.18
25	64.2 ±0.94	51.4±1.28	66.32 ±0.96	89.17 ±1.65	82.09 ±1.09
50	79.43 ±1.3	68.25±1.06	82.53 ±1.7	89.51 ±1.14	90.65 ±1.34
IC50 [b] **value µg/ml ± S.E.M**	13.31± 0.18	23.07± 0.07	13.8 ± 0.14	3.1± 0.08	12.9 ± 0.12

[a]SEM: standard error of the mean. [b]IC50: 50% effective concentration. IC50 is determined by using MasterPlex 2010 software (5 Parameters logistics).

4.2.2 Ferric reducing antioxidant power (FRAP) capacity of the crude extracts

As illustrated in Figure 4.2**,** the reducing ability of VN and CS extracts was in the range of 866.11-713.89 µmol Fe^{+2}/g, respectively. The FRAP values for VN extract was significantly lower than gallic acid, but higher than BHT and ascorbic acid. While the FRAP values for CS was significantly ($P<0.05$) lower than ascorbic acid and gallic acid, but significantly ($P<0.05$) higher than BHT as shown in Figure 4.2. Based on these readings, it is reasonable to extrapolate that VN extract has high antioxidant activity and CS extract must be containing sufficient acceptable level of anti-oxidant activity, supporting its free radical scavenging property, in helping the liver maintain its status quo.

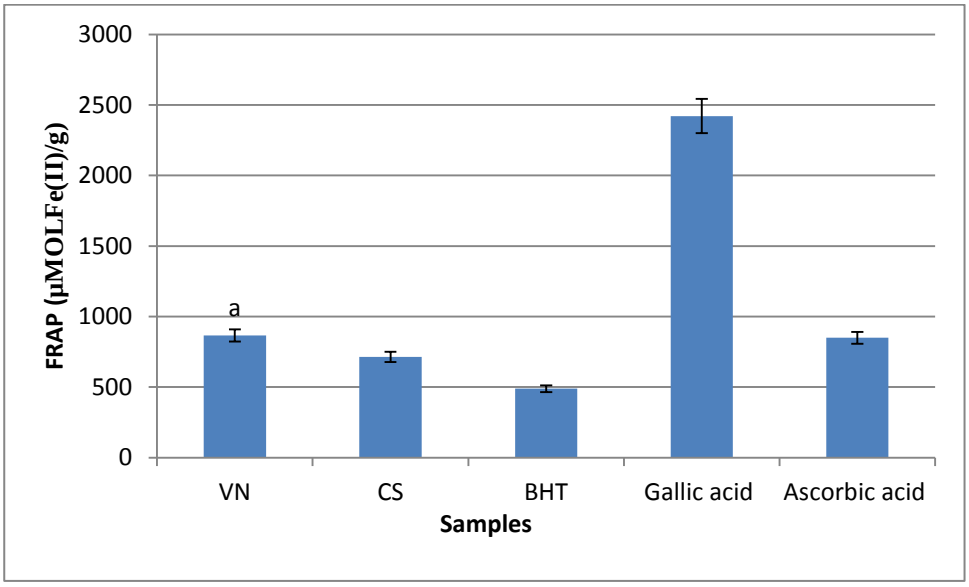

Figure 4.2: Ferric reducing antioxidant property (FRAP) of the leave extracts of VN and CS.

Values are presented as means ± SEM, [a] $P< 0.05$ versus BHT

4.2.3 Total phenolic and total flavonoids contents (TPC and TFC)

Figure 4.3 shows that both the plants extracts investigated had appreciable amounts of phenolic compounds. Ethanol extract of VN had phenolic and flavonoids contents values 249.00 ± 0.002 mg Quercetin / g extract and 120.9 ± 0.002 mg /g extract respectively. While the phenolic and flavonoids contents of the ethanol extract of CS were 196.0 ± 0.013 ± mg Quercetin / g extract and 131.8± 0.023 mg Quercetin / g extract respectively.

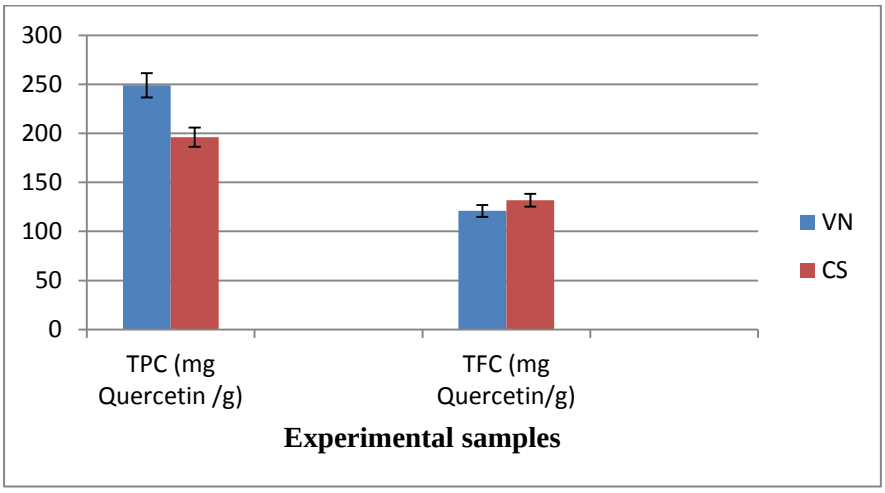

Figure 4.3**:** VN and CS total phenolic (TPC) and flavonoids (TFC) contents

4.2.4 *In vitro* antioxidant activity of VN and CS against H_2O_2 in WRL68 cell lines

The oxidative stress was induced by exposing WRL 68 cells to 1000 µM H_2O_2 for 2 hrs, while the protective effect of each plant extract reduces oxidative stress. Cells were first pre-incubated with VN and CS for 2 hrs and then treated with 1000 µM H_2O_2. The antioxidant activities of VN and CS were positively correlated with the improvement of the cell viability. It is obvious that H_2O_2 lead to the production of (ROS), which in consequence reduced the antioxidant enzymes such as SOD and GPx.

However, pre-treatment with plant extract decreased the free radical formation; therefore the antioxidant enzymes level became higher. Our results revealed that H_2O_2 exposed cells caused a statistically significant decrease, while cells with pre-incubation with VN or in CS revealed significantly increase ($P < 0.05$) in GPx activity.

On the other hand, lipid peroxidation value, measured by MDA production, significantly increased ($P < 0.05$) in H_2O_2 -induced oxidative stress group compared to the untreated cells. Whereas in cells pre-incubated with VN or CS extract, lipid peroxidation was significantly ($P < 0.05$) prevented (Table 4.4.).

Table 4.4: Effects of H_2O_2, VN and CS extracts on the antioxidant enzymes and MDA in H_2O_2 – induced WRL 68 cell line

Group	**SOD (U/mg protein)**	**GPx (nmol/ mg protein)**	**MDA (nmol/g protein)**
Normal Control	10.61 ± 0.010	27.14 ± 0.30	17.00 ± 1.019
H_2O_2	10.00 ± 0.065	10.98 ± 0.18[a]	46.94 ± 1.730[a]
VN extract	10.37 ± 0.150	22.05 ± 0.19[b]	23.17 ± 2.165[b]
CS extract	8.94 ± 0.025[b]	19.01 ± 1.110[b]	28.5 ± 6.830[b]

Values are presented as means ± SEM, [a] $P<0.05$ versus normal control group, [b] $P< 0.05$ versus H_2O_2 group

4.3 Hepatoprotective Effect of VN and CS Extracts on Liver Cirrhosis

4.3.1 Body weight

The mean body weight of all groups of rats which were treated with VN and CS is shown in Figure 4.4 respectively. Generally, just before sacrifice, marked growth retardation was noted in hepatotoxic group after 12 weeks of treatment. There was a significantly lower body weight ($P<0.05$) of TAA group in comparison to the normal control. Although there was increased of body weight in VN 300+TAA, VN 100+TAA , CS300+TAA and SY+TAA but still there was no significant change in body weights in these groups when compared to the TAA group. It was also noted that, there was a significant reduction in body weight in CS100+TAA in comparison to normal group.

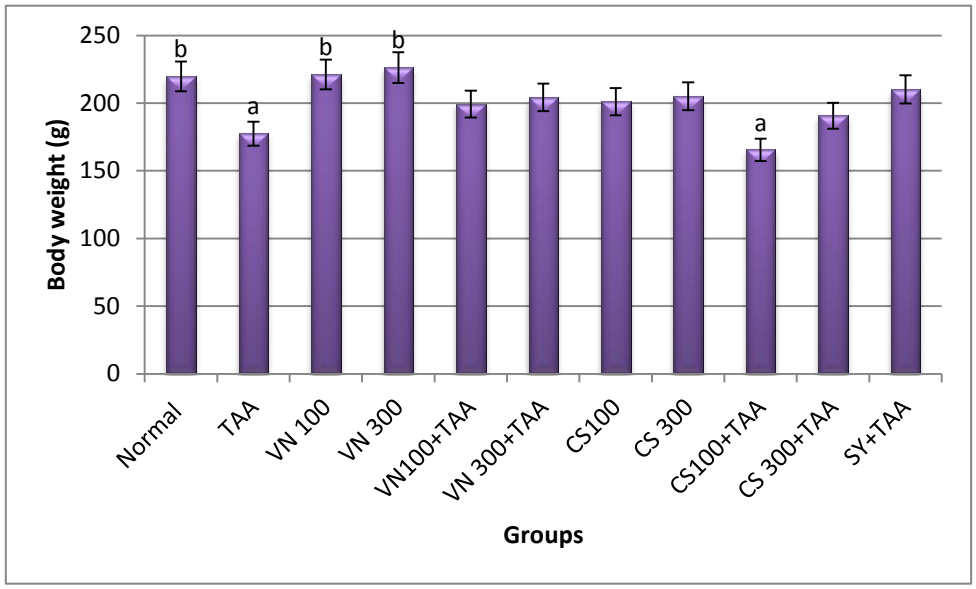

Figure 4.4: Effect of VN and CS crude extracts on the body weight from the rats at the end of the 12 weeks.

The data were stated as mean ±S.E.M. Means with different superscripts are significantly different. [a] $P < 0.05$ versus normal control group and [b] $P < 0.05$ versus TAA control group. SY stands for silymarin (standard hepatoprotective drug).

4.3.2 Gross anatomical analysis

Grossly, the livers of the TAA group were congested, and the liver surfaces showed many spots of nodules, firm in consistency and relatively harder in comparison with the normal gross features of the livers from VN100, VN300, CS100 and CS300. In contrary, the livers of VN100+TAA, VN300+TAA and CS300+TAA groups were with much fewer nodular spots, softer in consistency and with a comparatively normal liver size than the TAA group (Figure 4.5). On the other hand, CS100+TAA showed more nodular spots and larger in size in comparison to other extract treated groups (Figure 4.6).

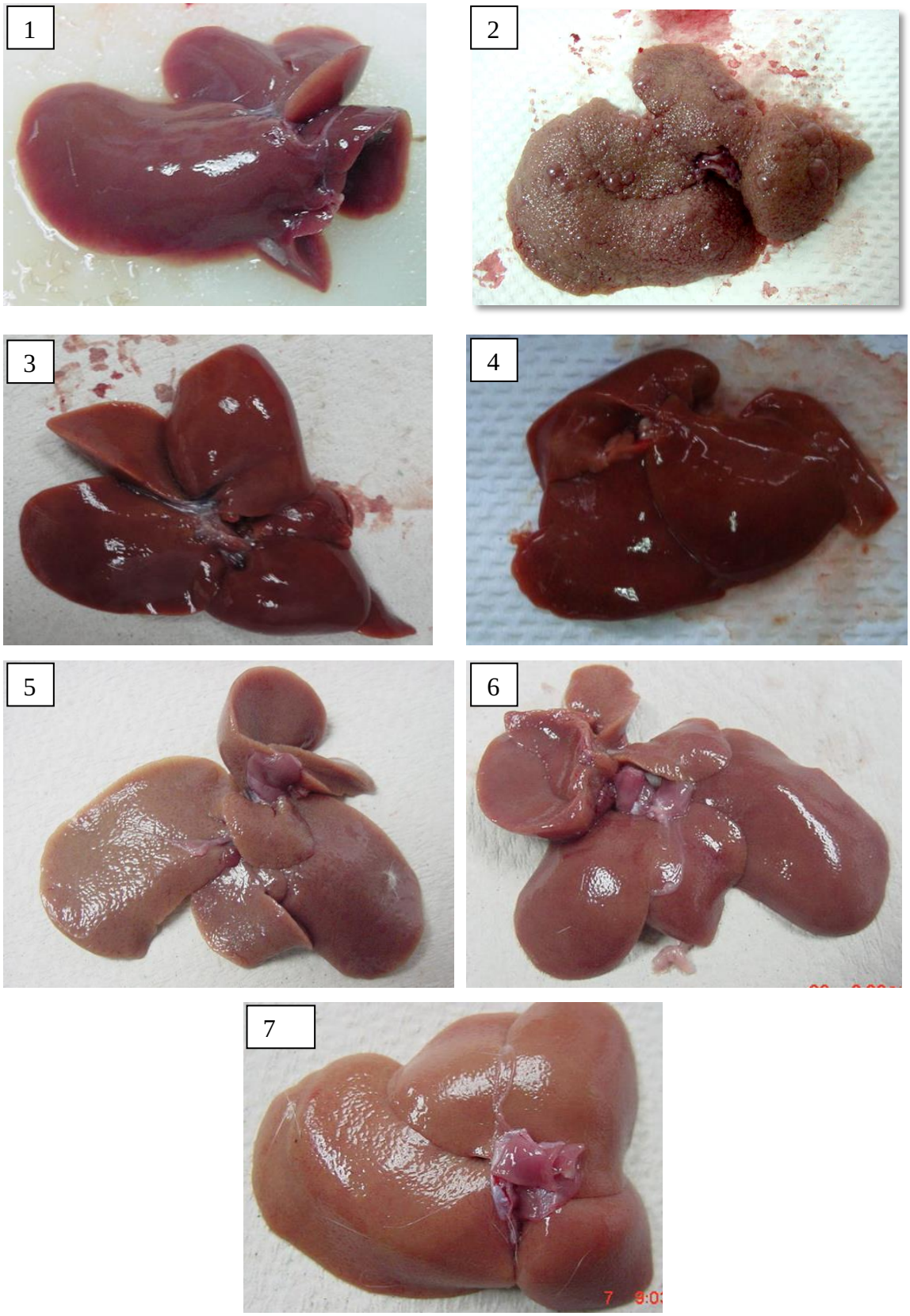

Figure 4.5: Photographs showing the macroscopic appearances of livers from different experimental groups treated with VN, SY and TAA.

1. Control group-showing regular smooth surface, **2**. TAA group (Hepatotoxic group)-showing shrinkage of the liver with multiple cirrhotic nodules on the whole surface of the liver, **3**.VN100 group- showing smooth surface **4** VN300 group-showing smooth surface, **5**. VN 100+TAA group-showing a nearly smooth surface, **6**. VN300 +TAA group-showing smooth surface, **7**. SY group-showing smooth surface.

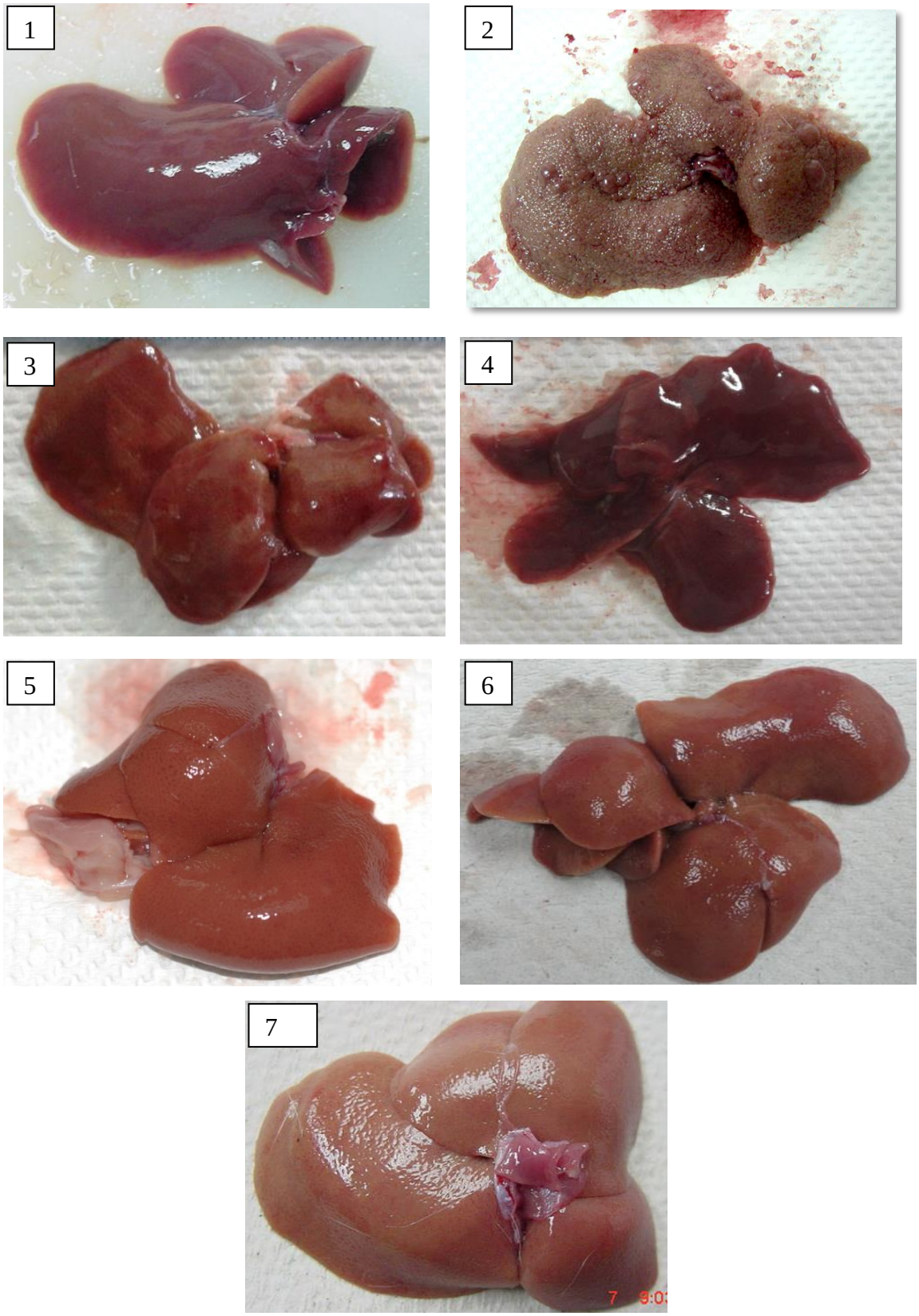

Figure 4.6: Photographs showing the macroscopic appearances of livers from different experimental groups treated with CS, SY and TAA.

1. Control group-showing regular smooth surface, 2. TAA group (Hepatotoxic group)-showing shrinkage of the liver with multiple cirrhotic nodules on the whole surface of the liver, 3. CS100 group-showing smooth surface, 4. CS300 group- showing smooth surface, 5. CS 100 +TAA group-showing micronodular surface, 6.CS300+TAA group- showing nearly smooth surface, 7. SY group-showing smooth surface.

4.3.3 Liver and spleen weights

The mean liver weight for all groups of rats is shown in Figure 4.7. There was a significant increase in liver weight ($P < 0.05$) in TAA group in comparison to normal group. At the same time there was significant ($P < 0.05$) decrease in liver weight in VN300+TAA group in comparison to TAA group. However, there was no significant change in liver weight between any other extract-treated groups in comparison to TAA group. Concurrently, the liver to body weight ratio showed a corresponding significant ($P < 0.05$) difference between the SY and VN-treated groups compared to TAA group, while there was no significant ($P < 0.05$) change in CS-treated group in comparison to TAA (Figure 4.8). Furthermore, a significant change in the weight of the spleen and spleen index for all groups of rats in comparison to TAA group was noticed (Figure 4.7).

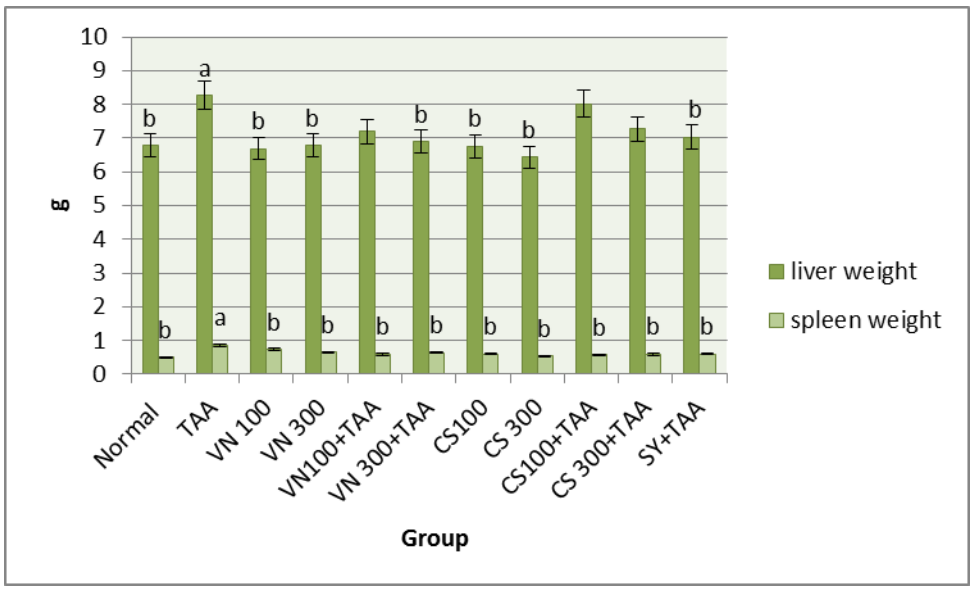

Figure 4.7 : Liver and spleen weights of the rats at the end of 12 weeks of treatment.

The data were stated as mean ± S.E.M. Means with different superscripts are significantly different. [a] $P<0.05$ versus normal control group and [b] $P< 0.05$ versus TAA control group SY stands for silymarin (standard hepatoprotective drug).

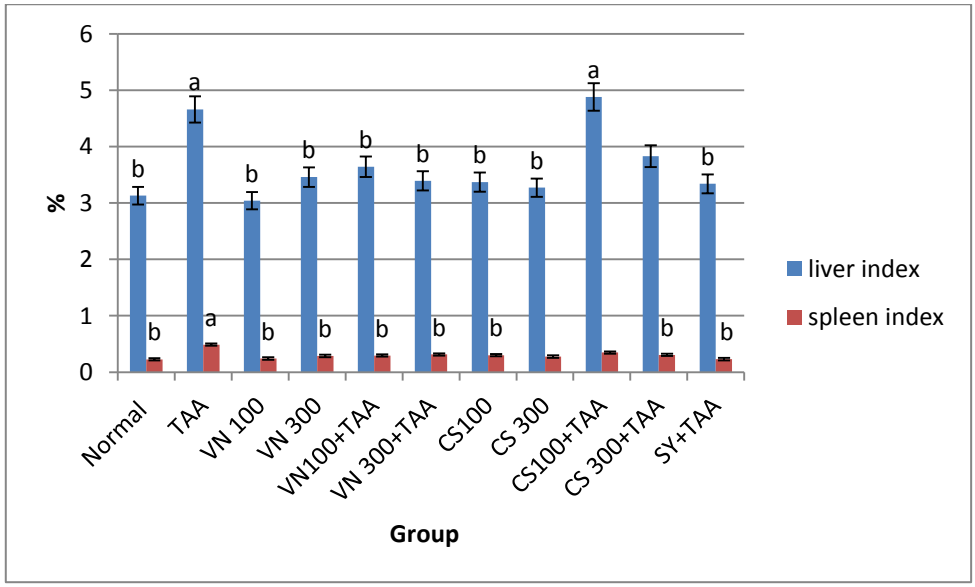

Figure 4.8: Liver and spleen indexes of the rats at the end of 12 weeks.

The data were stated as mean ± S.E.M. Means with different superscripts are significantly different. [a] $P<0.05$ versus normal control group and [b] $P< 0.05$ versus TAA control group. SY stands for silymarin (standard hepatoprotective drug).

4.3.4 Biochemical analysis

4.3.4.1 Liver enzymes activity

The mean level of ALT, AST, and AP enzymes of all groups of rats is shown in Figure 4.9. In general there was a significant ($P < 0.05$) higher level in the mean level of ALT, AST, and AP enzymes in TAA group in comparison to normal group. Besides that, there was a significant ($P < 0.05$) lower level in ALT, AST, AP enzymes in all low and high doses for VN and CS groups in comparison to TAA group Figure 4.9. All VN100+TAA, VN 300+TAA and SY+TAA groups showed significant ($P < 0.05$) lower level in ALT, AST and AP enzymes in comparison to TAA group.

In CS300+TAA group, there was significant lower level ($P < 0.05$) of AST and AP enzymes in comparison to TAA group. Although ALT level was lower in CS300+TAA group, there was no significant change in comparison to TAA group.

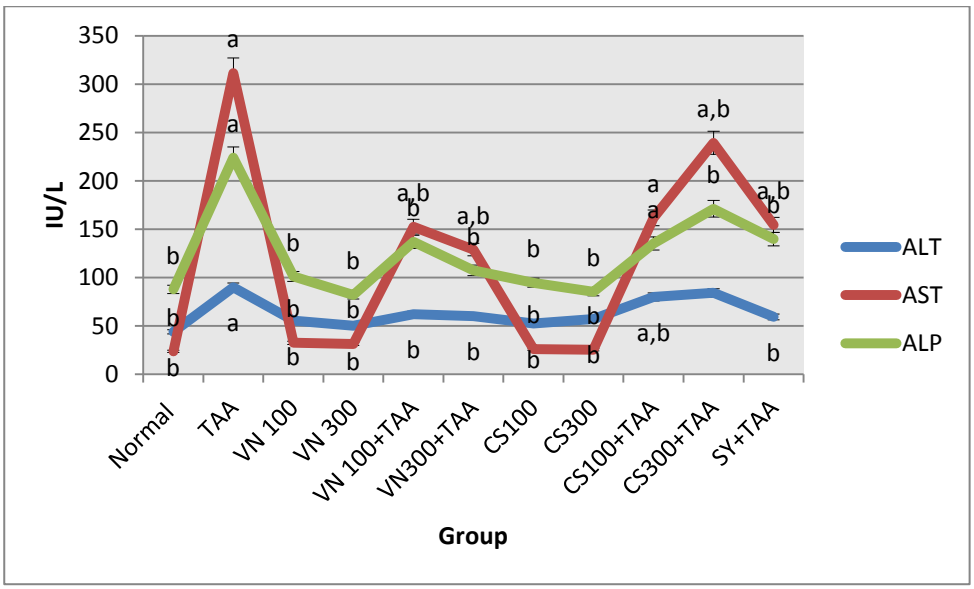

Figure 4.9: The mean liver enzymes activity in all groups of rats after 12 weeks of treatment.

The data were stated as mean ± S.E.M. Means with different superscripts are significantly different. [a] P<0.05 versus normal control group and [b] P< 0.05 versus TAA control group. SY stands for Silymarin (standard hepatoprotective drug).

4.3.4.2 Bilirubin level

The mean serum bilirubin level in all groups of rats is shown in Figure 4.10. The mean serum bilirubin level of the TAA group showed the highest level (P < 0.05) in comparison to normal group, followed by significant (P < 0.05) higher level in CS100+TAA group in comparison to normal. At the same time, SY+TAA, all VN-treated groups with low and high doses and CS-treated groups with low and high doses except CS100+TAA, showed significant (P < 0.05) lower level in bilirubin in comparison to TAA.

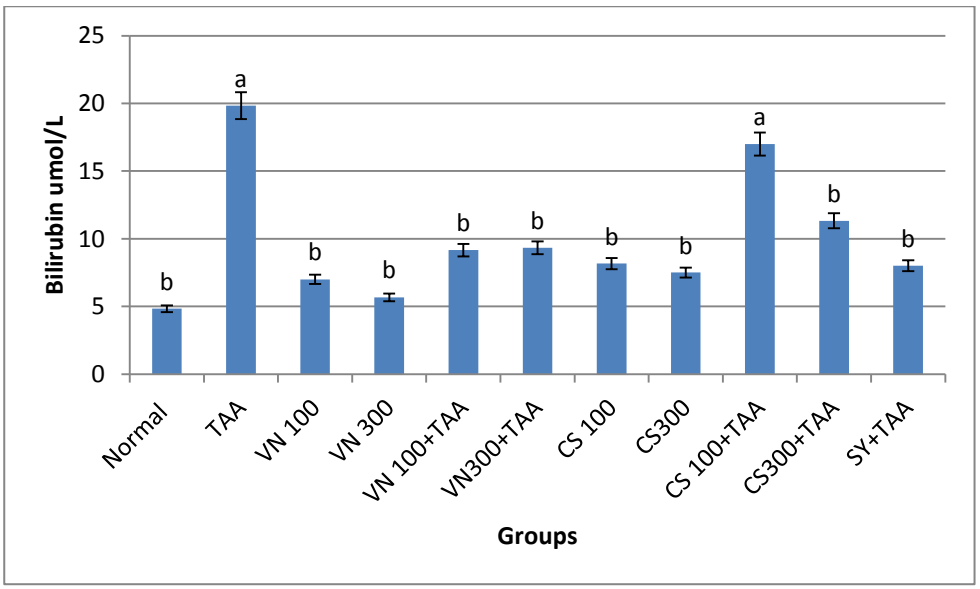

Figure 4.10: The mean serum bilirubin level in all groups of rats after 12 weeks of treatment.

The data were stated as mean ± S.E.M. Means with different superscripts are significantly different. [a] P<0.05versus normal control group and [b] P< 0.05 versus TAA control group. SY stands for silymarin (standard hepatoprotective drug).

4.3.4.3 Total serum protein level

The mean total serum protein level of all groups of rats is shown in Figure 4.11. After 12 weeks of treatment, there was a lower level of the mean total serum protein of TAA group, but still no significant change. As for other experimental groups, generally, there was no significant increase in total serum protein level in comparison to TAA group.

a. Albumin level

The mean albumin level of all groups of rats is shown in Figure 4.11. There was a significant lower level (P < 0.05) of the mean serum albumin in TAA group compared

to the normal control group. SY+TAA, all VN-treated groups and all CS-treated groups showed significant higher level of albumin in comparison to TAA group, except CS100+TAA group which showed significant lower level of albumin in comparison to normal group (Figure 4.11).

b. Globulin level

The mean globulin level of all groups of rats is shown in Figure 4.11. Against that reduction of albumin level, there was a significant ($P < 0.05$) higher level in the globulin in TAA group in comparison to normal control group. SY+TAA, VN100, VN300, VN100+TAA, VN300+TAA, CS100 and CS300 showed significant ($P < 0.05$) lower globulin level in comparison to TAA group.

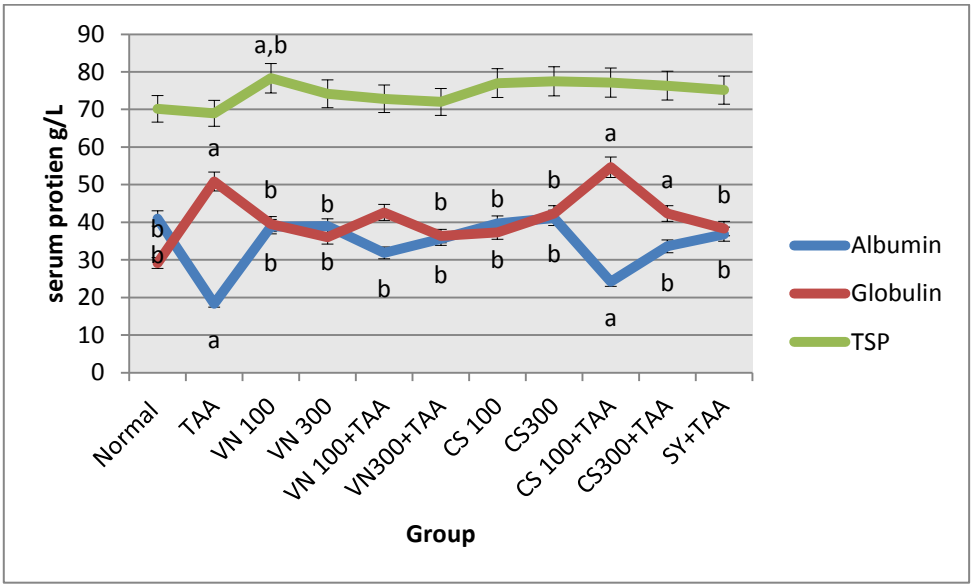

Figure 4.11**:** The mean total serum protein, albumin and globulin level in all groups of rats after 12 weeks of treatment.

The data were stated as mean ±S.E.M. Means with different superscripts are significantly different. [a] P<0.05 versus normal control group and [b]P < 0.05 versus TAA control group. SY stands for silymarin (standard hepatoprotective drug).

4.3.4.4 Gamma glutamyl transpeptidase activity (GGT)

The mean albumin level of all groups of rats is shown in Figure 4.12. There was a significant higher level (P < 0.05) in the mean GGT in TAA group in comparison to normal group. SY+TAA, all VN-treated groups and all CS-treated groups showed significant higher level in GGT in comparison to TAA group, except CS100+TAA group showed significant higher level in GGT in comparison to normal control group.

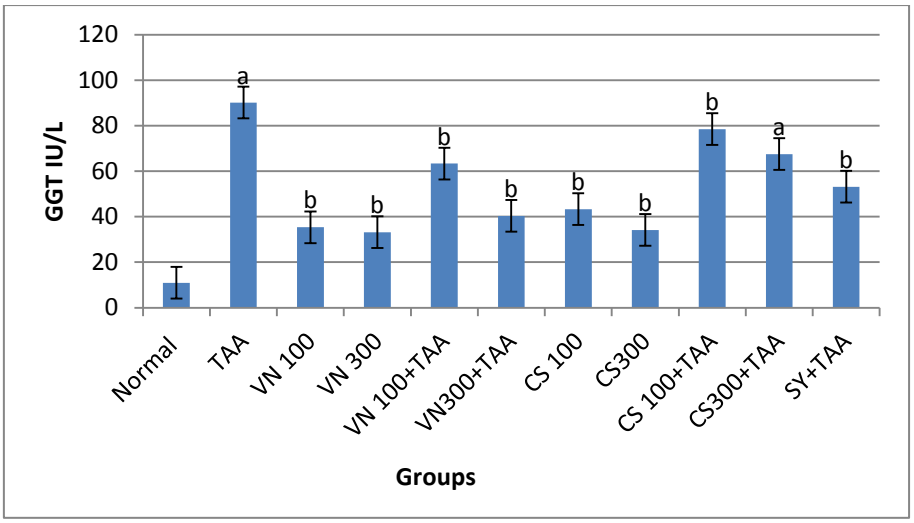

Figure 4.12: The mean gamma glutamyl transpeptidase activity in all groups of rats after 12 weeks of treatment.

The data were stated as mean ±S.E.M. Means with different superscripts are significantly different. [a] P<0.05 versus normal control group and [b]P< 0.05 versus TAA control group. SY stands for silymarin (standard hepatoprotective drug).

4.3.4.5 Lactate dehydrogenase activity (LDH)

The mean LDH of all groups of rats is shown in Figure 4.13. There was a significant higher level in LDH in TAA group in comparison to the normal control group. There was a significant lower level in LDH level all experimental groups in comparison to TAA group.

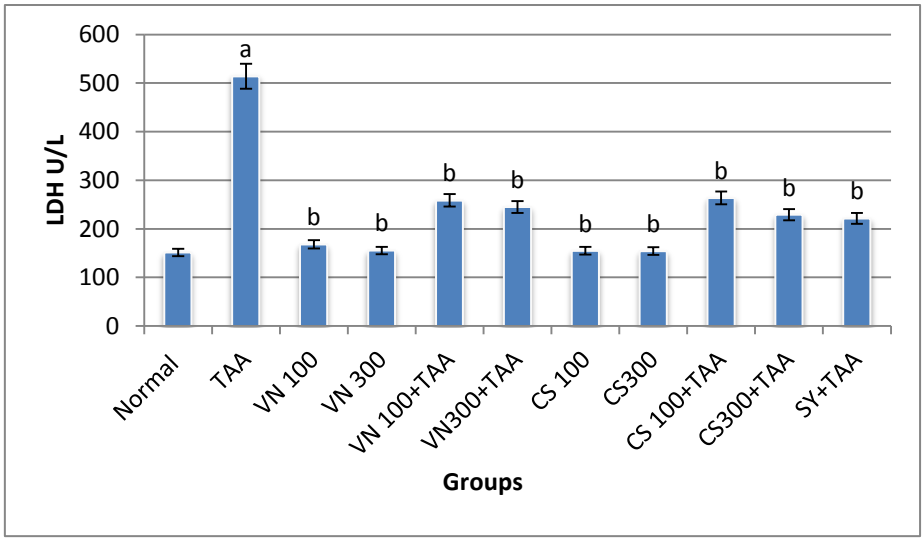

Figure 4.13: The mean lactate dehydrogenase activity in all groups of rats after 12 weeks of treatment.

The data were stated as mean ±S.E.M. Means with different superscripts are significantly different. [a] P<0.05 versus normal control group and [b]P < 0.05 versus TAA control group. SY stands for silymarin (standard hepatoprotective drug).

4.3.4.6 Lipid profile parameters

a. Total serum cholesterol level

The mean serum cholesterol level of all groups of rats is shown in Figure 4.14. There was significant (P < 0.05) higher level in the serum cholesterol in TAA in comparison to normal group. VN300, CS300, CS100 and CS300+TAA groups showed

significant (P < 0.05) lower serum cholesterol level in comparison to TAA group. Although SY+TAA ,VN 300+TAA, VN 300+TAA and CS100+TAA showed lower cholesterol level in comparison to TAA group, but still no significant (P < 0.05) change has been shown.

b. Triglyceride level

The mean serum triglyceride level of all groups of rats is shown in Figure 4.14. There was significant (P<0.05) higher level in serum triglyceride in TAA in comparison to normal group. All the experimental treated groups showed significant (P < 0.05) lower level in serum triglyceride in comparison to TAA group.

c. Low density lipoprotein (LDL)

The mean serum LDL level of all groups of rats is shown in Figure 4.14. There was significant (P < 0.05) higher level in LDL in TAA in comparison to normal group. All the experimental treated groups showed significant (P < 0.05) lower level in LDL in comparison to TAA group, except for CS100+TAA showed significant (P < 0.05) higher LDL level in comparison to the normal control group.

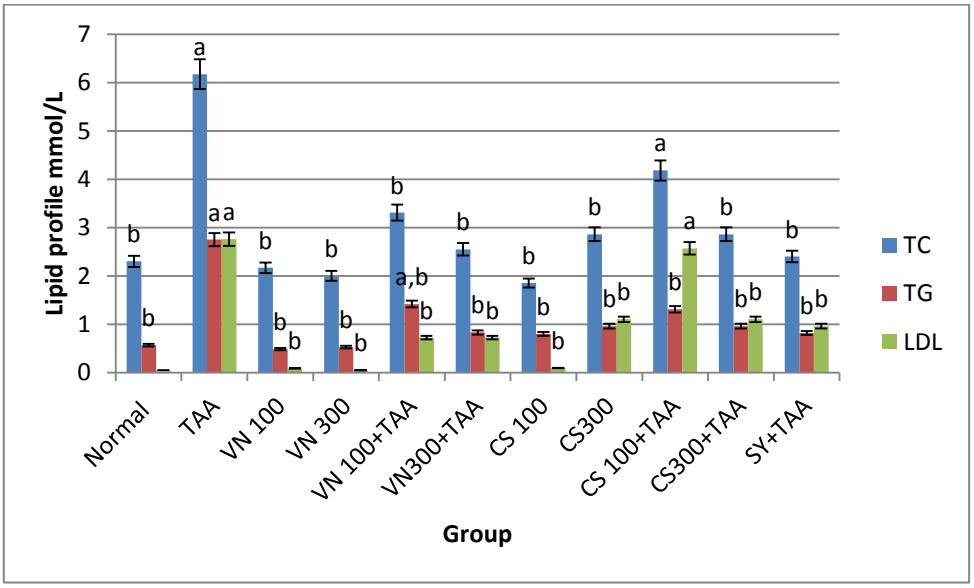

Figure 4.14: Effect of TAA, SY, VN and CS ethanolic extract on lipid profile parameters in TAA-induced liver fibrosis.

The data were stated as mean ±S.E.M. Means with different superscripts are significantly different. [a] P<0.05 versus normal control group and [b]P < 0.05 versus TAA control group. SY stands for silymarin (standard hepatoprotective drug).

4.3.4.7 Serum glucose level

The mean serum glucose level of all groups of rats is shown in Figure 4.15. There was significant (P < 0.05) higher level in serum glucose in TAA in comparison to normal group. VN100, VN300, CS100 and CS 300 groups showed significant (P<0.05) lower level in glucose in comparison to TAA group.

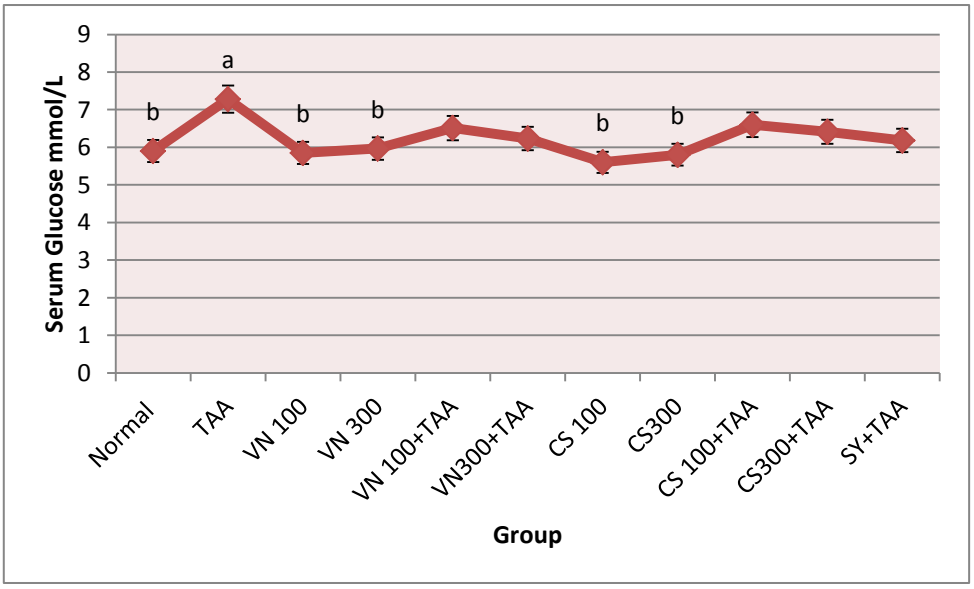

Figure 4.15: The mean serum glucose level in all groups of rats after 12 weeks of treatment.

The data were stated as mean ±S.E.M. Means with different superscripts are significantly different. [a] P<0.05 versus normal control group and [b]P< 0.05 versus TAA control group. SY stands for silymarin (standard hepatoprotective drug).

4.3.4.8 Sub-chronic toxicity

In the present study, oral dosing of the tested extracts to rats in doses of 100 and 300 mg/kg for 12 weeks did not show any significant effect on the levels of ALT, AST, total bilirubin, total proteins, and albumin in their as compared to normal control group as shown in Figure 4.9; page 102, Figure 4.10; page 103 and Figure 4.11; page 104. No significant change in the mean values of lipid profile parameters and serum glucose was estimated in serum of rats following 12 weeks of extracts administration at doses of 100 and 300 mg/kg when compared with the control as illustrated in (Figure 4.14; page 107 and Figure 4.15; page 108).

4.3.4.9 Oxidative stress marker

Oxidative stress parameter (liver tissue homogenate MDA) is shown in Figure 4.16. Generally, rats treated with TAA only, had significantly higher levels of oxidative stress biomarkers ($P<0.05$) than normal rats and the experimental treatment groups. Notably, experimental rats treated with low dose and high dose VN extract, low dose and high dose CS extract and SY- treated rats had significantly lower levels ($P< 0.05$) of liver MDA compared to TAA group. These results suggest that treatment with VN and CS extracts have the ability to protect hepatic cells from further damage during liver injury.

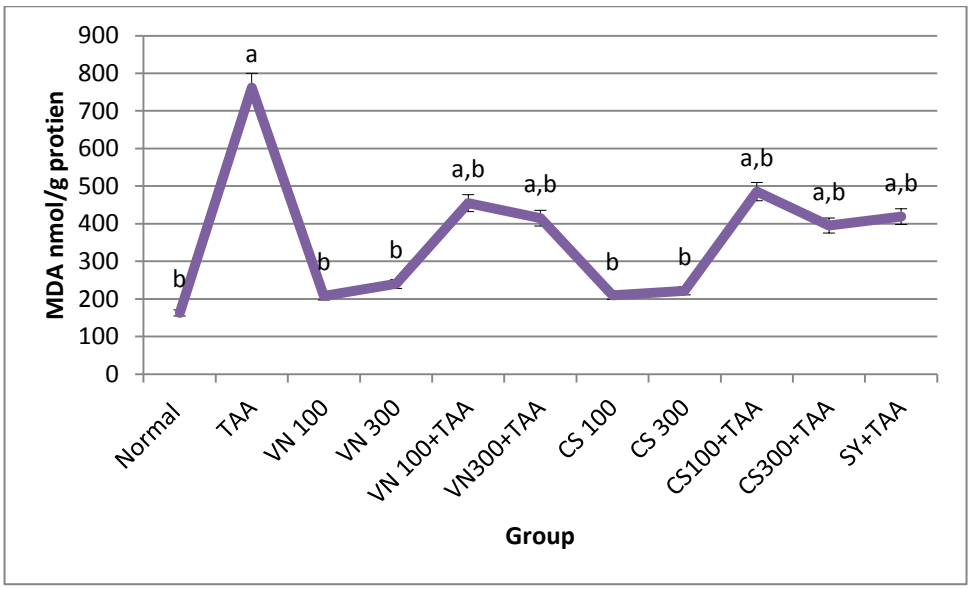

Figure 4.16: Effect of VN and CS extract on MDA liver homogenate in rats at the end of 12 weeks.

The data were stated as mean ±S.E.M. Means with different superscripts are significantly different. $^{a}P < 0.05$ versus normal control group and $^{b}P < 0.05$ versus TAA control group. SY stands for silymarin (standard hepatoprotective drug).

4.3.4.10 Hepatocellular antioxidant enzymes

CAT, SOD, and GPx are some of the components of intrinsic antioxidant defence system were significantly ($P<0.05$) increased in high dose treatment groups of both plants and SY, while decreased in TAA induced groups due to long term excretion of free radicals. These antioxidant enzymes are responsible for dissemination of free radicals such as superoxide radicals. During oxidative stress the body uses its defence mechanism to minimize the process of lipid peroxidation by using these antioxidant enzymes, thus, the activity of those enzymes become higher in the early stages of TAA induction. However, when the insult continues for long period, the enzymes become depleted and unable to fight against the free radicals. This means that in advance stages of peroxidation due to TAA the activity of CAT, SOD, and GPx declined as shown in

Figure 4.17, Figure 4.18 and Figure 4.19. While these enzymes levels continue to be high in the treated groups, because of the antioxidant properties of plant extracts against TAA-induced free radicals.

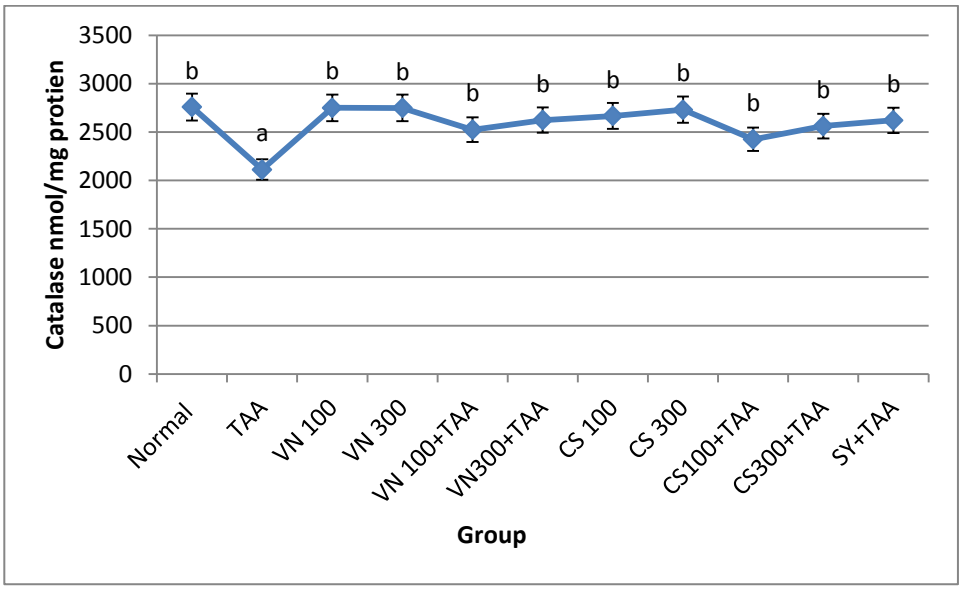

Figure 4.17: Effect of VN and CS extracts on liver homogenate level of CAT in rats at the end of 12 weeks.

The data were stated as mean ±S.E.M. Means with different superscripts are significantly different. [a] $P < 0.05$ versus normal control group and [b] $P < 0.05$ versus TAA control group. SY stands for silymarin (standard hepatoprotective drug), CAT stands for catalase enzyme.

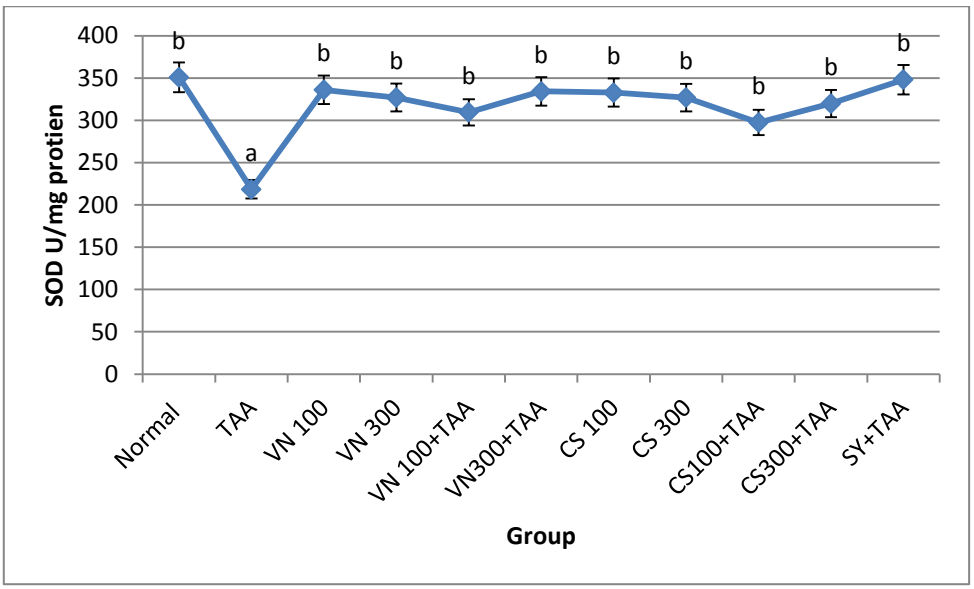

Figure 4.18: Effect of VN and CS extracts on liver homogenate level of SOD in rats at the end of 12 weeks.

The data were stated as mean ±S.E.M. Means with different superscripts are significantly different. $^{a}P < 0.05$ versus normal control group and $^{b}P < 0.05$ versus TAA control group. SY stands for silymarin (standard hepatoprotective drug), SOD stands for supraoxide dismutase enzyme.

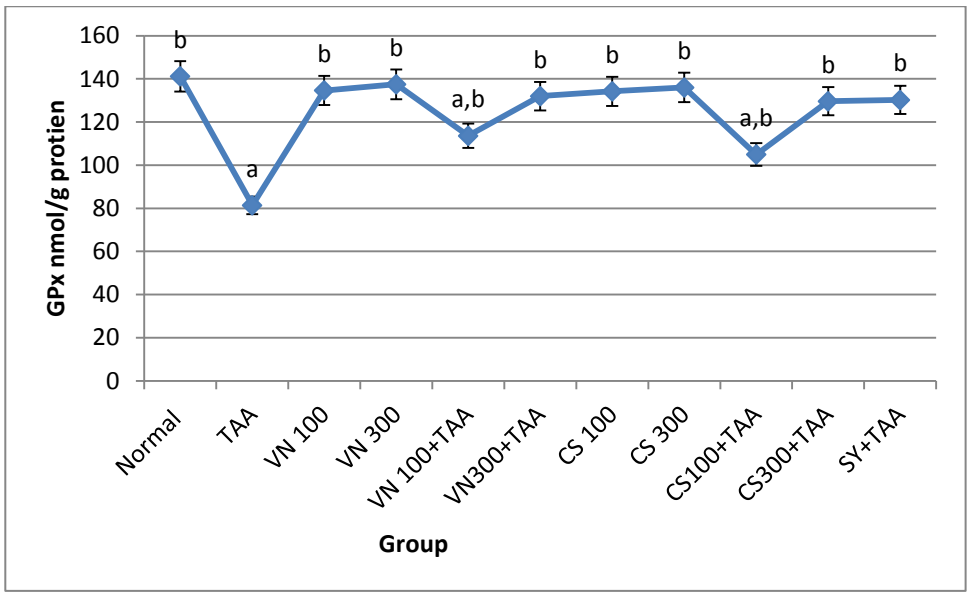

Figure 4.19: Effect of VN and CS extracts on liver homogenate level of GPx in rats at the end of 12 weeks.

The data were stated as mean ±S.E.M. Means with different superscripts are significantly different. $^{a}P < 0.05$ versus normal control group and $^{b}P < 0.05$ versus TAA control group. SY stands for silymarin (standard hepatoprotective drug), GPx stands for glutathione peroxidase enzyme.

4.3.4.11 Hepatic CYP2E1 levels

The results of the effect of VN and CS extracts on the hepatic cytochrome enzyme CYP2E1 are shown in Figure 4.20. Animals from hepatotoxic (TAA) group had significantly ($P<0.05$) higher levels (3.32 ± 0.87 ng/ml) of CYP2E1 compared with normal group (1.64 ± 0.62 ng/ml) and SY-treated group (1.76 ± 0.51 ng/ml). High dose VN-treated rats showed significantly ($P<0.05$) lower levels (1.78 ± 0.81 ng/ml) when compared with TAA group. On the other hand, there was no significant difference between the low doses of VN, CS-treated animals and high dose CS-treated animals

which had similar CYP2E1 levels (2.26 ± 0.62, 2.72 ± 0.37 and 2.53 ± 0.52 ng/ml), respectively in comparison to normal and TAA control groups.

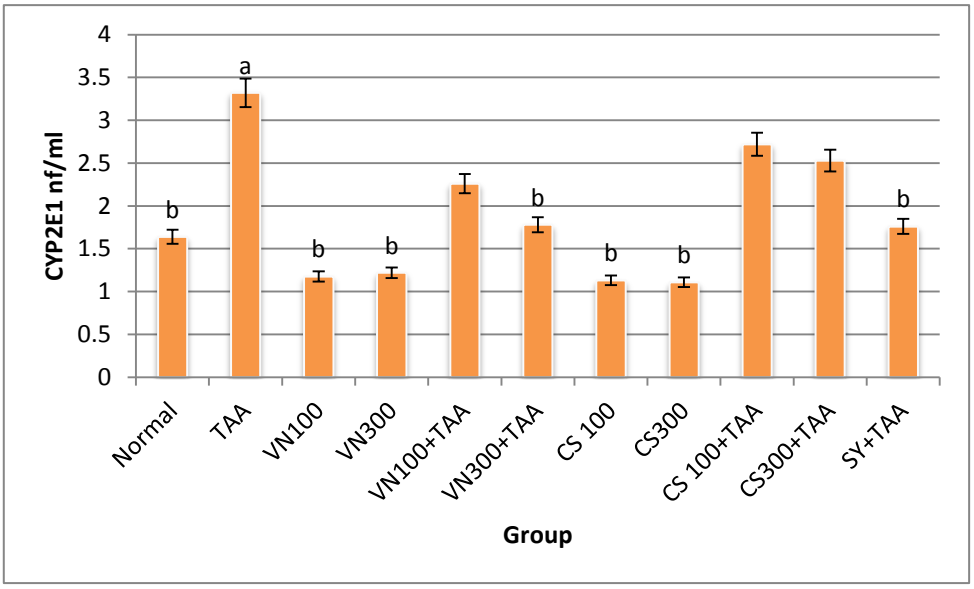

Figure 4.20: Effect of VN and CS crude extracts on hepatic levels of CYP2E1 in rats at the end of 12 weeks.

The data were stated as mean ±S.E.M. Means with different superscripts are significantly different. $^{a}P < 0.05$ versus normal control group and $^{b}P < 0.05$ versus TAA control group. SY stands for silymarin (standard hepatoprotective drug).

4.3.4.12 Hepatic MMP-2, MMP-9 and TIMP-1

The effect of VN and CS extracts treatment on the liver tissue homogenate levels of MMP-2, MMP-9 and TIMP-1 from all experimental animals are illustrated in Figure 4.21. The levels of the tested enzymes were significantly higher ($P<0.05$) in the TAA group compared to all other experimental groups. On the other hand, administration of VN extract to the animals significantly ($P<0.05$) attenuated the enzymatic level of MMP-2, MMP-9 and TIMP-1 to approach the values of the reference

or standard control group (SY+TAA) which indicates the efficacy of the plant extract treatment in a dose-dependent manner. Furthermore, oral administration of low and high doses of CS-treated animals also reduced the level of MMP-9 in their liver homogenates to approach the values of SY-treated group. These results recommend VN more than CS-treatment in inhibiting extracellular matrix deposition in the rat livers via down-expression of MMP-2, MMP-9 and TIMP-1.

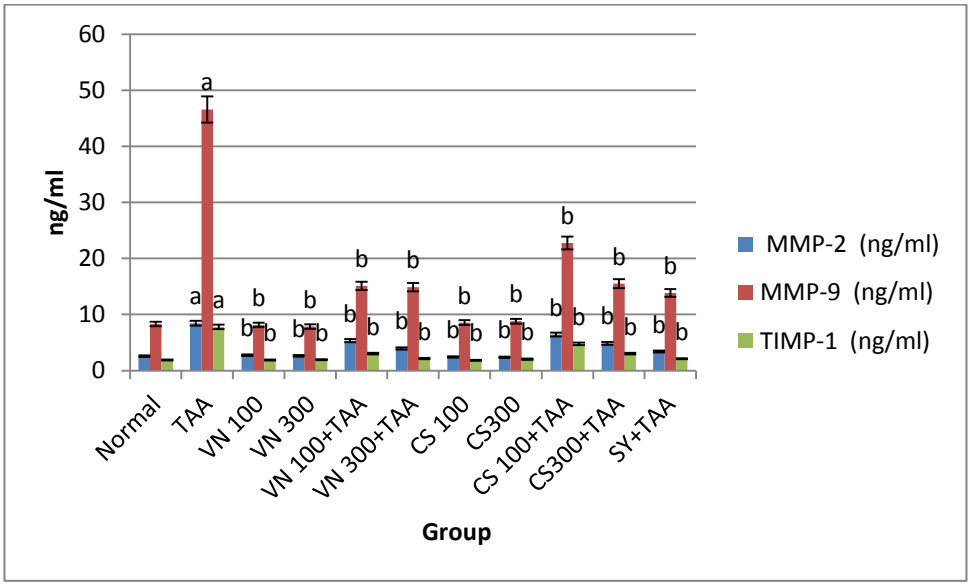

Figure 4.21: Correlation between MMP-2, MMP-9 and TIMP-1 levels in the rat liver homogenates collected from all animal groups at the end of 12 weeks.

The data were stated as mean ±S.E.M. Means with different superscripts are significantly different. $^{a}P < 0.05$ versus normal control group and $^{b}P < 0.05$ versus TAA control group. SY stands for silymarin (standard hepatoprotective drug).

4.3.5 Histopathological findings of the liver

Livers were taken from both normal (Figure 4.22), VN100, VN300. CS100 and CS300 groups showed normal liver architecture with distinct hepatic cells, sinusoidal spaces and a central vein. The hepatocytes are polygonal cells with well-preserved cytoplasm, nucleus with prominent nuclei. Hepatocytes and portal tracts showed no significant changes.

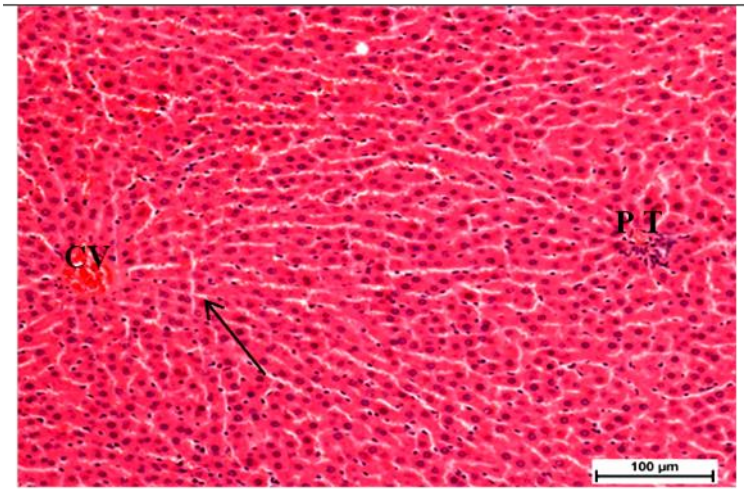

Figure 4.22: Liver histology of normal group. H & stain,(LM, Scale bar, 100µm).

Figure 4.22 showing normal plates of hepatocytes separated by sinusoidal capillaries (arrow), central vein (CV) and portal tract (PT).

On the other hand, the histological examination of liver tissue in the hepatotoxic group (TAA) showed loss of normal architecture by the presence of regenerating nodules separated by fibrous septa extending from the central vein and some inflammatory cells, abnormal appearance of portal tracts and twinning of cell plates (TCP) due to regenerating activity of the hepatocytes with cytoplasmic vacuolation, fatty change, sinusoidal dilatation, proliferation of bile duct, centrilobular necrosis,

displayed bundles of collagen surrounding the lobules, which resulted in huge fibrous septa and distorted tissue architecture (Figure 4.23).

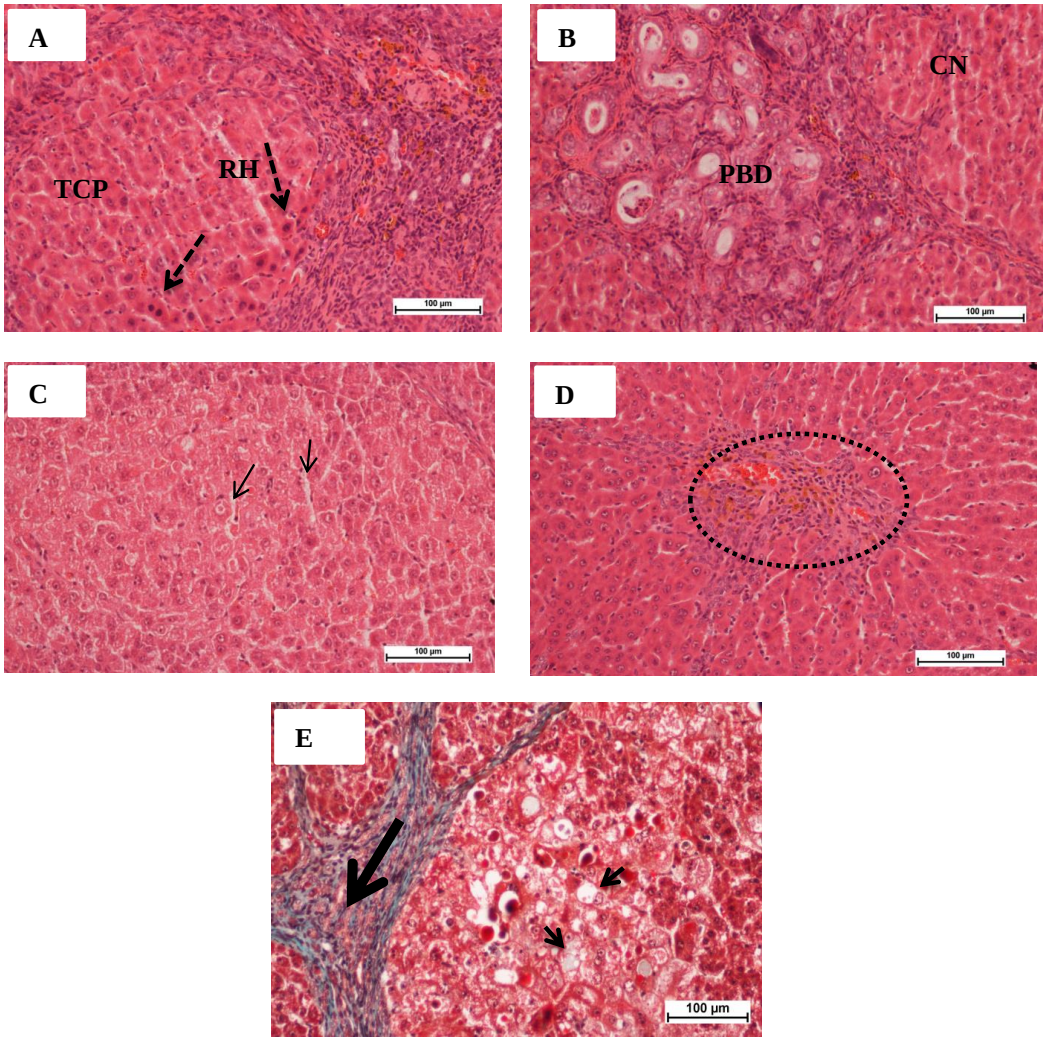

Figure 4.23: Liver histology of TAA group

A: showing regenerative hyperplastic cells (RH), necrotic cells (dotted arrows) among the hepatocytes and twining of the cell plates (TCP), (LM, Scale bar, 100µm). **B**: showing, proliferation of bile duct (PBD) with some inflammatory cells within the fibrous septa and cirrhotic nodules (CN), (LM, Scale bar, 100µm). **C:** showing sinusoidal dilatation, (LM, Scale bar, 100µm). **D:** showing the cholestasis and greenish discoloration (dotted circle), (LM, Scale bar, 100µm). H and E stain. **E:** showing thick

fibrous septa (big thick arrow) and fatty degeneration (short thick arrows), (LM, Scale bar: 100μm). Masson's Trichome stain.

By using H and E staining technique, the cirrhotic nodules which were obtained, showed thick purple bundles of collagen fibers separating the regenerative nodules (Figure 4.23). While, from the Masson's trichrome stained section, the thick bundles of collagen appeared green and separated the regenerative nodules Figure 4.23).

In VN and CS-treated animals, the liver sections showed mild inflammation and mild necrosis of hepatocytes with the presence of mild cytoplasmic vacuolation. Histopathological examination also showed good recovery of TAA-induced necrosis by both plant ethanolic extracts compared to SY. Animals treated with the low dose ethanolic extract showed regeneration of hepatocytes surrounded by fibrous tissue septa with a significant increase in bile ductules, fat storing cells, and Kupffer cells. Animals treated with the higher dose of both plant extracts showed remarkable histological regeneration compared to those of the low dosed groups. They showed nearly normal patterns with an increase normal hepatocytes parenchyma and a reduced development of fibrous septa and lymphocytes infiltration. Results of the histopathological examination are shown in the Figure 4.24 and Figure 4.25.

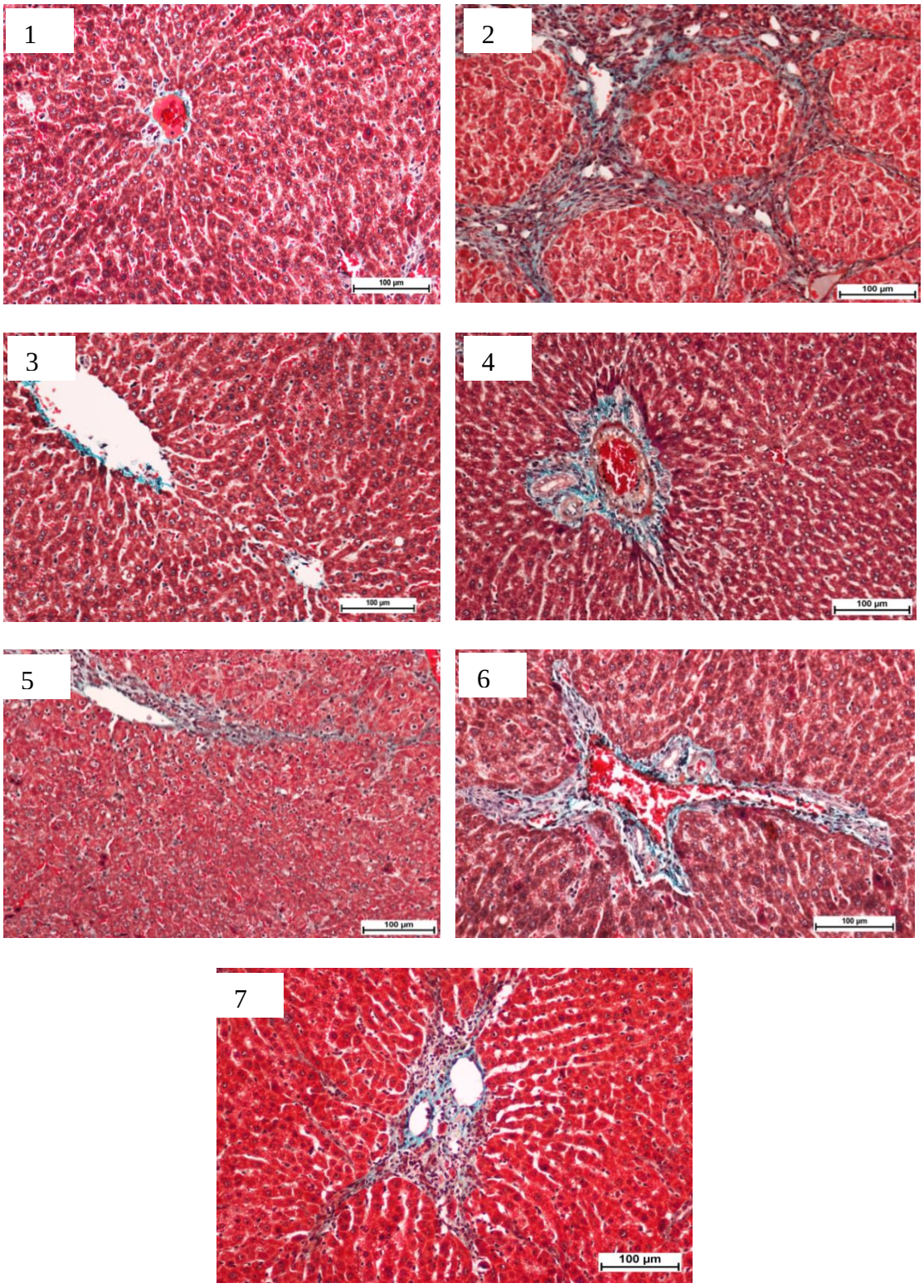

Figure 4.24: Photomicrographs showing the histopathological images of livers from experimental groups treated with VN, SY and TAA.

1. Control group-showing normal liver architecture, **2.** TAA group (Hepatotoxic group)-showing proliferation of bile duct and thick fibrous septa, **3**. VN100 group-showing normal liver architecture. **4.** VN 300 group-showing normal liver architecture, **5.** VN 100 + TAA group- showing moderate fibrous septa, **6.**VN 300 + TAA group-showing mild fibrous septa, **7.** SY group-showing mild fibrous septa**.** Masson's Trichrome stain.(Scale Bar: 100µm).

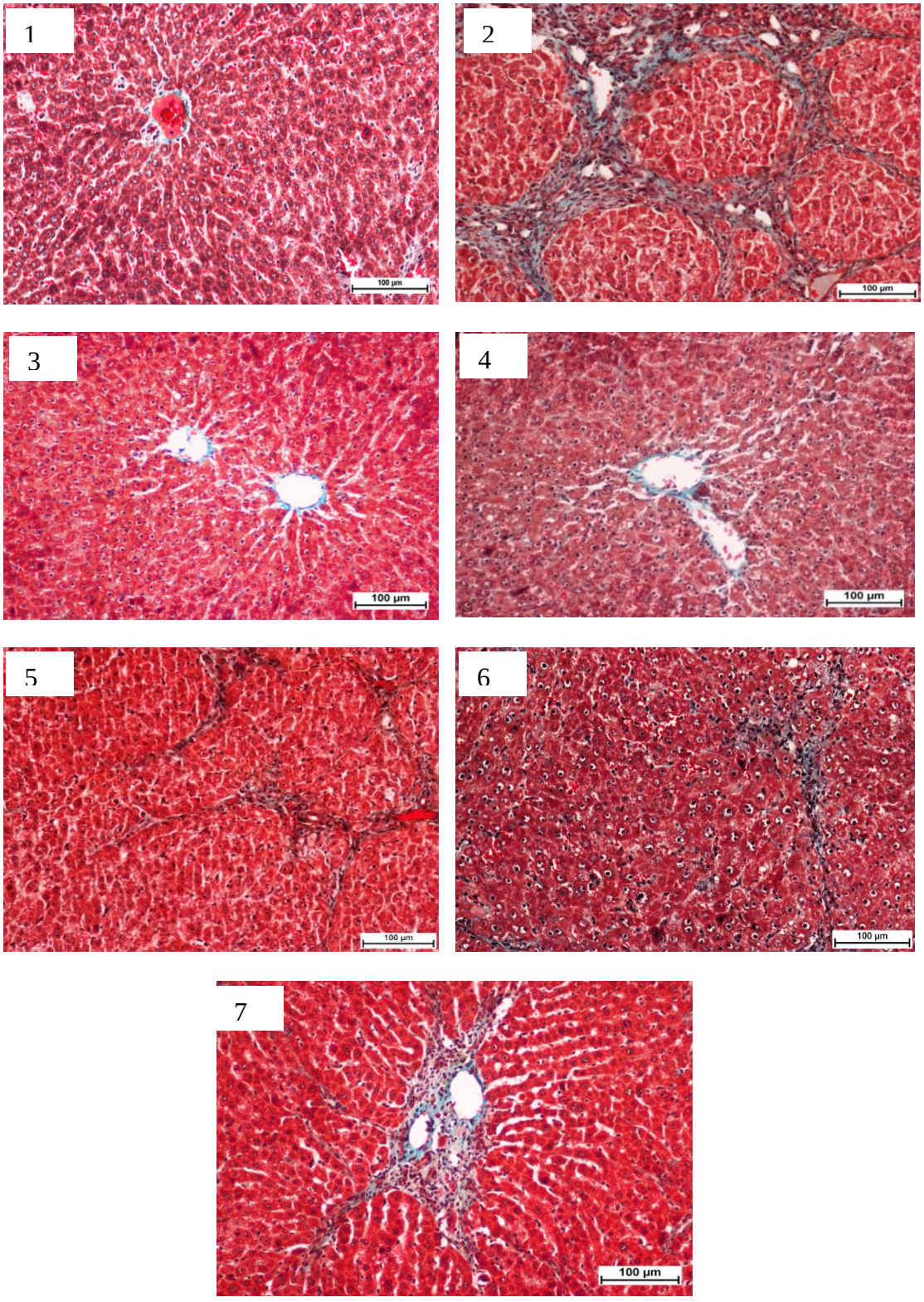

Figure 4.25: Photomicrographs showing the histopathological images of livers from the experimental groups treated with CS, SY and TAA.

1. Control group-showing normal liver architecture, **2.** TAA group (Hepatotoxic group)-showing proliferation of bile duct and thick fibrous septa, **3**. CS100 group-showing normal liver architecture. **4.** CS 300 group-showing normal liver architecture, **5.** CS 100+ TAA group- showing multiple nodules with moderate fibrous septa and fewer cirrhotic nodules, **6**. CS 300 + TAA group-showing mild fibrous septa, **7.** SY group-showing mild fibrous septa**.** Masson's Trichrome stain. (Scale Bar: 100µm).

4.3.5.1 Staging of liver cirrhosis

There was a significant ($P<0.05$) increase of fibrosis in TAA group in comparison to normal control group, as well as a significant ($P< 0.05$) decrease of fibrosis in all VN and CS-treated groups (Figure 4.26).

.

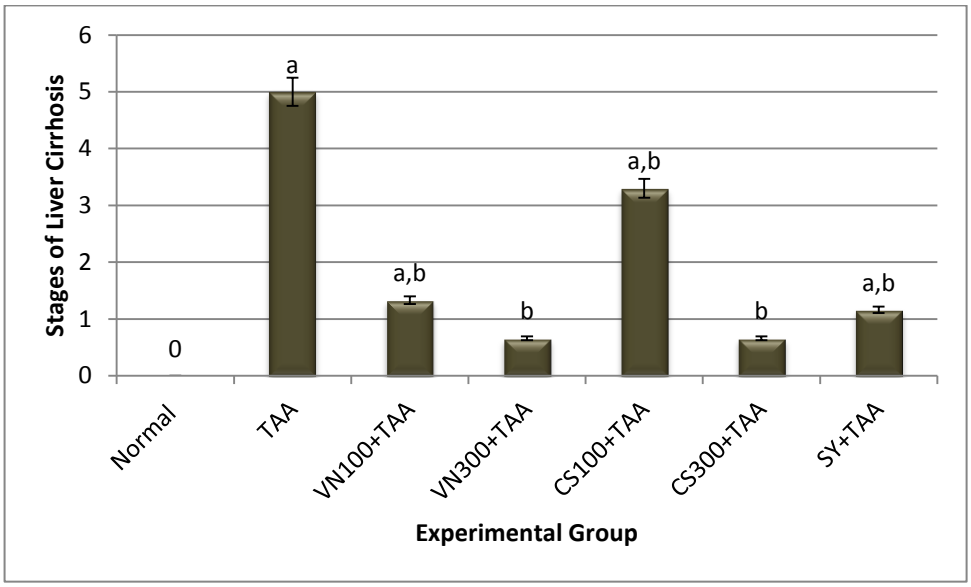

Figure 4.26: Stages of liver cirrhosis in all groups of rats after 12 weeks of treatment

The data were stated as mean ±S.E.M. Means with different superscripts are significantly different. $^{a}P < 0.05$ versus normal control group and $^{b}P < 0.05$ versus TAA control group. SY stands for silymarin (standard hepatoprotective drug).

4.3.5.2 Immunohistochemistry of TGF-β1 and α-SMA

TGF-β1 and α-SMA staining of hepatocytes from the livers of VN and CS-treated groups are shown in Figure 4.27 and Figure 4.28. Hepatocytes of liver tissues from TAA-group rats showed up-regulation of TGF-β1 and α-SMA expressions while in the normal control group, there was down-regulation of TGF-β1 and α-SMA. As for the SY-treated rats, there was down-regulation of TGF-β1 and α-SMA expressions. Down-regulation of TGF- β1 and α-SMA expressions indicates lower levels of fibrosis. Thus, rats treated with low dose and high dose VN and CS extracts help inhibit hepatocyte fibrosis as indicated by the down-regulated TGF-β1 and α-SMA expressions. It was noted that low dose CS extract still showed moderately high expression for TGF-β1 within the hepatocytes and near the central vein areas. These findings support the idea of VN and CS extracts-induced hepatoprotective activities against progressive liver damage by inhibiting fibrosis of hepatocytes and ameliorating their proliferation.

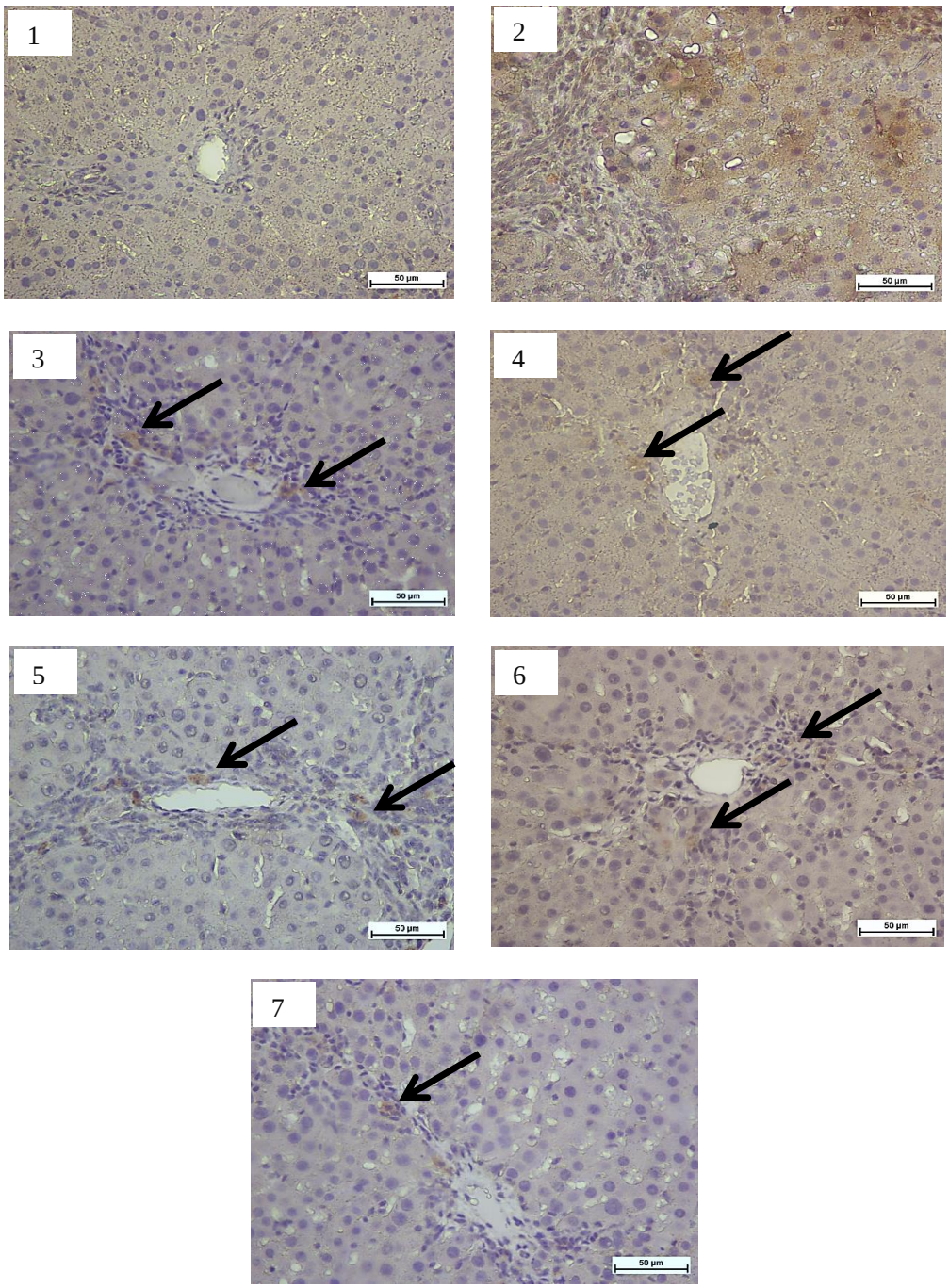

Figure 4.27: Photomicrographs showing Immunohistochemistry staining of TGF-β1of livers from different experimental groups.

1. Control group-showing normal liver architecture, **2.** TAA group (Hepatotoxic group)-showing more TGF-β1 expression, **3** VN 100+TAA group-showing moderate TGF-β1 expression. **4.** VN 300 + TAA group-showing very less TGF-β1 expression and near to normal group. **5.** CS 100+TAA group-showing moderate TGF-β1 expression. **6**. CS 300+TAA group-showing mild TGF-β1 expression. **7.** SY group-showing mild TGF-β1-positive hepatocytes in the liver and near to normal group**.** (Scale Bar: 50µm).

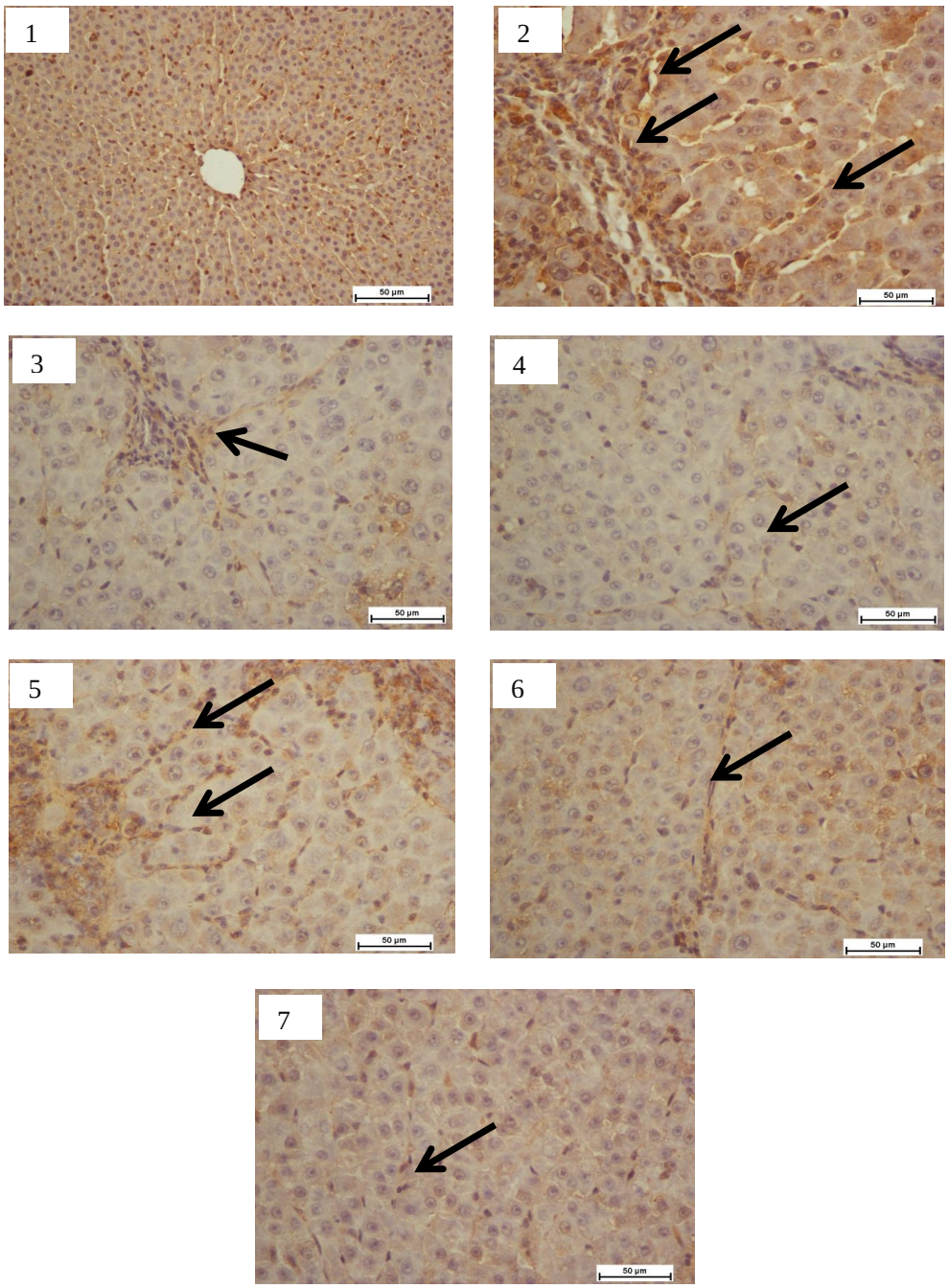

Figure 4.28: Photomicrographs showing Immunohistochemistry staining of α-SMA of livers from different experimental groups.

1. Control group-showing normal liver architecture, **2.** TAA group (Hepatotoxic group)-showing more α-SMA expression in between the hepatocytes, at the sinusoidal capillaries and within the fibrous septa, **3.**VN 100+TAA group-showing moderate α-SMA expression at the sinusoidal capillaries. **4.** VN 300 + TAA group-showing negative α-SMA expression and near to normal group. **5.** CS 100+TAA group-showing moderate α-SMA expression at the sinusoidal capillaries. **6**. CS 300+TAA group-showing mild α-SMA expression. **7.** SY group-showing negative α-SMA-expression in the liver**.** (Scale bar: 10µm).

4.3.6 Expression of TGF-β1, α-SMA and PCNA by Western blot analysis

Remarkable thick bands of TGF-β1, α-SMA and PCNA expressions were observed in TAA group and decreased in (SY+TAA) group. Both (VN100+TAA) and (CS100+TAA) groups revealed slight TGF-β1, α-SMA and PCNA expressions (Figure 4.29). In (VN300+TAA) and (CS300+TAA) groups, the expressions of TGF-β1, α-SMA and PCNA were all slight in comparison to TAA group.

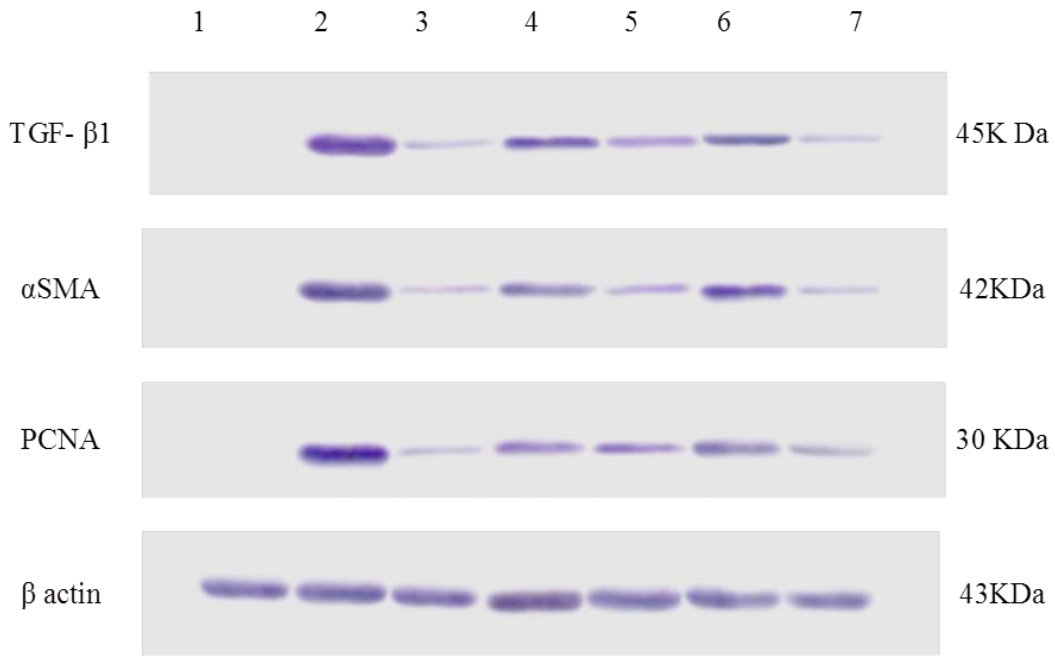

Figure 4.29: Western blot analysis of TGF-β1, α-SMA and PCNA levels in liver tissue for all experimental groups.

1. Normal control group, 2. TAA group (Hepatotoxic group), 3. SY+TAA group, 4.VN 100+ TAA, 5. VN 300+ TAA, 6. CS 100+TAA group, 7. CS 300+TAA group.

The quantitative analysis of Western blot results using Image J program showed that the treatment of liver cirrhosis with VN300 and CS 300 reduced the expression of TGF-β1 and α-SMA in a level comparable with SY+TAA as illustrated in Figure 4.30 (A and B).

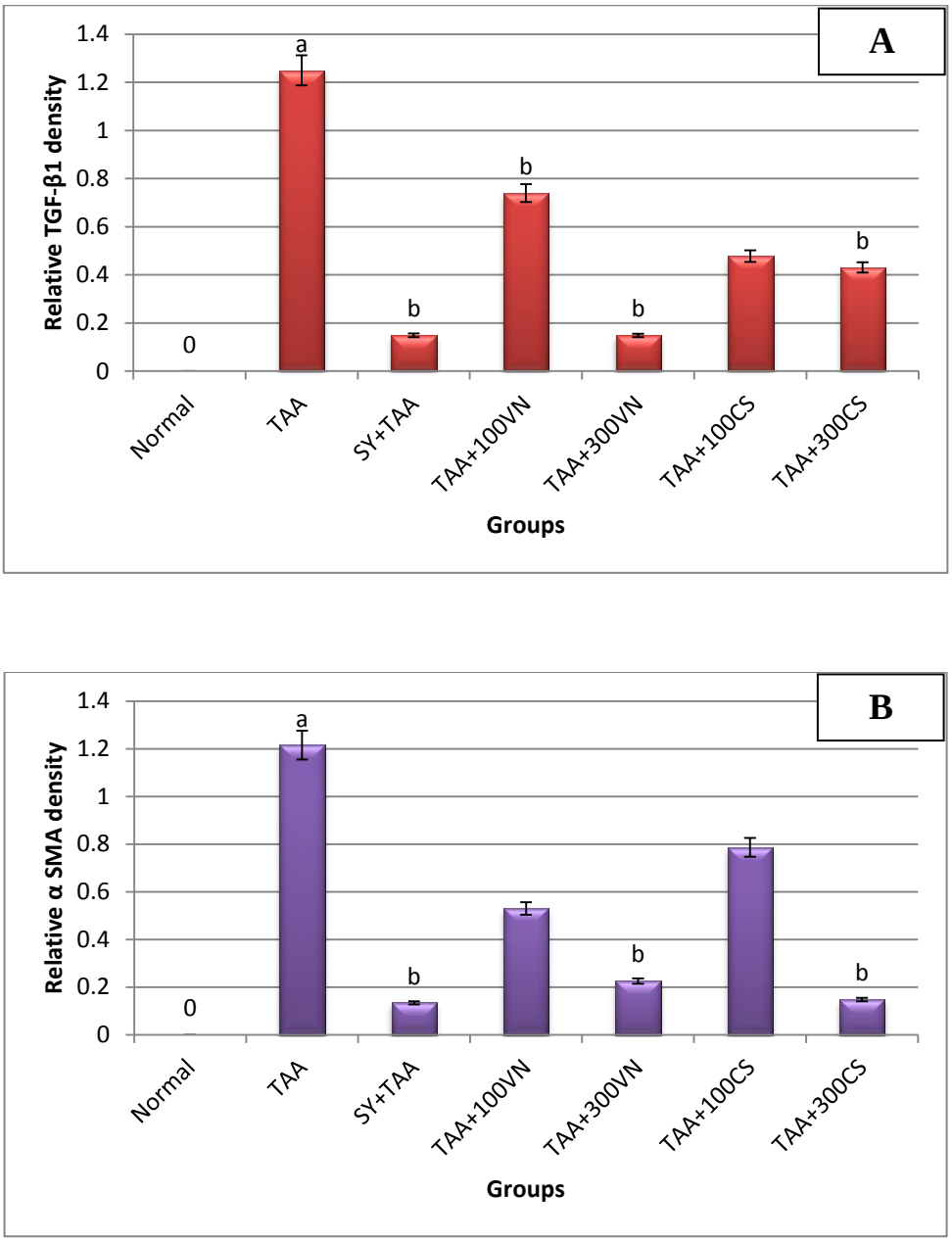

Figure 4.30: Protein expressions from Western blots in all experimental groups are quantitated using Image J program. (A) TGF-β1 density. (B) α-SMA density.

The data were stated as mean ± S.E.M. (n = 3). Means with different superscripts are significantly different. [a] $P < 0.05$ versus normal control group and [b] $P < 0.05$ versus TAA control group. SY stands for Silymarin (standard hepatoprotective drug).

4.4 Cytotoxic and Antiproliferative Effects on WRL68 and HepG2 Cells

4.4.1 Cytotoxic effect of VN extract on HepG2 and WRL 68 cell lines

Cytotoxicity of VN extract on HepG2 and WRL68 cells was assessed using MTT assay. Responses of HepG2 cells toward increased concentrations were exponential. HepG2 cells experienced a significant increase in inhibition at low concentrations of VN extract, with an eventual decline at the highest concentrations tested and with the increasing in the incubation period. The estimated IC50 values of VN extract (concentration causing death of 50% of HepG2 cells) were 66.46 µg/ml, 57.36 µg/ml and 65.12 µg/ml at 24hrs, 48 hrs and 72 hrs incubation respectively (Table 4.5) This means that increasing the concentration used and with longer time of incubation with VN extract has an impact on increasing the ability of inhibition of proliferation. This is indicated by the declining number of living cells with increasing concentrations and incubation time of HepG2 cells (Figure 4.31).

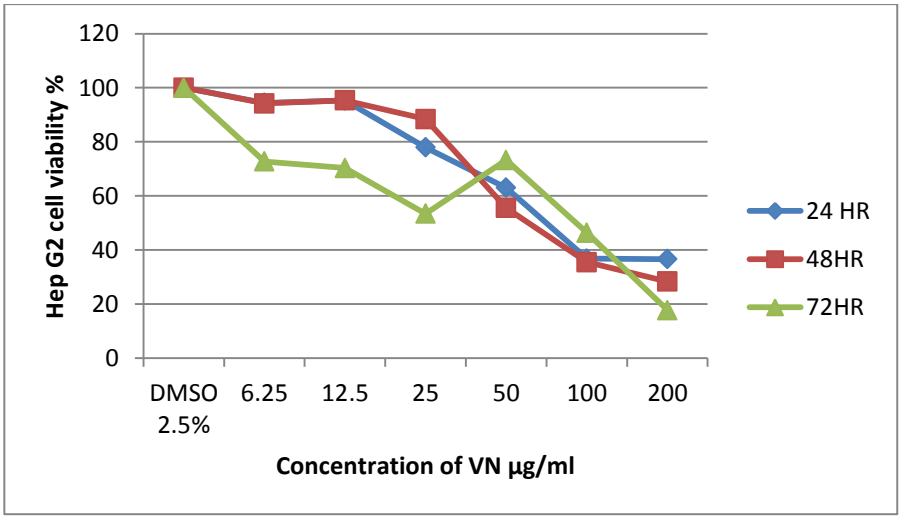

Figure 4.31: Effect of VN treatment in HepG2 cell lines viability

The cytotoxicity of the crude extract expressed as the inhibitory of concentration (IC50). The sensitivity of HepG2 cells to VN is characterised by IC50. The lower the IC50 value indicated the higher anticancer effect of the sample. These results indicate that elevated anticancer effects strengthened with dose time of exposure.

The *in vitro* dosage-and time-dependant effects of VN extract against the cell viability for the cultured WRL68 cells showed lesser cytotoxicity effect with no IC50 as shown in Figure 4.32.

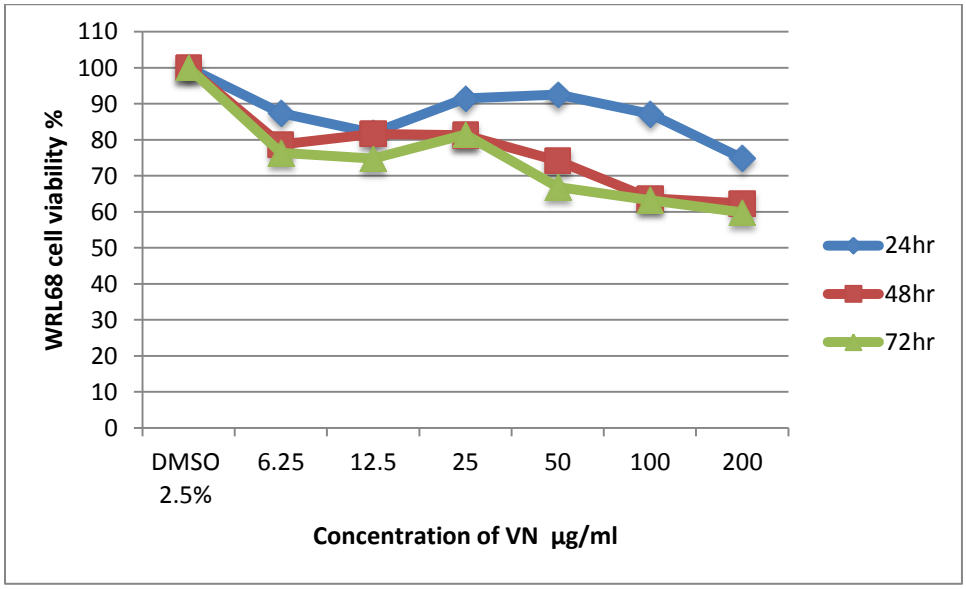

Figure 4.32: Effect of VN treatment in WRL68 cell lines viability

4.4.2 Cytotoxic effect of CS ethanolic extract on HepG2 and WRL68 cell lines

Cytotoxicity of CS crud extract on HepG2 and WRL68 cells was assessed using MTT assay. Responses of HepG2 cells toward increased concentrations were exponential. HepG2 cells experienced a significant increase in inhibition at low concentrations of CS extract, with an eventual decline at the highest concentrations tested and with the increasing incubation period (Figure 4.33). The estimated IC50

values of CS extract (concentration causing death of 50% of HepG2 cells) ranged between 88.89µg/ml and 84.87µg/ml after 48 hrs and 72 hrs respectively Table 4.5.

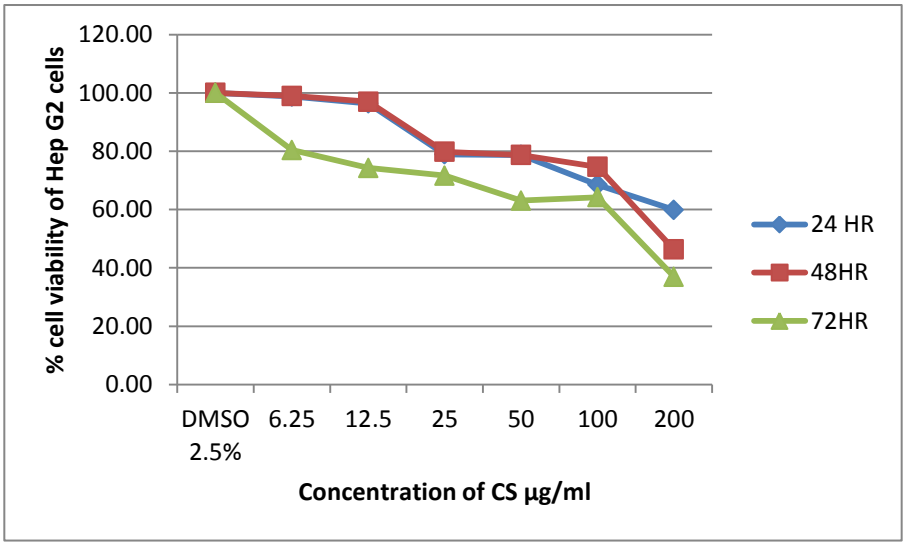

Figure 4.33: Effect of CS treatment in HepG2 cell lines viability

The *in vitro* dosage-and time-dependent effects of CS extract against the cell viability for the WRL68 are shown in Figure 4.34. There was no estimated IC50 of CS extract at 24 and 48 hrs. The estimated IC50 value was 163.40 µg/ml at 72 hrs, as compared to untreated control cells (Table 4.5).

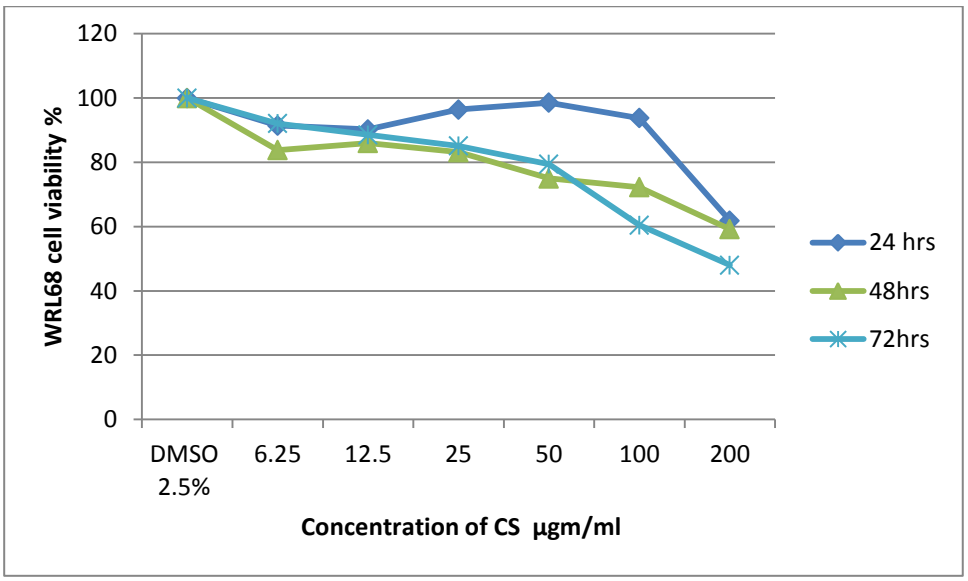

Figure 4.34: Effect of CS treatment in WRL68 cell lines viability

Table 4.5: Comparison of IC50 values for HepG2 and WRL 68 cells obtained from MTT assay following exposure to VN and CS extracts for 24, 48 and 72 hrs.

Cell line	Extract	Duration(Hour)	IC50 µg/ml
WRL 68	VN	24	-
		48	-
		72	-
HepG2	VN	24	66.46±2.8
		48	57.36±1.3
		72	65.12±1.8
WRL 68	CS		
		24	-
		48	-
		72	163.40±1.5
HepG2	CS	24	-
		48	88.89±2.5
		72	84.87±1.7

The IC_{50} value is defined as the concentration of sample necessary to inhibit 50% of the cells. IC_{50} is determined by using Masterplex2010 software (5Parameters logistics)

4.4.3 Morphological observation by inverted microscope

Light microscopic observation of the VN and CS ethanolic extract-treated HepG2 cell line after 72 hrs of exposure showed typical morphological features of apoptosis. The characterisation of morphological changes observed showed reduction in cell volume, cell shrinkage, reduction in chromatin condensation and formation of cytoplasmic blebs as shown in Figure 4.35.

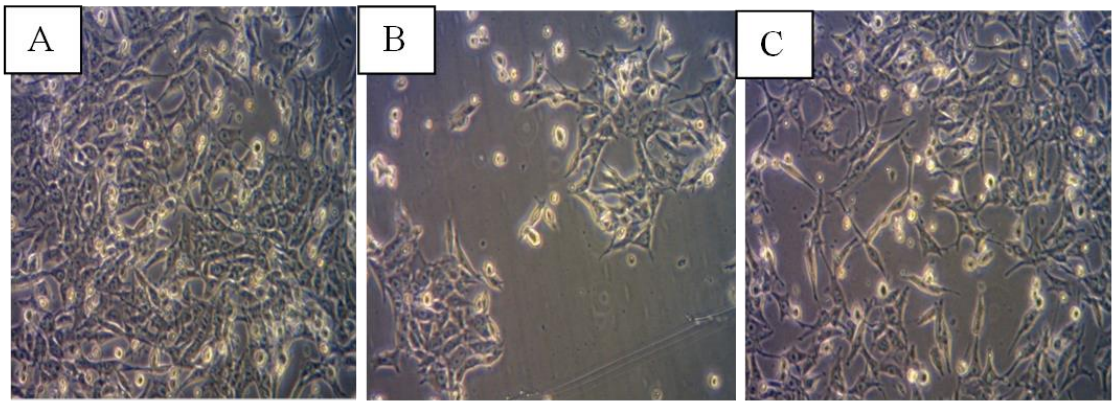

Figure 4.35: Photomicrographs showing the comparison of the morphology of $HepG_2$ cells before and after treatment with VN and CS extracts.

A. untreated cells (control), **B**.VN treated cells, **C**. CS treated cells (magnification ×10).

4.4.4 Morphological observation by acridine orange and ethidium bromide (AO/EB) staining

Induction of apoptotic cell death among HepG2 cells was confirmed by morphological observation of the cells after Acridine Orange/Ethidium Bromide (AO/EB) staining assessed by fluorescence microscopy. As shown in Figure 4.36, the cells treated with VN and CS showed a marked decrease in the number of live cells compared to the untreated control.

.

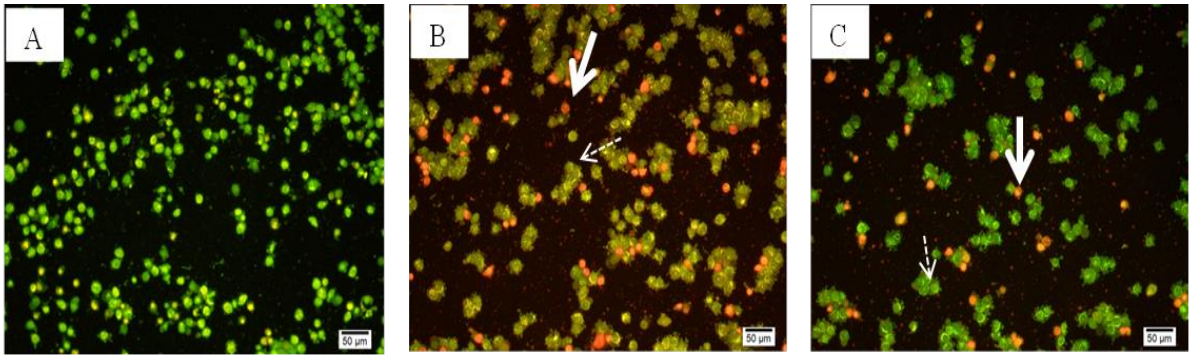

Figure 4.36: Effect of VN and CS on morphology of HepG2 cells.

A. Untreated controlled cells (control), **B.**VN treated cells, **C.** CS treated cells. Full white head arrows: apoptotic cells and dashed dotted arrow indicated cell with fragmented nuclei. AO/EB staining, fluorescence microscope, Bar=50µm.

4.4.5 Caspase-3 activity (extracts induce apoptosis)

Caspase-3 activation is a momentous element in the apoptotic signalling cascade. Although VN and CS extracts were not selectively the cytotoxic of choice to HepG2 cells, we were enthusiastic to check if the cytotoxicity to Hep G2 cells treated with VN or CS were mediated by apoptosis. To further elucidate the mechanism of cell death induced by VN or CS, a caspase-3 colorimetric assay was conducted to establish the level of caspase-3 activation both before and after treatment with the extract. The

results of this experiment showed that treatment of HepG2 cells with VN or CS extract strongly induces increased caspase-3 activity with increasing the incubation period as shown in Figure 4.37.

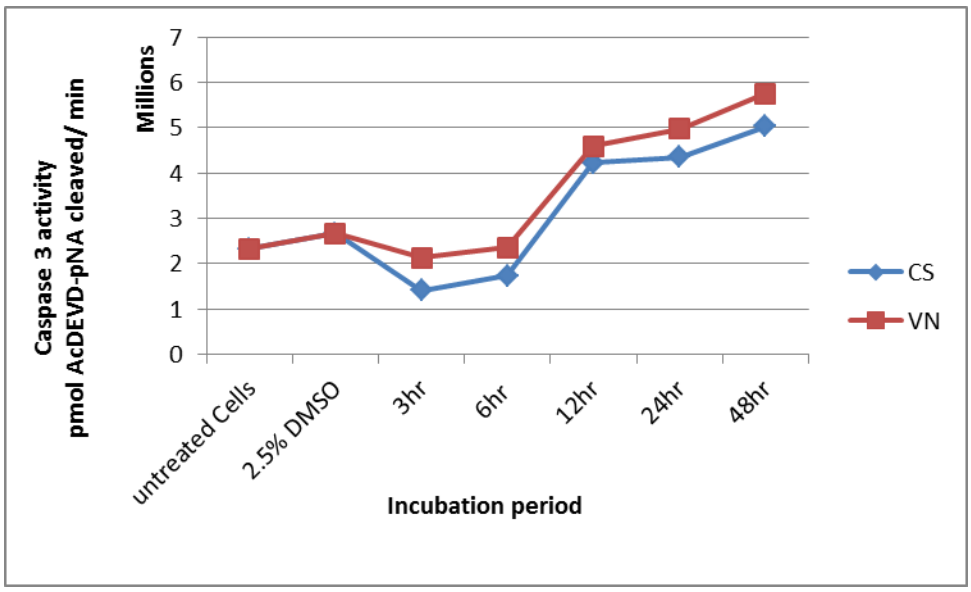

Figure 4.37: Caspase-3 activity of HepG2 cells treated with VN and CS extract

Figure 4.37 showed the maximum caspase-3 activity was 574845 at 48 hrs with 100 µg/ml concentration of VN extract, while the maximum caspase-3 activity was 5×10^7 at 48 hrs with 100 µg/ml concentration of CS extract. This suggests the involvement of caspase-3 in triggering apoptosis in VN and CS-treated HepG2 cells.

4.4.6 Lactate dehydrogenase enzyme activity

LDH is an enzyme located in the cell and catalyses the inter-conversion of lactate to pyruvate. It is another indicator for cell viability through the evaluation of membrane integrity. The LDH activity is measured externally as it leaks from dead cells or disturbed cells where in both cases the LDH activity increases. In the present study,

LDH assay was carried out to evaluate the *in vitro* cytotoxic effect of VN extract on WRL 68 and HepG2 cells. Figure 4.38 showed that the lowest LDH release was in WRL 68 cells at 50 µg/ml within 24 hrs incubation period and it was activated with the increase of VN concentration and the incubation period. On the other hand, Hep G2 cells were more sensitive to VN as compared to WRL 68 cells, LDH was released in a time and dose dependent manner (Figure 4.38).

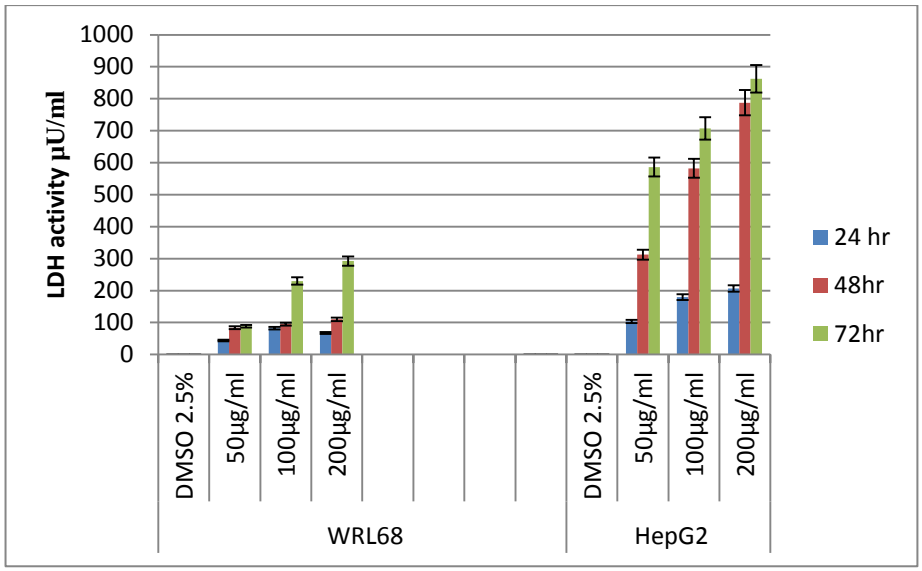

Figure 4.38: Effect of VN treatment in WRL68 and HepG2 cell lines on LDH release

The *in vitro* cytotoxic effect of CS extract on WRL 68 and HepG2 cells. Figure 4.39 showed that the lowest LDH release was in WRL 68 cells at 50 µg/ml within 24 hrs incubation period and it was activated with the increase of CS concentration and the incubation period. On the other hand, HepG2 cells were more sensitive to CS as compared to WRL 68 cells, LDH was released in a time and dose dependent manner (Figure 4.39).

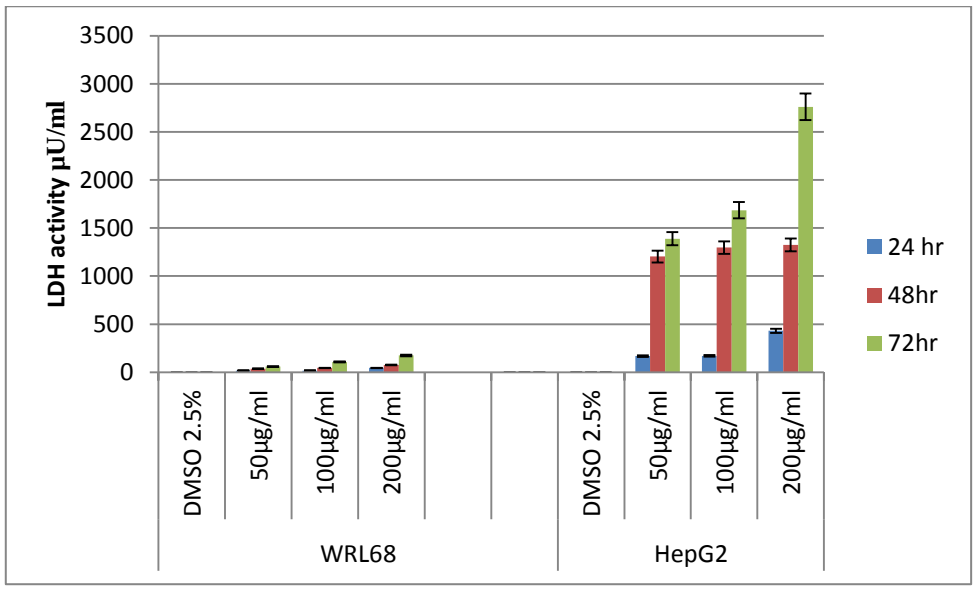

Figure 4.39: Effect of CS treatment in WRL68 and HepG2 cell lines on LDH release

Chapter 5

Discussion

5.1 PASS Assisted Biological Activities

In order to find out the specific bioactivities of VN and CS isolated compounds, the chemical structures of all these compounds were computed through PASS software for prediction of their activities. The spectra of the biological activities assisted by PASS include hepatoprotection, antioxidant, radical scavenging, lipid peroxidase inhibition, caspase-3 stimulation and antiproliferative activities are presented in Table 4.1 and Table 4.2.

VN extract is composed of eight isolated compounds. It is found that 70% probability of being hepatoprotective drug was shown by two compounds of VN extract, negundoside and vitegnoside. The antioxidant activity was expressed mainly by vitegnoside and 7, 8 dimethyl herbacetin 3- rhamnoside. On the other hand, 5,3'-dihydroxy-7,8,4'-trimethoxy flavanone showed highest antiproliferative activity while 7,8-dimethyl herbacetin 3-rhamnoside revealed the strongest caspase-3stimulant. Similarly, CS extract contains twelve compounds, among them, sappanchalcone, which shows the drug likeness as hepatoprotective and antioxidant. Based on the structural formulae, predictions of biological activity and drug likeness have been implemented for the phytochemical constituents in the selected medicinal herbs, which revealed hepatoprotective effect. These findings are in agreement with previous studies, which show the effective anti-inflammatory and anticancer activity (Hade, 2012).

From these results, it can be concluded that PASS software gave a fair approach for the corresponding reported activities of the phytoconstituents and determining the other valuable insights of other medicinal uses.

5.2 Choice of Materials

5.2.1 Choice of animals

The *Sprague Dawley* rats were taken as an animal model in this study because they have a close analogous genetic and physiological match to humans and have a short lifespan/time between generations. Its main advantage is its calmness and ease to handle. Only the male rats were selected in this experiment to avoid any differences that might arise if both sexes were used.

5.2.2 Rationale of using TAA to induce liver cirrhosis

The model of cirrhosis induced in rats by specific patterns and doses of administration of TAA was characterised previously by clinical, biochemical and histopathological methods and proven to be a reliable and satisfactory model of hepatic injury (Hamza, 2010; Nakajima et al., 1998). Previous studies reported that a single dose of TAA could produce multiple macro and micro cirrhotic nodules with evidence of centrilobular hepatic necrosis (Amin et al., 2012).

Various TAA administration methods including, intraperitoneal, subcutaneous injection and administering the toxin with food or drinking water have been used in experimental animals to produce hepatic injury (Yeh et al., 2004). In this study, liver cirrhosis was induced by administering 0.03% TAA in the drinking water of rats daily for 12 weeks duration (Natarajan et al., 2006). It was reported that the toxic effect of

TAA is due to peroxidation of cell membrane by free radicals (Pawa & Ali, 2004). Extreme macroscopic changes of cirrhotic liver with nodules on the external surface as well as on the cut surface with variation in the size, color, shape and consistency were observed. It was proven in previous studies that histopathological finding after chronic administration of TAA is similar closely to those for liver cirrhosis in humans (Ljubuncic et al., 2005).

5.3 Plants Extracts and the Potential Antioxidant Activities

The role of free radicals and tissue damage in diseases, such as atherosclerosis, heart failure, neurodegenerative disorders, aging diabetes mellitus, hypertension and several other diseases is gaining a lot of recognition (Flora, 2007). ROS are prospective carcinogenic substances because they generate free radicals, including hydroxyl, superoxide, peroxyl, hydroperoxyl, and alkoxyl radicals, which participate in tumour promotion, mutagenesis and progression (Turrens, 2003). If there is no effective regulation, the excess ROS would damage proteins, lipids and DNA and in turn cause inhibition of the normal function, modulation of gene expression, cell cycle, cell metabolism, cell adhesion and cell death (Deshpande et al., 2013).

Medicinal plants have been suggested to contain rich sources of natural antioxidants that counter balance the ROS by neutralizing the free radicals and minimizing the damage of the tissues. In this study, we have tested the crude ethanol extract of VN and CS for their radical scavenging potentials.

In DPPH method, it was demonstrated that the DPPH free radicals were reduced through the existence of the plants' extracts following the trend ascorbic acid > gallic acid > BHT > VN > CS as shown in Figure **4.1**; page 90. The optimum concentration of

VN and CS that achieved maximum inhibition of DPPH was at 50 µmol/ml with IC50 = 13.31 µg/ml and 33.86µg/ml respectively. The different relative scavenging activity of the tested compounds against radicals may be explained by the different mechanisms involved in the radical–antioxidant reactions or might be due to solubility of these compounds or due to the different testing systems which could affect the capacity of the individual compound to react and quench different radicals and also depend on various extraction procedures and solvents that were utilized for track down the multiple active components of each plant (Kadir et al, 2011).

VN and CS free radical scavenging activity from low concentration (3.125 µmol/ml) with inhibition of (2.35%) and (6.75%) respectively, to the highest concentration (50 µmol/ml), with inhibition of (79.34%) and (68.25%) respectively, has some logical arguments. VN and CS are rich in phenolic compounds and provided wide range of antioxidant properties, which seem to be directly related to the hydroxyl groups attached to aromatic rings. This broad spectrum of antioxidant formula provides the best possible protection against free radicals. It could be attributed to bond dissociation energy (BDE; O-H) of each hydroxyl group attached to the benzene ring. BDE is the energy needed to break one mole of the bond to give separated atoms. It plays a central role in determining antioxidant efficacy, and is one of the most important physical parameters used for evaluating antioxidant activity in chemical compounds that were used as inhibitors of free radical reactions. In general, compounds having lower BDE have been reported to have better antioxidant properties. Hence, VN and/or CS have a wide variety of hydroxyl groups and therefore, exert a wide variety of BDE, forming a synergistic system (antioxidant and co-antioxidant together) by regeneration of antioxidants by co-antioxidant. For instance, α-Tocophenol (α-TOH) and polyphenols can be played as synergistic antioxidant system. α-TOH is consumed from the

beginning of the oxidation reaction forming α-TO• radical which completely preserved until all co-antioxidant (CoAH) has been consumed (Scheme 5.1). Due to this peculiar behavior, polyphenolic species are ideal co-antioxidants to be used together with a small amount of α-TOH (Amorati et al., 2003; Yehye et al., 2012)

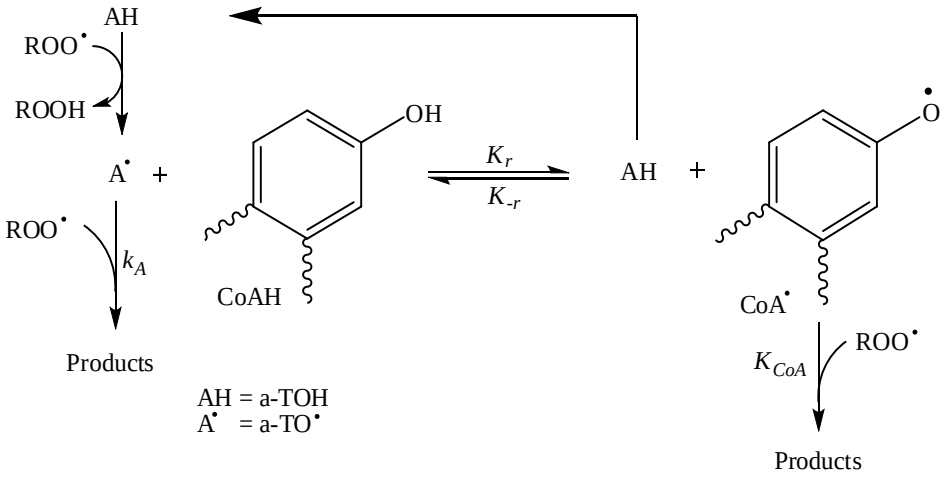

Scheme 5.1: CoAH effectively recycles α-TOH

In FRAP method, the antioxidant activity of VN and CS is determined on the basis of the ability of antioxidant in these plants extracts to reduce Fe^{3+} iron to Fe^{2+} iron. Both plants showed a high power to reduce the ferric ions. Generally, FRAP assay was used due to its simplicity and reproducibility. FRAP assay treats the antioxidants in the sample as a reductant in a redox-linked colorimetric reaction (Prasad et al., 2010). The trend for ferric ion reducing activity of VN and CS against BHT, gallic acid and ascorbic acid are shown in Figure 4.2; page 91. VN exhibited the strongest free radical scavenging power compared with two commercial antioxidants, BHT and ascorbic acid, while CS showed antioxidant power compared to BHT only. These findings seem to suggest that VN and CS extract can donate an electron easily. This activity is believed to be mainly due to their redox properties. Hence, VN and CS extracts should be able to

donate electrons to stable free radicals in the actual biological and food system. The ethanolic extracts of VN and CS were found to be effective scavengers of DPPH and FRAP, possessed a good reducing power activity. The high antioxidant activity of VN enhanced the potential interest in this plant for improving the efficacy of different products as nutraceutical and pharmacological agents.

The antioxidant activities of VN and CS ethanolic extracts could be attributed to their phenolic and flavonoid contents, which are powerful *in vitro* antioxidant molecules (Rice-Evans, 2001). These activities due to their reducing properties as hydrogen or electron-donating agents (Rice-Evans, 2001) (Sharma et al., 2012).

It is a worthy note that our results in PASS were strongly paralleled and supportive to these values. It can be assumed that VN extract has high radical scavenging activity due to the presence of 7,8-dimethyl herbacetin 3-rhamnoside (97.3%) and vitegnoside (95.6). While sappanchalcone in CS extract showed the highest radical scavenging activity which reached up to 81%. These results seem to be in agreement with the a recent study (Sharma et al., 2010) who proposed that the whole parts of VN plant show a potent source of natural antioxidants, which was due to the involvement of polyphenolic compounds. Besides, it is encouraging to compare the findings with a very recent study which revealed that the methanol and aqueous extracts of VN leaves and flowers showed scavenging of DPPH free radicals *in vitro* (Rabeta & An Nabil, 2013). Furthermore, a previous study has shown the powerful antioxidant activity of ethyl acetate, methanol and water extracts of CS as evidenced by the low IC50 values in both DPPH and nitric oxide methods when compared with rutin and ascorbic acid (Sarumathy et al., 2011).

A previous review stated that VN crud extract contains different fractions from chromatography analysis, including flavones, alkaloid and saponin, which are powerful

antioxidants (Singh et al., 2011). These compounds are capable of scavenging hydroxyl radicals and effectively reducing the extent of oxidation of low density lipoproteins (Rice-Evans, 2001). Therefore, it is reasonable to assume that, the widespread use of VN as a traditional practice of medicine in South-Eastern Asia countries could be attributed to the content of these antioxidant phytochemicals.

Recently, research has proven that several species of CS are being used traditionally for a wide variety of ethnomedical properties, presumably, due to the presence of several flavones and phenols, including brazilin, which is a phenolic oxygen hetrocycle (Sarumathy et al., 2011).

Our bodies have adapted to the changes required over time to develop defence systems to reduce the damages done by ROS. Antioxidants are the main defence mechanism of the body acting as free radical scavengers (Flora, 2007). They are produced within the body and include dismutase, peroxidase, and catalase enzymes, as well as glutathione and cytochrome (Garrett & Kirkendall, 2000). GPx is the major endogenous antioxidant scavenger that protects cells from oxidative stress through its ability to bind to and reduce ROS (Theiss et al., 2007). In an attempt to elucidate the baseline levels of antioxidant enzymes status in WRL68 cell lines, which are exposed to an oxidant agent H_2O_2, we have measured the activities of SOD, GAT, GPx and MDA content. The results explored the possible *in vitro* antioxidant effect of VN and CS in WRL68 cell lines by measuring exogenous antioxidant level for this type of cells when they are exposed to H_2O_2 and treated with different concentrations of VN and CS extracts. It has been highly suggested that in the process of carcinogenesis, there is excessive accumulation of ROS which play an important role in causing oxidative damage (Mena et al., 2009). In attempting to defend the stimulation, it was found that the antioxidant enzymes activities were higher in WRL68 cells treated with VN and CS

extracts in comparison to H_2O_2 control group. Moreover, VN and CS crude extracts showed significant reduction in MDA content in WRL68 exposed to oxidative stimulant as shown in Table 4.4 page 93. These results revealed that both VN and CS extracts exhibited a strong radical scavenging effect against H_2O_2. Such observation could be due to modulations of the defence system in the cell lines in relation to their growth and maintenance or reflect an idiosyncrasy of the *in vitro* system used in this study.

5.4 Hepatoprotective Activities of VN and CS

5.4.1 General Observation

Liver cirrhosis is a pathological condition that reflects irreversible chronic injury of hepatic parenchyma in association with extensive fibrosis. Once cirrhosis is established, normal hepatic architecture is altered, thus compromising the intrahepatic anatomy that leads to marked portal and systemic hemodynamic alterations (Crawford, 2002). Generally, the oral feeding with VN and CS ethanolic extract did not have any adverse effects on the experimental rats. There was neither mortality nor toxicity symptoms throughout the period of the experiment. Many clinical and toxicological studies were carried out for medicinal plant extracts to ensure the secure use and safeties of these plants. In Global Harmonized System of Classification and Labelling of Chemicals and Environmental Protection Agency: Health Effects Test Guidelines, stated that when the LD_{50} value of plant extracts are higher than 5000 mg/kg they are practically safe (McQueen, 2010).

Therefore, the investigated plants' extracts are toxicologically safe by oral administration since they did not show any signs of body weight loss, no behavioral abnormalities were observed, and no significant differences were found in the VN and

CS-treated groups in comparison to the control group with regards to liver and other serum analysis tests. Thus, our findings support the traditional usage of these plants in Malaysian folk medicine.

5.4.2 Body weight

A marked reduction in body weight of TAA group in comparison to the normal and other VN and CS-treated groups is shown in Figure 4.4 page 94. These findings confirm the toxic effect of TAA throughout the period of experiment, which is considered to be the most reliable and consistent symptoms of toxicity among the experimental animals (Al-Bader et al., 2000). It could be due to reduced food intake or due to impairment and disabling transport of some nutrients into the blood circulation, and could also be due to inhibition of nutrients breakdown into usable substances (Ighodaro et al., 2010). The study findings showed non-significant increase in body weight of all VN and CS-treated rats in comparison to TAA. However, this normal increase in body weight for the experimental rats treated with both VN and CS extracts, indicating the overwhelming safety of these two plants.

5.4.3 Gross findings

The morphological findings of nodular lesions in the hepatotoxic group in our study demonstrated the extreme changes to the liver gross appearance after TAA injection. The nodular lesions were more abundant and variable in size but were usually coarse when compared to normal and other VN and CS-treated groups (Figure 4.5; page 96). In addition**,** multiple dark green to black spots distributed around the whole surface of the liver in the TAA group were detected, indicating considerable deterioration in liver morphology. These dark spots could be either haemorrhagic spots resulting from

over congestion of hepatic venules or bile-staining nodules of biliary cirrhosis (Cooke & Stewart, 2004). These findings give a rough idea for the amount of scarring and its distribution. In fact, the reason for the congestion in the liver is the presence of the thick fibrous network in between the regenerative nodules distributed at the perivenular, periportal and intralobular regions together with sinusoidal fibrosis. The capillary dilatation is probably due to scar formation in the space of Disse, which plays a role in decreasing the fenestrae or even disappearance in the endothelial wall. Increased in the basement membrane thickness results in the tightening of the sinusoidal wall and elevation of intra sinusoidal pressure which explains their dilatation in advance cirrhosis (Vlad et al., 2007).

In contrary, the livers from SY+TAA, VN100+TAA, VN300+TAA, CS100+TAA and CS300+TAA groups showed normal morphology and this pattern are consistent with other previous supported studies (Sarumathy et al., 2011) (Mahalakshmi et al., 2010). These findings suggested that the protective effects of both plants are comparable to SY+TAA group (Figure 4.5 page 96).

In the TAA group, there was an obvious increase in liver weight and significant high liver index in comparison with normal, SY+TAA, VN+TAA and CS+TAA groups. It was shown that the concurrent treatment with VN and CS extracts had effectively maintained the liver weight comparable with SY+TAA group as shown in Figure 4.7 page 100. Thus, it could be suggested that there is a strong association between the *in vitro* free radical scavenging activities and *in vivo* hepatoprotective effects of VN and CS extracts since TAA-induced hepatotoxicity is through its bioactivation to TAA-S-oxide which covalently binds to the macromolecules and induces oxidative stress (Pallottini et al., 2006).

Although there was no significant change in body weight, but there was a significant change in liver weight in all the different experimental groups. The higher liver weight and the higher liver to the body weight ratio has been obtained in TAA-treated rats compared to other groups Figure 4.8 page 100. In fact, we noticed that the measurement of liver body weight ratio is more accurate approach to determine the changes in the liver size compared to the measurement of body weight or liver weight alone, as the liver weight is mainly dependant on the size of the rat (Wong et al., 2012).

5.4.4 Biochemical analysis

There was a significantly higher level in ALT, AST, and AP enzymes in the TAA group compared to normal group (Figure 4.9 page 102). This is probably due to the toxic effect of TAA on permeability of the cellular membranes for cells containing ALT and AST enzymes. This finding is in agreement with the previous study where a similar TAA dose and application time were applied (Müller et al., 1988). However, with the concurrent treatment with VN and CS extract, ALT, AST and AP enzymes showed lower significant level in VN and CS groups than TAA group, probably due to the effect of the herbs inhibiting the effect of TAA (Figure 4.9 page 102). Although the serum levels of both ALT and AST were elevated when liver cells were injured, the degree of elevation was sometimes not parallel with the degree of injury. This is because the mechanism of the elevation was affected by many factors, such as etiology of the liver disease or severity of the liver cell necrosis (Lascelles & Donaldson, 1990). However, ALT is of particular value for the diagnosis of liver disease and a high concentration of this enzyme is found in acute exacerbations of uncompensated cirrhosis, and acute hepatitis (Giannini et al., 2005). The slight increases in

transaminases in cirrhotic rats are due to increase in protein synthesis in rat liver after TAA intoxication (Chakrabarty et al., 1982).

For human, the ratio of AST to ALT is calculated. A ratio of AST to ALT ratio more than or equal to 1.00 suggested a predictive value for the diagnosis of cirrhosis in patients (Šídlová et al., 2002). However, the AST and ALT enzyme levels in the blood of the rats are far different from that of the human because the activities of rat liver enzymes in different strains, species are different and inter-individual variation exists in liver microsomal cytochrome P450 enzyme (Pearce et al., 1992). Thus, the ratio of AST to ALT is not applicable for this study.

AP enzyme usually rises in any disease involving the structural and functional integrity of the liver, including hepatocellular necrosis and cirrhosis. However, highest levels of AP occur in cholestatic disorder as it is a canalicular enzyme that plays a role in bile production (Giannini et al., 2005). The study result is consistent with this explanation.

The study findings also showed hyperbilirubinemia in TAA group in comparison to normal control and plants-treated groups (Figure 4.10; page103). This is probably due to defect in the transportation of bilirubin from the serum into the hepatic cells or deficient uptake by the hepatic cells or it results from impaired flow of bile into the intestine, as in patients with biliary obstruction (Fevery & Blanckaert, 1986). This high level of conjugated bilirubin may secondarily elevate the level of unconjugated bilirubin, the possible cause is the reduction in hepatic clearance of unconjugated bilirubin that results from competition with conjugated bilirubin for uptake or excretion (Giannini et al., 2005).

On the other hand, a significantly high activity of serum GGT activity was observed in this study. It was found that GGT level increases in diseases of the liver and biliary system (Levison & Reid, 2008). In this aspect, it is similar to AP in detecting disease of the biliary tract. Indeed, the two markers correlate well, although there is conflicting data about whether GGT has better sensitivity (Tameda et al., 2005). Generally, AP is still the first test for biliary disease. The main value of GGT over AP is in verifying that AP elevations are in fact due to biliary disease. AP can also increase in certain bone diseases, but GGT is not (Giannini et al., 2005). The mechanism for this elevation is unclear. However, a number of drugs and chemicals such as hexachlorocyclohexane, CCl_4 and TAA are known to increase GGT activity by the induction of microsomal enzymes (Trivedi & Rawal, 2000).

Since the metabolism of proteins, amino acids, synthesis of other amino acids and urea occur in the liver, we anticipated variations in the concentration and characteristics of these materials would be present in liver disease. The total serum albumin concentration in the normal control, SY+TAA, VN100+TAA, VN300+TAA, CS100+TAA and CS300+TAA groups were significantly higher in comparison to TAA group (Figure 4.11 page 104).

As some of the globulins are synthesised by the liver, while others are synthesised by the immune system, this could explain the slight significant elevation in the serum globulin (Geoffrey et al., 1995). Usually these alterations are more marked in chronic conditions, as in our case of cirrhosis. Reduced level of albumin usually follows the severity of the condition and it is a reliable index of the prognosis. While the serum globulin concentrations were slightly increased in CS100+TAA group in comparison to the normal group (Figure 4.11; page 104), it could be normal or slightly increased in acute hepatitis and cirrhosis. Generally, the continuation of hypoalbuminemia and

hyperglobulinemia indicates a progress or a change to a chronic state (Thapa & Walia, 2007).

A cellular enzyme, LDH is an essentially enzyme present in all tissues involved in glycolysis. Under certain conditions of intense activity, the muscle operates anaerobically converting glucose to lactate (Atakisi et al., 2006). The cycling of lactate and glucose between muscle and liver in the Cori cycle passes through the blood stream before being picked up by the liver, which converts the lactate back to glucose. Hence, any damage in liver tissues, result in enormous accumulation of lactate, which explains the significant elevation of LDH level as in the TAA group as compared to the normal group, VN and CS-treated groups in this study (Figure 4.13; page 106).

The synthesis of lipid and lipoproteins occurs in liver, and the levels of the various lipid molecules change in both acute and chronic liver diseases. Previous studies reported that cholesterol level was elevated in cholestatic form of liver diseases while triglyceride level was elevated in acute liver diseases (Bayless & Diehl, 2005). However, because of the individual differences in these lipid values as well as their dependence on nutritional status, there is no reliable way to use them for assessing hepatic function. This explains the significant elevation in the cholesterol level in TAA group in comparison to normal and other plants-treated groups (Figure 4.14; page 107). These findings are consistent with a previous study which had shown small changes in serum cholesterol level after CCl_4-induced liver injury (Hui-Mei et al., 2008). However, the test is generally not sensitive, in comparison to transaminase which is a more reliable test (Geoffrey et al., 1995).

Furthermore, in the current study, there was significantly high glucose level in TAA and CS100+TAA groups in comparison to normal other plants-treated groups

(Figure 4.15 page 108). This elevation in glucose level could be mainly due to resistance to insulin hormone, which was produced by injury to the hepatic cells, resulting in no more glucose uptake by the liver, leading to high serum glucose level and Type II diabetes mellitus (Friedman & Schiano, 2004).

The hepatoprotective effects of the investigated plants are not only evidenced in *in vitro* antioxidant activities, but also through endogenous oxidative enzyme systems involved in the hepatic defence system like CAT, SOD and GPx. This counter balance the oxidative stress induced by TAA (Huang et al., 2011) (Kuo et al., 2010), (Figure 4.17; Figure 4.18 and Figure 4.19). According to the PASS results, the antioxidant activities are most probably due to the activity of 7,8-dimethyl herbacetin 3-rhamnoside and vitegnoside in VN extract which showed 87.4% and 79.8%, respectively (Table 4.1). On the other hand, sappanchalcone, the active compound in CS extract revealed 83% antioxidant activity as explained in Table 4.2.

TAA administration has been reported to produce ROS that is followed by lipid peroxidation (Sun et al., 2000), glutathione depletion and reduction in the SH-thiol groups (Zaragoza et al., 2000). The present finding demonstrated that TAA administration caused severe damage to the rats endogenous antioxidant system as represented by the down-regulation of the total antioxidant capacity of the rats. Furthermore, there was lipid peroxidation characterised by up-regulation of MDA levels (Figure 4.16) and disturbance of antioxidant enzymes (CAT, SOD and GPx) activities which led to decrease in their levels. These results are in agreement with the previous research which reported that treatment of experimental rats with TAA caused an increase in the MDA levels and decrease in the GPx levels (Balkan et al., 2001). Moreover, other study displayed that TAA administration to rats resulted in significant ($P < 0.05$) decrease in the activities of SOD, CAT, GPx (Yogalakshmi et al., 2010).

VN and CS crude ethanol extracts attenuated the levels of antioxidant enzymes; CAT, SOD, GPx and MDA to their normal levels after tissue damage induced by TAA. These results are consistent with our findings in PASS (Table 4.1 and Table 4.2) which revealed a high percentage of lipid peroxidation inhibition. This is mainly related to the presence of 7,8-dimethyl herbacetin 3-rhamnoside in VN extract (95.2%) and sappanchalcone in CS extract (81%), respectively. Therefore, it could be anticipated that VN and CS ethanolic extracts have the therapeutic ability to reduce the lipid peroxidation reaction in hepatocytes against TAA action. The constant exposure of the tissue to the herbal supplementation in the current study schedule and under the continuous administration of TAA might have been able in modifying the extent of lipid peroxidation reaction or result as a secondary effect rather than primary mediating mechanism in hepatic fibrosis. This modifying mechanism may either be mutual biomolecular interaction among the reactive radicals or by interaction with herbal bioactive molecules. There is a possibility that VN and CS extracts could exert antioxidant activities, and the fact that TAA administration causes elevation in liver enzymes might have played a role. In this study, VN and CS extracts reduced ECM and lipid peroxidation in TAA-treated animals.

To summarise, normal liver weight, lower liver enzymes, lower bilirubin, and decreased MDA level in TAA-treated rats were enhanced by feeding with VN and CS extracts. Thus, the results were in line with the reported antioxidant action of VN and CS. This action appears to reflect some variations in the metabolic activation and interaction with the hepatotoxin. The study results confirmed that the plant is hepatoprotective and this effect is seemingly time–dependent. This synergistic action obviously warrants further investigation.

TAA is metabolized by CYP2E1 enzymes present in liver microsomes and is converted to toxic reactive intermediate compound called TAA-sulfer dioxide through oxidation (Kadir et al., 2011). The level of CYP2E1 inhibition and attenuating drug-induced hepatotoxicity is measured in this study. The inhibitory effect of VN and CS extracts to CYP2E1 may be one of the significant factors in their hepatoprotective activity. This is by inhibiting the metabolism of TAA and blocking the release of ROS responsible for inducing damage to the hepatocytes (Figure 4.20). Parallel findings were consistent with this study, which showed that *Curcuma longa* possessed protective effect against TAA (Salama et al., 2013).

Additionally, based upon our *in vitro* findings, we anticipated that ethanolic extract of VN and CS would be hepatoprotective and would thus ameliorate the hepatotoxic actions of TAA. In fact, the findings from this study revealed that administration of the plants extracts alleviated the hepatotoxic actions of TAA, presumably, via the reduction of high levels of cytokines in rats through the suppression activity of certain phytoconstituents in both extracts. This was attributed mainly to negundoside and agnuside compounds in VN extract and sappanchalcone in CS extract which showed hepatoprotective activity of 98.6%, 98.3% and 92%, respectively.

However, it should be noted that the effect of these plants depends basically on the response of the body cells to a particular agent, which is determined by a variety of factors such as dose, mode of administration, age, sex, species, strain, physiological and nutritional status of the animal (Ighodaro et al., 2010).

Hence, these data highlight an important principle when conducting research into the supposed beneficial actions of the medicinal plants. Our observations from using both *in vitro* and *in vivo* techniques indicated the importance of the combined approach. Data obtained from *in vitro* experiments are useful for identifying the effect

of plants extracts and giving an indication of their cytotoxic potential. The results from this study suggested that complementing *in vitro* experiments with those involving animals are essential steps in establishing the safety of medicinal plants and validating the supposed effects.

The *in vivo* and *in vitro* collaboration would scale down the release of anti-inflammatory and antifibrotic mediators that would prevent progressive liver damage. On the other hand, as mentioned earlier (section 2.3.1.2), liver cirrhosis activates the HSC which in turn increases the ECM synthesis and causes a relative imbalance between production and degradation of MMPs. In addition, the activated HSCs constitute various collagenases and tissue inhibitors of metalloproteinases to remodel the ECM (Bruck et al., 2001). ECM is mainly controlled by MMPs, which are a group of proteolytic enzymes that are able to degrade the ECM (Abraham et al., 2005).

TIMPs regulate tightly the activity of MMPs (Parsons et al., 2004) (Shi & Li, 2005). MMP-9 and TIMP-1 were verified as the molecular signatures during the progress of liver cirrhosis induced by TAA (An et al., 2006). A study revealed that TAA increased MMP-2 expression in the liver tissues of rats and reported that the balance of MMPs and TIMPs is the key factor of liver fibrogenesis (Park et al., 2010). In our research, we studied the effect of VN and CS extracts on the level of MMP-2, MMP-9 and TIMP-1 in the rats' livers intoxicated with TAA. The results showed significant down-regulation in the hepatic levels of MMP-2, MMP-9 and TIMP-1 in the cirrhotic livers of rats treated with VN similar to that of SY, the reference drug used for this study. In addition, CS extract treatment significantly down-regulated the level of MMP-9 in the rat liver (Figure 4.21). These findings are in agreement with a previous study confirming the hepatoprotective effect of curcumin the active antioxidant compound of *C. longa* rhizomes (Salama et al., 2013).

5.4.5 Histopathological patterns of the liver

Liver cirrhosis can be characterised by scarring and regeneration resulting in distortion of the normal liver architecture (Kumar et al., 2009). Normal liver of the rats showed plates of hepatocytes of one cell thick radiating from portal tracts, which contain terminal branches of portal vein, hepatic artery and bile ducts. The plates of hepatocytes are separated by endothelium-lined sinusoids; the hepatocytes have fine granular cytoplasm and a central nucleus (Gartner et al., 2007). This normal cellular architecture was seen in the livers of the normal group in the present study (Figure 4.22; page 116).

Histological patterns of TAA-induced liver cirrhosis forming nodules of various sizes were demonstrated throughout this study. The nodules were separated by thin fibrous septa which was stained dark purple in colour and surrounding the regenerating hepatocytes (Figure 4.23 page117). The regenerating activity of the hepatocytes produced further distortion as the twinning of cell plates caused expansion. Ductular reaction is a lesion characterised by small ductules, often without a visible lumen, fibrosis and inflammatory cells were frequently found in the scar tissues without any intervening parenchyma (Curran, 1982) (Millward-Sadler et al., 1992). Multiple and interrupted portal tracts among chronic inflammatory cells could also be seen, and the normal portal tracts were rarely found. In our study, the findings from TAA group were consistent with the above description.

In the TAA group, chronic intoxication with TAA induces liver damage with cholangiolar cell proliferation (proliferation of bile ducts), damage of liver cell membranes (Kumar et al., 2009) and distorted liver architecture (Figure 4.23 page 117). It is explained by regeneration of the liver cells and hyperplasia of the fibrous

connective tissue. Hyperplasia or hypertrophy of the liver cells was indicated by increases of relative liver weights in the TAA group. This finding is consistent with the previous study (Fu et al., 2007) stated that acute poisoning causes massive hepatotoxicity with haemorrhagic necrosis may take place in the liver, lungs, and blood vessels, while exposure for a longer period of time causes cell enlargement (megalocytosis), veno-occlusion in the liver, fatty degeneration, nuclei enlargement with increasing nuclear chromatin, loss of metabolic function, proliferation of biliary tract epithelium, liver cirrhosis, nodular hyperplasia and adenomas or carcinomas. Three major mechanisms involved in the generation of cirrhosis include: cell death, aberrant extracellular matrix deposition (fibrosis) and vascular reorganization (Guyot, et al., 2006).

In this regard, the histological patterns obtained from the TAA group, showed severe liver distortion, larger nodules which contained more than one portal tract inside their fibrous boundaries. Nodular regeneration without fibrosis usually indicates a problem with the vascular supply to the liver, particularly portal venous insufficiency as established by a previous study (Roskams et al., 2003). Presence of binucleation of hepatocytes in TAA group, indicates the presence of mitosis in hepatic cells which can be assessed as an index of liver proliferative capacity in response to toxin-induced injury (Lee et al., 2007).

Hepatic fibrosis is an indication of the wound healing response of the liver to repeated injuries and is associated with increased inflammatory cell infiltration. This may involve different inflammatory mediators, which is a common stage in most chronic liver disease (Hui-Mei et al., 2008). As the portal tracts are the sites at which circulating lymphoid cells first gain access to the liver (Hübscher, 2006), hence, portal inflammation is common in many liver diseases, inflammatory cells and proliferations

of the bile ducts at the portal area as seen in the TAA and CS100+TAA groups. The proliferation of bile duct is characteristically seen in primary biliary cirrhosis, probably represents the bile continues to be drained from the liver in spite of interruption of ducts (Figure 4.23 and Figure 4.24).

Furthermore, we also noticed spillover of inflammatory cells, mainly mononuclear and lymphocytic cells from the portal area to the adjacent liver parenchyma with presumed damage to the periportal hepatocytes. This is referred to as 'piecemeal necrosis', this lesion was suggested to be important in the pathogenesis of periportal fibrosis (Hübscher, 2006). The presence of necrotic and inflammatory cells as well as the sign of cholestasis was the most prominent pathological features associated with hepatic parenchymal fibrosis. This is because inflammation occurs in response to tissue damage, with the formation of a provisional matrix favouring cell migration and proliferation in the lesion (Guyot et al., 2006). All the above informations are consistent with the findings of this study. Therefore, it could be suggested that the use of VN and CS herbs successfully capable of overcoming the toxicity induced by TAA.

The study results indicated that TAA group experienced higher degree of oxidative DNA damage than the rats in SY, VN and CS-treated groups, which showed an ongoing hepatoprotective effect (Figure 4.24; page 119).

The utilization of the combination of H and E and Masson's Trichrome staining techniques enabled us confidently to detect regenerative nodules of established cirrhosis (Ferrell & Greenberg, 2007). The areas of the established fibrosis in cirrhotic groups and the remaining residual normal portal areas demonstrated dense, thick bundles of collagen, which were also darker blue to green with Masson's Trichrome stain. Elastic fibers were present between the nodules in all the cirrhotic livers.

In this study, the microscopic appearances depend on the methods that used to demonstrate the fat in ordinary method for preparation of tissue for microscopic examination; the fixed tissue is dehydrated in ascending concentrations of alcohol and this treatment dissolves out all fat and lipid substances which are thus demonstrated by their absence or less availability in the liver sections (Kadir et al., 2011).

The non-parenchymal cells in hepatic sinusoids (Kupffer cells, hepatic stellate cells and sinusoidal endothelial cells) which can be identified under an electron microscope have an important role in the pathogenesis of many liver diseases, but are relatively less important in routine liver biopsy diagnosis (Hübscher, 2006).

The ethanolic extracts of VN and CS are shown to be more effective in reducing the fibrotic process of the cirrhotic liver, this effect suggests that these two plants possess bioactive compounds that could prevent the oxidative stress induced by TAA. These compounds most probably belong to negundoside and vitegnoside in VN extract and sappanchalcone in CS extract, thus alleviating the degree of liver injury. The morphological status of the liver corresponds to the ALT, AST and AP enzymes level of the various groups. However, a histological scoring is needed as it is the most reliable and confirmative way to evaluate the degree of their protective effect on the liver (Figure 4.24; page 119).

In this study, the analysis on the staging of fibrosis showed that for TAA group, it was approximately similar to those results established in previous studies (Ljubuncic et al., 2005). Fibrotic score in VN100+TAA and CS100+TAA groups showed a lower scores than TAA group, but the lowest and significant scores were shown in VN 300+TAA and CS300+TAA groups together with SY+TAA group in comparison to TAA group (Figure 4.26). Therefore, it can be concluded that VN and CS extracts provided a hepatoprotective action by alleviating the toxic effect of TAA-treated rats.

These results are similar to previous study, using *Moringa oleifera Lam* seed extract to reduce the liver fibrosis score (Hamza, 2010). However, more elaboration for the mechanism of action for VN and CS extracts is recommended.

In the present study results, since the levels of TGF-β1 and α-SMA did not change in the normal control group, this supports the idea that the HSCs were still in their quiescent state. However, these HSCs were activated in the presence of TAA that led to the high production of ECM and consequently, high expression of TGF-β1 and α-SMA (Figure 4.27; page 124 and Figure 4.28; page 125).

HSC, the main cellular source of ECM during chronic liver injury, undergo a transition into α-SMA expressing myofibroblast-like cells. Activation of HSC is associated with cell proliferation, increased contractility and enhancement of matrix production (Reeves & Friedman, 2002). It was demonstrated that α-SMA was mainly retained in between the plates of hepatocytes, the portal tract and accompanied by the proliferation of the bile ducts, corresponding to the distribution of collagen. It was explained that ROS-induced HSC activation can be inhibited by antioxidants (Yu et al., 1993). Based on these findings, VN and CS treatment during the development of liver fibrosis were successfully reduced α-SMA expression in comparison to the hepatotoxic group which showed markedly high expression of α-SMA in the portal areas and fibrous septa accompanied with bile duct proliferation. Thus, it can be conclude that VN and CS extracts have potential action to suppress HSC activation, through inhibition of ROS.

Since TGF-β1 has multiple pharmacological actions, the balance among these actions is required to maintain tissue homeostasis and the aberrant expression of TGF-β1 is involved in the pathogenesis of liver diseases (Poli, 2000). It is known that TGF-β1 is the crucial cytokine involved in early stages of liver fibrosis and oxidative stress,

the latter stimulates ECM production and deposition (Poli, 2000). Therefore, one of the effective strategies to produce antifibrotic drugs is to find anti TGF-β1agents.

From the study findings, immunohistochemical analysis of liver tissue from hepatotoxic group showed that the cells were positive for TGF-β1 in the portal areas and around the central veins, while concurrent administration of VN and CS ethanolic extracts in TAA-treated rats down-regulated TGF-β1 expression which is corresponded to the reduction in α-SMA expression. These findings suggest that both plants extracts have effective TGF-β1 inhibitor (Figure 4.27; page 124 and Figure 4.28; page 125). These results confirm the findings of previous study (Zhang et al., 2008). From Western blot assay, it was observed that TAA increased TGF-β1 and α-SMA proteins expression which suggests that these proteins participate in liver injury or as an early reaction of liver cirrhosis (Figure 4.29; page 126, Figure 4.30; page 127). Interestingly, TAA treatment caused sharp bands to be formed, in contrast to smeared bands in the normal group. Since the internal control β actin is clearly detected, this result was not due to experimental errors, such as revers transcription failures or RNA degradation (Park et al., 2010).

Furthermore, daily feeding of animals with VN and CS extracts along with TAA administration for 12 weeks attenuated hepatocyte proliferation and regeneration (Sakr & Shalaby, 2012). This was indicated in Western blot analysis by a significant decrease in PCNA in the liver tissue from the plant extracts-treated groups similar to that in the SY-treated group (Figure 4.29; page 126). These results are consistent with previous reports which showed that curcumin the active polyphenol ingredient of *c. longa* extract had an inhibitory effect on hepatocyte proliferation (Wang et al., 2012). Treating the animals with the plant extracts inhibited the necrotic effect due to TAA administration by modifying necrosis into apoptosis, which may be via a cytochrome release from

mitochondria or caspase activation (Malhi et al., 2006). This *in vivo* modification would scale down the release of inflammatory mediators that would prevent the progression of liver damage.

We speculate that the steps of alteration in TAA-treated rats are as following:

i. TAA bioactivates into TAA-S-oxide and other ROS (Chilakapati et al., 2005) causes lipid peroxidation evidenced by the elevation of MDA level, alters the antioxidant defence system of CAT, SOD and GPx (Yogalakshmi et al., 2010). TAA also activates the HSCs, which in turn releases more ECM and subsequently increases in the TGF-β1 and α-SMA expressions that affect the release of MMP1 then TIMP1.

ii. Thus, development of scar tissue resulting in loss of its normal functions, anatomical shape and architecture (Mormone et al., 2011).

iii. Treatment with VN and CS ethanolic extracts significantly reduced the impact of TAA toxicity, firstly, through removing the causative stimuli of TAA, neutralizing the ROS by their high antioxidant content and attenuation of endogenous antioxidant enzymes to their normal levels. Secondly, maintaining the HSCs in their quiescent state. Thirdly, through reducing the release of TGF-β1and α-SMA to counter balance and complete remodelling of the hepatocyte cellular system that preserves or sustains the normal liver function, shape and appearance.

iv. These findings confirm the previous study (Wills & Asha, 2007) who suggested that the hepatoprotective role of *Lygodium flexuosum* plant extract is due to reduction of the mRNA levels of the growth factors, pro inflammatory cytokines and other signaling molecules, which are

involved in hepatic fibrosis including TGF-β1, α-SMA, procollagen-I, and TIMP-1. Also (Chen et al., 2009) had demonstrated the hepatoprotective effects of silymarin against TAA-induced liver damage to be due to down-regulation of hepatic MMP-2, TIMP-1,TGF-β1, COL-α1 and other genes in the mouse model of chronic liver fibrosis. While the antifibrotic and hepatoprotective properties of silybin–phosphatidylcholine-α (TOH) complex in the rat model of hepatic fibrosis induced by bile duct ligation and dimethylnitrosamine administration was postulated to attribute reduced mRNA levels of procollagen type I, TGF-β1, TIMP-1 and MMP-2 genes expression. Besides, the administration of that complex has been reported to reduce HSCs activation and proliferation with collagen deposition (Di Sario et al., 2005).

Finally, recent studies have shown that plant-derived polyphenols are promising nutraceuticals for the control of various disorders such as cardiovascular, neurological and neoplastic diseases (Ullah & Khan, 2008). In addition, the use of such compounds were utilized as hepatoprotective agents, against different types of liver damage inducers like CCl_4 (Shimoda et al., 2008), paracetamol (Chen et al., 2009) and TAA (Madani et al., 2008) which explains the high interest and initiation of many researchers to study the biological activity and bio-availabilities of the polyphenolic compounds.

5.5 Cytotoxic Role of VN and CS

The immune system is one of the body's defence systems to detect the different pathogens by producing immediate responses and activation of immune cells, chemokines, cytokines and release of inflammatory mediators, which in turn modulate and adapt the immune system (Singh, V. et al., 2011). The identification of many medical plants derived compound having the capacity to interfere with carcinogenic processes besides possessing a significant role as an antitumour agent has received great interest lately (Wong et al., 1994). The naturally derived immunomodulators have great and green future for advancing towards new pharmaceutical products and serve as the initial point in the development of modern medicines (Ganju et al., 2003).

The ethanolic extracts of VN and CS have been shown to inhibit the survival of HepG2 cell lines and induce their apoptosis by releasing caspase-3 and LDH enzymes as illustrated in Figure 4.37; page 134, Figure 4.38; page 135 and Figure 4.39; page 136. Evidence shows the reduction of the general cytotoxicity is not easy due to the fact that cancerous cells and noncancerous cells are very similar. However, several attempts have been made to report the immunomodulatory roles of VN to protect different types of cells by its action against nitric oxide production (Manikandan et al., 2011). Additionally, CS derivatives has shown a wide variety of immune modulator action by protecting human dental pulp and human periodontal ligament cells from the cytotoxicity of H_2O_2 (Jeong et al., 2010). Besides that, anticancer activity of several isolated compounds from CS has been reported to be involved in cell proliferation and changes in the cell morphology (Zhang et al., 2010). Generally, PASS prediction for VN extract phytoconstituents compounds in terms of caspase-3 stimulant and antiproliferative activity showed an encouraging results but the main attribution is

related to 7,8-dimethyl herbacetin 3-rhamnoside (81.2%) and, 5,3'-dihydroxy-7,8,4'-trimethoxy flavanone (88.6%), respectively (Table 4.1). On the other hand, PASS results of CS extract showed the highest caspase-3 stimulant (89.9%) attributed to 3-deoxy sappanchalcone while sappanchalcone represented the strongest antiproliferative activity (87.1%) among all other active constituents (Table 4.2).

To date, no ideal cytotoxicity test has been developed, hence, in this study, VN and CS plants were screened, which are native to South Eastern Asia's countries. They are commonly used for treating a variety of ailments, including cancer, by using two-cell lines, WRL68 and HepG2 cells.

MTT assay was used to measure the amount of cell viability. This method is based on the quantification of purple-coloured formazan, which was formed by the reduction of MTT [3-(4,5-dimethylthiazole-2-yl)-2,5-diphenyl]. The potential antiproliferative effect of VN and CS extract was investigated to determine their effects on the viability of HepG2 and WRL 68. Since there was reduction of MTT proportional to the number of active mitochondria in the live cells, this result indicated that VN extract caused significant inhibition of HepG2 cells in a dose and time-dependent manner. Generally, it was found that VN extract at 57.36 µg/ml IC50 concentrations was cytotoxic for HepG2 cell lines after 48 hrs of exposure. Meanwhile, there was no IC50 value of VN extract against WRL 68 cell lines in all the concentrations and incubation periods as shown in Table 4.5 page 131. On the other hand, CS extract showed the highest cytotoxic effect against HepG2 and WRL68 cell lines at 72 hrs with IC50 value equal to 84.87 µg/ml and 163.40 µ/ml, respectively.

Since recent studies suggest that LDH is the more reliable and accurate marker of cytotoxicity, because damaged cells are fragmented completely during the path of prolonged incubation with substances (Hubert et al., 2011) (Sivalokanathan et al.,

2006). Therefore, in this study, the LDH amount from HepG2 cells was released in a time and dose dependent manner as shown in Figure 4.38 and Figure 4.39. This indicates that VN and CS extract are less cytotoxic on WRL 68 cell lines and the highest toxicity of VN on HepG2 cells was at 48 hrs. Based on MTT spectrophotometric assay, VN showed higher antiproliferative activities toward HepG2 cell lines in a dose and time-dependent manner than CS. The sensitivity of HepG2 cells to VN and CS is characterised by IC50 value. These results indicate that the antiproliferative effects increase with the dose and time of exposure. This observation was based on the average of three sets of experiments.

To prove that apoptosis has been influenced by VN and CS ethanolic extracts, HepG2 cells were examined in the presence of acridine orange and ethidium bromide staining (AO/EB staining). AO is a vital dye that will stain both live and dead cells, whereas EB will only stain those cells that have lost their membrane integrity (Raju et al., 2004). Green staining cells are viable cells, whereas reddish or orange staining ones are the late apoptotic cells. HepG2 cells treated with 100 µg/ml and 200 µg/ml of VN and CS ethanolic extracts, respectively showed changes in cellular morphology, including chromatin condensation, membrane blebbing, and fragmented nuclei as shown in Figure 4.36; page 133. Therefore, it could be assumed that the stronger apoptosis is associated with high concentration of VN and CS extracts. This high antiproliferative effect of VN and CS was related to the presence of bioactive compounds such as alkaloid, flavonoids like flavones, luteolin-7-glucoside, casticin, iridoid, glycosides, essential oil and other constituents like Vitamin C, carotene, glucononital, benzoic acid and β-sitosterol (Gautam et al., 2010). These findings are consistent with previous study which indicated that glycosides and flavones compounds

possessing potent anticancer properties against MCF-7 human breast cancer cells (Arulvasu et al., 2010).

Cell proliferation could be balanced by apoptosis. This represents an effective way to alleviate damaged cells through the activation of protease called caspase (Ramos et al., 2005). Human caspase cascade is involved in chemical-induced apoptosis, caspase-3 may cleave essential cellular proteins or activate additional caspases by proteolytic cleavage (Sivalokanathan et al., 2006).

To understand the molecular mechanism of VN or CS induced growth inhibition, we found that there was a marked increase in the activation of caspase-3, suggesting that caspase-3 dependent apoptotic death could be another mechanism for the beneficial effects of VN and CS. This is because of the activation of caspase-3 which leads to degradation of cellular proteins, cell shrinkage, DNA fragmentation, loss of plasma membrane potential and membrane blebbing (Timmer & Salvesen, 2006). The activation of caspase-3 induced chromosomal DNA break and finally the occurrence of apoptosis (Anantharam et al., 2002).

In the present investigation, VN and CS extracts showed activation of caspase-3 enzyme- mediated apoptosis in HepG2 cells (Figure 4.37; page 134). This might be due to the presence of glycosides and flavones. Similarly, there was a report that certain products from plants can induce apoptosis in cancerous cells like OCM-1, MCF-7 and HT-29 (Arulvasu et al., 2010).

In summary, the obtained findings showed the ability of VN and CS extracts to inhibit HepG2 cells proliferation via the induction of apoptosis and by the induction of caspase-3 activity. The observation of cells containing fragmented nuclei, suggesting the possible potent anticancer activity *in vitro* and chemoprotective role of VN and CS,

was presumably, due to their high antioxidant and free radical scavenging activities which have been identified to innate immune responses and acts as therapeutic pathways for controlling cancerous diseases (Agarwal & Singh, 1999). Further studies are needed to determine the molecular mechanism of the active components and to evaluate the potential *in vivo* anticancer activity of the both extracts

Chapter 6

Conclusion

1. PASS-predicted VN and CS activity has successfully been applied; the results have efficiently helped us in selecting the most promising pharmaceutical properties with high accuracy. PASS has saved for us unnecessary waste of chemicals and time. From PASS, it is clear that the most probable activities of VN and CS are antioxidant, hepatoprotectants and antiproliferative.
2. VN and CS had relevant amounts of phenolic and flavone contents and exhibited potent antioxidant activity *in vitro* by virtue of DPPH radical scavenging activity and ferric reducing antioxidant power.
3. VN and CS possessed significant *in vitro* hepatoprotective effect against H_2O_2-induced oxidative stress in WRL68 cell lines.
4. VN and CS were significantly effective in maintaining the macroscopic and microscopic features in TAA-induced liver cirrhosis in male rats.
5. VN and CS did significantly maintain the normal level of liver function test parameters, lipid profile, serum glucose and endogenous antioxidant enzymes in TAA - induced liver cirrhosis in male rats.
6. VN and CS have promising hepatoprotective activities through the reduction of lipid peroxidation product of liver, hepatic CYP2E1, MMP-2 and MMP-9 and TIMP-1 by monitoring the expression of TGF-β1and α-SMA proteins.
7. VN and CS possess significant *in vitro* cytotoxic and antiproliferative effect in HepG2 cells through the activation of caspase-3 enzyme.

Recommendations by the Examiners

The following points are addressed here for future research in this topic:

1. The scope of this project is to use the crude ethanol extracts of VN and CS for their hepatoprotective activity in thioacetamide-induced liver injury in rats, however, a substantial method and money are required to separate and identify the components of these extracts by using thin layer chromatography (TLC) or high performance liquid chromatography (HPLC) was recommended.

2. To identify the cytokines of liver fibrosis (i.e. TGF-β1, α SMA and PCNA), a Real-time PCR technique was recommended. However, Western Blot analysis and immunohistochemical analysis carried out were sufficient to support our findings.

3. To identify the cytokines of antiproliferative activity (caspase-3) of VN and CS, Western Blot analysis was recommended. However, enzyme linked immunosorbent assay (ELISA) was sufficient to support our findings.

4. To identify the phenol compounds in VN and CS extracts, Fourier transform infrared (FTIR) spectroscopy method was recommended. In this study, total phenolic content (TPC) satisfactorily support our findings

5. To identify hepatic MMP-2, MMP-9 and TIMP-1 enzymes, Western Blot and immunohistochemical analysis were recommended. However, enzyme linked immunosorbent assay (ELISA) sufficiently support our findings.

6. Further investigations of the pancreatic functions such as measuring amylase, lipase and trypsin levels together with immunohistochemical analysis were recommended to exclude pancreatic causes on the high serum glucose level.

Future Study

Potential Hepatoprotective Drugs

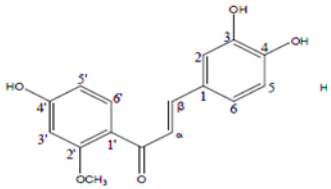

sappanchalcone

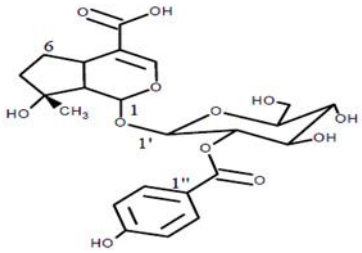

Negundoside

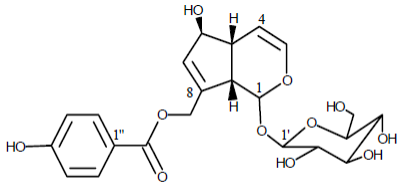

Agnuside

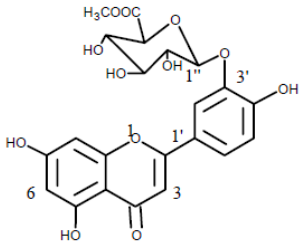

Vitegnoside

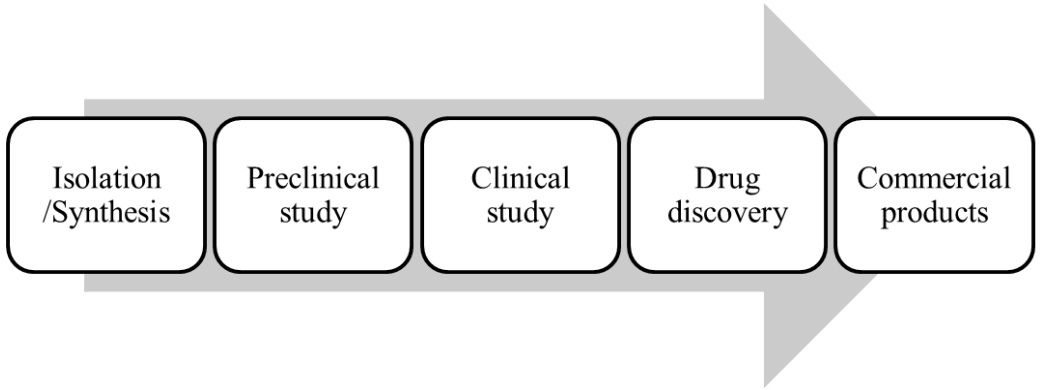

References

Abelson, J., Simon, M., & Reed, J. (2000). *Apoptosis*: Elsevier Science.

Abraham, D., Ponticos, M., & Nagase, H. (2005). Connective tissue remodeling: cross-talk between endothelins and matrix metalloproteinases. *Current vascular pharmacology, 3*(4), 369-379.

Abrahams, P., Boon, J., Spratt, J., & Hutchings, R. (2008). *McMinn's Clinical Atlas of Human Anatomy*: Elsevier/Mosby.

Agarwal, M., Srivastava, V. K., Saxena, K. K., & Kumar, A. (2006). Hepatoprotective activity of Beta vulgaris against CCl4-induced hepatic injury in rats. *Fitoterapia, 77*(2), 91-93.

Agarwal, S., & Singh, V. (1999). *Immunomodulators: a review of studies on Indian medicinal plants and synthetic peptides: Part I. Medicinal plants.* Paper presented at the Proc. Indian Natl. Sci. Acad.

Al-Bader, A., Mathew, T., Khoursheed, M., Asfar, S., Al-Sayer, H., & Dashti, H. (2000). Thioacetamide Toxicity and the Spleen: Histological and Biochemical Analysis. *Anatomia, Histologia, Embryologia, 29*(1), 3-8. doi: 10.1046/j.1439-0264.2000.00207.x

Al-Qubaisi, M., Rozita, R., Yeap, S., Omar, A., Ali, A., & Alitheen, N. (2011). Selective cytotoxicity of goniothalamin against hepatoblastoma HepG2 cells. *Molecules, 16*(4), 2944-2959. doi: 10.3390/molecules16042944

Allen, R., Hunter, W., & Agrawal, D. (1997). Morphological and biochemical characterization and analysis of apoptosis. *Journal of Pharmacological and Toxicological Methods, 37*(4), 215-228.

Amali, A., Rekha, R., Lin, C., Wang, W., Gong, H., Her, G., & Wu, J. (2006). Thioacetamide induced liver damage in zebrafish embryo as a disease model for steatohepatitis. *Journal of biomedical science, 13*(2), 225-232.

Amin, Z., Bilgen, M., Alshawsh, M., Ali, H., Hadi, A., & Abdulla, M. (2012). Protective Role of Phyllanthus niruri Extract against Thioacetamide-Induced Liver Cirrhosis in Rat Model. *Evidence-Based Complementary and Alternative Medicine, 2012*, 9. doi: 10.1155/2012/241583

Amorati, R., Ferroni, F., Pedulli, G., & Valgimigli, L. (2003). Modeling the Co-Antioxidant Behavior of Monofunctional Phenols. Applications to Some Relevant Compounds. *The Journal of Organic Chemistry, 68*(25), 9654-9658. doi: 10.1021/jo0351825

An, J., Seong, J., Oh, H., Kim, W., Han, K., & Paik, Y. (2006). Protein expression profiles in a rat cirrhotic model induced by thioacetamide. *The Korean journal of hepatology, 12*(1), 93-102.

Anantharam, V., Kitazawa, M., Wagner, J., Kaul, S., & Kanthasamy, A. (2002). Caspase-3-dependent proteolytic cleavage of protein kinase Cδ is essential for oxidative stress-mediated dopaminergic cell death after exposure to methylcyclopentadienyl manganese tricarbonyl. *The Journal of neuroscience, 22*(5), 1738-1751.

Antoine, M., Wirz, W., Tag, C., Gressner, A., Marvituna, M., Wycislo, M., Hellerbrand, C., & Kiefer, P. (2007). Expression and function of fibroblast growth factor (FGF) 9 in hepatic stellate cells and its role in toxic liver injury. *Biochemical and Biophysical Research Communications, 361*(2), 335-341. doi: 10.1016/j.bbrc.2007.06.189

Arthur, M. (1998). Fibrosis and altered matrix degradation. *Digestion, 59*(4), 376-380.

Arulvasu, C., Prabhu, D., Manikandan, R., Srinivasan, P., Dinesh, D., Babu, G., & Sellamuthu, S. (2010). Induction of apoptosis by the aqueous and ethanolic leaf extract of Vitex negundo L. in MCF-7 human breast cancer cells. *International Journal of Drug Discovery, 2*(1), 1-7.

Asselah, T., Bieche, I., Sabbagh, A., Bedossa, P., Moreau, R., Valla, D., Vidaud, M., & Marcellin, P. (2009). Gene expression and hepatitis C virus infection. *Gut, 58*(6), 846-858.

Atakisi, E., Karapehlivan, M., Atakisi, O., Kontas, T., & Marasli, S. (2006). Adenosine deaminase and biochemical liver function tests in the dermatophytic cattle. *Bulletin-Veterinary Institute in Pulawy, 50*(4), 481.

Athina, G., Poroikov, V., Salutin, V., Macaev, F., Babaev, E., Voronina, T., Proenca, F., Dearden, J., & Belzung, K. (2007, October 1-3). [Computer-aided selection and biological testing of anxiolytics, anticonvulsants and cognition enhancers in divers set of chemical compounds].

Atzori, L., Poli, G., & Perra, A. (2009). Hepatic stellate cell: a star cell in the liver. *The International Journal of Biochemistry & Cell Biology, 41*(8), 1639-1642.

Avadhoot, Y., & Rana, A. (1991). Hepatoprotective effect of Vitex negundo against carbon tetrachloride-induced liver damage. *Archives of pharmacal research 14*(1), 96-98.

Badami, S., Moorkoth, S., & Suresh, B. (2004). Caesalpinia sappan–A medicinal and dye yielding plant. *Nat Prod Radiance, 3*, 75-82.

Balkan, J., Dogğru-Abbasoğlul, S., Çevikbas, U., Aykaç-Toker, G., & Uysal, M. (2001). Taurine has a protective effect against thioacetamide-induced liver cirrhosis by decreasing oxidative stress. *Human & experimental toxicology, 20*(5), 251-254.

Bancroft, J., & Cook, H. (1994). *Manual of histological techniques and their diagnostic application*: Churchill Livingstone.

Bass, N. (1999). Is there any use for nontraditional or alternative therapies in patients with chronic liver disease? *Current gastroenterology reports, 1*(1), 50-56.

Bauer, R. (1998). Quality Criteria and Standardization of Phytopharmaceuticals: Can Acceptable Drug Standards be Achieved? *Drug Information Journal, 32*(1), 101-110. doi: 10.1177/009286159803200114

Bayless, T., & Diehl, A. (2005). *Advanced Therapy in Gastroenterology and Liver Disease, Fifth Edition*: Pmph Bc Decker.

Bedossa, P., Houglum, K., Trautwein, C., Holstege, A., & Chojkier, M. (1994). Stimulation of collagen α1 (I) gene expression is associated with lipid peroxidation in hepatocellular injury: a link to tissue fibrosis? *Hepatology, 19*(5), 1262-1271.

Benzie, I. (1999). Ferric reducing/antioxidant power assay: direct measure of total antioxidant activity of biological fluids and modified version for simultaneous measurement of total antioxidant power and ascorbic acid concentration. *Method Enzymol., 299*, 15-27.

Bergendi, L., Beneš, L., Ďuračková, Z., & Ferenčik, M. (1999). Chemistry, physiology and pathology of free radicals. *Life sciences, 65*(18), 1865-1874.

Block, K., & Mead, M. (2003). Immune system effects of echinacea, ginseng, and astragalus: a review. *Integrative cancer therapies, 2*(3), 247-267.

Boigk, G., Stroedter, L., Herbst, H., Waldschmidt, J., Riecken, E., & Schuppan, D. (1997). Silymarin retards collagen accumulation in early and advanced biliary fibrosis secondary to complete bile duct obliteration in rats. *Hepatology, 26*(3), 643-649.

Brandon, E., Raap, C., Meijerman, I., Beijnen, J., & Schellens, J. (2003). An update on in vitro test methods in human hepatic drug biotransformation research: pros and cons. *Toxicology and Applied Pharmacology, 189*(3), 233-246. doi: http://dx.doi.org/10.1016/S0041-008X(03)00128-5

Bruck, R., Aeed, H., Shirin, H., Matas, Z., Zaidel, L., Avni, Y., & Halpern, Z. (1999). The hydroxyl radical scavengers dimethylsulfoxide and dimethylthiourea protect

rats against thioacetamide-induced fulminant hepatic failure. *Journal of hepatology, 31*(1), 27-38.

Bruck, R., Genina, O., Aeed, H., Alexiev, R., Nagler, A., Avni, Y., & Pines, M. (2001). Halofuginone to prevent and treat thioacetamide-induced liver fibrosis in rats. *Hepatology, 33*(2), 379-386. doi: 10.1053/jhep.2001.21408

Bucio, L., Souza, V., Albores, A., Sierra, A., Chávez, E., Cárabez, A., & Gutiérrez-Ruiz, M. (1995). Cadmium and mercury toxicity in a human fetal hepatic cell line (WRL-68 cells). *Toxicology, 102*(3), 285-299. doi: 10.1016/0300-483x(95)03095-w

Buijnsters, M., Bicanic, D., Chirtoc, M., Nicoli, M. C., & Min-Kuo, Y. (2001). Evaluation of anti-oxidative activity of some antioxidants by means of a combined optothermal window and a DPPH free-radical colorimetry. *Journal of Analytic Science and Spectroscopy 17*, 544-546.

Casini, A., Pinzani, M., Milani, S., Grappone, C., Galli, G., Jezequel, A., & Surrenti, C. (1993). Regulation of extracellular matrix synthesis by transforming growth factor beta 1 in human fat-storing cells. . *Gastroenterology, 105* (1), 245-253.

Cassiman, D., Denef, C., Desmet, V., & Roskams, T. (2001). Human and rat hepatic stellate cells express neurotrophins and neurotrophin receptors. *Hepatology, 33*(1), 148-158.

Cawston, T. (1998). Matrix metalloproteinases and TIMPs: properties and implications for the rheumatic diseases. *Molecular Medicine Today, 4*(3), 130-137.

Chakrabarty, P., Chattopadhyay, S., & Schneider, W. (1982). Molecular basis for increased synthesis of albumin in rat liver after thioacetamide administration. *Cancer Res, 42*(2), 421-428.

Chen, H., Yan, X., Zhu, P., & Lin, J. (2006). Antioxidant activity and hepatoprotective potential of agaro-oligosaccharides in vitro and in vivo. *Nutr J, 5*(1), 31.

Chen, X., Sun, C., Han, G., Peng, J., Li, Y., Liu, Y., Lv, Y., Liu, K., Zhou, Q., & Sun, H. (2009). Protective effect of tea polyphenols against paracetamol-induced hepatotoxicity in mice is significanly correlated with cytochrome P450 suppression. *World Journal of gastroenterology., 15*(15), 1829.

Chilakapati, J., Shankar, K., Korrapati, M., Hill, R., & Mehendale, H. (2005). Saturation toxicokinetics of thioacetamide: role in initiation of liver injury. *Drug metabolism and Disposition, 33*(12), 1877-1885.

Chrungoo, V., Singh, K., & Singh, J. (1997). Silymarin mediated differential modulation of toxicity induced by carbon tetrachloride, paracetamol and D-

galactosamine in freshly isolated rat hepatocytes. *Indian J Exp Biol, 35*(6), 611-617.

Cinghită, D., Radovan, C., & Dascălu, D. (2008). Anodic Voltammetry of Thioacetamide and its Amperometric Determination in Aqueous Media. *Sensors, 8*(8), 4560-4581.

Clark, J., Gebhart, G., Gonder, J., Keeling, M., & Kohn, D. (1997). The 1996 guide for the care and use of laboratory animals. *ILAR journal, 38*(1), 41-48.

Cooke, R., & Stewart, B. (2004). *Color Atlas Anatomical Pathology 3e*: Churchill Livingstone.

Corrao, G., Lepore, A., Torchio, P., Valenti, M., Galatola, G., D'Amicis, A., Aricò, S., & di Orio, F. (1994). The effect of drinking coffee and smoking cigarettes on the risk of cirrhosis associated with alcohol consumption. *European Journal of Epidemiology, 10*(6), 657-664. doi: 10.1007/bf01719277

Cotelle, N. (2001). Role of flavonoids in oxidative stress. *Current topics in medicinal chemistry, 1*(6), 569-590.

Cragg, G., & Newman, D. (2005). Plants as a source of anti-cancer agents. *Journal of Ethnopharmacology, 100*(1), 72-79.

Crawford, J. (Ed.). (2002). *Liver cirrhosis. Pathology of the Liver.* (4th edition ed.). London: Churchill Livingstone.

Cruz, A., Padillo, F., Torres, E., Navarrete, C., Muñoz, C., Caballero, F., Briceño, J., Marchal, T., Túnez, I., & Montilla, P. (2005). Melatonin prevents experimental liver cirrhosis induced by thioacetamide in rats. *Journal of Pineal Research, 39*(2), 143-150.

Cunningham, C., & Van Horn, C. (2003). Energy availability and alcohol-related liver pathology. *Alcohol Research and Health 27*(4), 281–299.

Curran, R. (Ed.). (1982). *Colour Atlas of Histopathology.* (2nd edition ed.). England: Harvey Miller, M. LTD.

Dashti, H., Mathew, T., Jadaon, M., & Ashkanani, E. (1997). Zinc and liver cirrhosis: biochemical and histopathologic assessment. *Nutrition, 13*(3), 206-212.

Dehmlow, C., Erhard, J., & De Groot, H. (1996). Inhibition of Kupffer cell functions as an explanation for the hepatoprotective properties of silibinin. *Hepatology, 23*(4), 749-754.

Derek, G. (Ed.). (1994). *Systemic Pathology: Liver, Biliary tract and Exocrine Pancreas.* (11th edition ed.). Churchill Livingstone: Timothy Horne.

Deshpande, N., Kandi, S., Kumar, P., Ramana, K., & Muddeshwar, M. (2013). Effect of Alcohol Consumption on Oxidative Stress Markers and its Role in the Pathogenesis and Progression of Liver Cirrhosis. *American Journal of Medical and Biological Research, 1*(4), 99-102.

Di Sario, A., Bendia, E., Taffetani, S., Omenetti, A., Candelaresi, C., Marzioni, M., De Minicis, S., & Benedetti, A. (2005). Hepatoprotective and antifibrotic effect of a new silybin–phosphatidylcholine–Vitamin E complex in rats. *Digestive and Liver Disease, 37*(11), 869-876.

Durrieu, C., Degraeve, P., Carnet-Pantiez, A., & Martial, A. (2005). Assessment of the immunomodulatory activity of cheese extracts by a complete and easy to handle invitro screening methodology. *Biotechnology letters, 27*(14), 969-975.

Eroschenko, V., & di Fiore, M. (2012). *DiFiore's Atlas of Histology with Functional Correlations*: Wolters Kluwer Health/Lippincott Williams & Wilkins.

Ewelina, V., Rafal, J., & Grzegorz, L. (2013). Media Effects on the Mechanism of Antioxidant Action of Silybin and 2,3-Dehydrosilybin: Role of the Enol Group. *The Journal of Organic Chemistry, 78*(18), 9102-9112. doi: 10.1021/jo401296k

Fan, G., & Steer, C. (Eds.). (2006). *Cellular Biology of The Normal Liver. Comprehensive Clinical Hepatology. In: Bacon BR, O'Grady JG, Di Bisceglie AM, Lake JR editors.* (2nd edition ed.). USA: Elsevier Mosby.

Fantozzi, R., Brunelleschi, S., Rubino, A., Tarli, S., Masini, E., & Mannaioni, P. (1986). FMLP-activated neutrophils evoke histamine release from mast cells. *Inflammation Research, 18*(1), 155-158.

Ferrell, L., & Greenberg, M. (2007). Special stains can distinguish hepatic necrosis with regenerative nodules from cirrhosis *Liver International, ISSN 1478-3223.*

Fevery, J., & Blanckaert, N. (1986). What can we learn from analysis of serum bilirubin? . *Journal of Hepatology 2*(1), 113-121.

Flora, S. (2007). Role of free radicals and antioxidants in health and disease. *Cell Mol Biol 53*(1), 1-2.

Friedman, L., & Keeffe, E. (2011). *Handbook of Liver Disease*: Elsevier Health Sciences.

Friedman, S. (1997). Molecular mechanisms of hepatic fibrosis and principles of therapy. *Journal of Gastroenterology, 32*(3), 424-430.

Friedman, S. (2000). Molecular regulation of hepatic fibrosis, an integrated cellular response to tissue injury. *Journal of Biological Chemistry, 275*(4), 2247-2250.

Friedman, S., & Schiano, T. (Eds.). (2004). *Cirrhosis and its sequelea. In Goldman L, Ausiello D, Textbook of Medicine* (22nd edition. ed.). Philadelphia: Pa, Saunders.

Fu, L., Huang, X., Lai, Z., Hu, Y., Liu, H., & Cai, X. (2008). A new 3-benzylchroman derivative from Sappan Lignum (Caesalpinia sappan). *Molecules, 13*(8), 1923-1930.

Fu, P., Xia, Q., Chou, M., & Lin, G. (2007). Detection, hepatotoxicity, and tumorigenicity of pyrrolizidine alkaloids in Chinese herbal plants and herbal dietary supplements. *Journal of Food and Drug Analysis, 15*(4), 400.

Fuchs, E., Weyhenmeyer, R., & Weiner, O. (1997). Effects of silibinin and of a synthetic analogue on isolated rat hepatic stellate cells and myofibroblasts. *Arzneimittel-Forschung, 47*(12), 1383.

Galato, D., Ckless, K., Susin, M., Giacomelli, C., Ribeiro-do-Valle, R., & Spinelli, A. (2001). Antioxidant capacity of phenolic and related compounds: correlation among electrochemical, visible spectroscopy methods and structure–antioxidant activity. *Redox Report, 6*(4), 243-250.

Ganju, L., Karan, D., Chanda, S., Srivastava, K., Sawhney, R., & Selvamurthy, W. (2003). Immunomodulatory effects of agents of plant origin. *Biomedicine & pharmacotherapy, 57*(7), 296-300.

Garrett, W., & Kirkendall, D. (2000). *Exercise and sport science.*

Gartner, L., Hiatt, J., & Strum, J. (Eds.). (2007). *Cell Biology And Histology.* (5th edition. ed.). Philadelphia:: Lippincott Williams & Wilkins. .

Gautam, L., Shrestha, S., Wagle, P., & Tamrakar, B. (2010). Chemical constituents from Vitex negundo (Linn.) of nepalese origin. *Scientific world, 6*(6), 27-32.

Geoffrey, L., William, W., & Dennis, E. (Eds.). (1995). *Principles of Biochemistry. Integration of Metabolism and Hormone Action.* United States of America:: Wm. C. Brown Publishers.

George, J., Pera, N., Phung, N., Leclercq, I., Yun Hou, J., & Farrell, G. (2003). Lipid peroxidation, stellate cell activation and hepatic fibrogenesis in a rat model of chronic steatohepatitis. *Journal of hepatology, 39*(5), 756-764. doi: 10.1016/s0168-8278(03)00376-3

George, S., Bhalerao, S. V., Lidstone, E. A., Ahmad, I. S., Abbasi, A., Cunningham, B. T., & Watkin, K. L. (2010). Cytotoxicity screening of Bangladeshi medicinal plant extracts on pancreatic cancer cells. *BMC Complement Altern Med, 10*, 52. doi: 10.1186/1472-6882-10-52

Ghadir, M., Riahin, A., Havaspour, A., Nooranipour, M., & Habibinejad, A. (2010). The relationship between lipid profile and severity of liver damage in cirrhotic patients. *Hepat Mon, 10*(4), 285-288.

Giannini, E., Testa, R., & Savarino, V. (2005). Liver enzyme alteration: a guide for clinicians. *Canadian Medical Association Journal, 172*(3), 367-379.

Goodman, Z. (2007). Grading and staging systems for inflammation and fibrosis in chronic liver diseases. *Journal of hepatology, 47*(4), 598-607.

Gorinstein, S., Belloso, O. M., Katrich, E., Lojek, A., Miguel, M. N. G., Haruenkit, R., Seo Park, Y., Teck Jung, S., & Trakhtenberg, S. (2003). Comparison of the contents of the main biochemical compounds and the antioxidant activity of some Spanish olive oils as determined by four different radical scavenging tests. *Journal of Nutritional Biochemistry 14*(3), 154-159.

Gressner, O., Weiskirchen, R., & Gressner, A. (2007). Evolving concepts of liver fibrogenesis provide new diagnostic and therapeutic options. *Comparative hepatology, 6*(1), 7.

Guengerich, F. (2007). Mechanisms of cytochrome P450 substrate oxidation: MiniReview. *Journal of Biochemical and Molecular Toxicology, 21*(4), 163-168. doi: 10.1002/jbt.20174

Gülçin, Ý., Elias, R., Gepdiremen, A., Boyer, L., & Köksal, E. (2007). A comparative study on the antioxidant activity of fringe tree (Chionanthus virginicus L.) extracts. *African Journal of Biotechnology, 6*(4).

Gutiérrez-Ruíz, M., Robles-Díaz, G., & Kershenobich, D. (2002). Emerging concepts in inflammation and fibrosis. *Archives of medical research, 33*(6), 595-599.

Guyot, C., Lepreux, S., Combe, C., Doudnikoff, E., Bioulac-Sage, P., Balabaud, C., & Desmoulière, A. (2006). Hepatic fibrosis and cirrhosis: the (myo) fibroblastic cell subpopulations involved. *The international journal of biochemistry & cell biology, 38*(2), 135-151.

Hade, S. (2012). Exploration of new therapeutic potential of phytoconstituents in anti-inflammatory plants by PASS. *Journal of Chemical and Pharmaceutical Research, 4*(4), 1925-1937.

Hamza, A. (2010). Ameliorative effects of Moringa oleifera Lam seed extract on liver fibrosis in rats. *Food and Chemical Toxicology, 48*(1), 345-355.

Hanaa, M. (2007). Biochemical studies on thioacetamide toxicity in male albino rats and the role of tomato juice as an antioxidant, *Mansoura Journal of Forensic Medicine and clinical Toxicology, 15*(2), 99-115.

Harborne, J., & Williams, C. (2000). Advances in flavonoid research since 1992. *Phytochemistry, 55*(6), 481-504. doi: http://dx.doi.org/10.1016/S0031-9422(00)00235-1

Hasani-Ranjbar, S., Larijani, B., & Abdollahi, M. (2009). A systematic review of the potential herbal sources of future drugs effective in oxidant-related diseases. *Inflammation & Allergy-Drug Targets (Formerly??? Current Drug Targets, 8*(1), 2-10.

Heidelbaugh, J., & Bruderly, M. (2006). Cirrhosis and Chronic Liver Failure: Part I. Diagnosis and Evaluation. . *American Family Physician 72*(5), 756-762.

Horwitz, W. (1980). *Official Methods of Analysis of the Association of Official Analytical Chemists. 13th Ed*: Assoc. Off. Anal. Chem.

Hsiao, T., Liao, H., Hsieh, P., & Wong, R. (2007). Risk of betel quid chewing on the development of liver cirrhosis: a community-based case-control study. *Annals of epidemiology, 17*(6), 479-485.

Hu, J., Yan, X., Wang, W., Wu, H., Hua, L., & Du, L. (2008). Antioxidant activity in vitro of three constituents from Caesalpinia sappan L. *Tsinghua Science and Technology 13*(4), 474-479.

Huang, G., Deng, J., Huang, S., Shao, Y., Chen, C., & Kuo, Y. (2011). Protective effect of antrosterol from Antrodia camphorata submerged whole broth against carbon tetrachloride-induced acute liver injury in mice. *Food Chemistry*.

Hubert, D., Dawe, A., Florence, N., Gilbert, K., Angele, T., Buonocore, D., Finzi, P., Vidari, G., Bonaventure, N., & Marzatico, F. (2011). In vitro hepatoprotective and antioxidant activities of crude extract and isolated compounds from Ficus gnaphalocarpa. *Inflammopharmacology, 19*(1), 35-43.

Hübscher, S. (2006). Histological assessment of non-alcoholic fatty liver disease. *Histopathology, 49*(5), 450-465.

Hui-Mei, L., Hsien-Chun, T., Chau-Jong, W., Jin-Jin, L., Chia-Wen, L., & Fen-Pi, C. (2008). Hepatoprotective effects of Solanum nigrum Linn extract against CCl4-induced oxidative damage in rats. *Chem Biol Interact, 171*, 283-293.

Ighodaro, O., Omole, J., & Uwaifo, A. (2010). Effects of Chronic Ethanol Administration on Body Weight, Reduced Glutathione (GSH), Malondialdehyde (MDA) Levels and Glutathione-s-transferase Activity (GST) in Rats. *New York Science Journal, 3*, 39-47.

Jeffrey, B. (Ed.). (2000). *Atlas of Functional Histology*. (2nd edition ed.). London: Harcourt Publisher Limited.

Jeong, G., Lee, D., Li, B., Lee, H., Kim, E., & Kim, Y. (2010). Effects of sappanchalcone on the cytoprotection and anti-inflammation via heme oxygenase-1 in human pulp and periodontal ligament cells. *European Journal of Pharmacology, 644*, 230-237.

Jia, J., Bauer, M., Cho, J., Ruehl, M., Milani, S., Boigk, G., Riecken, E., & Schuppan, D. (2001). Antifibrotic effect of silymarin in rat secondary biliary fibrosis is mediated by downregulation of procollagen α1 (I) and TIMP-1. *Journal of hepatology, 35*(3), 392-398.

Jones, W., Chin, Y., & Kinghorn, A. (2006). The role of pharmacognosy in modern medicine and pharmacy. *Curr Drug Targets, 7*(3), 247-264.

Junqueira, L., & Carneiro, J. (2005). *Basic Histology: Text and Atlas*: McGraw-Hill.

Kadir, F., Othman, F., Abdulla, A., Hussan, F., & Hassandarvish, P. (2011). Effect of Tinospora crispa on thioacetamide-induced liver cirrhosis in rats. *Indian Journal of Pharmacology, 43*(1), 64-68.

Kaplowitz, N., & DeLeve, L. (2007). *Drug-induced liver disease*: Informa Healthcare.

Katiyar, S., Korman, N., Mukhtar, H., & Agarwal, R. (1997). Protective effects of silymarin against photocarcinogenesis in a mouse skin model. *Journal of the National Cancer Institute, 89*(8), 556-565.

Keith, L., Arthur, F., & Anne, M. (Eds.). (2009). *Clinically Oriented Anatomy* (6th edition ed.): Lippincott Williams & Wilkins.

Kim, S., Park, S., Lee, J., Yang, J., Cho, M., Choi, S., & Cho, Y. (2009). Caesalpinia sappan extracts for improving and treating acne *Repub. Korean Kongkae Taeho Kongbo KR 2009055261 A 20090602*.

Kirtikar, K., & Basu, B. (Eds.). (2008). *Indian medicinal plants* (Vol. 3). Dehradun: International Book Distributors.

Koehn, F., & Carter, G. (2005). The evolving role of natural products in drug discovery. *Nature Reviews Drug Discovery, 4*(3), 206-220.

Koek, G., Bast, A., & Driessen, A. (2007). The encyclopedia of vitamin E: Liver cirrhosis and vitamin E status. . Retrieved from http://bookshop.cabi.org. website:

Křen, V., & Walterova, D. (2009). Silybin and silymarin–new effects and applications. *Biomedical papers, 149*(1), 29-41.

Kropacova, K., Misurova, E., & Hakova, H. (1998). Protective and therapeutic effect of silymarin on the development of latent liver damage. *Radiats Biol Radioecol, 38*, 411-415.

Kumar, V., Abbas, A., Aster, J., & Robbins, S. (2012). *Robbins Basic Pathology*: Elsevier/Saunders.

Kumar, V., Abbas, A., Fausto, N., & Aster, J. (2009). *Robbins & Cotran Pathologic Basis of Disease*: Elsevier Health Sciences.

Kuntz, E., & Kuntz, H. (2008). *Hepatology: Textbook and Atlas : History, Morphology, Biochemistry, Diagnostics, Clinic, Therapy*: Springer Berlin Heidelberg.

Kuo, D., Kang, W., Shieh, P., Chen, F., Chang, C., Tsai, M., Cheng, A., Ho, C., & Pan, M. (2010). Protective effect of Pracparatum mungo extract on carbon tetrachloride-induced hepatotoxicity in rats. *Food Chemistry, 123*(4), 1007-1012.

Kuzu, N., Metin, K., Dagli, A., Akdemir, F., Orhan, C., Yalniz, M., Ozercan, I., Sahin, K., & Bahcecioglu, I. (2007). Protective role of genistein in acute liver damage induced by carbon tetrachloride. *Mediators of inflammation, 1*, 36381.

Lagunin, A., Gomazkov, A., Filimonov, D., Gureeva, A., Dilakyan, A., Kugaevskaya, E., Elisseeva, Y., Solovyeva, N., & Poroikov, V. (2003). Computer-Aided Selection of Potential Antihypertensive Compounds with Dual Mechanism of Action
J. Med. Chem, 46, 3326-3332.

Lascelles, P., & Donaldson, D. (1990). *Diagnostic Function Tests in Chemical Pathology*: Kluwer Academic.

Lee, C., Shih, P., Hsu, C., & Yen, G. (2007). Hepatoprotection of tea seed oil (Camellia oleifera Abel.) against CCl4-induced oxidative damage in rats. *Food Chem Toxicol, 45*(6), 888-895. doi: 10.1016/j.fct.2006.11.007

Lee, J., & Min, K. (2011). Antimicrobial activity and bactericidal activity of Caesalpinia sappan L. extract *Hangug Hwangyeong Bogeon Haghoeji 37*(2), 133-140.

Lee, Y., Jeong, G., Lim, H., An, R., Kim, Y., & Kim, E. (2010). Isoliquiritigenin 2'-methyl ether induces growth inhibition and apoptosis in oral cancer cells via heme oxygenase-1 *Toxicology in Vitro 24*(3), 776-782.

Leonard, R. (1995). *Human Gross Anatomy: An Outline Text*: Oxford University Press.

Levison, D., & Reid, R. (Eds.). (2008). *MUIR'S Text book of Pathology.* (14th edition ed.). London: Edward Arnold. Ltd.

Liaw, Y., Tai, D., Chu, C., & Chen, T. (1988). The development of cirrhosis in patients with chronic type B hepatitis: a prospective study. *Hepatology, 8*(3), 493-496.

Lisina, K., Ragavendran, P., Sophia, D., Rajamanikandan, S., Sindhu, T., Durgapriya, D., & Gopalakrishnan, V. (2011). A comparitive study of Justicia adhatoda, Mimosa pudica AD Vitex negundo against hepatoprotective activity albi o rats-in vivo evaluation. *Pharmacologyonline, 1*, 481-491.

Ljubuncic, P., Song, H., Cogan, U., Azaizeh, H., & Bomzon, A. (2005). The effects of aqueous extracts prepared from the leaves of Pistacia lentiscus in experimental liver disease. *Journal of Ethnopharmacology, 100*(1-2), 198-204.

Luper, S. (1998). A review of plants used in the treatment of liver disease: part 1. *Altern Med Rev, 3*(6), 410-421.

Luxon, B. (Ed.). (2006). *Functions of the Liver. Comprehensive Clinical Hepatology* (2nd edition. ed.). USA: Elsevier Mosby. .

MacSween, R. (1994). *Pathology of the liver*: Churchill Livingstone.

Mahalakshmi, R., Rajesh, P., Balasubramanian, V., & Rajesh Kanan, V. (2010). Hepatoprotective activity on Vitex negundo Linn.(Verbanaceae) by using Wistar albino rats in Ibuprofen induced model. *International Journal of Pharmacology, 6*(5), 658-663.

Malhi, H., Gores, G., & Lemasters, J. (2006). Apoptosis and necrosis in the liver: a tale of two deaths? *Hepatology, 43*(2 Suppl 1), S31-44. doi: 10.1002/hep.21062

Mallikadevi, T., Paulsamy, S., Jamuna, S., & Karthika, K. (2012). Analysis for phytoceuticals and bioinformatics approach for the evaluation of therapetic properties of whole plant methanolic extract of mukia maderaspatana (l.) M.roem. (cucurbitaceae) – a traditional medicinal plant in western districts of Tamil nadu, India.. *Asian Journal of Pharmaceutical & Clinical Research., 5*(4), 163.

Manikandan, R., Thiagarajan, R., Beulaja, S., Sivakumar, M., Meiyalagan, V., Sundaram, R., & Arumugam, M. (2011). 1,2 di-substituted idopyranose from Vitex negundo L. protects against streptozotocin-induced diabetes by inhibiting nuclear factor-kappa B and inducible nitric oxide synthase expression *Microscopy Research and Technique 74*(4), 301-307.

Mann, R., Smart, R., & Govoni, R. (2003). The epidemiology of alcoholic liver disease. *Alcohol Research and Health, 27*, 209-219.

Mathew, S., & Abraham, T. (2006). In vitro antioxidant activity and scavenging effects of Cinnamomum verum leaf extract assayed by different methodologies. *Food and chemical toxicology: an international journal published for the British Industrial Biological Research Association, 44*(2), 198.

Matsumoto, K., Masui, S., Yokoyama, Y., Yoshihama, K., Kuroda, H., & Suzuki, M. (1993). A hair growth promoter containing extract of Vitex negundo L.var.cannabifolia or Vitex negundo L. . *Jpn. Kokai Tokkyo Koho, JP 05139938 A 19930608*.

McEwen, D. (1996). Management of Alcoholic Cirrhosis of the Liver. *ARON Journal, 64*(2), 209-216.

McPhee, S., & Hammer, G. (2009). *Pathophysiology of Disease An Introduction to Clinical Medicine, Sixth Edition*: McGraw-Hill.

McQueen, C. (2010). *Comprehensive Toxicology*: Elsevier Science.

Mena, S., Ortega, A., & Estrela, J. (2009). Oxidative stress in environmental-induced carcinogenesis. *Mutation Research/Genetic Toxicology and Environmental Mutagenesis, 674*(1), 36-44.

Millward-Sadler, G., Wright, R., & Arthur, J. (1992). *Wright's liver and biliary disease: pathophysiology, diagnosis and management*: W.B. Saunders.

Moon, C. (1986). Drugs from Caesalpinia. *Ger. Offen, DE 3511609 A1 19861002.* .

Moon, C., Park, K., Kim, S., Won, H., & Chung, J. (1992). Brazilin protects cultured rat hepatocytes from bromochloroform-induced toxicity. *Drug and Chemical Toxicology 15*(1), 81-91.

Moon, H., Chung, I., Seo, S., & Kang, E. (2010). Protective effects of 3’-deoxy-4-O-methylepisappanol from Caesalpinia sappan against glutamate-induced neurotoxicity inprimary cultured rat cortical cells *Phytotherapy Research 24*(3), 463-465

Mormone, E., George, J., & Nieto, N. (2011). Molecular pathogenesis of hepatic fibrosis and current therapeutic approaches. *Chem Biol Interact, 193*(3), 225-231.

Morton, D., Foreman, K., & Albertine, K. (2011). *The Big Picture: Gross Anatomy*. F. K. In: Morton DA, Albertine KH, eds. (Ed.) *Foregut*

Müller, A., Machnik, F., Zimmermann, T., & Schubert, H. (1988). Thioacetamide-induced cirrhosis-like liver lesions in rats usefulness and reliability of this animal model. *Experimental Pathology, 34*(4), 229-236. doi: 10.1016/s0232-1513(88)80155-5

Muñoz, T. (1991). Experimental thioacetamide-induced cirrhosis of the liver. *Histology and histopathology, 6*(1), 95-100.

Muriel, P., Garciapina, T., Perez-Alvarez, V., & Mourelle, M. (1992). Silymarin protects against paracetamol-induced lipid peroxidation and liver damage. *J Appl Toxicol, 12*(6), 439-442.

Muriel, P., Suarez, O., Gonzalez, P., & Zuņiga, L. (1994). Protective effect of S-adenosyl-l-methionine on liver damage induced by biliary obstruction in rats: a histological, ultrastructural and biochemical approach. *Journal of hepatology, 21*(1), 95-102.

Murray, C., & Lopez, A. (1997). Alternative projections of mortality and disability by cause 1990-2020: Global Burden of Disease Study. *Lancet, 349*(9064), 1498-1504.

Nakajima, M., Iwata, K., Yamamoto, T., Funae, Y., Yoshida, T., & Kuroiwa, Y. (1998). Nicotine metabolism in liver microsomes from rats with acute hepatitis or cirrhosis. *Drug metabolism and Disposition, 26*(1), 36-41.

Natarajan, S., Thomas, S., Ramamoorthy, P., Basivireddy, J., Pulimood, A., Ramachandran, A., & Balasubramanian, K. (2006). Oxidative stress in the development of liver cirrhosis: A comparison of two different experimental models. *Journal of Gastroenterology and Hepatology, 21*(6), 947-957. doi: 10.1111/j.1440-1746.2006.04231.x

Negi, A., Kumar, J., Luqman, S., Shanker, K., Gupta, M., & Khanuja, S. (2008). Recent advances in plant hepatoprotectives: a chemical and biological profile of some important leads. *Medicinal research reviews, 28*(5), 746-772.

Newman, D., Cragg, G., & Snader, K. (2003). Natural products as sources of new drugs over the period 1981-2002. *Journal of Natural Products, 66*(7), 1022-1037.

Nugraheni, M., Santoso, U., & Suparmo, W. (2011). In vitro antioxidant, antiproliferative and apoptosis effect of Coleus tuberosus L. *African Journal of Food Science, 5*(4), 232-241.

Nussler, A., Wildemann, B., Freude, T., Litzka, C., Soldo, P., Friess, H., Hammad, S., Hengstler, J., Braun, K., Trak-S., Godoy, P., & Ehnert, S. (2014). Chronic CCl4 intoxication causes liver and bone damage similar to the human pathology of hepatic osteodystrophy: a mouse model to analyse the liver–bone axis. *Archives of Toxicology*, 1-10. doi: 10.1007/s00204-013-1191-5

Okazaki, I., Ninomiya, Y., Kyuichi, T., & Friedman, S. (2003). *Extracellular Matrix and the Liver: Approach to Gene Therapy*: Academic Press.

Ovalle, W., Nahirney, P., & Netter, F. (2013). *Netter's Essential Histology: With Student Consult Access*: Elsevier Science Health Science Division.

Pallottini, V., Martini, C., Bassi, A., Romano, P., Nanni, G., & Trentalance, A. (2006). Rat HMGCoA reductase activation in thioacetamide-induced liver injury is related to an increased reactive oxygen species content. *Journal of hepatology, 44*(2), 368-374.

Panasiuk, A., Zak, J., Kasprzycka, E., Janicka, K., & Prokopowicz, D. (2005). Blood platelet and monocyte activations and relation to stages of liver cirrhosis. *World J Gastroenterol, 11*(18), 2754-2758.

Park, S., Shin, H., Lee, K., Lee, M., & Jang, J. (2010). Differential expression of matrix metalloproteinases and tissue inhibitors of metalloproteinases in thioacetamide-induced chronic liver injury. *Journal of Korean Medical Science, 25*(4), 570-576.

Park, W., Lee, M., Kim, J., & Jung, Y. (2008). Pharmaceutical composition containing Caesalpinia sappan extract for preventing and treating arteriosclerosis *Repub. Korean Kongkae Taeho Kongbo, KR 2008076343 A 20080820*

Parsons, C., Bradford, B., Pan, C., Cheung, E., Schauer, M., Knorr, A., Krebs, B., Kraft, S., Zahn, S., & Brocks, B. (2004). Antifibrotic effects of a tissue inhibitor of metalloproteinase-1 antibody on established liver fibrosis in rats. *Hepatology, 40*(5), 1106-1115.

Pawa, S., & Ali, S. (2004). Liver necrosis and fulminant hepatic failure in rats: protection by oxyanionic form of tungsten. *Biochimica et Biophysica Acta (BBA) - Molecular Basis of Disease, 1688*(3), 210-222. doi: http://dx.doi.org/10.1016/j.bbadis.2003.12.004

Pearce, R., Greenway, D., & Parkinson, A. (1992). Species differences and interindividual variation in liver microsomal cytochrome P450 2A enzymes: Effects on coumarin, dicumarol, and testosterone oxidation. *Archives of Biochemistry and Biophysics, 298*(1), 211-225. doi: 10.1016/0003-9861(92)90115-d

Pierce, R., Glaug, M., Greco, R., Mackenzie, J., Boyd, C., & Deak, S. (1987). Increased procollagen mRNA levels in carbon tetrachloride-induced liver fibrosis in rats. *Journal of Biological Chemistry, 262*(4), 1652.

Pogrebnyak, A. (1998). Computer-Assisted Mechanism-ofAction Analysis of Large Databases, Including 250,000 Open NCI Database Compounds. *Plant Resources, 34*(1), 61-64.

Poli, G. (2000). Pathogenesis of liver fibrosis: role of oxidative stress. *Molecular aspects of medicine, 21*(3), 49-98.

Portmann, B. (Ed.). (2006). *Development and Anatomy of the Normal Liver. In: Bacon BR, O'Grady JG, Di Bisceglie AM, Lake JR, editors. Comprehensive Clinical Hepatology* (2nd edition ed.). USA:: Elsevier Mosby.

Poynard, T., Bedossa, P., & Opolon, P. (1997). Natural history of liver fibrosis progression in patients with chronic hepatitis C. The OBSVIRC, METAVIR, CLINIVIR, and DOSVIRC groups. *Lancet, 349*(9055), 825-832.

Pradhan, S., & Girish, C. (2006). Hepatoprotective herbal drug, silymarin from experimental pharmacology to clinical medicine. *Indian J Med Res, 124*, 491-504.

Pradhan, S., & Girish, C. (2013). Hepatoprotective herbal drug, silymarin from experimental pharmacology to clinical medicine. *Indian Journal of Medical Research, 137*(2).

Pramely, R., & Leon, S. (2012). Prediction of biological activity spectra of a few phytoconstituents of Azadirachta indicia A. Juss. *Journal of Biochemical Technology, 3*(4), 375-379.

Prasad, K., Chew, L., Khoo, H., Kong, K., Azlan, A., & Ismail, A. (2010). Antioxidant capacities of peel, pulp, and seed fractions of Canarium odontophyllum Miq. fruit. *BioMed Research International, 2010*.

Puerta, R., Martinez, E., Bravo, L., & Ahumada, M. (1996). Effect of silymarin on different acute inflammation models and on leukocyte migration. *Journal of pharmacy and pharmacology, 48*(9), 968-970.

Qiang, Y. (2007). Antitumor compositions containing brazilin and its derivatives for the treatment of tumors *Faming Zhuanli Shenqing Gongkai Shuomingshu CN 101045046 A 20071003*

Rabeta, M., & An Nabil, Z. (2013). Total phenolic compounds and scavenging activity in Clitoria ternatea and Vitex negundo linn. *International Food Research Journal, 20*(1), 495-500.

Raju, J., Patlolla, J., Swamy, M., & Rao, C. (2004). Diosgenin, a steroid saponin of Trigonella foenum graecum (Fenugreek), inhibits azoxymethane-induced aberrant crypt foci formation in F344 rats and induces apoptosis in HT-29 human colon cancer cells. *Cancer Epidemiology Biomarkers & Prevention, 13*(8), 1392-1398.

Ramón, B., & David, B. (2001). Hepatic Stellate Cells as a Target for the Treatmentof Liver Fibrosis. . *Seminar Liver Disease, 21*, 437-452.

Ramos, S., Alía, M., Bravo, L., & Goya, L. (2005). Comparative effects of food-derived polyphenols on the viability and apoptosis of a human hepatoma cell line (HepG2). *Journal of agricultural and food chemistry, 53*(4), 1271-1280.

Rashed, M. (2011). The role of trace elements on hepatitis virus infections: A review. *Journal of Trace Elements in Medicine and Biology, 25*(3), 181-187. doi: http://dx.doi.org/10.1016/j.jtemb.2011.07.001

Reeves, H., & Friedman, S. (2002). Activation of hepatic stellate cells-a key issue in liver fibrosis. *Front Biosci, 7*(4), 808-826.

Reid, R., Muir, R., Levison, D., & Burt, A. (2008). *Muir's textbook of pathology*: Hodder Arnold.

Reif, S., Aeed, H., Shilo, Y., Reich, R., Kloog, Y., Kweon, Y., & Bruck, R. (2004). Treatment of thioacetamide-induced liver cirrhosis by the Ras antagonist, farnesylthiosalicylic acid. *Journal of hepatology, 41*(2), 235-241.

Rice-Evans, C. (2001). Flavonoid antioxidants. *Current medicinal chemistry, 8*(7), 797-807.

Rice-Evans, C. (2004). Flavonoids and isoflavones: absorption, metabolism, and bioactivity. *Free radical biology & medicine, 36*(7), 827.

Rigby, S., & Schwarz, K. (Eds.). (2001). *Nutrition and Liver Disease. Nutrition in the Prevention and Treatment of Disease* (2nd edition ed.). Maryland: Academic Press. .

Roskams, T., Baptista, A., Bianchi, L., Burt, A., Callea, F., Denk, H., De Groote, J., Desmet, V., Hubscher, S., Ishak, K., MacSween, R., Portmann, B., Poulson, H., Scheuer, P., Terracciano, L., & Thaler, H. (2003). Histopathology of portal hypertension: a practical guideline. *Histopathology, 42*(1), 2-13.

Saad, B., Dakwar, S., Said, O., Abu-Hijleh, G., Battah, F. A., Kmeel, A., & Aziazeh, H. (2006). Evaluation of medicinal plant hepatotoxicity in co-cultures of hepatocytes and monocytes. *Evidence Based Complementary and Alternative Medicine, 3*(1), 93-98.

Sakr, S., & Shalaby, S. (2012). Metiram-induced histological and histochemical alterations in Liver and kidney of pregnant mice. *Life Sci J, 9*(1).

Salama, S., Abdulla, M., AlRashdi, A., Ismail, S., Alkiyumi, S., & Golbabapour, S. (2013). Hepatoprotective effect of ethanolic extract of Curcuma longa on thioacetamide induced liver cirrhosis in rats. *BMC Complement Altern Med, 13*, 56. doi: 10.1186/1472-6882-13-56

Sarumathy, K., Vijay, T., Palani, S., Sakthivel, K., & Rajan, M. (2011). Antioxidant and hepatoprotective effects of Caesalpinia sappan against acetaminophen-induced hepatotoxicity in rats. *International Journal of pharmacology and Therapeutics*(1).

Sarumathya, K., Vijay, T., Jayakanthia, J., & Dhana, M. (2011). A Protective effect of Caesalpinia sappan (CS) on acetaminophen induced nephrotoxicity and oxidative stress in male albino rats. *J Pharmacol Toxicol, 2*, 11-21.

Schuppan, D., & Afdhal, N. H. (2008). Liver cirrhosis. *The Lancet, 371*(9615), 838-851.

Shaker, E., Mahmoud, H., & Mnaa, S. (2010). Silymarin, the antioxidant component and Silybum marianum extracts prevent liver damage. *Food and Chemical Toxicology, 48*(3), 803-806. doi: http://dx.doi.org/10.1016/j.fct.2009.12.011

Sharma, K., Bhatia, S., Sharma, A., Shinde, V., & Mahadik, K. (2010). Antioxidant activity of methanol extracts of Vitex negundo Linn. *Pharmacologyonline, 2*, 975-986.

Sharma, P., Jha, A., Dubey, R., & Pessarakli, M. (2012). Reactive Oxygen Species, Oxidative Damage, and Antioxidative Defense Mechanism in Plants under Stressful Conditions. *Journal of Botany, 2012*, 26. doi: 10.1155/2012/217037

Sharma, P., Yelne, M., & Dennis, T. (Eds.). (2005). *Database on Medicinal Plants used in Ayurveda* (Reprint Edition ed. Vol. 3). New Delhi: CCRAS Publication.

Sheldon, H. (Ed.). (1994). *Boyd's introduction to the study of disease* (11th edition ed.). Philadelphia: Lippincott Williams and Wilkins.

Shi, G., & Li, Q. (2005). Effects of oxymatrine on experimental hepatic fibrosis and its mechanism in vivo. *World J Gastroenterol, 11*(2), 268-271.

Shimoda, H., Tanaka, J., Kikuchi, M., Fukuda, T., Ito, H., Hatano, T., & Yoshida, T. (2008). Walnut polyphenols prevent liver damage induced by carbon tetrachloride and d-galactosamine: hepatoprotective hydrolyzable tannins in the kernel pellicles of walnut. *Journal of agricultural and food chemistry, 56*(12), 4444-4449.

Shinde, A., & Ganu, J. (2009). Role of antioxidant supplementation in alcoholic cirrhosis induced oxidative stress. *JARBS, 1*(2), 46-51.

Shirin, H., Sharvit, E., Aeed, H., Gavish, D., & Bruck, R. (2013). Atorvastatin and rosuvastatin do not prevent thioacetamide induced liver cirrhosis in rats. *World J Gastroenterol, 19*(2), 241-248. doi: 10.3748/wjg.v19.i2.241

Shukla, M. (2013). Plant extract composition for the treatment of liver dysfunction.: WO Patent 2,013,021,295.

Šídlová, K., Pechová, M., Kotaška, K., & Průša, R. (2002). Insulin-Like Growth Factor Binding Protein-3 in Patients with Liver Cirrhosis. *Physiological Research 51*, 587-590.

Singh, P., Mishra, G., Srivastava, S., Sangeeta, K., & Khosa, R. (2011). Phytopharmacological Review of Vitex Negundo (Sambhalu). *Pharmacologyonline, 2*, 1355-1385.

Singh, V., Sharma, P., Dudhe, R., & Kumar, N. (2011). Immunomodulatory effects of some traditional medicinal plants. *J. Chem. Pharm. Res., 3*(1), 675-684.

Sivalokanathan, S., Vijayababu, M., & Balasubramanian, M. (2006). Effects of Terminalia arjuna bark extract on apoptosis of human hepatoma cell line HepG2. *World Journal of Gastroenterology, 12*(7), 1018.

Spira, B., & Raw, I. (2000). The effect of thioacetamide on the activity and expression of cytosolic rat liver glutathione-S-transferase. *Molecular and Cellular Biochemistry, 211*(1), 103-110.

Srilakshmi, V., Vijayan, P., Raj, P., Dhanaraj, S., & Chandrashekhar, H. (2010). Hepatoprotective properties of Caesalpinia sappan Linn. heartwood on carbon tetrachloride induced toxicity. *Indian journal of experimental biology, 48*, 905-910.

Sun, F., Hayami, S., Ogiri, Y., Haruna, S., Tanaka, K., Yamada, Y., Tokumaru, S., & Kojo, S. (2000). Evaluation of oxidative stress based on lipid hydroperoxide, vitamin C and vitamin E during apoptosis and necrosis caused by thioacetamide in rat liver. *Biochimica et Biophysica Acta (BBA)-Molecular Basis of Disease, 1500*(2), 181-185.

Swanson, T., & Kim, S. (2004). *Gross Anatomy: Clinically Relevant Anatomy!* : Lippincott Williams & Wilkins.

Tameda, M., Shiraki, K., Ooi, K., Takase, K., Kosaka, Y., Nobori, T., & Tameda, Y. (2005). Aspartate aminotransferase-immunoglobulin complexes in patients with chronic liver disease. *World J Gastroenterol, 11*(10), 1529-1531.

Tandon, V. (2005). Medicinal uses and biological activities of Vitex negundo. *Natural product radiance, 4*(3), 162-165.

Tandon, V., Khajuria, V., Kapoor, B., Kour, D., & Gupta, S. (2008). Hepatoprotective activity of Vitex negundo leaf extract against anti-tubercular drugs induced hepatotoxicity. *Fitoterapia, 79*(7-8), 533-538.

Tasduq, S., Kaiser, P., Gupta, B., Gupta, V., & Johri, R. (2008). Negundoside, an irridiod glycoside from leaves of Vitex negundo, protects human liver cells against calcium-mediated toxicity induced by carbon tetrachloride. *World Journal of Gastroenterology, 14*(23), 3693-3709.

Thapa, B., & Walia, A. (2007). Liver function tests and their interpretation. *Indian journal of pediatrics, 74*(7), 663-671.

Theiss, A., Idell, R., Srinivasan, S., Klapproth, J., Jones, D., Merlin, D., & Sitaraman, S. (2007). Prohibitin protects against oxidative stress in intestinal epithelial cells. *FASEB J, 21*(1), 197-206. doi: 10.1096/fj.06-6801com

Thurman, R., Bradford, B., Iimuro, Y., Frankenberg, M., Knecht, K., Connor, H., Adachi, Y., Wall, C., Arteel, G., & Raleigh, J. (1999). Mechanisms of alcohol-induced hepatotoxicity: studies in rats. *Front Biosci, 4*(1), 42.

Thyagarajan, S., Jayaram, S., Gopalakrishnan, V., Hari, R., Jeyakumar, P., & Sripathi, M. (2002). Herbal medicines for liver diseases in India. *Journal of Gastroenterology and Hepatology, 17*, S370-S376.

Timmer, J., & Salvesen, G. (2006). Caspase substrates. *Cell Death & Differentiation, 14*(1), 66-72.

Tortora, G., & Derrickson, B. (2008). *Principles of anatomy and physiology*: Wiley.

Toyokuni, S., Okada, S., Hamazaki, S., Fujioka, M., Li, J., & Midorikawa, O. (1989). Cirrhosis of the liver induced by cupric nitrilotriacetate in Wistar rats. An experimental model of copper toxicosis. *The American journal of pathology, 134*(6), 1263.

Trivedi, N., & Rawal, U. (2000). Hepatoprotective and toxicological evaluation of Andrographis paniculata on severe liver damage. *Indian Journal of Pharmacology, 32*(5), 288-293.

Tsukada, S., Parsons, C. J., & Rippe, R. A. (2006). Mechanisms of liver fibrosis. *Clinica Chimica Acta, 364*(1), 33-60.

Turrens, J. F. (2003). Mitochondrial formation of reactive oxygen species. *The Journal of Physiology, 552*(2), 335-344. doi: 10.1111/j.1469-7793.2003.00335.x

Ueki, T., Kaneda, Y., Tsutsui, H., Nakanishi, K., Sawa, Y., Morishita, R., Matsumoto, K., Nakamura, T., Takahashi, H., & Okamoto, E. (1999). Hepatocyte growth factor gene therapy of liver cirrhosis in rats. *Nature medicine, 5*(2), 226-230.

Ullah, M., & Khan, M. (2008). Food as medicine: potential therapeutic tendencies of plant derived polyphenolic compounds. *Asian Pac J Cancer Prev, 9*(2), 187-196.

Vasanth Raj, P., Nitesh, K., Sagar Gang, S., Hitesh Jagani, V., Raghu Chandrashekhar, H., Venkata Rao, J., Mallikarjuna Rao, C., & Udupa, N. (2010). Protective Role of Catechin on -Galactosamine Induced Hepatotoxicity Through a p53 Dependent Pathway. *Indian J Clin Biochem., 25*(4), 349-356.

Vlad, M., Ionescu, N., Ispas, A., STOICA, C., & Ungureanu, E. (2007). The histological changes of digestive organs in experimental decreases of hepatic venous outflow at the rat. *Romanian Journal of Morphology and Embryology, 48*(1), 33-39.

Wang, M., Chen, Y., Chen, I., Hsieh, S., Chen, S., & Chiu, C. (2012). Curcumin protects against thioacetamide-induced hepatic fibrosis by attenuating the inflammatory response and inducing apoptosis of damaged hepatocytes. *J Nutr Biochem, 23*(10), 1352-1366. doi: 10.1016/j.jnutbio.2011.08.004

Wang, X., Du, L., Lei, F., Xing, D., Wang, Y., Hu, J., Li, B., & Li, H. (2010). Application of brazilein extracted from Caesalpinia sappan to prepare medical preparations for treating 5-HT2 agonistassociated diseases *Faming Zhuanli Shenqing CN 101773493 A 20100714*.

Wanless, I. (2004). Pathogenesis of cirrhosis. *Journal of Gastroenterology and Hepatology, 19*, S369-S371.

Washiyama, M., Sasaki, Y., Hosokawa, T., & Nagumo, S. (2009). Anti-inflammatory constituents of Sappan Lignum *Biological & Pharmaceutical Bulletin 32*(5), 941-944.

Weinshilboum, R. (2003). Inheritance and drug response. *N Engl J Med, 348*(6), 529-537. doi: 10.1056/NEJMra020021

Wenzel, S., Stolte, H., & Soose, M. (1996). Effects of silibinin and antioxidants on high glucose-induced alterations of fibronectin turnover in human mesangial cell cultures. *Journal of Pharmacology and Experimental Therapeutics, 279*(3), 1520-1526.

Wilkening, S., Stahl, F., & Bader, A. (2003). Comparison of primary human hepatocytes and hepatoma cell line Hepg2 with regard to their biotransformation properties. *Drug Metab Dispos, 31*(8), 1035-1042. doi: 10.1124/dmd.31.8.1035

Wills, P. J., & Asha, V. V. (2007). Protective mechanism of Lygodium flexuosum extract in treating and preventing carbon tetrachloride induced hepatic fibrosis in rats. *Chem Biol Interact, 165*(1), 76-85. doi: 10.1016/j.cbi.2006.10.010

Wong, C., Leung, K., Fung, K., & Choy, Y. (1994). Immunomodulatory and anti-tumour polysaccharides from medicinal plants. *The Journal of international medical research, 22*(6), 299.

Wong, W., Abdulla, M., Chua, K., Kuppusamy, U., Tan, Y., & Sabaratnam, V. (2012). Hepatoprotective Effects of Panus giganteus (Berk.) Corner against Thioacetamide-(TAA-) Induced Liver Injury in Rats. *Evidence-Based Complementary and Alternative Medicine, 2012*.

Wu, C., Chamuleau. R, & Bosch, S. (1993). Protective effect of silymarin on rat liver injury induced by ischemia. *Virchows Arch B Cell Pathol Incl Mol Pathol, 64*, 259-263.

Wu, C., Giambrone, M., Howard, D., Rojkind, M., & Wu, G. (1982). The nature of the collagen in hepatic fibrosis in advanced murine schistosomiasis. *Hepatology, 2*(3), 366S-371S.

Xu, J., Shi, T., Zhang, S., Guo, S., Qiao, L., & Li, K. (2009). Manufacture and application of water extract of caesalpinia sappan for treating ascites tumor and leukemia *Faming Zhuanli Shenqing CN 101411739 A 20090422*

Yadav, N., Pal, A., Shanker, K., Bawankule, D., Gupta, A., Darokar, M., & Khanuja, S. (2008). Synergistic effect of silymarin and standardized extract of Phyllanthus amarus against CCl4-induced hepatotoxicity in Rattus norvegicus. *Phytomedicine, 15*(12), 1053.

Yang, J., Gu, Z., He, L., & Zhang, J. (2010). Traditional chinese medicine preparation for treating adiposis hepatica, alcoholic hepatitis and complicating diseases *Faming Zhuanli Shenqing Gongkai Shuomingshu CN 101745077 A 20100623*.

Yang, L., Yen, K., Kiso, Y., & Hikino, H. (1987). Antihepatotoxic actions of formosan plant drugs', Journal of Ethnopharmacology. *Journal of Ethnopharmacology, 19*, 103-110.

Yeh, C., Maitra, A., Lee, K., Jan, Y., & Chen, M. (2004). Thioacetamide-induced intestinal-type cholangiocarcinoma in rat: an animal model recapitulating the multi-stage progression of human cholangiocarcinoma. *Carcinogenesis, 25*(4), 631-636. doi: 10.1093/carcin/bgh037

Yehye, W., Abdul Rahman, N., Alhadi, A., Khaledi, H., Ng, S., & Ariffin, A. (2012). Butylated Hydroxytoluene Analogs: Synthesis and Evaluation of Their Multipotent Antioxidant Activities. *Molecules, 17*(7), 7645-7665.

Yodsaoue, O., Cheenpracha, S., Karalai, C., Ponglimanont, C., & Tewtrakul, S. (2009). Anti-allergic activity of principles from the roots and heartwood of Caesalpinia sappan on antigen-induced β- hexosaminidase release. *Phytotherapy Research 23*(7), 1028-1031.

Yogalakshmi, B., Viswanathan, P., & Anuradha, C. (2010). Investigation of antioxidant, anti-inflammatory and DNA-protective properties of eugenol in thioacetamide-induced liver injury in rats. *Toxicology, 268*(3), 204-212.

You-Zhi, W., Shi-Qin, S., & Ya-Bin, Z. (2011). Extract of the dried heartwood of Caesalpinia sappan L. attenuates collagen-induced arthritis. *Journal of Ethnopharmacology., 136*(1), 271-278. doi: http://dx.doi.org/10.1016/j.jep.2011.04.061

Yu, E., Choe, G., Gong, G., & Lee, I. (1993). Expression of alpha-smooth muscle actin in liver diseases. *Journal of Korean Medical Science, 8*(5), 367.

Zaragoza, A., Andrés, D., Sarrión, D., & Cascales, M. (2000). Potentiation of thioacetamide hepatotoxicity by phenobarbital pretreatment in rats. Inducibility of FAD monooxygenase system and age effect. *Chem Biol Interact, 124*(2), 87-101.

Zhang, B., Xu, D., Guo, Y., Ping, J., Chen, L., & Wang, H. (2008). Protection and antioxidant effect of berberine in rat liver induced fibrosis by multiple hepatotoxic factors. *Clinical and Experimental Pharmacology and Physiology, 35*(3), 303-309.

Zhang, X., Wang, G., & Ren, L. (2010). Study of Caesalpinia sappan aqueous extract's apoptosis-inducing effects on human ovarian cancer cell SKOV3 *Zhongliu Yanjiu Yu Linchuang 22*(6), 388-390.

Zhao, X., Wang, B., Li, X., & Wang, T. (2008). Newly proposed fibrosis staging criterion for assessing carbon tetrachloride- and albumin complex-induced liver fibrosis in rodents. *Pathol Int, 58*(9), 580-588. doi: 10.1111/j.1440-1827.2008.02274.x

Zheng, C., Huang, B., Han, T., Zhang, Q., Zhang, H., Rahman, K., & Qin, L. (2010). Antinociceptive activities of the liposoluble fraction from Vitex negundo seeds *Pharmaceutical Biology 48*(6), 651-658.

Zou, S., Xiao, Q., Li, Y., Cai, W., Li, X., Sun, H., Wu, Q., Li, L., & Liu, X. (2010). Effect of Caesalpinia sappan L phenol of cervical cancer cell. *Chongqing Ligong Daxue Xuebao, Ziran Kexue 24*(3), 33-35.

Appendices

Appendix A: Ethical Form

Appendix A1: Hepatoprotective ethic approval

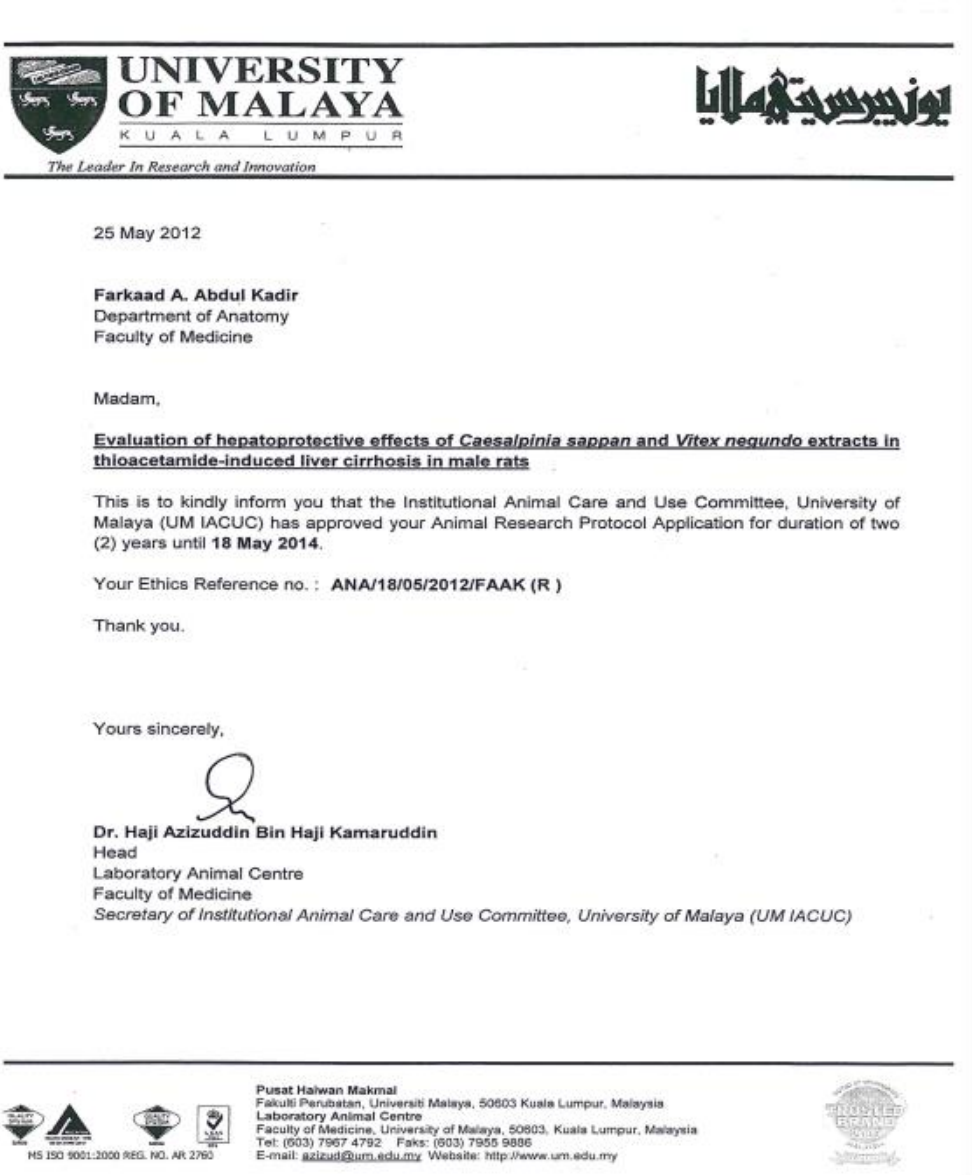

UNIVERSITY OF MALAYA
KUALA LUMPUR
The Leader In Research and Innovation

يونيورسيتي مالايا

25 May 2012

Farkaad A. Abdul Kadir
Department of Anatomy
Faculty of Medicine

Madam,

Evaluation of hepatoprotective effects of *Caesalpinia sappan* and *Vitex negundo* extracts in thioacetamide-induced liver cirrhosis in male rats

This is to kindly inform you that the Institutional Animal Care and Use Committee, University of Malaya (UM IACUC) has approved your Animal Research Protocol Application for duration of two (2) years until **18 May 2014**.

Your Ethics Reference no. : **ANA/18/05/2012/FAAK (R)**

Thank you.

Yours sincerely,

Dr. Haji Azizuddin Bin Haji Kamaruddin
Head
Laboratory Animal Centre
Faculty of Medicine
Secretary of Institutional Animal Care and Use Committee, University of Malaya (UM IACUC)

MS ISO 9001:2000 REG. NO. AR 2760

Pusat Haiwan Makmal
Fakulti Perubatan, Universiti Malaya, 50603 Kuala Lumpur, Malaysia
Laboratory Animal Centre
Faculty of Medicine, University of Malaya, 50603, Kuala Lumpur, Malaysia
Tel: (603) 7967 4792 Faks: (603) 7955 9886
E-mail: azizud@um.edu.my Website: http://www.um.edu.my

Appendix B: Analytical Techniques and Preparations

Appendix B1: DPPH free radical scavenging assay

Reagents

2, 2-diphenyl-1-picrylehydrazyl ($C_{18}H_{12}N_5O_0$) solution

Ascorbic acid (Vit. C)

Preparation of reagent

0.001761 g/ml Vit. C was prepared as a standard.

The DPPH solution was prepared by dissolving 0.001972 g of DPPH in 50 ml of absolute ethanol then stirred until the DPPH was completely dissolved.

Appendix B2: DPPH Standard curve

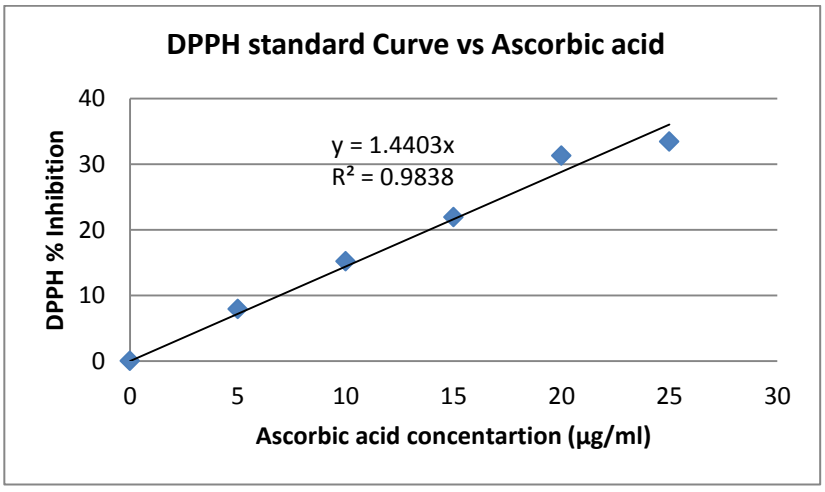

Appendix B3: Ferric reducing antioxidant power (FRAP) assay

Reagents

Iron (II) sulfate hepatohydrate ($FeSO_4$. $7H_2O$)

Sodium acetate trihydrate buffer ($C_2H_3O_2N_9$. $3H_2O$)

2,4,6-tris(2-pyridyl)-s-triazine (TPTZ) 98%

$FeCl_3$. $6H_2O$

Preparation of reagents

0.0278 g of $FeSO_4.7H_2O$ was dissolved in 100 ml dH_2O.

0.0775 g of acetate buffer was dissolved in 25 ml dH_2O mixed previously with 0.4 ml glacial acetic acid.

0.00781 g of TPTZ was dissolved in 2.5 ml dH_2O mixed previously with 0.1 ml (1M HCL).

0.0135 g $FeCl_3$. $6H_2O$ was dissolved in 2.5 ml dH_2O.

The freshly prepared: acetate buffer, TPTZ and $FeCl_3$. $6H_2O$ solutions were mixed and vortexed to obtain the ready to use FRAP reagent.

Appendix B4: $FeSO_4.7H_2O$ calibration plot

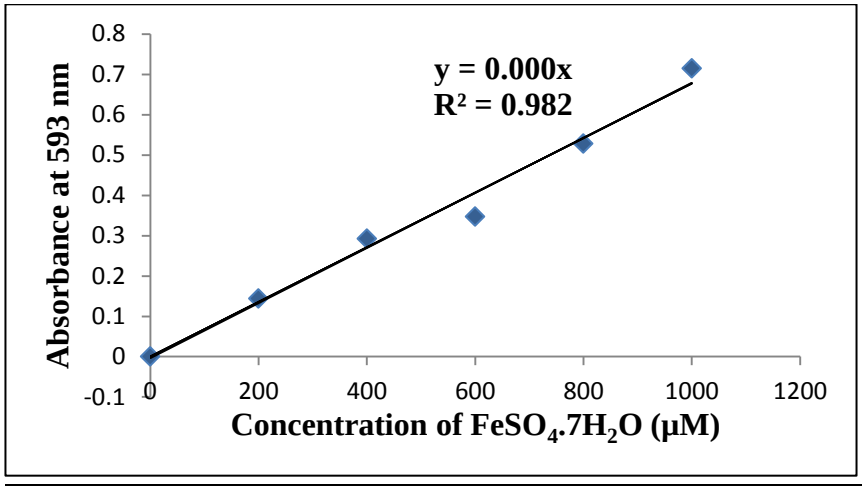

Appendix B5 Total Phenolic Content (TPC)

Reagents

Commercial Folin-Ciocalteu solution

Sodium carbonate

Gallic acid

Preparation of reagent

1- A ratio of (1:10) of Folin-Ciocalteu solution was prepared by diluting 10 ml of it with 90 ml dH_2O in a dark place.
2- 5.75 g of sodium carbonate was dissolved in 50 ml of dH_2O to give a final concentration of 0.115 mg/ml.
3- 0.2 mg/ml of quercitine solution was prepared and used as the standard solution.

Appendix B6 Quercetine calibration plot

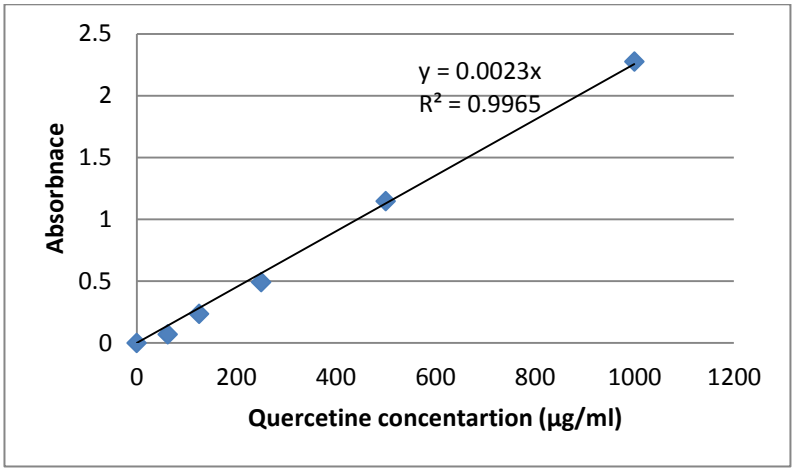

Appendix B7 Total flavonoid content (TFC)

Reagents

Aluminium trichloride (Al Cl_3)

Quercetin (Standard)

Potassium acetate (CH_3COOK)

Preparation of reagents

One gram of Al Cl_3 was dissolved in 10 ml dH_2O.

0.9815 g of potassium acetate was dissolved in 10 ml dH_2O.

And 0.02g of quercetin was dissolved in 4 ml (95%) methanol.

Appendix B8: Quercetine calibration plot

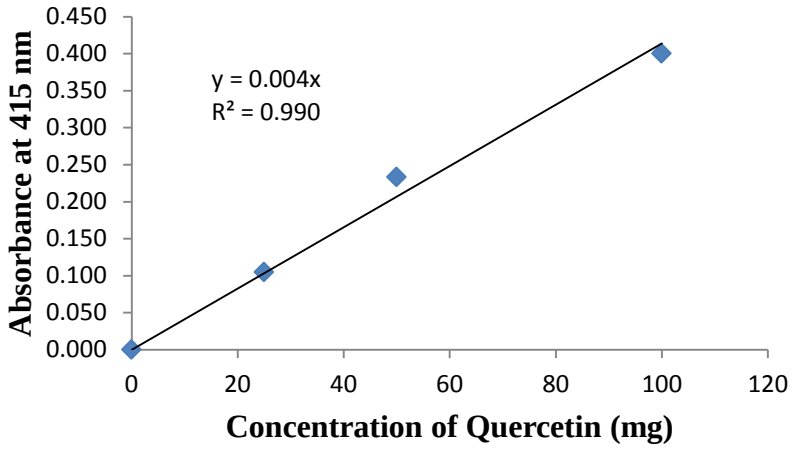

Appendix B9 TBARS (MDA) assay kit (Item No. 10009055 Cayman)

Tissue Homogenates

1. Weigh out approximately 25 mg of tissue into a 1.5 ml centrifuge tube.
2. Add 250 µl of RIPA buffer with protease inhibitors of choice (see **Interferences** section on page 19).
3. Sonicate for 15 seconds at 40V over ice.
4. Centrifuge the tube at 1,600 x g for 10 minutes at 4°C. Use the supernatant for analysis. Store supernatant on ice. If not assaying the same day, freeze at -80°C. The sample will be stable for one month.
5. Tissue homogenates do not need to be diluted before assaying.

Cell Lysates

1. Collect 2 x 10^7 cells in 1 ml of cell culture medium or buffer of choice, such as PBS.
2. Sonicate 3X for five second intervals at 40V setting over ice.
3. Use the whole homogenate in the assay, being sure to use the culture medium as a sample blank.
4. Cell lysates do not need to be diluted before assaying.

ASSAY PROTOCOL

Plate Set Up

There is no specific pattern for using the wells on the plate. A typical layout of standards and samples to be measured in duplicate is shown below in Figure 2. We suggest you record the contents of each well on the template sheet provided (see page 23).

	1	2	3	4	5	6	7	8	9	10	11	12
A	A	A	S1	S1	S9	S9	S17	S17	S25	S25	S33	S33
B	B	B	S2	S2	S10	S10	S18	S18	S26	S26	S34	S34
C	C	C	S3	S3	S11	S11	S19	S19	S27	S27	S35	S35
D	D	D	S4	S4	S12	S12	S20	S20	S28	S28	S36	S36
E	E	E	S5	S5	S13	S13	S21	S21	S29	S29	S37	S37
F	F	F	S6	S6	S14	S14	S22	S22	S30	S30	S38	S38
G	G	G	S7	S7	S15	S15	S23	S23	S31	S31	S39	S39
H	H	H	S8	S8	S16	S16	S24	S24	S32	S32	S40	S40

A-H = Standards
S1-S40 = Sample Wells

Figure 2. Sample plate format

Tissue Homogenates

1. Weigh out approximately 25 mg of tissue into a 1.5 ml centrifuge tube.
2. Add 250 µl of RIPA buffer with protease inhibitors of choice (see **Interferences** section on page 19).
3. Sonicate for 15 seconds at 40V over ice.
4. Centrifuge the tube at 1,600 x g for 10 minutes at 4°C. Use the supernatant for analysis. Store supernatant on ice. If not assaying the same day, freeze at -80°C. The sample will be stable for one month.
5. Tissue homogenates do not need to be diluted before assaying.

Cell Lysates

1. Collect 2 x 10^7 cells in 1 ml of cell culture medium or buffer of choice, such as PBS.
2. Sonicate 3X for five second intervals at 40V setting over ice.
3. Use the whole homogenate in the assay, being sure to use the culture medium as a sample blank.
4. Cell lysates do not need to be diluted before assaying.

ASSAY PROTOCOL

Plate Set Up

There is no specific pattern for using the wells on the plate. A typical layout of standards and samples to be measured in duplicate is shown below in Figure 2. We suggest you record the contents of each well on the template sheet provided (see page 23).

	1	2	3	4	5	6	7	8	9	10	11	12
A	A	A	S1	S1	S9	S9	S17	S17	S25	S25	S33	S33
B	B	B	S2	S2	S10	S10	S18	S18	S26	S26	S34	S34
C	C	C	S3	S3	S11	S11	S19	S19	S27	S27	S35	S35
D	D	D	S4	S4	S12	S12	S20	S20	S28	S28	S36	S36
E	E	E	S5	S5	S13	S13	S21	S21	S29	S29	S37	S37
F	F	F	S6	S6	S14	S14	S22	S22	S30	S30	S38	S38
G	G	G	S7	S7	S15	S15	S23	S23	S31	S31	S39	S39
H	H	H	S8	S8	S16	S16	S24	S24	S32	S32	S40	S40

A-H = Standards
S1-S40 = Sample Wells

Figure 2. Sample plate format

Appendix B10: Superoxide dismutase assay kit (Item No. 706002 Cayman)

ASSAY PROTOCOL

Plate Set Up

There is no specific pattern for using the wells on the plate. A typical layout of SOD standards and samples to be measured in duplicate is given below in Figure 2. We suggest you record the contents of each well on the template sheet provided (see page 19).

	1	2	3	4	5	6	7	8	9	10	11	12
A	A	A	S2	S2	S10	S10	S18	S18	S26	S26	S34	S34
B	B	B	S3	S3	S11	S11	S19	S19	S27	S27	S35	S35
C	C	C	S4	S4	S12	S12	S20	S20	S28	S28	S36	S36
D	D	D	S5	S6	S13	S13	S21	S21	S29	S29	S37	S37
E	E	E	S6	S6	S14	S14	S22	S22	S30	S30	S38	S38
F	F	F	S7	S7	S15	S15	S23	S23	S31	S31	S39	S39
G	G	G	S8	S8	S16	S16	S24	S24	S32	S32	S40	S40
H	S1	S1	S9	S9	S17	S17	S25	S25	S33	S33	S41	S41

A-G = Standards
S1-S41 = Sample Wells

Figure 2. Sample plate format

Pipetting Hints

- It is recommended that an adjustable pipette be used to deliver reagents to the wells.
- Before pipetting each reagent, equilibrate the pipette tip in that reagent (*i.e.*, slowly fill the tip and gently expel the contents, repeat several times).
- Do not expose the pipette tip to the reagent(s) already in the well.

General Information

- The final volume of the assay is 230 µl in all the wells.
- It is not necessary to use all the wells on the plate at one time.
- The assay temperature is 25°C.
- All reagents except samples and xanthine oxidase must be equilibrated to room temperature before beginning the assay.
- It is recommended that the samples and SOD standards be assayed at least in duplicate.
- Monitor the absorbance at 440-460 nm using a plate reader.

Standard Preparation

Dilute 20 µl of the SOD Standard (Catalog No. 706005) with 1.98 ml of Sample Buffer (dilute) to obtain the SOD stock solution. Take seven clean glass test tubes and mark them A-G. Add the amount of SOD stock and Sample Buffer (dilute) to each tube as described in Table 1 on page 12.

Tube	SOD Stock (µl)	Sample Buffer (µl)	Final SOD Activity (U/ml)
A	0	1,000	0
B	20	980	0.025
C	40	960	0.05
D	80	920	0.1
E	120	880	0.15
F	160	840	0.2
G	200	800	0.25

Table 1. Superoxide Dismutase standards

Performing the Assay

1. **SOD Standard Wells** - add 200 µl of the diluted radical detector and 10 µl of standard (tubes A-G) per well in the designated wells on the plate (see sample plate format, Figure 2, page 10).
2. **Sample Wells** - add 200 µl of the diluted radical detector and 10 µl of sample to the wells. *NOTE: If using an inhibitor, add 190 µl of the diluted radical detector, 10 µl of inhibitor, and 10 µl of sample to the wells. The amounts of sample added to the well should always be 10 µl. Samples should be diluted with Sample Buffer (dilute) or concentrated with an Amicon centrifuge concentrator with a molecular weight cut-off of 10,000 to bring the enzymatic activity to fall within the standard curve range.*
3. Initiate the reactions by adding 20 µl of diluted xanthine oxidase to all the wells you are using. Make sure to note the precise time you started and add the xanthine oxidase as quickly as possible. *NOTE: If assaying sample backgrounds, add 20 µl of sample buffer instead of xanthine oxidase.*
4. Carefully shake the 96-well plate for a few seconds to mix. Cover with the plate cover.
5. Incubate the plate on a shaker for 20 minutes at room temperature. Read the absorbance at 440-460 nm using a plate reader.

ANALYSIS

Calculations

1. Calculate the average absorbance of each standard and sample. If assayed, subtract sample background absorbance from the sample.
2. Divide standard A's absorbance by itself and divide standard A's absorbance by all the other standards and samples absorbances to yield the linearized rate (LR) (*i.e.*, LR for Std A = Abs Std A/Abs Std A; LR for Std B = Abs Std A/Abs Std B).
3. Plot the linearized SOD standard rate (LR) (from step 2 above) as a function of final SOD Activity (U/ml) from Table 1. See Figure 3 (on page 14) for a typical standard curve.
4. Calculate the SOD activity of the samples using the equation obtained from the linear regression of the standard curve substituting the linearized rate (LR) for each sample. One unit is defined as the amount of enzyme needed to exhibit 50% dismutation of the superoxide radical. SOD activity is standardized using the cytochrome c and xanthine oxidase coupled assay

$$\text{SOD (U/ml)} = \left[\left(\frac{\text{sample LR - y-intercept}}{\text{slope}}\right) \times \frac{0.23 \text{ ml}}{0.01 \text{ ml}}\right] \times \text{sample dilution}$$

Performance Characteristics

Precision:

When a series of 60 SOD standard measurements were performed on the same day, the intra-assay coefficient of variation was 3.2%. When a series of 60 SOD standard measurements were performed on five different days under the same experimental conditions, the inter-assay coefficient of variation was 3.7%.

Assay Range:

Under the standardized conditions of the assay described in this booklet, the dynamic range of the kit is 0.025-0.25 units/ml SOD.

Plasma and Erythrocyte Lysate

1. Collect blood using an anticoagulant such as heparin, citrate, or EDTA.
2. Centrifuge the blood at 700-1,000 x g for 10 minutes at 4°C. Pipet off the top yellow plasma layer without disturbing the white buffy layer. Store plasma on ice until assaying or freeze at -80°C. The plasma sample will be stable for at least one month.
3. Remove the white buffy layer (leukocytes) and discard.
4. Lyse the erythrocytes (red blood cells) in 4 volumes of ice-cold HPLC-grade water.
5. Centrifuge at 10,000 x g for 15 minutes at 4°C.
6. Collect the supernatant (erythrocyte lysate) for assaying and store on ice. If not assaying the same day, freeze at -80°C. The sample will be stable for at least one month.

NOTE: It has been reported that heme peroxidase activity of hemoglobin can lead to falsely elevated GPx activity in erythrocyte lysates. There was no significant effect in the GPx activity when assayed with cumene hydroperoxide as the substrate. Therefore, it is not necessary to treat the sample with Drabkin's Reagent (potassium ferricyanide/potassium cyanide) to convert hemoglobin to cyanmethemoglobin before assaying.

Tissue Homogenization using the Precellys 24 Homogenizer

- Freeze organs immediately upon collection and then store at -80°C. Snap-freezing of tissues in liquid nitrogen is preferred.
- Add 1 ml of homogenization buffer (50 mM Tris-HCl, pH 7.5, 5 mM EDTA and 1 mM DTT) per 100 milligrams of tissue.
- Homogenize the sample using the Precellys 24 according to appropriate settings:

Organ	Speed (rpm)	Cycle Length (seconds)	Cycle Break (seconds)	Number of Cycles	Beads
Heart (aorta)	5,000	30	30	3	CK28 Large Ceramic

- Spin the tissue homogenates at 10,000 x g for 15 minutes at 4°C.
- Collect supernatant and assay samples according to the kit booklet protocol. Samples may need to be diluted appropriately for assay and should be normalized using a protein assay.

ASSAY PROTOCOL

Plate Set Up

There is no specific pattern for using the wells on the plate. However, it is necessary to have three wells designated as non-enzymatic or background wells. The absorbance rate of these wells must be subtracted from the absorbance rate measured in the GPx sample and control wells. We suggest that there be at least three wells designated as positive controls and that you record the contents of each well on the template sheet provided on page 19.

	1	2	3	4	5	6	7	8	9	10	11	12
A	B	B	B	7	7	7	15	15	15	23	23	23
B	C	C	C	8	8	8	16	16	16	24	24	24
C	1	1	1	9	9	9	17	17	17	25	25	25
D	2	2	2	10	10	10	18	18	18	26	26	26
E	3	3	3	11	11	11	19	19	19	27	27	27
F	4	4	4	12	12	12	20	20	20	28	28	28
G	5	5	5	13	13	13	21	21	21	29	29	29
H	6	6	6	14	14	14	22	22	22	30	30	30

B - Background Wells
C - Positive Control Wells
1-30 - Sample Wells

Figure 2. Sample plate format

Pipetting Hints

- It is recommended that an adjustable pipette be used to deliver reagents to the wells.
- Use different tips to pipette the assay buffer (dilute), co-substrate mixture, enzymes, and cumene hydroperoxide.
- Before pipetting each reagent, equilibrate the pipette tip in that reagent (*i.e.*, slowly fill the tip and gently expel the contents, repeat several times).
- Do not expose the pipette tip to the reagent(s) already in the well.

General Information

- The final volume of the assay is 190 µl in all the wells.
- It is not necessary to use all the wells on the plate at one time.
- The assay temperature is 25°C.
- Use the Assay Buffer (dilute) in the assay.
- Monitor the decrease in absorbance at 340 nm using a plate reader.

Performing the Assay

1. **Background or Non-enzymatic Wells** - add 120 µl of Assay Buffer and 50 µl of co-substrate mixture to three wells.
2. **Positive Control Wells (bovine erythrocyte GPx)** - add 100 µl of Assay Buffer, 50 µl of co-substrate mixture, and 20 µl of diluted GPx (control) to three wells.
3. **Sample Wells** - add 100 µl of Assay Buffer, 50 µl of co-substrate mixture, and 20 µl of sample to three wells. To obtain reproducible results, the amount of GPx added to the well should cause an absorbance decrease between 0.02 and 0.135/min. When necessary, samples should be diluted with Sample Buffer or concentrated with an Amicon centrifuge concentrator with a molecular weight cut-off of 10,000 to bring the enzymatic activity to this level. ***NOTE:*** *The amount of sample added to the well should always be 20 µl. To determine if an additional sample control should be performed see the Interferences section (page 14).*
4. Initiate the reactions by adding 20 µl of cumene hydroperoxide to all the wells being used. Make sure to note the precise time the reaction is initiated and add the cumene hydroperoxide as quickly as possible.
5. Carefully shake the plate for a few seconds to mix.
6. Read the absorbance once every minute at 340 nm using a plate reader to obtain at least 5 time points. ***NOTE:*** *The initial absorbance of the sample wells should not be above 1.2 or below 0.5.*

ASSAY PROTOCOL

Plate Set Up

There is no specific pattern for using the wells on the plate. We suggest that there be at least two wells designated as positive controls.

A typical layout of formaldehyde standards and samples to be measured in duplicate is shown in Figure 1. We suggest you record the contents of each well on the template sheet provided on page 23.

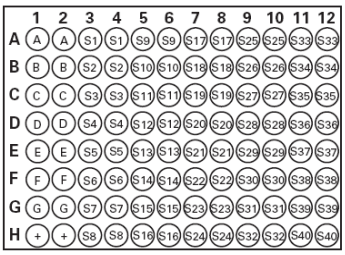

A-G = Standards
+ = Positive Controls
S1-S40 = Sample Wells

Figure 1. Sample plate format

Pipetting Hints

- It is recommended that an adjustable pipette be used to deliver reagents to the wells.
- Before pipetting each reagent, equilibrate the pipette tip in that reagent (*i.e.*, slowly fill the tip and gently expel the contents, repeat several times).
- Do not expose the pipette tip to the reagent(s) already in the well.

General Information

- The final volume of the assay is 240 µl in all the wells.
- All reagents except samples must be equilibrated to room temperature before beginning the assay.
- It is not necessary to use all the wells on the plate at one time.
- If the expected CAT activity of the sample is not known or if it is expected to be beyond the range of the standard curve, it is prudent to assay the sample at several dilutions.
- It is recommended that the samples and formaldehyde standards be assayed at least in duplicate.
- Use the Assay Buffer (dilute) in the assay.
- Monitor the absorbance at 540 nm using a plate reader.

Standard Preparation

1. Preparation of the Formaldehyde Standards - Dilute 10 µl of formaldehyde standard (vial #3) with 9.99 ml of Sample Buffer (dilute) to obtain a 4.25 mM formaldehyde stock solution. Take seven clean glass test tubes and mark them A-G. Add the amount of formaldehyde stock and Sample Buffer (dilute) to each tube as described in Table 1 (below).

Tube	Formaldehyde (µl)	Sample Buffer (µl)	Final Concentration (µM formaldehyde)*
A	0	1,000	0
B	10	990	5
C	30	970	15
D	60	940	30
E	90	910	45
F	120	880	60
G	150	850	75

Table 1

*Final formaldehyde concentration in the 170 µl reaction.

Performing the Assay

1. **Formaldehyde Standard Wells** - Add 100 µl of Assay Buffer (dilute), 30 µl of methanol, and 20 µl of standard (tubes A-G) per well in the designated wells on the plate (see sample plate format, Figure 1, page 12).
2. **Positive Control Wells (bovine liver CAT)** - Add 100 µl of Assay Buffer (dilute), 30 µl of methanol, and 20 µl of diluted CAT (control) to two wells.
3. **Sample Wells** - Add 100 µl of Assay Buffer (dilute), 30 µl of methanol, and 20 µl of sample to two wells. To obtain reproducible results, the amount of CAT added to the well should result in an activity between 0.25-4 nmol/min/ml. When necessary, samples should be diluted with Sample Buffer (dilute) or concentrated with an Amicon centrifuge concentrator with a molecular weight cut-off of 100,000 to bring the enzymatic activity to this level.
4. Initiate the reactions by adding 20 µl of hydrogen peroxide (dilute) to all the wells being used. Make sure to note the precise time the reaction is initiated and add the hydrogen peroxide as quickly as possible.
5. Cover the plate with the plate cover and incubate on a shaker for 20 minutes at room temperature.
6. Add 30 µl of potassium hydroxide to each well to terminate the reaction and then add 30 µl of Purpald (chromogen) to each well.
7. Cover the plate with the plate cover and incubate for 10 minutes at room temperature on the shaker.
8. Add 10 µl of potassium periodate to each well. Cover with plate cover and incubate five minutes at room temperature on a shaker.
9. Read the absorbance at 540 nm using a plate reader.

Appendix B13: Enzyme-linked immunosorbent assay Kit for Cytochrome P450 2E1. (CYP-2E1) SEA 988Ra

SEA988Ra 96 Tests
Enzyme-linked Immunosorbent Assay Kit
For Cytochrome P450 2E1 (CYP2E1)
Organism: Rattus norvegicus (Rat)
Instruction manual

FOR IN VITRO AND RESEARCH USE ONLY
NOT FOR USE IN CLINICAL DIAGNOSTIC PROCEDURES

10th Edition (Revised in June, 2013)

[INTENDED USE]

The kit is a sandwich enzyme immunoassay for in vitro quantitative measurement of CYP2E1 in rat serum, plasma, tissue homogenates, cell lysates, cell culture supernates and other biological fluids.

[REAGENTS AND MATERIALS PROVIDED]

Reagents	Quantity	Reagents	Quantity
Pre-coated, ready to use 96-well strip plate	1	Plate sealer for 96 wells	4
Standard (lyophilized)	2	Standard Diluent	1×20mL
Detection Reagent A (green)	1×120μL	Assay Diluent A (2 × concentrate)	1×6mL
Detection Reagent B (red)	1×120μL	Assay Diluent B (2 × concentrate)	1×6mL
TMB Substrate	1×9mL	Stop Solution	1×6mL
Wash Buffer (30 × concentrate)	1×20mL	Instruction manual	1

[MATERIALS REQUIRED BUT NOT SUPPLIED]

1. Microplate reader with 450 ± 10nm filter.
2. Precision single or multi-channel pipettes and disposable tips.
3. Eppendorf Tubes for diluting samples.
4. Deionized or distilled water.
5. Absorbent paper for blotting the microtiter plate.
6. Container for Wash Solution

[STORAGE OF THE KITS]

1. **For unopened kit:** All the reagents should be kept according to the labels on vials. The **Standard, Detection Reagent A, Detection Reagent B** and the **96-well strip plate** should be stored at -20°C upon receipt while the others should be at 4°C.
2. **For opened kit:** When the kit is opened, the remaining reagents still need to be stored according to the above storage condition. Besides, please return the unused wells to the foil pouch containing the desiccant pack, and reseal along entire edge of zip-seal.

Note:
It is highly recommended to use the remaining reagents within 1 month provided this is within the expiration date of the kit.

[SAMPLE COLLECTION AND STORAGE]

Tissue homogenates - The preparation of tissue homogenates will vary depending upon tissue type. For this assay, tissues were rinsed in ice-cold PBS(0.02mol/L,pH 7.0-7.2) to remove excess blood thoroughly and weighed before homogenization. Minced the tissues to small pieces and homogenized them in 5-10 mL of PBS with a glass homogenizer on ice(Micro Tissue Grinders woks, too). The resulting suspension was sonicated with an ultrasonic cell disrupter or subjected to two freeze-thaw cycles to further break the cell membranes. After that, the homogenates were centrifugated for 5 minutes at 5000×g. Remove the supernate and assay immediately or aliquot and store at ≤-20°C.

Other biological fluids - Centrifuge samples for 20 minutes at 1000×g. Remove particulates and assay immediately or store samples in aliquot at -20°C or -80°C. Avoid repeated freeze/thaw cycles.

Note:
1. Samples to be used within 5 days may be stored at 4°C, otherwise samples must be stored at -20°C (≤1 month) or -80°C (≤2 months) to avoid loss of bioactivity and contamination.
2. Sample hemolysis will influence the result, so hemolytic specimen can not be detected.
3. When performing the assay, bring samples to room temperature.

[REAGENT PREPARATION]

1. Bring all kit components and samples to room temperature (18-25°C) before use.
2. **Standard** - Reconstitute the **Standard** with 1.0mL of **Standard Diluent,** kept for 10 minutes at room temperature, shake gently(not to foam). The concentration of the standard in the stock solution is 10ng/mL. Please prepare 7 tubes containing 0.5mL Standard Diluent and produce a double dilution series according to the picture shown below. Mix each tube thoroughly before the next transfer. Set up 7 points of diluted standard such as 10ng/mL, 5ng/mL, 2.5ng/mL, 1.25ng/mL, 0.625ng/mL, 0.312ng/mL, 0.156ng/mL, and the last EP tubes with **Standard Diluent** is the blank as 0ng/mL.

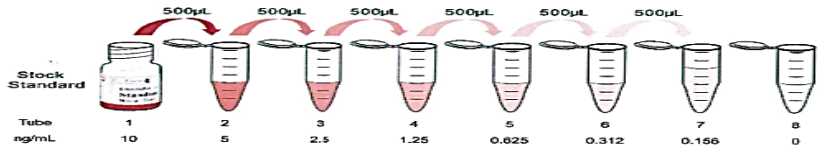

3. **Assay Diluent A and Assay Diluent B** - Dilute 6mL of Assay Diluent A or B Concentrate(2×) with 6mL of deionized or distilled water to prepare 12 mL of Assay Diluent A or B. **(In fact, more than 6mL Assay Diluent A and Assay Diluent B are contained in the bottles. Therefore, in every test, please precisely pipette required amount of Diluent and make double dilution in a new container. The prepared working dilution can't be frozen.)**

4. **Detection Reagent A and Detection Reagent B** - Briefly spin or centrifuge the stock Detection A and Detection B before use. Dilute to the working concentration with working **Assay Diluent A or B,** respectively (1:100).
5. **Wash Solution** - Dilute 20mL of Wash Solution concentrate (30×) with 580mL of deionized or distilled water to prepare 600 mL of Wash Solution (1×).
6. **TMB substrate** - Aspirate the needed dosage of the solution with sterilized tips and do not dump the residual solution into the vial again.

Note:

1. Making serial dilution in the wells directly is not permitted.
2. Prepare standard within 15 minutes before assay. Please do not dissolve the reagents at 37°C directly.
3. Please carefully reconstitute Standards or working Detection Reagent A and B according to the instruction, and avoid foaming and mix gently until the crystals are completely dissolved. To minimize imprecision caused by pipetting, use small volumes and ensure that pipettors are calibrated. It is recommended to suck more than 10μL for once pipetting.
4. The reconstituted Standards, Detection Reagent A and Detection Reagent B can be **used only once**.
5. If crystals have formed in the Wash Solution concentrate (30×), warm to room temperature and mix gently until the crystals are completely dissolved.
6. Contaminated water or container for reagent preparation will influence the detection result.

[SAMPLE PREPARATION]

1. Uscn, Inc. is only responsible for the kit itself, but not for the samples consumed during the assay. The user should calculate the possible amount of the samples used in the whole test. Please reserve sufficient samples in advance.
2. Please predict the concentration before assaying. If values for these are not within the range of the standard curve, users must determine the optimal sample dilutions for their particular experiments.
3. If the samples are not indicated in the manual, a preliminary experiment to determine the validity of the kit is necessary.
4. Tissue or cell extraction samples prepared by chemical lysis buffer may cause unexpected ELISA results due to the impacts from certain chemicals.
5. Due to the possibility of mismatching between antigen from other origin and antibody used in our kits (e.g., antibody targets conformational epitope rather than linear epitope), some native or recombinant proteins from other manufacturers may not be recognized by our products.
6. Influenced by the factors including cell viability, cell number or sampling time, samples from cell culture supernatant may not be detected by the kit.
7. Fresh samples without long time storage is recommended for the test. Otherwise, protein degradation and denaturalization may occur in those samples and finally lead to wrong results.

[ASSAY PROCEDURE]

1. Determine wells for diluted standard, blank and sample. Prepare 7 wells for standard, 1 well for blank. Add 100μL each of dilutions of standard (read Reagent Preparation), blank and samples into the appropriate wells. Cover with the Plate sealer. Incubate for 2 hours at 37°C.
2. Remove the liquid of each well, don't wash.
3. Add 100μL of **Detection Reagent A** working solution to each well. Incubate for 1 hour at 37°C after covering it with the Plate sealer.
4. Aspirate the solution and wash with 350μL of 1× Wash Solution to each well using a squirt bottle, multi-channel pipette, manifold dispenser or autowasher, and let it sit for 1~2 minutes. Remove the remaining liquid from all wells completely by snapping the plate onto absorbent paper. Totally wash 3 times. After the last wash, remove any remaining Wash Buffer by aspirating or decanting. Invert the plate and blot it against absorbent paper.
5. Add 100μL of **Detection Reagent B** working solution to each well. Incubate for 30 minutes at 37°C after covering it with the Plate sealer.
6. Repeat the aspiration/wash process for total 5 times as conducted in step 4.
7. Add 90μL of **Substrate Solution** to each well. Cover with a new Plate sealer. Incubate for 15 - 25 minutes at 37°C (Don't exceed 30 minutes). Protect from light. The liquid will turn blue by the addition of Substrate Solution.
8. Add 50μL of **Stop Solution** to each well. The liquid will turn yellow by the addition of Stop solution. Mix the liquid by tapping the side of the plate. If color change does not appear uniform, gently tap the plate to ensure thorough mixing.
9. Remove any drop of water and fingerprint on the bottom of the plate and confirm there is no bubble on the surface of the liquid. Then, run the microplate reader and conduct measurement at 450nm immediately.

Note:

1. **Assay preparation:** Keep appropriate numbers of wells for 1 experiment and remove extra wells from microplate. Rest wells should be resealed and stored at -20°C.
2. **Samples or reagents addition: Please use the freshly prepared Standard.** Please carefully add samples to wells and mix gently to avoid foaming. Do not touch the well wall. For each step in the procedure, total dispensing time for addition of reagents or samples to the assay plate should not exceed 10 minutes. This will ensure equal elapsed time for each pipetting step, without interruption. Duplication of all standards and specimens, although not required, is recommended. To avoid cross-contamination, change pipette tips between additions of standards, samples, and reagents. Also, use separated reservoirs for each reagent.
3. **Incubation:** To ensure accurate results, proper adhesion of plate sealers during incubation steps is necessary. Do not allow wells to sit uncovered for extended periods between incubation steps. Once reagents are added to the well strips, DO NOT let the strips DRY at any time during the assay. Incubation time and temperature must be controlled.
4. **Washing:** The wash procedure is critical. Complete removal of liquid at each step is essential for good performance. After the last wash, remove any remaining Wash Solution by aspirating or decanting and remove any drop of water and fingerprint on the bottom of the plate. Insufficient washing will result in poor precision and false elevated absorbance reading.
5. **Controlling of reaction time:** Observe the change of color after adding **TMB Substrate** (e.g. observation once every 10 minutes), if the color is too deep, add **Stop Solution** in advance to avoid excessively strong reaction which will result in inaccurate absorbance reading.
6. **TMB Substrate** is easily contaminated. Please protect it from light.
7. The environment humidity which is less than 60% might have some effects on the final performance, therefore, a humidifier is recommended to be used at that condition.

[TEST PRINCIPLE]

The microtiter plate provided in this kit has been pre-coated with an antibody specific to CYP2E1. Standards or samples are then added to the appropriate microtiter plate wells with a biotin-conjugated antibody preparation specific for CYP2E1. Next, Avidin conjugated to Horseradish Peroxidase (HRP) is added to each microplate well and incubated. After TMB substrate solution is added, only those wells that contain CYP2E1, biotin-conjugated antibody and enzyme-conjugated Avidin will exhibit a change in color. The enzyme-substrate reaction is terminated by the addition of sulphuric acid solution and the color change is measured spectrophotometrically at a wavelength of 450nm ± 10nm. The concentration of CYP2E1 in the samples is then determined by comparing the O.D. of the samples to the standard curve.

[CALCULATION OF RESULTS]

Average the duplicate readings for each standard, control, and samples and subtract the average zero standard optical density. Create a standard curve on log-log graph paper, with CYP2E1 concentration on the y-axis and absorbance on the x-axis. Draw the best fit straight line through the standard points and it can be determined by regression analysis. Using some plot software, for instance, curve expert 1.30, is also recommended. If samples have been diluted, the concentration read from the standard curve must be multiplied by the dilution factor.

[TYPICAL DATA]

In order to make the calculation easier, we plot the O.D. value of the standard (X-axis) against the known concentration of the standard (Y-axis), although concentration is the independent variable and O.D. value is the dependent variable. However, the O.D. values of the standard curve may vary according to the conditions of assay performance (e.g. operator, pipetting technique, washing technique or temperature effects), plotting log of the data to establish standard curve for each test is recommended. Typical standard curve below is provided for reference only.

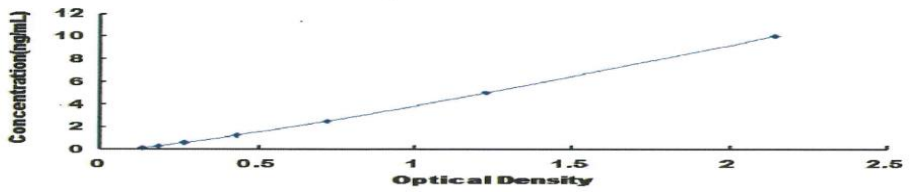

Typical Standard Curve for Rat CYP2E1 ELISA.

[DETECTION RANGE]

0.156-10ng/mL. The standard curve concentrations used for the ELISA's were 10ng/mL, 5ng/mL, 2.5ng/mL, 1.25ng/mL, 0.625ng/mL, 0.312ng/mL, 0.156ng/mL.

[IMPORTANT NOTE]

1. Limited by the current condition and scientific technology, we can't completely conduct the comprehensive identification and analysis on the raw material provided by suppliers. So there might be some qualitative and technical risks to use the kit.
2. The final experimental results will be closely related to validity of the products, operation skills of the end users and the experimental environments. Please make sure that sufficient samples are available.
3. Kits from different batches may be a little different in detection range, sensitivity and color developing time. Please perform the experiment exactly according to the instruction attached in kit while electronic ones from our website (www.uscnk.us; www.uscnk.cn; www.uscnk.com) is only for information.
4. Do not mix or substitute reagents from one kit lot to another. Use only the reagents supplied by manufacturer.
5. Protect all reagents from strong light during storage and incubation. All the bottle caps of reagents should be covered tightly to prevent the evaporation and contamination of microorganism.
6. There may be some foggy substance in the wells when the plate is opened at the first time. It will not have any effect on the final assay results. Do not remove microtiter plate from the storage bag until needed.
7. Wrong operations during the reagents preparation and loading, as well as incorrect parameter setting for the plate reader may lead to incorrect results. A microplate plate reader with a bandwidth of 10nm or less and an optical density range of 0-3 O.D. or greater at 450 ± 10nm wavelength is acceptable for use in absorbance measurement. Please read the instruction carefully and adjust the instrument prior to the experiment. For more information, please refer to the operation video (http://www.uscnk.com/homepage/operate-elisa.htm).
8. Even the same operator might get different results in two separate experiments. In order to get better reproducible results, the operation of every step in the assay should be controlled. Furthermore, a preliminary experiment before assay for each batch is recommended.
9. Each kit has been strictly passed Q.C test. However, results from end users might be inconsistent with our in-house data due to some unexpected transportation conditions or different lab equipments. Intra-assay variance among kits from different batches might arise from above factors, too.
10. Kits from different manufacturers with the same item might produce different results, since we haven't compared our products with other manufacturers.
11. Valid period: six months.
12. The instruction manual also suits for the kit of 48T, but all reagents of 48T kit are reduced by half.

[PRECAUTION]

The Stop Solution suggested for use with this kit is an acid solution. Wear eye, hand, face, and clothing protection when using this material.

Appendix B14: CYP2E1 standard curve

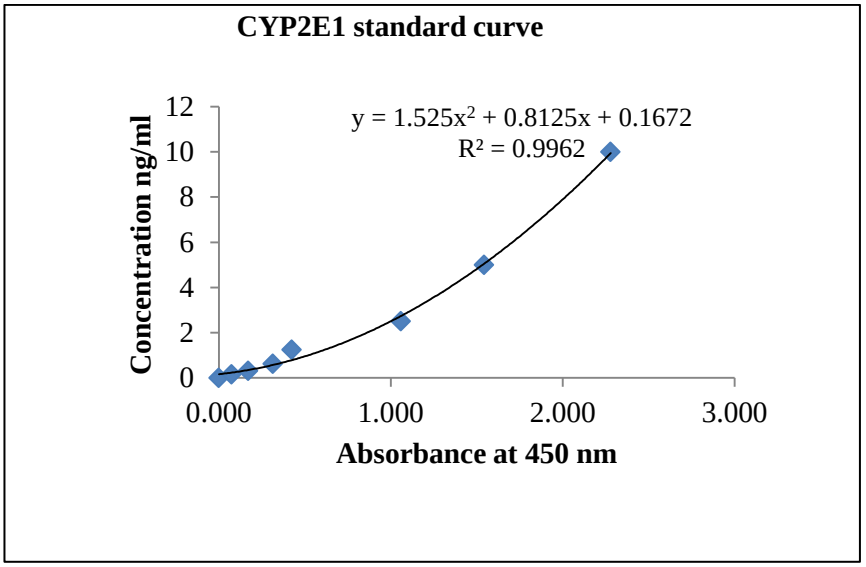

Appendix B15: Enzyme-linked immunosorbent assay Kit for measuring Matrix metalloproteinase enzyme 2 (MMP-2). E 90100 Ra

Uscn
Life Science Inc.

E90100Ra 96 Tests

Enzyme-linked Immunosorbent Assay Kit

For Matrix Metalloproteinase 2 (MMP2)
Organism: Rattus norvegicus (Rat)
Instruction manual
FOR IN VITRO USE AND RESEARCH USE ONLY
NOT FOR USE IN DIAGNOSTIC OR THERAPEUTIC PROCEDURES

[INTENDED USE]

The kit is a sandwich enzyme immunoassay for the in vitro quantitative measurement of MMP2 in rat serum, plasma and other biological fluids.

[REAGENTS AND MATERIALS PROVIDED]

Reagents	Quantity	Reagents	Quantity
Pre-coated, ready to use 96-well strip plate	1	Plate sealer for 96 wells	4
Standard (freeze dried)	2	Standard Diluent	1×20mL
Detection Reagent A (green)	1×120μL	Assay Diluent A (2 × concentrate)	1×6mL
Detection Reagent B (red)	1×120μL	Assay Diluent B (2 × concentrate)	1×6mL
TMB Substrate	1×9mL	Stop Solution	1×6mL
Wash Buffer (30 × concentrate)	1×20mL	Instruction manual	1

[MATERIALS REQUIRED BUT NOT SUPPLIED]

1. Microplate reader with 450 ± 10nm filter.
2. Precision single or multi-channel pipettes and pipette tips with disposable tips.
3. Eppendorf Tubes for diluting samples.
4. Deionized or distilled water.
5. Absorbent paper for blotting the microtiter plate.
6. Container for Wash Solution

[STORAGE OF THE KITS]

All the reagents should be kept acccrding to the labels on vials. The **Standard**, **Detection Reagent A**, **Detection Reagent B** and the **96-well strip plate** should be stored at -20°C upon being received. The unused strips should be kept in a sealed bag with the desiccant provided to minimize exposure to damp air. The test kit may be used throughout the expiration date of the kit (six months from the date of manufacture). Opened test kits will remain stable until the expiring date shown, provided it is stored as prescribed above.

[TEST PRINCIPLE]

The microtiter plate provided in this kit has been pre-coated with a monoclonal antibody specific to MMP2. Standards or samples are then added to the appropriate microtiter plate wells with a biotin-conjugated polyclonal antibody preparation specific for MMP2. Next, Avidin conjugated to Horseradish Peroxidase (HRP) is added to each microplate well and incubated. Then a TMB substrate solution is added to each well. Only those wells that contain MMP2, biotin-conjugated antibody and enzyme-conjugated Avidin will exhibit a change in color. The enzyme-substrate reaction is terminated by the addition of a sulphuric acid solution and the color change is measured spectrophotometrically at a wavelength of 450nm ± 10nm. The concentration of MMP2 in the samples is then determined by comparing the O.D. of the samples to the standard curve.

[SAMPLE COLLECTION AND STORAGE]

Serum - Use a serum separator tube and allow samples to clot for two hours at room temperature or overnight at 4°C before centrifugation for 20 minutes at approximately 1000×g. Assay freshly prepared serum immediately or store samples in aliquot at -20°C or -80°C for later use. Avoid repeated freeze/thaw cycles.

Plasma - Collect plasma using EDTA or heparin as an anticoagulant. Centrifuge samples for 15 minutes at 1000×g at 2 - 8°C within 30 minutes of collection. Remove plasma and assay immediately or store samples in aliquot at -20°C or -80°C for later use. Avoid repeated freeze/thaw cycles.

Other biological fluids - Centrifuge samples for 20 minutes at 1000×g. Remove particulates and assay immediately or store samples in aliquot at -20°C or -80°C for later use. Avoid repeated freeze/thaw cycles.

Note:

1. Samples to be used within 5 days may be stored at 2-8°C, otherwise samples must stored at -20°C (≤1 month) or -80°C (≤2 months) to avoid loss of bioactivity and contamination.
2. Sample hemolysis will influence the result, so hemolytic specimen can not be detected.
3. When performing the assay slowly bring samples to room temperature.

[REAGENT PREPARATION]

1. Bring all kit components and samples to room temperature (18-25°C) before use.
2. **Standard** - Reconstitute the **Standard** with 1.0mL of **Standard Diluent,** kept for 10 minutes at room temperature, shake gently(not to foam). The concentration of the standard in the stock solution is 5,000pg/mL. Please prepare 7 tubes containing 0.5mL Standard Diluent and produce a double dilution series according to the picture shown below. Mix each tube thoroughly before the next transfer. Set up 7 points of diluted standard such as 5,000pg/mL, 2,500pg/mL, 1,250pg/mL, 625pg/mL, 312pg/mL, 156pg/mL, 78pg/mL, and the last EP tubes with **Standard Diluent** is the blank as 0pg/mL.

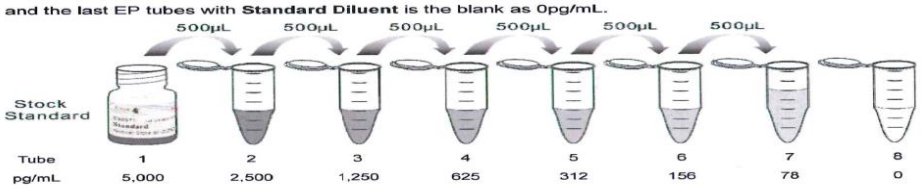

3. **Assay Diluent A and Assay Diluent B** - Dilute 6mL of Assay Diluent A or B Concentrate(2×) with 6mL of deionized or distilled water to prepare 12 mL of Assay Diluent A or B. **The prepared working dilution can't be frozen.**
4. **Detection Reagent A and Detection Reagent B** - Briefly spin or centrifuge the stock Detection A and Detection B before use. Dilute to the working concentration with working **Assay Diluent A or B,** respectively (1:100).
5. **Wash Solution** - Dilute 20mL of Wash Solution concentrate (30×) with 580mL of deionized or distilled water to prepare 600 mL of Wash Solution (1×).
6. **TMB substrate** - Aspirate the needed dosage of the solution with sterilized tips and do not dump the residual solution into the vial again.

Note:

1. Making serial dilution in the wells directly is not permitted.
2. Prepare standard within 15 minutes before assay. Please do not dissolve the reagents at 37°C directly.
3. Please carefully reconstitute Standards or working Detection Reagent A and B according to the instruction, and avoid foaming and mix gently until the crystals have completely dissolved. To minimize imprecision caused by pipetting, use small volumes and ensure that pipettors are calibrated. It is recommended to suck more than 10µL for once pipetting.
4. The reconstituted Standards, Detection Reagent A and Detection Reagent B can be **used only once.**
5. If crystals have formed in the Wash Solution concentrate (30×), warm to room temperature and mix gently until the crystals have completely dissolved.
6. Distilled water is recommended to be used to make the preparation for reagents or samples. Contaminated water or container for reagent preparation will influence the detection result.

[SAMPLE PREPARATION]

1. Uscn, Inc. is only responsible for the kit itself, but not for the samples consumed during the assay. The user should calculate the possible amoun: of the samples used in the whole test. Please reserve sufficient samples in advance.
2. Please predict the concentration before assaying. If values for these are not within the range of the standard curve, users must determine the optimal sample dilutions for their particular experiments.
3. Serum/plasma samples require about a 100-200 fold dilution. A suggested 100-fold dilution is 10µL Sample + 990µL PBS. Sample should be diluted by 0.02mol/L PBS(PH=7.0-7.2).
4. If the samples are not indicated in the manual, a preliminary experiment to determine the validity of the kit is necessary.
5. Tissue or cell extraction samples prepared by chemical lysis buffer may cause unexpected ELISA results due to the impacts of certain chemicals.
6. Owing to the possibility of mismatching between antigen from other resource and antibody used in our kits (e.g., antibody targets conformationa epitope rather than linear epitope), some native or recombinant proteins from other manufacturers may not be recognized by our products.
7. Influenced by the factors including cell viability, cell number and also sampling time, samples from cell culture supernatant may not be detected by the kit.
8. Fresh samples without long time storage is recommended for the test. Otherwise, protein degradation and denaturalization may occur in those samples and finally lead to wrong results.

[ASSAY PROCEDURE]

1. Determine wells for diluted standard, blank and sample. Prepare 7 wells for standard, 1 well for blank. Add 100µL each of dilutions of standard (read Reagent Preparation), blank and samples into the appropriate wells. Cover with the Plate sealer. Incubate for 2 hours at 37°C.
2. Remove the liquid of each well, don't wash.
3. Add 100µL of **Detection Reagent A** working solution to each well. Incubate for 1 hour at 37°C after covering it with the Plate sealer.
4. Aspirate the solution and wash with 350µL of 1× Wash Solution to each well using a squirt bottle, multi-channel pipette, manifold dispenser or autowasher, and let it sit for 1~2 minutes. Remove the remaining liquid from all wells completely by snapping the plate onto absorbent paper. Repeat 3 times. After the last wash, remove any remaining Wash Buffer by aspirating or decanting. Invert the plate and blot it against absorbent paper.
5. Add 100µL of **Detection Reagent B** working solution to each well. Incubate for 30 minutes at 37°C after covering it with the Plate sealer.
6. Repeat the aspiration/wash process for five times as conducted in step 4.
7. Add 90µL of **Substrate Solution** to each well. Cover with a new Plate sealer. Incubate for 15 - 25 minutes at 37°C (Don't exceed 30 minutes). Protect from light. The liquid will turn blue by the addition of Substrate Solution.
8. Add 50µL of **Stop Solution** to each well. The liquid will turn yellow by the addition of Stop solution. Mix the liquid by tapping the side of the plate. If color change does not appear uniform, gently tap the plate to ensure thorough mixing.
9. Remove any drop of water and fingerprint on the bottom of the plate and confirm there is no bubble on the surface of the liquid. Then, run the microplate reader and conduct measurement at 450nm immediately.

Note:

1. **Assay preparation:** Keep appropriate numbers of strips for 1 experiment and remove extra strips from microtiter plate. Removed strips should be resealed and stored at -20°C until the kits expiry date.
2. **Samples or reagents addition: Please use the freshly prepared Standard.** Please carefully add samples to wells and mix gently to avoid foaming. Do not touch the well wall as possible. For each step in the procedure, total dispensing time for addition of reagents or samples to the assay plate should not exceed 10 minutes. This will ensure equal elapsed time for each pipetting step, without interruption. Duplication of all standards and specimens, although not required, is recommended. To avoid cross-contamination, change pipette tips between additions of each standard level, between sample additions, and between reagent additions. Also, use separate reservoirs for each reagent.
3. **Incubation:** To ensure accurate results, proper adhesion of plate sealers during incubation steps is necessary. Do not allow wells to sit uncovered for extended periods between incubation steps. Once reagents have been added to the well strips, DO NOT let the strips DRY at any time during the assay. Incubation time and temperature must be observed.
4. **Washing:** The wash procedure is critical. Complete removal of liquid at each step is essential to good performance. After the last wash, remove any remaining Wash Solution by aspirating or decanting and remove any drop of water and fingerprint on the bottom of the plate. Insufficient washing will result in poor precision and falsely elevated absorbance reading.

5. **Controlling of reaction time:** Observe the change of color after adding **TMB Substrate** (e.g. observation once every 10 minutes), if the color is too deep, add **Stop Solution** in advance to avoid excessively strong reaction which will result in inaccurate absorbance reading.
6. **TMB Substrate** is easily contaminated. Please protect it from light.

[CALCULATION OF RESULTS]

Average the duplicate readings for each standard, control, and samples and subtract the average zero standard optical density. Create a standard curve on log-log graph paper, with MMP2 concentration on the y-axis and absorbance on the x-axis. Draw the best fit straight line through the standard points and it can be determined by regression analysis. Using some plot software, such as curve expert 1.30, is also recommended. If samples have been diluted, the concentration read from the standard curve must be multiplied by the dilution factor.

[TYPICAL DATA]

In order to make the calculation easier, we plot the O.D. value of the standard (X-axis) against the known concentration of the standard (Y-axis), although concentration is indeed the independent variable while O.D. value is the dependent variable. Further, in this part, in order to help the customer perform the assay more visual, we provide the customer with the raw data (not the log of data). However, plotting log of the data to construct the curve will be recommended. The O.D. values of the standard curve may vary according to the conditions of assay performance (e.g. operator, pipetting technique, washing technique or temperature effects). This curve is provided for demonstration only. The customers should establish their own standard curve for each test conducted.

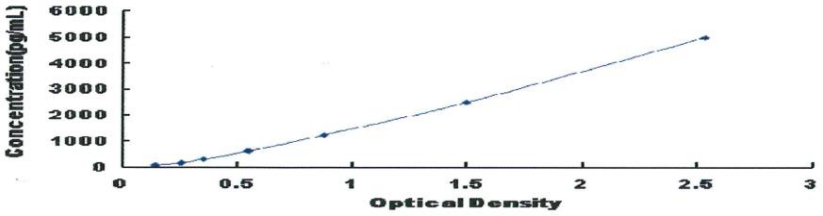

Typical Standard Curve for Rat MMP2 ELISA.

[DETECTION RANGE]

78-5,000pg/mL. The standard curve concentrations used for the ELISA's were 5,000pg/mL, 2,500pg/mL, 1,250pg/mL, 625pg/mL, 312pg/mL, 156pg/mL, 78pg/mL.

[SENSITIVITY]

The minimum detectable dose of rat MMP2 is typically less than 29pg/mL.
The sensitivity of this assay, or Lower Limit of Detection (LLD) was defined as the lowest protein concentration that could be differentiated from zero. It was determined the mean O.D. Value of 20 replicates of the zero standard added by their three standard deviations.

[SPECIFICITY]

This assay has high sensitivity and excellent specificity for detection of rat MMP2.
No significant cross-reactivity or interference between rat MMP2 and analogues was observed.
Note:
Limited by current skills and knowledge, it is impossible for us to complete the cross- reactivity detection between rat MMP2 and all the analogues, therefore, cross reaction may still exist.

[ASSAY PROCEDURE SUMMARY]

1. Prepare all reagents, samples and standards;
2. Add 100µL standard or sample to each well. Incubate 2 hours at 37°C;
3. Add 100µL prepared Detection Reagent A. Incubate 1 hour at 37°C;
4. Aspirate and wash 3 times;
5. Add 100µL prepared Detection Reagent B. Incubate 30 minutes at 37°C;
6. Aspirate and wash 5 times;
7. Add 90µL Substrate Solution. Incubate 15-25 minutes at 37°C;
8. Add 50µL Stop Solution. Read at 450nm immediately.

[IMPORTANT NOTE]

1. Limited by the current condition and scientific technology, we can't completely conduct the comprehensive identification and analysis on the raw material provided by suppliers. So there might be some qualitative and technical risks to use the kit.
2. The final experimental results will be closely related to validity of the products, operation skills of the end users and the experimental environments. Please make sure that sufficient samples are available.
3. Kits from different batches may be a little different in detection range, sensitivity and color developing time. Please perform the experiment exactly according to the instruction attached in kit while electronic ones from our website (www.uscnk.us; www.uscnk.cn; www.uscnk.com) is only for information.
4. Do not mix or substitute reagents from one kit lot to another. Use only the reagents supplied by manufacturer.
5. Protect all reagents from strong light during storage and incubation. All the bottle caps of reagents should be covered tightly to prevent the evaporation and contamination of microorganism.
6. There may be some foggy substance in the wells when the plate is opened at the first time. It will not have any effect on the final assay results. Do not remove microtiter plate from the storage bag until needed.
7. Wrong operations during the reagents preparation and loading, as well as incorrect parameter setting for the plate reader may lead to incorrect results. A microplate plate reader with a bandwidth of 10nm or less and an optical density range of 0-3 O.D. or greater at 450 ± 10nm wavelength is acceptable for use in absorbance measurement. Please read the instruction carefully and adjust the instrument prior to the experiment. For more information, please refer to the operation video (http://www.uscnk.com/homepage/operate-elisa.htm).
8. Even the same operator might get different results in two separate experiments. In order to get better reproducible results, the operation of every step in the assay should be controlled. Furthermore, a preliminary experiment before assay for each batch is recommended.

Appendix B16: MMP-2 standard curve

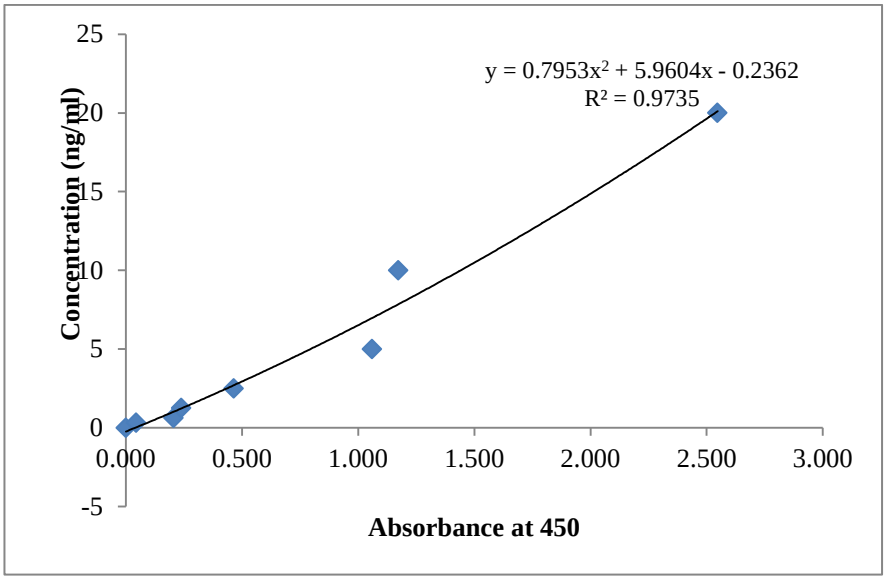

Appendix B17: Enzyme-linked immunosorbent assay Kit for measuring Matrix metalloproteinase enzyme 9 (MMP-9). SEA 553Ra

Uscn Life Science Inc.

SEA553Ra 96 Tests
Enzyme-linked Immunosorbent Assay Kit
For Matrix Metalloproteinase 9 (MMP9)
Organism: Rattus norvegicus (Rat)
Instruction manual

FOR IN VITRO AND RESEARCH USE ONLY
NOT FOR USE IN CLINICAL DIAGNOSTIC PROCEDURES

10th Edition (Revised in June, 2013)

[INTENDED USE]

The kit is a sandwich enzyme immunoassay for in vitro quantitative measurement of MMP9 in rat serum, plasma, tissue homogenates, cell lysates, cell culture supernates and other biological fluids.

[REAGENTS AND MATERIALS PROVIDED]

Reagents	Quantity	Reagents	Quantity
Pre-coated, ready to use 96-well strip plate	1	Plate sealer for 96 wells	4
Standard (lyophilized)	2	Standard Diluent -	1×20mL
Detection Reagent A (green)	1×120μL	Assay Diluent A (2 × concentrate)	1×6mL
Detection Reagent B (red)	1×120μL	Assay Diluent B (2 × concentrate)	1×6mL
TMB Substrate	1×9mL	Stop Solution	1×6mL
Wash Buffer (30 × concentrate)	1×20mL	Instruction manual	1

[MATERIALS REQUIRED BUT NOT SUPPLIED]

1. Microplate reader with 450 ± 10nm filter.
2. Precision single or multi-channel pipettes and disposable tips.
3. Eppendorf Tubes for diluting samples.
4. Deionized or distilled water.
5. Absorbent paper for blotting the microtiter plate.
6. Container for Wash Solution

[STORAGE OF THE KITS]

1. **For unopened kit:** All the reagents should be kept according to the labels on vials. The **Standard, Detection Reagent A, Detection Reagent B** and the **96-well strip plate** should be stored at -20°C upon receipt while the others should be at 4°C.
2. **For opened kit:** When the kit is opened, the remaining reagents still need to be stored according to the above storage condition. Besides, please return the unused wells to the foil pouch containing the desiccant pack, and reseal along entire edge of zip-seal.

[TEST PRINCIPLE]

The microtiter plate provided in this kit has been pre-coated with a monoclonal antibody specific to MMP9. Standards or samples are then added to the appropriate microtiter plate wells with a biotin-conjugated polyclonal antibody preparation specific for MMP9. Next, Avidin conjugated to Horseradish Peroxidase (HRP) is added to each microplate well and incubated. Then a TMB substrate solution is added to each well. Only those wells that contain MMP9, biotin-conjugated antibody and enzyme-conjugated Avidin will exhibit a change in color. The enzyme-substrate reaction is terminated by the addition of a sulphuric acid solution and the color change is measured spectrophotometrically at a wavelength of 450nm ± 10nm. The concentration of MMP9 in the samples is then determined by comparing the O.D. of the samples to the standard curve.

[SAMPLE COLLECTION AND STORAGE]

Serum - Use a serum separator tube and allow samples to clot for two hours at room temperature or overnight at 4°C before centrifugation for 20 minutes at approximately 1000×g. Assay freshly prepared serum immediately or store samples in aliquot at -20°C or -80°C for later use. Avoid repeated freeze/thaw cycles.

Plasma - Collect plasma using EDTA or heparin as an anticoagulant. Centrifuge samples for 15 minutes at 1000×g at 2 - 8°C within 30 minutes of collection. Remove plasma and assay immediately or store samples in aliquot at -20°C or -80°C for later use. Avoid repeated freeze/thaw cycles.

Tissue homogenates - The preparation of tissue homogenates will vary depending upon tissue type. For this assay, tissues were rinsed in ice-cold PBS(0.02mol/L,pH 7.0-7.2) to remove excess blood thoroughly and weighed before homogenization. Minced the tissues to small pieces and homogenized them in 5-10 mL of PBS with a glass homogenizer on ice(Micro Tissue Grinders woks, too). The resulting suspension was sonicated with an ultrasonic cell disrupter or subjected to two freeze-thaw cycles to further break the cell membranes. After that, the homogenates were centrifugated for 5 minutes at 5000×g. Remove the supernate and assay immediately or aliquot anc store at ≤-20°C.

Cell culture supernates and other biological fluids - Centrifuge samples for 20 minutes at 1000×g. Remove particulates and assay immediately or store samples in aliquot at -20°C or -80°C for later use. Avoid repeated freeze/thaw cycles.

Note:

1. Samples to be used within 5 days may be stored at 2-8°C, otherwise samples must stored at -20°C (≤1 month) or -80°C (≤2 months) to avoid loss of bioactivity and contamination.
2. Sample hemolysis will influence the result, so hemolytic specimen can not be detected.
3. When performing the assay slowly bring samples to room temperature.

[REAGENT PREPARATION]

1. Bring all kit components and samples to room temperature (18-25°C) before use.
2. **Standard** - Reconstitute the **Standard** with 1.0 mL of **Standard Diluent,** kept for 10 minutes at room temperature, shake gently(not to foam). The concentration of the standard in the stock solution is 50ng/mL. Please prepare 7 tubes containing 0.5mL Standard Diluent and produce a double dilution series according to the picture shown below. Mix each tube thoroughly before the next transfer. Set up 7 points of diluted standard such as 50ng/mL, 25ng/mL, 12.5ng/mL, 6.25ng/mL, 3.12ng/mL, 1.56ng/mL, 0.78ng/mL, and the last EP tubes with **Standard Diluent** is the blank as 0ng/mL.

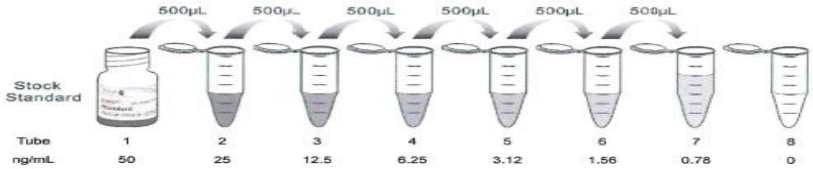

3. **Assay Diluent A and Assay Diluent B** - Dilute 6mL of Assay Diluent A or B Concentrate(2×) with 6mL of deionized or distilled water to prepare 12 mL of Assay Diluent A or B. **The prepared working dilution can't be frozen.**
4. **Detection Reagent A and Detection Reagent B** - Briefly spin or centrifuge the stock Detection A and Detection B before use. Dilute to the working concentration with working **Assay Diluent A or B,** respectively (1:100).
5. **Wash Solution** - Dilute 20mL of Wash Solution concentrate (30×) with 580mL of deionized or distilled water to prepare 600 mL of Wash Solution (1×).
6. **TMB substrate** - Aspirate the needed dosage of the solution with sterilized tips and do not dump the residual solution into the vial again.

Note:

1. Making serial dilution in the wells directly is not permitted.
2. Prepare standard within 15 minutes before assay. Please do not dissolve the reagents at 37°C directly.
3. Please carefully reconstitute Standards or working Detection Reagent A and B according to the instruction, and avoid foaming and mix gently until the crystals have completely dissolved. To minimize imprecision caused by pipetting, use small volumes and ensure that pipettors are calibrated. It s recommended to suck more than 10μL for once pipetting.
4. The reconstituted Standards, Detection Reagent A and Detection Reagent B can be **used only once**.
5. If crystals have formed in the Wash Solution concentrate (30×), warm to room temperature and mix gently until the crystals have completely dissolved.
6. Distilled water is recommended to be used to make the preparation for reagents or samples. Contaminated water or container for reagent preparation will influence the detection result.

[SAMPLE PREPARATION]

1. Uscn, Inc. is only responsible for the kit itself, but not for the samples consumed during the assay. The user should calculate the possible amount of the samples used in the whole test. Please reserve sufficient samples in advance.
2. Please predict the concentration before assaying. If values for these are not within the range of the standard curve, users must determine the optimal sample dilutions for their particular experiments.
3. Serum/plasma samples require about a 0-10 fold dilution. A suggested 10-fold dilution is 20μL Sample + 180μL PBS. Sample should be diluted by 0.02mol/L PBS(PH=7.0-7.2).
4. If the samples are not indicated in the manual, a preliminary experiment to determine the validity of the kit is necessary.
5. Tissue or cell extraction samples prepared by chemical lysis buffer may cause unexpected ELISA results due to the impacts of certain chemicals.
6. Owing to the possibility of mismatching between antigen from other resource and antibody used in our kits (e.g., antibody targets conformational epitope rather than linear epitope), some native or recombinant proteins from other manufacturers may not be recognized by our products.
7. Influenced by the factors including cell viability, cell number and also sampling time, samples from cell culture supernatant may not be detected by the kit.
8. Fresh samples without long time storage is recommended for the test. Otherwise, protein degradation and denaturalization may occur in those samples and finally lead to wrong results.
9. If the humidity level in the laboratory does not reach 60%, a humidifier is recommended to be used.

[ASSAY PROCEDURE]

1. Determine wells for diluted standard, blank and sample. Prepare 7 wells for standard, 1 well for blank. Add 100μL each of dilutions of standard (read Reagent Preparation), blank and samples into the appropriate wells. Cover with the Plate sealer. Incubate for 2 hours at 37°C.
2. Remove the liquid of each well, don't wash.
3. Add 100μL of **Detection Reagent A** working solution to each well. Incubate for 1 hour at 37°C after covering it with the Plate sealer.
4. Aspirate the solution and wash with 350μL of 1× Wash Solution to each well using a squirt bottle, multi-channel pipette, manifold dispenser or autowasher, and let it sit for 1~2 minutes. Remove the remaining liquid from all wells completely by snapping the plate onto absorbent paper. Repeat 3 times. After the last wash, remove any remaining Wash Buffer by aspirating or decanting. Invert the plate and blot it against absorbent paper.
5. Add 100μL of **Detection Reagent B** working solution to each well. Incubate for 30 minutes at 37°C after covering it with the Plate sealer.
6. Repeat the aspiration/wash process for five times as conducted in step 4.
7. Add 90μL of **Substrate Solution** to each well. Cover with a new Plate sealer. Incubate for 15 - 25 minutes at 37°C (Don't exceed 30 minutes). Protect from light. The liquid will turn blue by the addition of Substrate Solution.
8. Add 50μL of **Stop Solution** to each well. The liquid will turn yellow by the addition of Stop solution. Mix the liquid by tapping the side of the plate If color change does not appear uniform, gently tap the plate to ensure thorough mixing.
9. Remove any drop of water and fingerprint on the bottom of the plate and confirm there is no bubble on the surface of the liquid. Then, run the microplate reader and conduct measurement at 450nm immediately.

Note:

1. **Assay preparation:** Keep appropriate numbers of strips for 1 experiment and remove extra strips from microtiter plate. Removed strips should be resealed and stored at -20°C until the kits expiry date.
2. **Samples or reagents addition：Please use the freshly prepared Standard.** Please carefully add samples to wells and mix gently to avoid foaming. Do not touch the well wall as possible. For each step in the procedure, total dispensing time for addition of reagents or samples to the assay plate should not exceed 10 minutes. This will ensure equal elapsed time for each pipetting step, without interruption. Duplication of all standards and specimens, although not required, is recommended. To avoid cross-contamination, change pipette tips between additions of each standard level, between sample additions, and between reagent additions. Also, use separate reservcirs for each reagent.

[DETECTION RANGE]

0.78 -50ng/mL. The standard curve concentrations used for the ELISA's were 50ng/mL, 25ng/mL, 12.5ng/mL, 6.25ng/mL, 3.12ng/mL, 1.56ng/mL, 0.78ng/mL.

[SENSITIVITY]

The minimum detectable dose of rat MMP9 is typically less than 0.25ng/mL.
The sensitivity of this assay, or Lower Limit of Detection (LLD) was defined as the lowest protein concentration that could be differentiated from zero. It was determined the mean O.D. Value of 20 replicates of the zero standard added by their three standard deviations.

[SPECIFICITY]

This assay has high sensitivity and excellent specificity for detection of rat MMP9.
No significant cross-reactivity or interference between rat MMP9 and analogues was observed.
Note:
Limited by current skills and knowledge, it is impossible for us to complete the cross- reactivity detection between rat MMP9 and all the analogues, therefore, cross reaction may still exist.

[ASSAY PROCEDURE SUMMARY]

1. Prepare all reagents, samples and standards;
2. Add 100μL standard or sample to each well. Incubate 2 hours at 37°C;
3. Add 100μL prepared Detection Reagent A. Incubate 1 hour at 37°C;
4. Aspirate and wash 3 times;
5. Add 100μL prepared Detection Reagent B. Incubate 30 minutes at 37°C;
6. Aspirate and wash 5 times;
7. Add 90μL Substrate Solution. Incubate 15-25 minutes at 37°C;
8. Add 50μL Stop Solution. Read at 450nm immediately.

[IMPORTANT NOTE]

1. Limited by the current condition and scientific technology, we can't completely conduct the comprehensive identification and analysis on the raw material provided by suppliers. So there might be some qualitative and technical risks to use the kit.
2. The final experimental results will be closely related to validity of the products, operation skills of the end users and the experimental environments. Please make sure that sufficient samples are available.
3. Kits from different batches may be a little different in detection range, sensitivity and color developing time. Please perform the experiment exactly according to the instruction attached in kit while electronic ones from our website (www.uscnk.us; www.uscrk.cn; www.uscnk.com) is only for information.
4. Do not mix or substitute reagents from one kit lot to another. Use only the reagents supplied by manufacturer.
5. Protect all reagents from strong light during storage and incubation. All the bottle caps of reagents should be covered tightly to prevent the evaporation and contamination of microorganism.
6. There may be some foggy substance in the wells when the plate is opened at the first time. It will not have any effect on the final assay results. Do not remove microtiter plate from the storage bag until needed.
7. Wrong operations during the reagents preparation and loading, as well as incorrect parameter setting for the plate reader may lead to incorrect results. A microplate plate reader with a bandwidth of 10nm or less and an optical density range of 0-3 O.D. or greater at 450 ± 10nm wavelength is acceptable for use in absorbance measurement. Please read the instruction carefully and adjust the instrument prior to the experiment. For more information, please refer to the operation video (http://www.uscnk.com/homepage/operate-elisa.htm).
8. Even the same operator might get different results in two separate experiments. In order to get better reproducible results, the operation of every step in the assay should be controlled. Furthermore, a preliminary experiment before assay for each batch is recommended.
9. Each kit has been strictly passed Q.C test. However, results from end users might be inconsistent with our in-house data due to some unexpected transportation conditions or different lab equipments. Intra-assay variance among kits from different batches might arise from above factors, too.
10. Kits from different manufacturers for the same item might produce different results, since we haven't compared our products with other manufacturers.
11. Valid period: six months.
12. The instruction manual also suit for the kit of 48T, but all reagents of 48T kit is reduced by half.

[PRECAUTION]

The Stop Solution suggested for use with this kit is an acid solution. Wear eye, hand, face, and clothing protection when using this material.

Appendix B18: MMP-9 standard curve

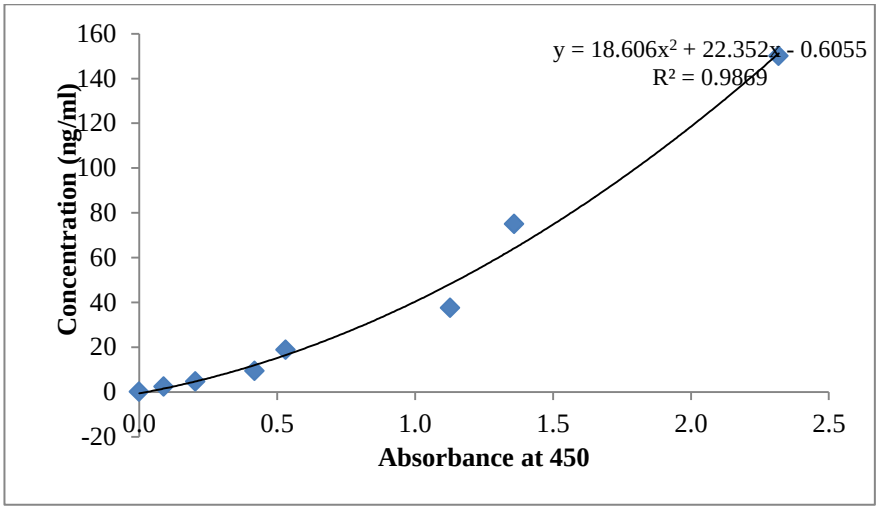

Appendix B19: Enzyme-linked immunosorbent assay Kit for measuring Tissue inhibitor metalloproteinase enzyme1 (TIMP-1). SEA 522Ra

Uscn Life Science Inc.

SEA552Ra 96 Tests
Enzyme-linked Immunosorbent Assay Kit
For Tissue Inhibitors Of Metalloproteinase 1 (TIMP1)
Organism: Rattus norvegicus (Rat)
Instruction manual

FOR IN VITRO AND RESEARCH USE ONLY
NOT FOR USE IN CLINICAL DIAGNOSTIC PROCEDURES

10th Edition (Revised in June, 2013)

[INTENDED USE]

The kit is a sandwich enzyme immunoassay for in vitro quantitative measurement of TIMP1 in rat serum, plasma, tissue homogenates, cell lysates, cell cullure supernates and other biological fluids.

[REAGENTS AND MATERIALS PROVIDED]

Reagents	Quantity	Reagents	Quantity
Pre-coated, ready to use 96-well strip plate	1	Plate sealer for 96 wells	4
Standard (lyophilized)	2	Standard Diluent	1×20mL
Detection Reagent A (green)	1×120μL	Assay Diluent A (2 × concentrate)	1×6mL
Detection Reagent B (red)	1×120μL	Assay Diluent B (2 × concentrate)	1×6mL
TMB Substrate	1×9mL	Stop Solution	1×6mL
Wash Buffer (30 × concentrate)	1×20mL	Instruction manual	1

[MATERIALS REQUIRED BUT NOT SUPPLIED]

1. Microplate reader with 450 ± 10nm filter.
2. Precision single or multi-channel pipettes and disposable tips.
3. Eppendorf Tubes for diluting samples.
4. Deionized or distilled water.
5. Absorbent paper for blotting the microtiter plate.
6. Container for Wash Solution

[STORAGE OF THE KITS]

1. **For unopened kit:** All the reagents should be kept according to the labels on vials. The **Standard, Detection Reagent A, Detection Reagent B** and the **96-well strip plate** should be stored at -20°C upon receipt while the others should be at 4 °C.
2. **For opened kit:** When the kit is opened, the remaining reagents still need to be stored according to the above storage condition. Besides, please return the unused wells to the foil pouch containing the desiccant pack, and reseal along entire edge of zip-seal.

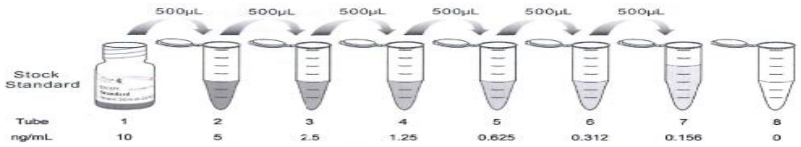

3. **Assay Diluent A and Assay Diluent B -** Dilute 6mL of Assay Diluent A or B Concentrate(2×) with 6mL of deionized or distilled water to prepare 12 mL of Assay Diluent A or B. **The prepared working dilution can't be frozen.**
4. **Detection Reagent A and Detection Reagent B -** Briefly spin or centrifuge the stock Detection A and Detection B before use. Dilute to the working concentration with working **Assay Diluent A or B,** respectively (1:100).
5. **Wash Solution** - Dilute 20mL of Wash Solution concentrate (30×) with 580mL of deionized or distilled water to prepare 600 mL of Wash Solution (1×).
6. **TMB substrate** - Aspirate the needed dosage of the solution with sterilized tips and do not dump the residual solution into the vial again.

Note:

1. Making serial dilution in the wells directly is not permitted.
2. Prepare standard within 15 minutes before assay. Please do not dissolve the reagents at 37°C directly.
3. Please carefully reconstitute Standards or working Detection Reagent A and B according to the instruction, and avoid foaming and mix gently until the crystals have completely dissolved. To minimize imprecision caused by pipetting, use small volumes and ensure that pipettors are calibrated. It is recommended to suck more than 10μL for once pipetting.
4. The reconstituted Standards, Detection Reagent A and Detection Reagent B can be **used only once**.
5. If crystals have formed in the Wash Solution concentrate (30×), warm to room temperature and mix gently until the crystals have completely dissolved.
6. Distilled water is recommended to be used to make the preparation for reagents or samples. Contaminated water or container for reagent preparation will influence the detection result.

[SAMPLE PREPARATION]

1. Uscn, Inc. is only responsible for the kit itself, but not for the samples consumed during the assay. The user should calculate the possible amount of the samples used in the whole test. Please reserve sufficient samples in advance.
2. Please predict the concentration before assaying. If values for these are not within the range of the standard curve, users must determine the optimal sample dilutions for their particular experiments.
3. Serum/plasma samples require about a 0-5 fold dilution. A suggested 5-fold dilution is 40μL Sample + 160μL PBS. Sample should be diluted by 0.02mol/L PBS(PH=7.0-7.2).
4. If the samples are not indicated in the manual, a preliminary experiment to determine the validity of the kit is necessary.

5. Tissue or cell extraction samples prepared by chemical lysis buffer may cause unexpected ELISA results due to the impacts of certain chemicals.
6. Owing to the possibility of mismatching between antigen from other resource and antibody used in our kits (e.g., antibody targets conformational epitope rather than linear epitope), some native or recombinant proteins from other manufacturers may not be recognized by our products.
7. Influenced by the factors including cell viability, cell number and also sampling time, samples from cell culture supernatant may not be detected by the kit.
8. Fresh samples without long time storage is recommended for the test. Otherwise, protein degradation and denaturalization may occur in those samples and finally lead to wrong results.

[ASSAY PROCEDURE]

1. Determine wells for diluted standard, blank and sample. Prepare 7 wells for standard, 1 well for blank. Add 100µL each of dilutions of standard (read Reagent Preparation), blank and samples into the appropriate wells. Cover with the Plate sealer. Incubate for 2 hours at 37°C.
2. Remove the liquid of each well, don't wash.
3. Add 100µL of **Detection Reagent A** working solution to each well. Incubate for 1 hour at 37°C after covering it with the Plate sealer.
4. Aspirate the solution and wash with 350µL of 1× Wash Solution to each well using a squirt bottle, multi-channel pipette, manifold dispenser or autowasher, and let it sit for 1~2 minutes. Remove the remaining liquid from all wells completely by snapping the plate onto absorbent paper. Repeat 3 times. After the last wash, remove any remaining Wash Buffer by aspirating or decanting. Invert the plate and blot it against absorbent paper.
5. Add 100µL of **Detection Reagent B** working solution to each well. Incubate for 30 minutes at 37°C after covering it with the Plate sealer.
6. Repeat the aspiration/wash process for five times as conducted in step 4.
7. Add 90µL of **Substrate Solution** to each well. Cover with a new Plate sealer. Incubate for 15 - 25 minutes at 37°C (Don't exceed 30 minutes). Protect from light. The liquid will turn blue by the addition of Substrate Solution.
8. Add 50µL of **Stop Solution** to each well. The liquid will turn yellow by the addition of Stop solution. Mix the liquid by tapping the side of the plate. If color change does not appear uniform, gently tap the plate to ensure thorough mixing.
9. Remove any drop of water and fingerprint on the bottom of the plate and confirm there is no bubble on the surface of the liquid. Then, run the microplate reader and conduct measurement at 450nm immediately.

Note:

1. **Assay preparation:** Keep appropriate numbers of strips for 1 experiment and remove extra strips from microtiter plate. Removed strips should be resealed and stored at -20°C until the kits expiry date.
2. **Samples or reagents addition: Please use the freshly prepared Standard.** Please carefully add samples to wells and mix gently to avoid foaming. Do not touch the well wall as possible. For each step in the procedure, total dispensing time for addition of reagents or samples to the assay plate should not exceed 10 minutes. This will ensure equal elapsed time for each pipetting step, without interruption. Duplication of all standards and specimens, although not required, is recommended. To avoid cross-contamination, change pipette tips between additions of each standard level, between sample additions, and between reagent additions. Also, use separate reservoirs for each reagent.
3. **Incubation:** To ensure accurate results, proper adhesion of plate sealers during incubation steps is necessary. Do not allow wells to sit uncovered for extended periods between incubation steps. Once reagents have been added to the well strips, DO NOT let the strips DRY at any time during the assay. Incubation time and temperature must be observed.
4. **Washing:** The wash procedure is critical. Complete removal of liquid at each step is essential to good performance. After the last wash, remove any remaining Wash Solution by aspirating or decanting and remove any drop of water and fingerprint on the bottom of the plate. Insufficient washing will result in poor precision and falsely elevated absorbance reading.
5. **Controlling of reaction time:** Observe the change of color after adding **TMB Substrate** (e.g. observation once every 10 minutes), if the color is too deep, add **Stop Solution** in advance to avoid excessively strong reaction which will result in inaccurate absorbance reading.
6. **TMB Substrate** is easily contaminated. Please protect it from light.

[CALCULATION OF RESULTS]

Average the duplicate readings for each standard, control, and samples and subtract the average zero standard optical density. Create a standard curve on log-log graph paper, with TIMP1 concentration on the y-axis and absorbance on the x-axis. Draw the best fit straight line through the standard points and it can be determined by regression analysis. Using some plot software, such as curve expert 1.30, is also recommended. If samples have been diluted, the concentration read from the standard curve must be multiplied by the dilution factor.

[TYPICAL DATA]

In order to make the calculation easier, we plot the O.D. value of the standard (X-axis) against the known concentration of the standard (Y-axis), although concentration is indeed the independent variable while O.D. value is the dependent variable. Further, in this part, in order to help the customer perform the assay more visual, we provide the customer with the raw data (not the log of data). However, plotting log of the data to construct the curve will be recommended. The O.D. values of the standard curve may vary according to the conditions of assay performance (e.g. operator, pipetting technique, washing technique or temperature effects). This curve is provided for demonstration only. The customers should establish their own standard curve for each test conducted.

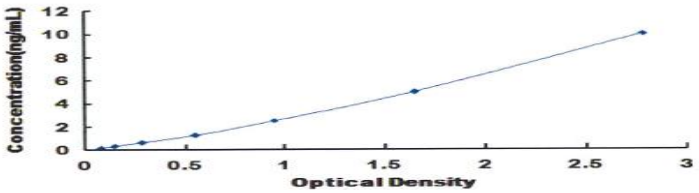

Typical Standard Curve for Rat TIMP1 ELISA.

[DETECTION RANGE]

0.156-10ng/mL. The standard curve concentrations used for the ELISA's were 10ng/mL, 5ng/mL, 2.5ng/mL, 1.25ng/mL, 0.625ng/mL, 0.312ng/mL, 0.156ng/mL.

[SENSITIVITY]

The minimum detectable dose of rat TIMP1 is typically less than 0.062ng/mL.
The sensitivity of this assay, or Lower Limit of Detection (LLD) was defined as the lowest protein concentration that could be differentiated from zero. It was determined the mean O.D. Value of 20 replicates of the zero standard added by their three standard deviations.

[SPECIFICITY]

This assay has high sensitivity and excellent specificity for detection of rat TIMP1.
No significant cross-reactivity or interference between rat TIMP1 and analogues was observed.
Note:
Limited by current skills and knowledge, it is impossible for us to complete the cross- reactivity detection between rat TIMP1 and all the analogues, therefore, cross reaction may still exist.

[ASSAY PROCEDURE SUMMARY]

1. Prepare all reagents, samples and standards;
2. Add 100μL standard or sample to each well. Incubate 2 hours at 37°C;
3. Add 100μL prepared Detection Reagent A. Incubate 1 hour at 37°C;
4. Aspirate and wash 3 times;
5. Add 100μL prepared Detection Reagent B. Incubate 30 minutes at 37°C;
6. Aspirate and wash 5 times;
7. Add 90μL Substrate Solution. Incubate 15-25 minutes at 37°C;
8. Add 50μL Stop Solution. Read at 450nm immediately.

[IMPORTANT NOTE]

1. Limited by the current condition and scientific technology, we can't completely conduct the comprehensive identification and analysis on the raw material provided by suppliers. So there might be some qualitative and technical risks to use the kit.
2. The final experimental results will be closely related to validity of the products, operation skills of the end users and the experimental environments. Please make sure that sufficient samples are available.
3. Kits from different batches may be a little different in detection range, sensitivity and color developing time. Please perform the experiment exactly according to the instruction attached in kit while electronic ones from our website (www.uscnk.us; www.uscnk.cn; www.uscnk.com) is only for information.
4. Do not mix or substitute reagents from one kit lot to another. Use only the reagents supplied by manufacturer.
5. Protect all reagents from strong light during storage and incubation. All the bottle caps of reagents should be covered tightly to prevent the evaporation and contamination of microorganism.
6. There may be some foggy substance in the wells when the plate is opened at the first time. It will not have any effect on the final assay results. Do not remove microtiter plate from the storage bag until needed.
7. Wrong operations during the reagents preparation and loading, as well as incorrect parameter setting for the

Appendix B20: TIMP-1 standard curve

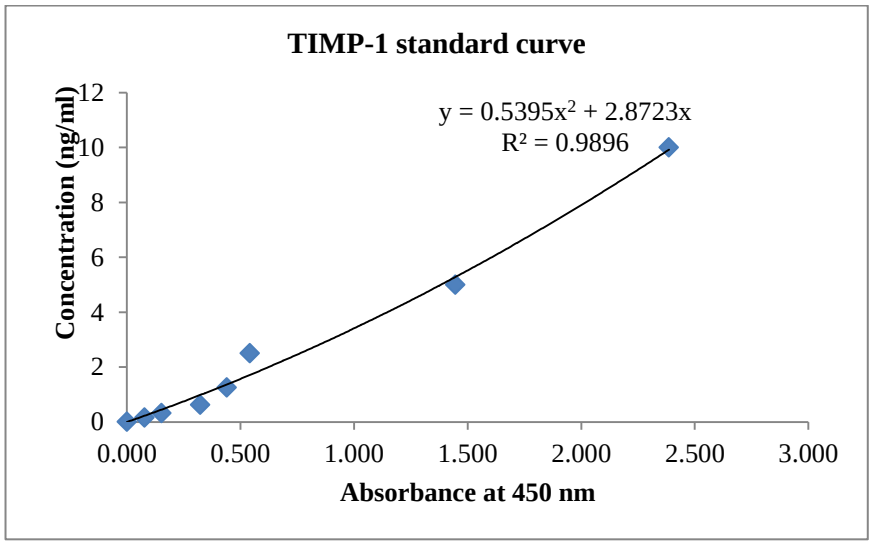

Appendix B 21: Tissue processing protocol

A. Dehydration:

50%Alcohol	-1 ½ hr
70% Alcohol	-1 ½ hr
80% Alcohol	-1 ½ hr
95% Alcohol	-1 ½ hr
100% Alcohol I	-1 ½ hr
100% Alcohol II	-1 ½ hr
100% Alcohol III	-1 ½ hr

B. Clearing:

Equal Alcohol and Toluene	-1/2 hr
Toluene	-Overnight

C. Infiltration and Impregnation:

Paraffin I	- 2 hr
Paraffin II	- 2 hr
Paraffin III	- 2 hr

Appendix B22: Preparation of hematoxylin and eosin stain

Reagents of hematoxylin

1. Pot or aluminium alum	6 gm
2. Mercuric oxide	1.25 gm
3. Hematoxylin	1.5 gm
4. Absolute alcohol	25 ml
5. Glacial Acetic acid	1 ml

Hematoxylin was dissolved in absolute alcohol, pot or aluminium alum was heated in 500 ml of distilled water until dissolved. Hematoxylin was added to mixture until boiled, then removed from heater and mercuric oxide was added. After it cooled, glacial acetic acid was added then filtered before use.

Reagents of ethyl eosin

1. Ethyl eosin	1 gm
2. Absolute alcohol	95 ml
3. Acetic acid	2 ml
4. Distilled water	5 ml

Mixed well and filtered before use.

Result

Fibrin – deep pink

Nucleus – blue to black

Appendix B23: Preparation of Masson's trichrome stain

Reagents

1. Lugol's Iodine

i. Iodine (1g).

ii. Potassium iodide (2 g).

iii. Distilled water (100 ml).

2. 5% sodium thiosulphate: 20 g of sodium thiosulphate dissolved in 400 ml distilled water.

3. Weigert iron hematoxylin

A. 10 g hematoxylin dissolved in 100 ml alcohol

B. 15 g ferric chloride dissolved in 100 ml distilled water

C. i) 10 ml from stock A mixed in 90 ml 95% alcohol

ii) 4 ml from stock B mixed with in 95 ml distilled water and 1 ml HCl

Equal part of solution (i) and (ii) were taken at time of use.

4. 1% acid alcohol: 99ml 70% OH mixed with 1 ml HCl pure.

5. 1% Ponceau fuschin: 4 g Ponceau fuschin dissolved in 400 ml of 1% acetic acid

6. 1% Phosphmolybdic acid: 4 g Phosphmolybdic acid dissolved in 400 ml distilled water.

7. 2% Light green: 8 g Light green dissolved in 400 ml 2% acetic acid.

8. 1% acetic acid: 1 ml acetic acid dissolved in 99 ml distilled water.

Result

Nucleus- blue to black

Fibrin- green

Appendix B24: Anti- TGF beta 1 antibody [2Ar2]. (ab64715).

abcam
discover more

Anti-TGF beta 1 antibody [2Ar2] (ab64715)

3 Abreviews | 5 References | 1 Image | URL for this product: http://www.abcam.com/TGF-beta-1-antibody-2Ar2-ab64715.html

Product overview

Description	Mouse monoclonal [2Ar2] to TGF beta 1
Host species	Mouse
Specificity	ab64715 neutralizes the biological activity of TGF beta 1 and TGF beta 1.2, (heterodimer of TGF beta 1 and TGF beta 2). In sandwich ELISA, less than 2% crossreactivity with TGF beta 3 and TGF beta 5 was observed and no crossreactivity was observed with other cytokines tested. With mouse RAW 264.7 cell lysates, a broad band is observed at ~45kD in Western Blot.
Tested applications	WB, ELISA, IHC-P, IHC-Fr, ICC, Neutralising, Flow Cyt
Cross reactivity	**Reacts with** Mouse, Rat, Human
Immunogen	Recombinant human TGF beta 1 and latent TGF beta 1 expressed from CHO cells.
Positive control	HT2 cells, RAW 264.7 cells, PC-3 cells

Target

Function	Multifunctional protein that controls proliferation, differentiation and other functions in many cell types. Many cells synthesize TGFB1 and have specific receptors for it. It positively and negatively regulates many other growth factors. It plays an important role in bone remodeling as it is a potent stimulator of osteoblastic bone formation, causing chemotaxis, proliferation and differentiation in committed osteoblasts.
Tissue specificity	Highly expressed in bone. Abundantly expressed in articular cartilage and chondrocytes and is increased in osteoarthritis (OA). Co-localizes with ASPN in chondrocytes within OA lesions of articular cartilage.
Involvement in disease	Defects in TGFB1 are the cause of Camurati-Engelmann disease (CE) [MIM:131300]; also known as progressive diaphyseal dysplasia 1 (DPD1). CE is an autosomal dominant disorder characterized by hyperostosis and sclerosis of the diaphyses of long bones. The disease typically presents in early childhood with pain, muscular weakness and waddling gait, and in some cases other features such as exophthalmos, facial paralysis, hearing difficulties and loss of vision.
Sequence similarities	Belongs to the TGF-beta family.
Post-translational modifications	Glycosylated. The precursor is cleaved into mature TGF-beta-1 and LAP, which remains non-covalently linked to mature TGF-beta-1 rendering it inactive.
Cellular localization	Secreted > extracellular space > extracellular matrix.

Target information above from: UniProt accession P01137 *The UniProt Consortium* ***The Universal Protein Resource (UniProt) in 2010*** Nucleic Acids Res. 38:D142-D148 (2010).

Alternative names	Camurati Engelmann disease antibody CED antibody Diaphyseal dysplasia 1 progressive antibody DPD1 antibody LAP antibody Latency-associated peptide antibody TGF beta 1 antibody TGF beta antibody TGF beta 1 protein antibody TGF-beta-1 antibody TGF-beta-5 antibody TGF-beta1 antibody TGFB antibody Tgfb-1 antibody TGFB1 antibody TGFB1_HUMAN antibody TGFbeta antibody TGFbeta1 antibody Transforming Growth Factor b1 antibody Transforming Growth Factor beta 1 antibody Transforming growth factor beta 1a antibody

Properties

Form	Liquid
Storage instructions	Store at -20ºC. Stable for 12 months at -20ºC
Storage buffer	Preservative: None Constituents: 5% Trehalose, 40% Glycerol, PBS, pH 7.2 See the website for more information on MSDS for this product.
Purity	Protein G purified
Clonality	Monoclonal
Clone number	2Ar2
Isotype	IgG1

Applications

WB	WB: Use a concentration of 1 - 2 µg/ml. Use under non reducing condition. Detects a band of approximately 45 kDa (predicted molecular weight: 45 kDa).(The detection limit for hTGF beta 1 is ~5ng/lane under non-reducing conditions.)
ELISA	ELISA: Use a concentration of 2 - 8 µg/ml.(Using 100µl/well will detect ~30-2000pg/ml)
IHC-P	IHC-P: Use a concentration of 8 - 25 µg/ml.Perform heat mediated antigen retrieval before commencing with IHC staining protocol.
IHC-Fr	IHC-Fr: Use a concentration of 8 - 25 µg/ml.
ICC	ICC: Use a concentration of 8 - 25 µg/ml.
Neutralising	Neut: Use a concentration of 0.3 - 1 µg/ml.(This dilution will neutralize 50% of the bioactivity due to 0.25ng/ml of rhTGF beta 1, using the HT2 cell line.)
Flow Cyt	Flow Cyt: Use a concentration of 25 µg/ml

Images (See the website for higher resolution images of this product)

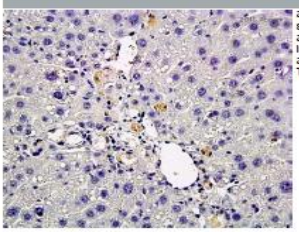

ab64715 staining TGF beta 1 in mouse liver tissue sections by IHC-P (Formaldehyde-fixed, Paraffin-embedded sections). Tissue samples were fixed with formaldehyde and blocked with 1% BSA for 30 minutes at 25ºC; antigen retrieval was by heat mediation in citrate buffer. The sample was incubated with primary antibody (1/50 in 1% BSA) at 4ºC for 12 hours. An undiluted HRP-conjugated polyclonal to mouse IgG was used as secondary antibody.
This image is courtesy of an Abreview submitted by Dr Robert Domitrovic

Appendix B25: Anti-alpha smooth muscle actin antibody- (ab5694)

abcam
discover more

Anti-alpha smooth muscle Actin antibody (ab5694)

63 Abreviews | 49 References | 9 Images | URL for this product: http://www.abcam.com/alpha-smooth-muscle-Actin-antibody-ab5694.html

Product overview

Description	Rabbit polyclonal to alpha smooth muscle Actin
Host species	Rabbit
Specificity	This antibody stains smooth muscle cells in vessel walls, gut wall, and myometrium. Myoepithelial cells in breast and salivary gland are also stained. It reacts with tumors arising from smooth muscles and myoepithelial cells. The other actins, such as beta- and gamma-cytoplasmic, striated muscle, and myocardium are not stained by this antibody.
Tested applications	IHC-FoFr, ICC, ICC/IF, WB, ELISA, IHC-P, IHC-Fr
Cross reactivity	**Reacts with** Mouse, Rat, Chicken, Guinea pig, Cow, Human, Pig
Immunogen	Synthetic peptide (Human) corresponding to N-terminus of smooth muscle alpha actin.

Target

Function	Actins are highly conserved proteins that are involved in various types of cell motility and are ubiquitously expressed in all eukaryotic cells.
Involvement in disease	Defects in ACTA2 are the cause of aortic aneurysm familial thoracic type 6 (AAT6) [MIM:611788]. AATs are characterized by permanent dilation of the thoracic aorta usually due to degenerative changes in the aortic wall. They are primarily associated with a characteristic histologic appearance known as 'medial necrosis' or 'Erdheim cystic medial necrosis' in which there is degeneration and fragmentation of elastic fibers, loss of smooth muscle cells, and an accumulation of basophilic ground substance.
Sequence similarities	Belongs to the actin family.
Cellular localization	Cytoplasm > cytoskeleton.

Target information above from: UniProt accession P62736 *The UniProt Consortium* ***The Universal Protein Resource (UniProt) in 2010*** *Nucleic Acids Res. 38:D142-D148 (2010).*

Alternative names

Alternative names

AAT6 antibody
ACTA_HUMAN antibody
ACTA2 antibody
Actin alpha 2 smooth muscle aorta antibody
Actin aortic smooth muscle antibody
Actin, aortic smooth muscle antibody
ACTSA antibody
ACTVS antibody
Alpha 2 actin antibody
Alpha actin 2 antibody
Alpha cardiac actin antibody
Alpha-actin 2 antibody
Alpha-actin-2 antibody
Cell growth inhibiting gene 46 protein antibody
Cell growth-inhibiting gene 46 protein antibody
Growth inhibiting gene 46 antibody

Storage instructions	Store at +4Â°C.
Storage buffer	Preservative: 0.02% Sodium Azide Constituents: PBS, pH 7.4 See the website for more information on MSDS for this product.
Purity	Immunogen affinity purified
Primary antibody notes	Actins are highly conserved proteins expressed in all eucaryotic cells. Actin filaments form part of the cytoskeleton and play essential roles in regulating cell shape and movement. Six distinct actin isotypes have been identified in mammalian cells. Each is encoded by a separated gene and is expressed in a developmentally regulated and tissue-specific manner, alpha and beta cytoplasmic actins are expressed in a wide variety of cells; whereas, expression of alpha skeletal, alpha cardiac, alpha vascular, and gamma enteric actins are more restricted to specialized muscle cell type. Smooth muscle alpha actin is of further interest because it is one of a few genes whose expression is relatively restricted to vascular smooth muscle cells. Further more, expression of smooth muscle alpha actin is regulated by hormones, cell proliferation , and altered by pathological conditions including oncogenic transformation and atherosclerosis.
Clonality	Polyclonal
Isotype	IgG

Applications

IHC-FoFr	IHC-FoFr: Use at an assay dependent dilution.
ICC	ICC: Use at an assay dependent concentration.
ICC/IF	ICC/IF: 1/100.
WB	WB: Use a concentration of 0.5 - 2.0 Âµg/ml.Predicted molecular weight: 42 kDa.
ELISA	ELISA: Use a concentration of 0.1 - 1.0 Âµg/ml.
IHC-P	IHC-P: 1/100 - 1/400. Perform heat mediated antigen retrieval before commencing with IHC staining protocol.
IHC-Fr	IHC-Fr: 1/200. (PubMed: 18559614Fix with acetone.)

Images (See the website for higher resolution images of this product)

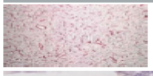

Human Leiomyoma stained with ab5694.

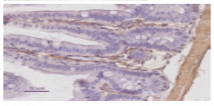

This picture shows formalin-fixed, paraffin embedded mouse intestine and mesentery, the optimal dilution is 1:1600 to 1:3200, incubation overnight at 4°C, counterstained with Hematoxylin.

This image was kindly supplied as part of the review by JQ Zhang.

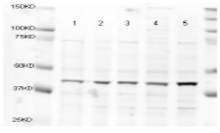

All lanes : Anti-alpha smooth muscle Actin antibody (ab5694) at 1 Âµg/ml

Lane 1 : HeLa Nuclear
Lane 2 : HeLa whole cell
Lane 3 : A431 cell lysate
Lane 4 : Jurkat cell lysate
Lane 5 : HEK293 cell lysate

Lysates/proteins at 20 Âµg per lane.

Secondary
Alexa Fluor anti-rabbit at 1/5000 dilution

Performed under reducing conditions.

Predicted band size : 42 kDa
Observed band size : 42 kDa
Additional bands at : 30 kDa,35 kDa,37 kDa,50 kDa,75 kDa. We are unsure as to the identity of these extra bands.

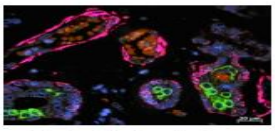

Please note that ab5694 does not appear to be specific to smooth muscle.

Ab5694 positively staining smooth muscle cells in blood vessels and myoepithelial cells in the frozen tissue of cancerous human mammary gland (pink) at 1/100 dilution. Secondary: CY5 conjugated goat anti rabbit (1/100). Co immunostaining of glandular cell cytokeratin can be seen stained by FITC (green). Auto fluorescent erythrocytes that are present within blood vessels are shown (red), whilst the DAPI counter stain may clearly be seen staining nuclei (blue).

This image is courtesy of an Abreview submitted by on **22 August 2005**. We do not have any further information relating to this image.

All lanes : Anti-alpha smooth muscle Actin antibody (ab5694) at 1/500 dilution

Lane 1 : Rat2 myofibroblasts (untreated before treatment-0 days)
Lane 2 : Rat2 myofibroblasts (untreated for 5 days)
Lane 3 : Rat2 myofibroblasts (treated with 1ng/mL TGF beta)
Lane 4 : Rat2 myofibroblasts (treated with 10ng/mL TGF beta)
Lane 5 : Positive control (NIH3T3)
Lane 6 : Negative control (MDA-MB-468 breast carcinoma cells)

Lysates/proteins at 10 Âµg per lane.

Secondary
Donkey anti rabbit (HRP) at 1/2500 dilution

Performed under reducing conditions.

Predicted band size : 42 kDa

This image is and edited version of an image submitted courtesy of an Abreview on **20 September 2005**. We do not have any further information relating to this image.

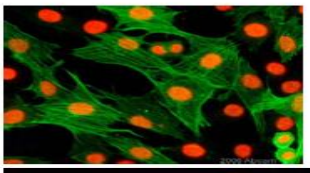

ab5694 at 1/500 staining rat myofibroblast cells by Immunocytochemistry/ Immunofluorescence. The cells were formaldehyde fixed and blocked with 5% serum prior to incubation with the antibody for 2 hours. A FITC conjugated goat anti-rabbit IgG was used as the secondary. Nuclei were counterstained with propidium iodide.

This image is courtesy of an Abreview submitted by Dr Jianyuan Chai

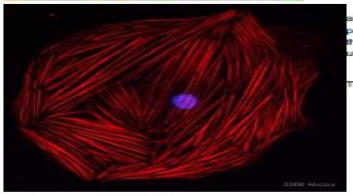

ab5694 staining human fetal heart cells by ICC/IF. Cells were fixed with PFA and permeabilized in 0.1% saponin prior to blocking in 10% serum for 45 minutes at 37°C. The primary antibody was diluted 1/400 and incubated with the sample for 1 hour at 37°C. A Alexa Fluor® 594 conjugated goat polyclonal to rabbit IgG (H+L), diluted 1/600 was used as secondary antibody.

This image is courtesy of an anonymous Abreview

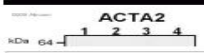

All lanes : Anti-alpha smooth muscle Actin antibody (ab5694) at 1/1000 dilution

Lane 1 : Lysates prepared from pig hear tissue from normal control animals

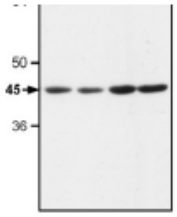

Lane 2 : Lysates prepared from pig hear tissue from normal control animals
Lane 3 : Lysates prepared from pig hear tissue from experimental animals
Lane 4 : Lysates prepared from pig hear tissue from experimental animals

Lysates/proteins at 4 Âµg per lane.

Secondary
HRP-conjugated goat polyclonal to rabbit IgG at 1/20000 dilution

Performed under reducing conditions.

Predicted band size : 42 kDa
Observed band size : 45 kDa (why is the actual band size different from the predicted?)

Exposure time : 1 minute

This image is a courtesy of Mario Torrado

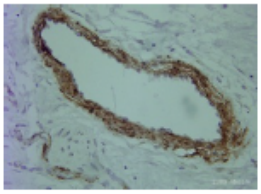

ab5694 staining alpha smooth muscle Actin in human skin tissue section by ImmunoHistochemistry (Formalin/PFA-fixed paraffin-embedded sections). Tissue underwent formaldehyde fixation before heat mediated antigen retrieval in Citrate pH 6.0 and then blocked with 10% serum for 1 hour at RT. The primary antibody was diluted 1/300 and incubated with sample in 2% serum for 15 hours at 4°C. A Biotin conjugated goat polyclonal to rabbit IgG was used at dilution at 1/500 as secondary antibody.

This image is courtesy of an anonymous Abreview

Our Abpromise to you: Quality guaranteed and expert technical support

If the product does not perform as described on this datasheet, we will offer a refund or replacement. For full details of the Abpromise, please visit http://www.abcam.com/abpromise or contact our technical team.

Appendix B26: Anti-PCNA [PC10] antibody ab29

Anti-PCNA [PC10] antibody ab29

47 Abreviews | 49 References | 13 Images

Overview

Product name	Anti-PCNA [PC10] antibody
Description	Mouse monoclonal [PC10] to PCNA
Specificity	This antibody is specific for PCNA p36 protein expressed at high levels in proliferating cells.
Tested applications	IHC-P, IP, WB, ICC/IF, IHC-Fr, Flow Cyt
Species reactivity	**Reacts with:** Mouse, Rat, Chicken, Human, Pig, Fruit fly (Drosophila melanogaster), Monkey, Zebrafish, Dogfish/Catshark, Thornback ray **Predicted to work with:** Cow
Immunogen	Protein A-rat PCNA (proliferating cell nuclear antigen) fusion obtained from pC2T
Positive control	WB: DT40 B lymphoma cell lysate, 293 cell lysate (see review), Hela, HEK293, A431 whole cell lysates. IHC-P: mouse hippocampus (see review), Normal human tonsil, developing chick brain. IHC-Fr: rat intestine. Flow Cyt: HeLa.

Properties

Form	Liquid
Storage instructions	Store at +4°C short term (1-2 weeks). Aliquot and store at -20°C or -80°C. Avoid repeated freeze / thaw cycles.
Storage buffer	Preservative: 0.02% Sodium Azide Constituents: PBS
Purity	IgG fraction
Clonality	Monoclonal
Clone number	PC10
Myeloma	Sp2/0-Ag14
Isotype	IgG2a
Light chain type	kappa
Research Areas	Cell Biology → Cell Cycle → Markers Epigenetics and Nuclear Signaling → DNA methylation → Methylated DNA Binding Tags & Cell Markers → Cell Type Markers → Replication Epigenetics and Nuclear Signaling → DNA / RNA → DNA Synthesis → Other Epigenetics and Nuclear Signaling → Chromatin Binding Proteins → DNA / RNA binding Cancer → Cell cycle → Cell division Cancer → Tumor biomarkers → Tumor antigens

Product Datasheet

weight: 29 kDa).

ICC/IF	ICC/IF: Use a concentration of 0.5 - 1 µg/ml. Methanol fixation recommended
IHC-Fr	IHC-Fr: Use at an assay dependent concentration.
Flow Cyt	Flow Cyt: Use 1µg for 10^6 cells.

Target

Function	This protein is an auxiliary protein of DNA polymerase delta and is involved in the control of eukaryotic DNA replication by increasing the polymerase's processibility during elongation of the leading strand. Induces a robust stimulatory effect on the 3'-5' exonuclease and 3'-phosphodiesterase, but not apurinic-apyrimidinic (AP) endonuclease, APEX2 activities. Has to be loaded onto DNA in order to be able to stimulate APEX2.
Sequence similarities	Belongs to the PCNA family.
Post-translational modifications	Upon methyl methanesulfonate-induced DNA damage, mono-ubiquitinated by the UBE2B-RAD18 complex on Lys-164. This induces non-canonical polyubiquitination on Lys-164 through 'Lys-63' linkage of ubiquitin moieties by the E2 complex UBE2N-UBE2V2 and the E3 ligases, HLTF, RNF8 and SHPRH, which is required for DNA repair. 'Lys-63' polyubiquitination prevents genomic instability on DNA damage. Monoubiquitination at Lys-164 also takes place in undamaged proliferating cells, and is mediated by the DCX(DTL) complex, leading to enhance PCNA-dependent translesion DNA synthesis. Acetylated in response to UV irradiation. Acetylation disrupts interaction with NUDT15 and promotes degradation.
Cellular localization	Nucleus. Forms nuclear foci representing sites of ongoing DNA replication and vary in morphology and number during S phase. Together with APEX2, is redistributed in discrete nuclear foci in presence of oxidative DNA damaging agents.

Target information above from: UniProt accession P12004

The UniProt Consortium

The Universal Protein Resource (UniProt) in 2010

Nucleic Acids Res. 38:D142-D148 (2010) .

Database links

- Entrez Gene: 373984 Chicken
- Entrez Gene: 515499 Cow
- Entrez Gene: 37290 Fruit fly (Drosophila melanogaster)
- Entrez Gene: 5111 Human
- Entrez Gene: 18538 Mouse
- Entrez Gene: 25737 Rat
- Entrez Gene: 30678 Zebrafish
- Omim: 176740 Human
- SwissProt: Q9DEA3 Chicken
- SwissProt: Q3ZBW4 Cow
- SwissProt: P17917 Fruit fly (Drosophila melanogaster)
- SwissProt: P12004 Human
- SwissProt: P17918 Mouse
- SwissProt: P04961 Rat
- SwissProt: Q9PTP1 Zebrafish
- Unigene: 4751 Fruit fly (Drosophila melanogaster)
- Unigene: 147433 Human
- Unigene: 728886 Human
- Unigene: 7141 Mouse
- Unigene: 223 Rat
- Unigene: 35605 Zebrafish

Alternative names

Cyclin antibody
DNA polymerase delta auxiliary protein antibody
HGCN8729 antibody
MGC8367 antibody
Mutagen-sensitive 209 protein antibody
OTTHUMP00000030189 antibody

Product **Datasheet**

OTTHUMP00000030190 antibody
PCNA antibody
Pcna/cyclin antibody
PCNA_HUMAN antibody
PCNAR antibody
Polymerase delta accessory protein antibody
Proliferating Cell Nuclear Antigen antibody

Anti-PCNA [PC10] antibody images

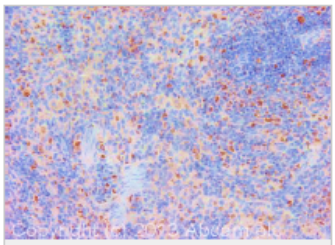

Immunohistochemistry (Formalin/PFA-fixed paraffin-embedded sections) - Anti-PCNA [PC10] antibody (ab29)

IHC image of PCNA staining in rat spleen formalin fixed paraffin embedded tissue section, performed on a Leica Bond system using the standard protocol F. The section was pre-treated using heat mediated antigen retrieval with sodium citrate buffer (pH6, epitope retrieval solution 1) for 20 mins. The section was then incubated with ab29, 1/30,000 dilution for 15 mins at room temperature and detected using an HRP conjugated compact polymer system. DAB was used as the chromogen. The section was then counterstained with haematoxylin and mounted with DPX.

For other IHC staining systems (automated and non-automated) customers should optimize variable parameters such as antigen retrieval conditions, primary antibody concentration and antibody incubation times.

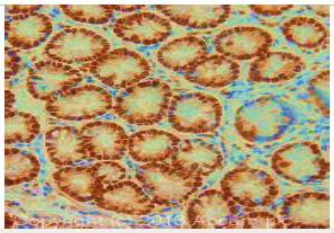

Immunohistochemistry (Formalin/PFA-fixed paraffin-embedded sections) - Anti-PCNA antibody [PC10] - Proliferation Marker (ab29)

IHC image of PCNA staining in rat large intestine formalin fixed paraffin embedded tissue section, performed on a Leica Bond system using the standard protocol F. The section was pre-treated using heat mediated antigen retrieval with sodium citrate buffer (pH6, epitope retrieval solution 1) for 20 mins. The section was then incubated with ab29, 0.025µg/ml, for 15 mins at room temperature and detected using an HRP conjugated compact polymer system. DAB was used as the chromogen. The section was then counterstained with haematoxylin and mounted with DPX.

For other IHC staining systems (automated and non-automated) customers should optimize variable parameters such as antigen retrieval conditions, primary antibody concentration and antibody incubation times.

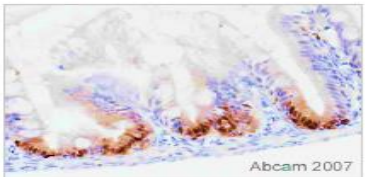

Immunohistochemistry (Frozen sections) - PCNA antibody [PC10] - Proliferation Marker (ab29)
Carl Hobbs, CARD, KCL, UK

Mouse monoclonal [PC10] to PCNA - Proliferation Marker (ab29) used in immunohistochemistry (Formalin/PFA-fixed paraffin-embedded sections;1/6000 for 2h at RT) on intestine of adult Zebra fish). Antigen retrieval step: Heat mediated. Blocking step: 1% BSA for 10 mins at RT. Incubation time: Secondary Antibody: Biotin conjugated goat anti mouse Igs (1/200). NB: The crypt nuclei on this image of zebrafish intestine, are positive for the PCNA/PC10 clone conforming to accepted localisation data for PCNA in other species.

Product **Datasheet**

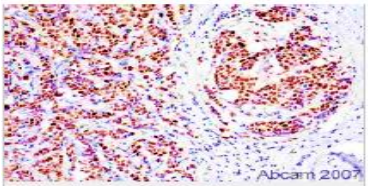

Immunohistochemistry (Formalin/PFA-fixed paraffin-embedded sections) - PCNA antibody [PC10] - Proliferation Marker (ab29)
Carl Hobbs, CARD, KCL, UK

Mouse monoclonal [PC10] to PCNA - Proliferation Marker (ab29) used in immunohistochemistry (Formalin/PFA-fixed paraffin-embedded sections; 1/6000 for 2h at RT) on Human Tissue sections (Paget's disease of the nipple). Antigen retrieval step: Heat mediated. Blocking step: 1% BSA for 10 mins at RT. Incubation time: Secondary Antibody: Biotin conjugated goat anti mouse Igs (1/200).

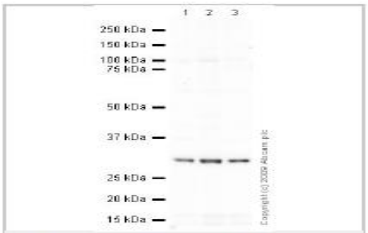

Western blot - PCNA antibody [PC10] - Proliferation Marker (ab29)

All lanes : Anti-PCNA [PC10] antibody (ab29) at 5 µg/ml

Lane 1 : HeLa (Human epithelial carcinoma cell line) Whole Cell Lysate
Lane 2 : HEK293 (Human embryonic kidney cell line) Whole Cell Lysate
Lane 3 : A431 (Human epithelial carcinoma cell line) Whole Cell Lysate

Lysates/proteins at 10 µg per lane.

Secondary
Goat polyclonal to Mouse IgG - H&L - Pre-Adsorbed (HRP) at 1/3000 dilution

Performed under reducing conditions.

Predicted band size : 29 kDa
Observed band size : 29 kDa

Exposure time : 4 minutes

Product **Datasheet**

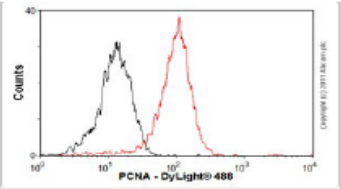

Flow Cytometry - Anti-PCNA antibody [PC10] - Proliferation Marker (ab29)

Overlay histogram showing HeLa cells stained with ab29 (red line). The cells were fixed with 80% methanol (5 min) and then permeabilized with 0.1% PBS-Tween for 20 min. The cells were then incubated in 1x PBS / 10% normal goat serum / 0.3M glycine to block non-specific protein-protein interactions followed by the antibody (ab29, 1µg/1x10^6 cells) for 30 min at 22ºC. The secondary antibody used was DyLight® 488 goat anti-mouse IgG (H+L) (ab96879) at 1/500 dilution for 30 min at 22ºC. Isotype control antibody (black line) was mouse IgG2a [ICIGG2A] (ab91361, 2µg/1x10^6 cells) used under the same conditions. Acquisition of >5,000 events was performed.

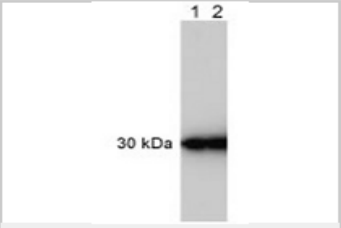

Western blot - PCNA antibody [PC10] - Proliferation Marker (ab29)
Taken from an Abreview submitted by Javier di Noia

All lanes : Anti-PCNA [PC10] antibody (ab29) at 1/5000 dilution

Lane 1 : Human 293 total cell extract
Lane 2 : Chicken DT40 total cell extract

Performed under reducing conditions.

Predicted band size : 29 kDa
Observed band size : 30 kDa

Exposure time : 5 seconds
Taken from an Abreview submitted by Javier di Noia

Blocking for 2 hours in 5% milk. Primary antibody incubated for 1 hour.

Immunoprecipitation - PCNA antibody [PC10] - Proliferation Marker (ab29)
This Image is courtesy of an anonymous Abreview

ab29 at a 1/500 dilution used in immunoprecipitation.

Lane 1: Beads only + HeLa whole cell lysate

Lane 2: Beads only + SupT1 whole cell lysate

Lane 3: Beads + ab29 + HeLa whole cell lysate

Lane 4: Beads + ab29 + SupT1 whole cell lysate

A 50KDa band is precipitated which is IgG heavy chain whilst the 30kDa band is PCNA.

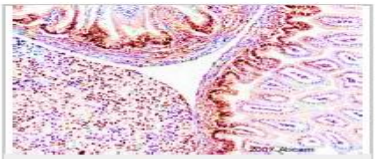

Immunohistochemistry (Formalin/PFA-fixed paraffin-embedded sections) - PCNA antibody [PC10] - Proliferation Marker (ab29)
This Image is courtesy of an Abreview submitted by Mr Carl Hobbs

ab29 at 1/6000 staining mouse embryo (day 17) liver and gut tissue sections by IHC-P. The tissue was formaldehyde fixed and a heat mediated antigen retrieval step in Tris buffer was performed. The tissue was blocked before incubation with the antibody for 2 hours. A biotinylated goat polyclonal antibody was used as the secondary.

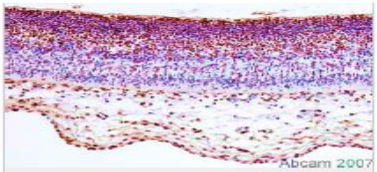

Immunohistochemistry (Formalin/PFA-fixed paraffin-embedded sections) - PCNA antibody [PC10] - Proliferation Marker (ab29)
Carl Hobbs, CARD, KCL, UK

Mouse monoclonal [PC10] to PCNA - Proliferation Marker (ab29) used in immunohistochemistry (Formalin/PFA-fixed paraffin-embedded sections; 1/6000 for 2h at RT) on E6 developing chick brain). Antigen retrieval step: Heat mediated. Blocking step: 1% BSA for 10 mins at RT. Incubation time: Secondary Antibody: Biotin conjugated goat anti mouse Igs (1/200). NB: This image shows developing brain/overlying skin.

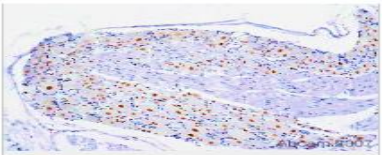

Immunohistochemistry (Formalin/PFA-fixed paraffin-embedded sections) - PCNA antibody [PC10] - Proliferation Marker (ab29)
Carl Hobbs, CARD, KCL, London, UK

Immunohistochemistical staining (Formaldehyde/PFA-fixed paraffin-embedded sections) for PCNA antibody [PC10] - Proliferation Marker (ab29) on Rat Tissue sections (adult spinal cord DRG). Antigen retrieval step: Heat mediated. Blocking step: 1% BSA for 10 mins at RT. Primary Antibody used at 1/6000 for 2 minutes at RT. Secondary Antibody: Biotin labelled goat anti mouse Igs (1/200).

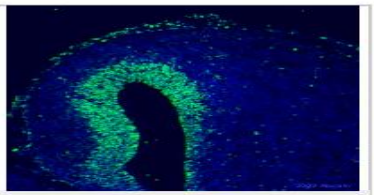

Immunohistochemistry (Frozen sections) - PCNA antibody [PC10] - Proliferation Marker (ab29)
This Image is a courtesy of Anonymous Abreview

ab29 staining PCNAin mouse embryonic brain tissue section by Immunohistochemistry (Frozen sections). Tissue samples were fixed with paraformaldehyde and permeabilized with 0.1% PBS-Tween before blocking with 5% BSAfor 1 hour at 22^{0}C. The sample was incubated with primary antibody (1/500) in 5% BSAin 0.3% PBS-Triton-X100 for 14 hours at 22^{0}C. An Alexa Fluor$^{®}$488-conjugated Goat polyclonal to mouse IgG was used as secondary antibody at 1/500 dilution.

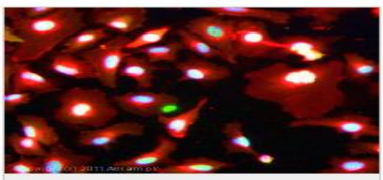

Immunocytochemistry/ Immunofluorescence - PCNA antibody [PC10] - Proliferation Marker (ab29)

ICC/IF image of ab29 stained HeLa cells. The cells were 100% methanol fixed (5 min) and then incubated in 1%BSA / 10% normal goat serum / 0.3M glycine in 0.1% PBS-Tween for 1h to permeabilise the cells and block non-specific protein-protein interactions. The cells were then incubated with the antibody (ab29, 5µg/ml) overnight at +4°C. The secondary antibody (green) was DyLight® 488 goat anti-mouse IgG - H&L, pre-adsorbed (ab96879) used at a 1/250 dilution for 1h. Alexa Fluor® 594 WGA was used to label plasma membranes (red) at a 1/200 dilution for 1h. DAPI was used to stain the cell nuclei (blue) at a concentration of 1.43µM.

Our Abpromise to you: Quality guaranteed and expert technical support

As standard

- Replacement or refund for products not performing as stated on the datasheet
- Valid for 12 months from date of delivery**
- Response to your inquiry within 24 hours

In addition

- We provide support in Chinese, English, French, German, Japanese and Spanish
- Extensive multi-media technical resources to help you
- We investigate all quality concerns to ensure our products perform to the highest standards

If the product does not perform as described on this datasheet, we will offer a refund or replacement. For full details of the Abpromise, please visit http://www.abcam.com/abpromise or contact our technical team.

Terms and conditions

- Guarantee only valid for products bought direct from Abcam or one of our authorized distributors
- **Regional variations to our Abpromise may apply to the following countries: China, Korea, Singapore, Malaysia, Taiwan and Thailand, which operate a 120 day guarantee. Please contact your regional office for further details
- Antibodies tested only in recombinant samples are not covered for use on endogenous samples. Please check the datasheet for information on tested species
- "Predicted to react" information on datasheets is based on sequence homology and provided for reference only
- "Predicted to react" species are not guaranteed, as they have not been tested
- Fast Track products are not covered under the Abpromise. Please see Fast Track terms and condition for additional information
- Abcam biochemicals are novel compounds and we have not tested their biological activity in house. Please use the literature to identify how to use these products effectively. If you require further assistance please contact the scientific support team

abcam®
discover more

Cambridge Office
Abcam plc
330 Cambridge Science Park Cambridge CB4 0FL UK
Tel: +44 (0)1223 696000
Fax: +44 (0)1223 215 215
Email: orders@abcam.com

Boston Office
Abcam Inc.
1 Kendall Square, Suite B2304 Cambridge, MA 02139-1517 USA
Tel: (888) 77-ABCAM (22226)
Fax: (877) 774-8286
These numbers are toll free in the US/Canada
Email: us.orders@abcam.com

Appendix B27: (MTT) assay

Reagents

3-(4, 5-Dimethyl-2-thiazolyl)-2,3-diphenyl-2H-tetrazolium bromide (MTT) reagent

RPMI media

Preparation of reagents

1- 5 mg / ml MTT reagent prepared in PBS and filtered through sterilized filter 0.22 µm.
2- RPMI media reconstitute with 10% (v/v) Fetal bovine serum (FBS).

Appendix B28: Preparation of Ethidium Bromide and Acridine Orange (EB/AO) stain

Reagents:

1 µl Acridine Orange Stock (5 mg/ml)

1 µl Ethidium Bromide Stock (3 mg/ml)

1 ml PBS

Method

AO-EB Working Solution

1) Add AO and EB to PBS and mix well.

2) Store at room temperature for up to 2 weeks.

To use

1) Dilute cells with equal volume of AO-EB working solution.

2) Immediately look at cells under fluorescence microscope.

Results

Red Cells = Dead

Green Cells = Live

BioVision rev. 04/11

For research use only

Caspase-3/CPP32 Colorimetric Assay Kit

(Catalog #K106-25, -100, -200, -400; Store kit at –20°C)

I. Introduction:

Activation of ICE-family proteases/caspases initiates apoptosis in mammalian cells. The **Caspase-3/CPP32 Colorimetric Assay Kit** provides a simple and convenient means for assaying the activity of caspases that recognize the sequence DEVD. The assay is based on spectrophotometric detection of the chromophore *p*-nitroaniline (*p*NA) after cleavage from the labeled substrate DEVD-*p*NA. The *p*NA light emission can be quantified using a spectrophotometer or a microtiter plate reader at 400- or 405-nm. Comparison of the absorbance of *p*NA from an apoptotic sample with an uninduced control allows determination of the fold increase in CPP32 activity.

II. Kit Contents:

Components	K106-25 25 assays	K106-100 100 assays	K106-200 200 assays	K106-400 400 assays	Part Number
Cell Lysis Buffer	25 ml	100 ml	100 ml	100 ml	K106-XX(X)-1
2X Reaction Buffer	2 ml	4 x 2 ml	16 ml	32 ml	K106-XX(X)-2
DEVD-*p*NA (4 mM)	125 µl	0.5 ml	2 x 0.5 ml	2 x 1 ml	K106-XX(X)-3
DTT (1 M)	100 µl	0.4 ml	0.4 ml	0.4 ml	K106-XX(X)-4
Dilution Buffer	25 ml	100 ml	200 ml	400 ml	K106-XX(X)-5

III. Caspase-3 Assay Protocol:

A. General Considerations

- Aliquot enough 2X Reaction Buffer for the number of assays to be performed. Add DTT to the 2X Reaction Buffer immediately before use (10 mM final concentration: add 10 µl of 1.0 M DTT stock per 1 ml of 2X Reaction Buffer).
- Protect DEVD-*p*NA from light.

B. Assay Procedure

1. Induce apoptosis in cells by desired method. Concurrently incubate a control culture *without* induction.
2. Count cells and pellet 1-5 x 10^6 cells.
3. Resuspend cells in 50 µl of chilled Cell Lysis Buffer and incubate cells on ice for 10 minutes.
4. Centrifuge for 1 min in a microcentrifuge (10,000 x g).
5. Transfer supernatant (cytosolic extract) to a fresh tube and put on ice for immediate assay or aliquot and store at –80°C for future use.
6. Assay protein concentration.
7. Dilute 50-200 µg protein to 50 µl Cell Lysis Buffer for each assay.
8. Add 50 µl of 2X Reaction Buffer (containing 10 mM DTT) to each sample.
9. Add 5 µl of the 4 mM DEVD-*p*NA substrate (200 µM final conc.) and incubate at 37°C for 1-2 hour.
10. Read samples at 400- or 405-nm in a microtiter plate reader, or spectrophotometer using a 100-µl micro quartz cuvette (Sigma), or dilute sample to 1 ml with Dilution Buffer and using regular cuvette (note: Dilution of the samples proportionally decreases the reading).

    You may also perform the entire assay directly in a 96-well plate.

    Fold-increase in CPP32 activity can be determined by comparing these results with the level of the uninduced control.

    Note: Background reading from cell lysates and buffers should be subtracted from the readings of both induced and the uninduced samples before calculating fold increase in CPP32 activity.

IV. Storage and Stability:

Store kit at –20°C (Store Lysis Buffer, Reaction Buffer, and Dilution Buffer at 4°C after opening). All reagents are stable for at least 6 months under proper storage conditions.

VI. Related Products:

Apoptosis Detection Kits & Reagents
- Annexin V Kits & Bulk Reagents
- Caspase Assay Kits & Reagents
- Mitochondrial Apoptosis Kits & Reagents
- Nuclear Apoptosis Kits & Reagents
- Apoptosis Inducers and Set

Cell Fractionation System
- Mitochondria/Cytosol Fractionation Kit
- Nuclear/Cytosol Fractionation Kit
- Membrane Protein Extraction Kit
- Cytosol/Particulate Rapid Separation Kit
- Mammalian Cell Extraction Kit
- FractionPREP Fractionation System

Cell Proliferation & Senescence
- Quick Cell Proliferation Assay Kit
- Senescence Detection Kit
- High Throughput Apoptosis/Cell Viability Assay Kits
- LDH-Cytotoxicity Assay Kit
- Bioluminescence Cytotoxicity Assay Kit
- Live/Dead Cell Staining Kit

Cell Damage & Repair
- HDAC & HAT Fluorometric & Colorimetric Assays & Drug Discovery Kits
- DNA Damage Quantification Kit
- Glutathione, GST, & Nitric Oxide Fluorometric & Colorimetric Assay Kits

Signal Transduction
- cAMP & cGMP Assay Kits
- Akt & JNK Activity Assay Kits
- Beta-Secretase Activity Assay Kit

Adiponectin & Lipid Transfer
- Recombinant Adiponectin, Survivin, & Leptin

Page 1

Appendix B30: LDH Assay Kit (Item No. 10008882 Cayman)

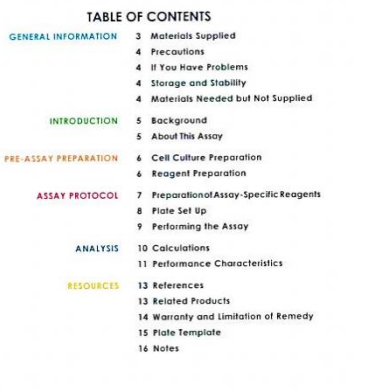

TABLE OF CONTENTS

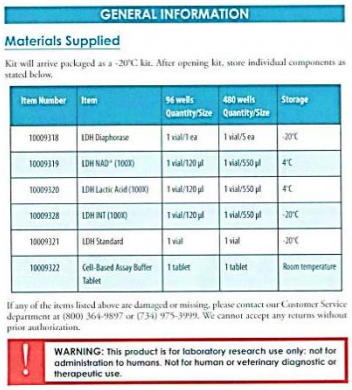

GENERAL INFORMATION

Materials Supplied

Kit will arrive packaged as a -20°C kit. After opening kit, store individual components as stated below.

Item Number	Item	96 wells Quantity/Size	480 wells Quantity/Size	Storage
10009318	LDH Diaphorase	1 vial/1 ea	1 vial/5 ea	-20°C
10009319	LDH NAD+ (100X)	1 vial/120 µl	1 vial/550 µl	4°C
10009320	LDH Lactic Acid (100X)	1 vial/120 µl	1 vial/550 µl	4°C
10009328	LDH INT (100X)	1 vial/120 µl	1 vial/550 µl	-20°C
10009321	LDH Standard	1 vial	1 vial	-20°C
10009322	Cell-Based Assay Buffer Tablet	1 tablet	1 tablet	Room temperature

If any of the items listed above are damaged or missing, please contact our Customer Service department at (800) 364-9897 or (734) 975-3999. We cannot accept any returns without prior authorization.

WARNING: This product is for laboratory research use only; not for administration to humans. Not for human or veterinary diagnostic or therapeutic use.

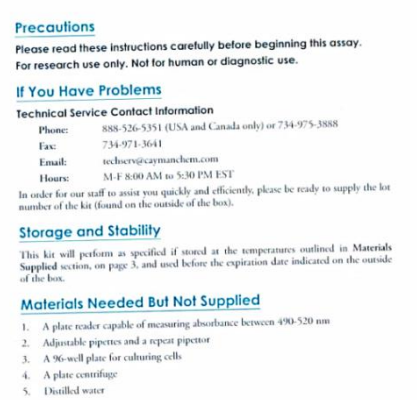

Precautions

Please read these instructions carefully before beginning this assay.
For research use only. Not for human or diagnostic use.

If You Have Problems

Technical Service Contact Information

Phone: 888-526-5351 (USA and Canada only) or 734-975-3888
Fax: 734-971-3641
Email: techserv@caymanchem.com
Hours: M-F 8:00 AM to 5:30 PM EST

In order for our staff to assist you quickly and efficiently, please be ready to supply the lot number of the kit (found on the outside of the box).

Storage and Stability

This kit will perform as specified if stored at the temperatures outlined in **Materials Supplied** section, on page 3, and used before the expiration date indicated on the outside of the box.

Materials Needed But Not Supplied

1. A plate reader capable of measuring absorbance between 490-520 nm
2. Adjustable pipettes and a repeat pipettor
3. A 96-well plate for culturing cells
4. A plate centrifuge
5. Distilled water

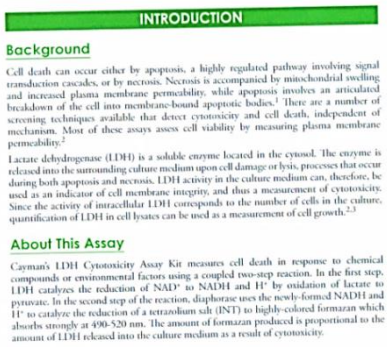

INTRODUCTION

Background

Cell death can occur either by apoptosis, a highly regulated pathway involving signal transduction cascades, or by necrosis. Necrosis is accompanied by mitochondrial swelling and increased plasma membrane permeability, while apoptosis involves an articulated breakdown of the cell into membrane-bound apoptotic bodies.[1] There are a number of screening techniques available that detect cytotoxicity and cell death, independent of mechanism. Most of these assays assess cell viability by measuring plasma membrane permeability.[2]

Lactate dehydrogenase (LDH) is a soluble enzyme located in the cytosol. The enzyme is released into the surrounding culture medium upon cell damage or lysis, processes that occur during both apoptosis and necrosis. LDH activity in the culture medium can, therefore, be used as an indicator of cell membrane integrity, and thus a measurement of cytotoxicity. Since the activity of intracellular LDH corresponds to the number of cells in the culture, quantification of LDH in cell lysates can be used as a measurement of cell growth.[2,3]

About This Assay

Cayman's LDH Cytotoxicity Assay Kit measures cell death in response to chemical compounds or environmental factors using a coupled two-step reaction. In the first step, LDH catalyzes the reduction of NAD^+ to NADH and H^+ by oxidation of lactate to pyruvate. In the second step of the reaction, diaphorase uses the newly-formed NADH and H^+ to catalyze the reduction of a tetrazolium salt (INT) to highly-colored formazan which absorbs strongly at 490-520 nm. The amount of formazan produced is proportional to the amount of LDH released into the culture medium as a result of cytotoxicity.

PRE-ASSAY PREPARATION

Cell Culture Preparation

1. Seed cells in a 96-well plate at a density of 10^4-10^5 cells/well in 120 µl of culture medium without components to be tested. We recommend that each treatment be performed in triplicate.
2. Culture the cells in a CO_2 incubator at 37°C for 24-48 hours.

Reagent Preparation

Some of the kit components are in lyophilized or concentrated form and need to be reconstituted or diluted prior to use. Follow the directions carefully to ensure proper volumes of LDH Assay Buffer are used to reconstitute or dilute the vial components.

1. **Assay Buffer Preparation**

Dissolve the Cell Based Assay Buffer Tablet (Item No. 10009322) in 100 ml of distilled water. This buffer should be stable for approximately one year at room temperature.

2. **LDH Diaphorase**

1 ea vial LDH Diaphorase (96-well kit; Item No. 10009318): Reconstitute with 550 µl Assay Buffer.

OR

5 ea vial LDH Diaphorase (480-well kit; Item No. 10009318): Reconstitute with 600 µl Assay Buffer.

Keep on ice during use. Store at -20°C when not in use. Freezing and thawing of the solution should be limited to a single time. If you plan to use this solution in multiple experiments, we recommend that you aliquot it for storage at -20°C.

3. **LDH Reaction Solution**

To make 10 ml of Reaction Solution, sufficient for use on one 96-well plate, add 110 µl of the following to 9.6 ml of the Assay Buffer:

% LDH (100X) (Item No. 10009319)
Lactic Acid (100X) (Item No. 10009320)
INT (100X) (Item No. 10009328)
Reconstituted Diaphorase (prepared in Step 2)

ASSAY PROTOCOL

Preparation of Assay-Specific Reagents

NOTE: Read entire assay AND remove LDH and other well samples with the media of the assay. We recommend that you use culture medium containing a low percentage of FBS (such as 1%) or serum free culture medium for the assay. If the culture medium containing a high percentage of FBS (such as 10%) is used with containing this same medium should be included in the assay as a control.

LDH Standard

Immediately prior to use, reconstitute the contents of the LDH Standard (Item No. 10009321) in 0.6 ml of Assay Buffer. The standard should be kept on ice during use. The standard is unstable, and degrades rapidly at room temperature. If you plan to use the standard in multiple experiments, we recommend that you aliquot the reconstituted solution and store at -20°C. The reconstituted standard should be frozen and thawed only once. Do not freeze, use gently.

To prepare the standard for use in the LDH assay, obtain six clean test tubes and label them #1 through #6. Aliquot 175 µl of culture medium into tubes #1 and 250 µl into tubes #2-#6. Transfer 25 µl of the reconstituted LDH standard into tube #1 and mix thoroughly. The concentration of this standard, the first point on the standard curve, is 10 mU/well (100 mU/ml). Serially dilute the standard by removing 250 µl from tube #1 and place into tube #2 and mix thoroughly. Next, remove 250 µl from tube #2 and place into tube #3, mix thoroughly. Repeat this procedure for tubes #4 and #5. Do not add any standard to tube #6; this tube will be your blank.

NOTE: 1 U/ml = 1/3 the amount of LDH that catalyzes the reduction of 1 µmol of substrate per minute.

Plate Set Up

Each plate should contain a standard curve, wells without cells, and wells containing cells with experimental treatment or vehicle. We recommend that standards be run in duplicate and that each treatment be performed in triplicate. A suggested plate format is shown below in Figure 1. The user may vary the location and type of wells present as necessary for each particular experiment. We suggest that you record the contents of each well on the template sheet provided (see page 15).

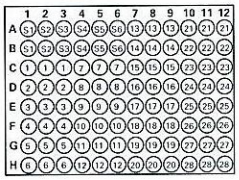

S1-S6 - Standards 1-6
1-28 - Samples

Figure 1. Sample plate format

Performing the Assay

Pipetting Hints

- It is recommended that a repeating pipettor be used to deliver reagents to the wells. This saves time and helps to maintain more precise incubation times.
- Before pipetting each reagent, equilibrate the pipette tip in that reagent (*i.e.*, slowly fill the tip and gently expel the contents, repeat several times).
- Do not expose the pipette tip to the reagent(s) already in the well.

NOTE: If you anticipate a high rate of cell death and you are planning to use the LDH Standard to calculate the level of cytotoxicity, serial dilution of your samples may be required to obtain values that fall on the standard curve.

Procedure

1. Centrifuge the 96-well tissue culture plate at 400 x g for five minutes.
2. Using a new 96-well plate, transfer 100 µl of the standards prepared above into the appropriate wells. We recommend that the standards be run in duplicate.
3. Transfer 100 µl of each supernatant from each well of the cultured cells to corresponding wells on the new plate.
4. Add 100 µl of Reaction Solution (prepared in Step 3) to each well using a repeating pipettor.
5. Incubate the plate with gentle shaking on an orbital shaker for 30 minutes at room temperature.
6. Read the absorbance at 490 nm with a plate reader.

ANALYSIS

Calculations

Subtract the Blanks

Average the absorbance value of the wells containing assay buffer medium only (standard #6) and subtract this from the absorbance values of all the other wells.

Plot the Standard Curve

Make a plot of absorbance at 490 nm as a function of LDH concentration and determine the equation of the line. See figure 2, on page 11, for a typical standard curve.

Determine the Sample Concentration

Determination of LDH activity present in the sample

$$\text{LDH Activity (µU)} = \frac{(A_{490\text{ nm}} - \text{y-intercept})}{\text{slope}}$$

$$\text{Total LDH Activity (µU/ml) in sample} = \frac{\text{Value from LDH activity assay (µU)}}{\text{x sample volume assayed (usually 0.1 ml)}}$$

Sensitivity:

The assay can detect as few as 10^3 cells, depending on cell type.

Performance Characteristics

Sample Data

The standard curve presented here is an example of the data typically produced in culture medium RPMI 1640 without FBS. However, your results will not be identical to these. You **must** run a new standard curve with each experiment.

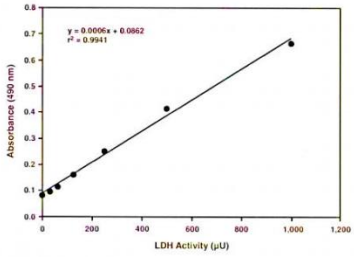

Figure 2. Typical standard curve
LDH standard was dissolved in 100 µl of RPMI 1640 without FBS. 100 µl of the reaction solution was then added to each well and incubated at room temperature for 30 minutes.

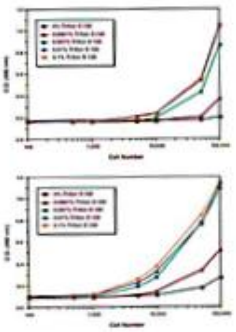

Figure 3. Release of cellular LDH by Triton X-100
Raw 264.7 cells (top panel, adherent cells) or Jurkat cells (bottom panel, suspension cells) were seeded in a 96-well plate in 100 µl of culture medium without FBS at the density indicated on the chart. The cells were incubated at 37°C in a CO_2 cell culture incubator. After several hours of incubation, the cells were treated with 0%, 0.0001%, 0.001%, 0.01%, and 0.1% of Triton X-100 and gently shaken for 10 minutes on an orbital shaker at room temperature. Samples were assayed according to the protocol described in **Performing the Assay** on page 9.

RESOURCES

References

1. Bonfoco, E., Krainc, D., Ankarcrona, M., *et al.* Apoptosis and necrosis: Two distinct events induced, respectively, by mild and intense insults with N-methyl-D-aspartate or nitric oxide/superoxide in cortical cell cultures. *Proc. Natl. Acad. Sci. USA* **92**, 7162-7166 (1995).
2. Horkan, C., Wyatt, D., and Kinos, D.A. Estimating the number of viable animal cells in multi-well cultures based on their lactate dehydrogenase activities. *Cytotechnology* **32**, 63-75 (2000).
3. Wiskerbeck, H.Th. and van der Meer, J.A.M. Optimization, application, and interpretation of lactate dehydrogenase measurements in microwell determination of cell number and toxicity. *ASSAY and Drug Development Technologies* **3(6)**, 675-682 (2005).

Related Products

Apoptosis Blebs Assay Kit - Item No. 10010736
Caspase-3 Fluorescence Assay Kit - Item No. 10009135
Cholesterol Cell-Based Detection Assay Kit - Item No. 10009779
Cytochrome *c* Cell-Based Detection Kit (Blue Fluorescence) - Item No. 600360
Glycolysis Cell-Based Assay Kit - Item No. 600450
JC-1 Mitochondrial Membrane Potential Assay Kit - Item No. 10009172
Lysosomal Cytotoxicity Dual Staining Kit - Item No. 600350
MTT Cell Proliferation Assay Kit - Item No. 10009365
Multi-Drug Resistance Assay Kit (Calcein AM) - Item No. 600370
Multi-Parameter Apoptosis Assay Kit - Item No. 600330
WST-1 Cell Proliferation Assay Kit - Item No. 10008883
WST-8 Cell Proliferation Assay Kit - Item No. 10010199
XTT Cell Proliferation Assay Kit - Item No. 10010200

Appendix C: Research Fund and Publication

1. This work was supported by two research Grants from University of Malaya, Malaysia (PG087-2012B) and (HIR F000009-21001/ 2012).

2. **Farkaad A. Kadir,** Normadiah M. Kassim, Mahmood A. Abdulla, and Wageeh A. Yehye. Hepatoprotective Role of Ethanolic Extract of *Vitex negundo* in Thioacetamide-Induced Liver Fibrosis in Male Rats. Evidence-Based Complementary and Alternative Medicine. Volume 2013, Article ID 739850, 9 pages.

3. **Farkaad A. Kadir,** Normadiah M. Kassim,Mahmood A. Abdulla,and Wageeh A. Yehye. PASS-Predicted *Vitex negundo* Activity: Antioxidant and Antiproliferative Properties on Human Hepatoma cells-An in vitro Study. BMC Complementary and Alternative Medicine 2013, **13**:343 doi:10.1186/1472-6882-13-343.

4. **Farkaad Kadir,** Normadiah Binti M. Kassim, Mahmood A. Abdulla, Behnam Kamalidehghan, Fatemeh Ahmadipour, and Wageeh Yehye. PASS-Predicted Hepatoprotective Activity of *Caesalpinia sappan* in Thioacetamide-induced Liver Fibrosis in Rats. The Scientific World Journal. 2014. Volume 2014 (2014), Article ID 301879, 12 pages.

Hindawi Publishing Corporation
Evidence-Based Complementary and Alternative Medicine
Volume 2013, Article ID 739850, 9 pages
http://dx.doi.org/10.1155/2013/739850

Research Article

Hepatoprotective Role of Ethanolic Extract of *Vitex negundo* in Thioacetamide-Induced Liver Fibrosis in Male Rats

Farkaad A. Kadir,[1] Normadiah M. Kassim,[1] Mahmood A. Abdulla,[2] and Wageeh A. Yehye[3]

[1] *Department of Anatomy, Faculty of Medicine, University of Malaya, 50603 Kuala Lumpur, Federal Territory, Malaysia*
[2] *Department of Biomedical Science, Faculty of Medicine, University of Malaya, 50603 Kuala Lumpur, Federal Territory, Malaysia*
[3] *Nanotechnology & Catalysis Research Centre (NANOCAT), Block 3A, Institute of Postgraduate Studies Building, University of Malaya, 50603 Kuala Lumpur, Federal Territory, Malaysia*

Correspondence should be addressed to Normadiah M. Kassim; normadiah_mk@um.edu.my

Received 23 November 2012; Revised 9 April 2013; Accepted 29 April 2013

Academic Editor: Adair Roberto Soares Santos

The hepatoprotective activity of ethanolic extract from the leaves of *Vitex negundo* (VN) was conducted against thioacetamide-(TAA-) induced hepatic injury in *Sprague Dawley* rats. The therapeutic effect of the extract was investigated on adult male rats. Rats were divided into seven groups: control, TAA, Silymarin (SY), and VN high dose and low dose groups. Rats were administered with VN extract at two different doses, 100 mg/kg and 300 mg/kg body weight. After 12 weeks, the rats administered with VN showed a significantly lower liver to body weight ratio. Their abnormal levels of biochemical parameters and liver malondialdehyde were restored closer to the normal levels and were comparable to the levels in animals treated with the standard drug, SY. Gross necropsy and histopathological examination further confirmed the results. Progression of liver fibrosis induced by TAA in rats was intervened by VN extract administration, and these effects were similar to those administered with SY. This is the first report on hepatoprotective effect of VN against TAA-induced liver fibrosis.

1. Introduction

Liver is a vital organ of metabolism and excretion in the body. It is involved in the biochemical conversions of varied administered substances which significantly increased the reactive oxygen species generation [1]. These liberated radicals can be produced by hepatotoxins, such as thioacetamide (TAA). Several investigations have approved that single dose of this hepatotoxic agent could produce centrilobular hepatic necrosis, and chronic administration led to cirrhosis [2].

Although the modern medicinal system has developed phenomenally, discovering a new drug for treating liver diseases is still a dream. Therefore, a number of therapeutic plants are used in the traditional system of medicine for the management of liver disorders. However, many of them have not been investigated for their effects. VN is one such medicinal plant credited with numeral curative qualities validated by modern science and used since ancient times. VN belongs to a family of Verbenaceae and commonly called five-leaved chaste tree [3]. It is mainly distributed in tropical to temperate regions, especially in India [4], which is traditionally used by the native medical practitioners for the treatment of various ailments, including stomach-ache, disease of the eye, inflammation, enlargement of spleen, bronchitis, asthma, and painful teething in children [5].

The leaves are aromatic, tonic, and vermifuge [6]; the juice from the leaves was used for the treatment of ulcers and swelling of joints [7]. Preliminary phytochemical screening of the extract and literature survey shows the presence of alkaloid, flavonoids-like flavones, luteolin-7-glucoside, casticin, iridoid, glycosides, an essential oil, and other constituents like vitamin C, carotene, gluconolinal, benzoic acid, β-sitosterol,s and glycoside [3]. The literature reviews reveal that the plant VN possesses analgesic and antinociceptive activity [8], hepatoprotective activities against antitubercular drugs [3], CCl_4 [9], and ibuprofen via inhibition of lipid peroxidation [10].

Kadir et al. BMC Complementary and Alternative Medicine 2013, 13:343
http://www.biomedcentral.com/1472-6882/13/343

BMC Complementary & Alternative Medicine

RESEARCH ARTICLE Open Access

PASS-predicted Vitex negundo activity: antioxidant and antiproliferative properties on human hepatoma cells-an in vitro study

Farkaad A Kadir[1†], Normadiah M Kassim[1*], Mahmood A Abdulla[2†] and Wageeh A Yehye[3†]

Abstract

Background: Hepatocellular carcinoma is a common type of tumour worldwide with a high mortality rate and with low response to current cytotoxic and chemotherapeutic drugs. The prediction of activity spectra for the substances (PASS) software, which predicted that more than 300 pharmacological effects, biological and biochemical mechanisms based on the structural formula of the substance was efficiently used in this study to reveal new multitalented actions for *Vitex negundo* (VN) constituents.

Methods: Experimental studies based on antioxidant and antiproliferative assays verified the predictions obtained by the PASS-predicted design strategy. Antioxidant activity of VN extract was studied using 1,1-diphenyl-2-picrylhydrazyl (DPPH) and Ferric reducing or antioxidant power (FRAP) assays. The antiproliferative activity of VN extract against WRL68 and HepG2 was investigated based on methylthiazol tetrazolium (MTT) spectrophotometric assay.

Results: VN extract showed 79.43% inhibition of DPPH stable radical with IC_{50} 13.31 ± 0.18 μg/mL. This inhibition was too closed to butylated hydroxyl toluene (BHT) 82.53% (IC_{50}13.8 ± 0.14) and gallic acid 89.51% (IC_{50} 3.1 ± 0.08). VN extract exhibited the strongest free radical scavenging power compared with two commercial antioxidants, BHT and ascorbic acid. VN increased the activities of antioxidant enzymes in normal embryonic liver cells (WRL68) including, superoxide dismutase (SOD) and glutathione peroxidase (GPX) compared with to H_2O_2 group. The ethanolic extract of VN showed cytotoxicity to HepG2 cells in a dose and time-dependent manner with IC_{50} 66.46 μg/ml, 57.36 μg/ml and 65.12 μg/ml at 24, 48, and 72-hours incubation respectively, with no sensitivity in WRL68 cells. This was associated with significant elevation in lactate dehydrogenase (LDH) release in HepG2 cells. In addition, the activation of caspase-3 enzyme suggesting that the observed cytotoxicity was mediated via an intrinsic apoptosis pathway.

Conclusions: PASS-predicted plant activity could efficiently help in selecting a promising pharmaceutical leads with high accuracy and required antioxidant and antiproliferative properties. This is the first report on PASS-predicted VN activity.

Keywords: Antioxidant, Caspase 3, HepG2, LDH, MTT, PASS, *Vitex negundo*, WRL68

*Correspondence: normadiah_mk@um.edu.my
†Equal contributors
[1]Department of Anatomy, Faculty of Medicine, University of Malaya, 50603, Kuala Lumpur, Malaysia
Full list of author information is available at the end of the article

Hindawi Publishing Corporation
The Scientific World Journal
Volume 2014, Article ID 301879, 12 pages
http://dx.doi.org/10.1155/2014/301879

Research Article

PASS-Predicted Hepatoprotective Activity of *Caesalpinia sappan* in Thioacetamide-Induced Liver Fibrosis in Rats

Farkaad A. Kadir,[1] Normadiah M. Kassim,[1] Mahmood Ameen Abdulla,[2] Behnam Kamalidehghan,[3] Fatemeh Ahmadipour,[3] and Wageeh A. Yehye[4]

[1] *Department of Anatomy, Faculty of Medicine, University of Malaya, 50603 Kuala Lumpur, Malaysia*
[2] *Department of Biomedical Science, Faculty of Medicine, University of Malaya, 50603 Kuala Lumpur, Malaysia*
[3] *Department of Pharmacy, Faculty of Medicine, University of Malaya, 50603 Kuala Lumpur, Malaysia*
[4] *Nanotechnology & Catalysis Research Centre (NANOCAT), University of Malaya, Block 3A, Institute of Postgraduate Studies Building, 50603 Kuala Lumpur, Malaysia*

Correspondence should be addressed to Normadiah M. Kassim; normadiah_mk@um.edu.my

Received 22 October 2013; Accepted 5 January 2014; Published 20 February 2014

Academic Editors: S. G. Clark, M. Pretterklieber, and M. Tsang

The antifibrotic effects of traditional medicinal herb *Caesalpinia sappan* (CS) extract on liver fibrosis induced by thioacetamide (TAA) and the expression of transforming growth factor β1 (TGF-β1), α-smooth muscle actin (αSMA), and proliferating cell nuclear antigen (PCNA) in rats were studied. A computer-aided prediction of antioxidant and hepatoprotective activities was primarily performed with the Prediction Activity Spectra of the Substance (PASS) Program. Liver fibrosis was induced in male Sprague Dawley rats by TAA administration (0.03% w/v) in drinking water for a period of 12 weeks. Rats were divided into seven groups: control, TAA, Silymarin (SY), and CS 300 mg/kg body weight and 100 mg/kg groups. The effect of CS on liver fibrogenesis was determined by Masson's trichrome staining, immunohistochemical analysis, and western blotting. *In vivo* determination of hepatic antioxidant activities, cytochrome P450 2E1 (CYP2E1), and matrix metalloproteinases (MPPS) was employed. CS treatment had significantly increased hepatic antioxidant enzymes activity in the TAA-treated rats. Liver fibrosis was greatly alleviated in rats when treated with CS extract. CS treatment was noted to normalize the expression of TGF-β1, αSMA, PCNA, MMPs, and TIMP1 proteins. PASS-predicted plant activity could efficiently guide in selecting a promising pharmaceutical lead with high accuracy and required antioxidant and hepatoprotective properties.

1. Introduction

Liver fibrosis is known to result in distortion of normal tissue architecture of the liver. This alteration resulted from chronic liver damage as seen in chronic alcoholic abuse, viral hepatitis, or inherited metabolic disease [1]. Several biological and biochemical disturbances may also lead to hepatic cirrhosis [2]. A fibrotic liver may contain a substantial increase in most of the matrix proteins, in particular, the interstitial collagen types I and III which are under the influences of cytokines like transforming growth factor beta 1 (TGF-β1) and α-smooth muscle actin (αSMA) [3, 4]. These cytokines not only are present in greater amounts but also are deposited in abnormal sites within the liver microanatomy [5]. In case of thioacetamide- (TAA-) induced liver cirrhosis, other parameters such as oxidative stress have been postulated to be major molecular mechanisms basic to tissue alteration [6].

Caesalpinia sappan (CS), commonly named as Brazil or Sappan, belongs to the family of Caesalpiniaceae, a native plant in Southeast Asia [7]. Several studies have shown that CS has antimicrobial and bactericidal activity [8] and antiallergic [9], neuroprotective [10], and hypoglycaemic effects [11]. Others found that extract from CS can be used for treating ascites, tumour, leukaemia [12], and arteriosclerosis [13]. This could be due to its antioxidant activity